

Assessing Playas as Point Sources for Recharge of the High Plains Aquifer, Western Kansas



William C. Johnson, Randy L. Stotler, Mark W. Bowen, Jude H. Kastens, Daniel R. Hirmas, Dakota J. Burt, and Kaitlin A. Salley

Prepared for

U.S. Environmental Protection Agency and Kansas Water Office

Kansas Geological Survey Open-File Report 2019-2

Cover image: Aerial view north of the Ehmke playa (Lane County, Kansas) during a rainy period in August, 2016. (W. Johnson)

***Assessing Playas as Point Sources for Recharge of the High Plains Aquifer,
Western Kansas***

Wetland Program Development Grant (WPDG) FFY 2014-17

Playa Mapping and Assessment

By

William C. Johnson, Randy L. Stotler, Mark W. Bowen, Jude H. Kastens, Daniel R. Hirmas,
Dakota J. Burt, and Kaitlin A. Salley

Department of Geography and Atmospheric Science
University of Kansas

For

Kansas Water Office

Prepared in fulfillment of KWO Contract CD-97746601, KUCR # KAN0073725

August 31, 2018
(Revised 5/15/2019)

Wetland Program Development Grant (WPDG) FFY 2014

Playa Lake Recharge

Report Date: August 31, 2018

Report Period: FINAL REPORT

Grant Recipient: Kansas Water Office

Grant Number: CD-97746601

Submitted by: Kirk Tjelmeland, Kansas Water Office

Project Description: Playas of the High Plains provide many functions, including providing wildlife habitat and maintaining regional biodiversity. Playa lakes have been promoted as potential point sources of recharge to the High Plains Aquifer. A “Vision for the Future of Water in Kansas” is under development, and one of the two main focus areas is conserving and extending the life of the Ogallala aquifer, which is contained within the High Plains aquifer. This project seeks to determine the degree to which functioning Playas contribute to recharge of the aquifer, which in turn extends its useful life by providing additional water input. If recharge can be demonstrated and measured in Kansas conditions, renovation and protection of Playa lakes could be enhanced by state policy and programs. This investigation addresses two activities in the WPP: (1) Support Playa Lakes Joint Venture (PLJV) efforts to assess historic impacts to playas and determine their current condition. (p.5, KS WPP); and (2) support PLJV efforts to promote ecosystem services provided by playas, especially aquifer recharge. (p.5, KS WPP).

While extensive recharge studies have been associated with the Playas of the Southern Great Plains (Texas), no known studies have been conducted in the Central Great Plains (Kansas), where the soils and substrate differ significantly from that to the south. Investigations that have been undertaken in the Southern Great Plains have tended to be of singular design i.e., based exclusively on water-budget calculations, infiltration data, or unsaturated-zone techniques. In contrast, this investigation will adopt a multifaceted approach by a team with diverse and complementary expertise.

This multifaceted approach to assessing the role of Playa recharge contribution to the High Plains Aquifer will provide direct and indirect data to answer this question, which when combined with a knowledge of the impact of Playa basin sedimentation, will greatly enhance our understanding and importance of Playa function within the central Great Plains and beyond.

Background for the Study: The High Plains aquifer (HPA) extends across eight states, encompasses $450,656 \text{ km}^2$ ($174,000 \text{ mi}^2$), and is responsible for approximately 23% of the total groundwater use nationally (Figure 1) (Gutentag et al., 1984; Maupin and Barber, 2005). In Kansas, approximately 3.36 billion m^3 (887 billion gallons, 2.72 million acre-ft,) was withdrawn in 2016, 91% of which was used for irrigation (Maupin and Barber, 2005; Water Information Management and Analysis System, 2018). Central Kansas annual recharge rates to the HPA are

estimated around 925 million m³ (244 billion gallons, 0.75 million acre-ft.), which is approximately 28% of the quantity pumped annually (Buchanan et al., 2015). This results in substantial reductions in the saturated aquifer thickness (Buchanan et al., 2015). In Kansas, large-scale groundwater development began in the 1950s, with the invention of the center-pivot irrigation system and improvements in drilling and pumping technology which resulted in less-expensive, more efficient wells (Gutentag et al., 1984; Buchanan et al., 2015). From predevelopment (1950) to 2014-2016, some areas of the aquifer have experienced over 60% reduction in the saturated thickness, with water levels declining by over 50 m (164 ft) in some areas in southwestern Kansas (McGuire, 2009; Scanlon et al., 2012; Buchanan et al., 2015). Although isolated regions in the northwest and central part of Kansas have witnessed water level increases since predevelopment, the majority of the Kansas HPA is experiencing water level declines (Scanlon et al., 2012; Buchanan et al., 2015). Under current pumping rates and average climatic conditions, water-level declines and water quality degradation will continue, likely compromising future use of the aquifer (Whittemore et al., 2016).

Recharge rates have been studied across the HPA and are spatially variable, with precipitation and recharge generally greater in the northern High Plains (NHP), evapotranspiration generally greater in the southern High Plains (SHP), and the Central High Plains (CHP) between these two extremes (Figure 1) (Gurdak et al., 2007). Previously published recharge estimates for Kansas (5 to 54 mm yr⁻¹) indicate a travel time of 270 to over 1000 years for infiltrated water to travel through the 15 to 100 m-thick vadose zone to the aquifer (Gurdak et al., 2007).

Notwithstanding, the presence of agricultural contaminants in the aquifer indicates recharge of modern water (since the 1950s), which is indicative of a <100-year travel time to the water table (McMahon et al., 2006). The faster paths to the aquifer are likely through focused recharge and preferential flow paths, including areas with ponded surface water such as ephemeral streambeds, ditches, shallow depressions, irrigated cropland and playas (Gurdak et al., 2007, 2008; Meixner et al., 2016). Fluid flux through these areas of preferential flow often exceeds diffuse recharge (>100 yrs), which represents movement of water between individual pore spaces. Preferential flow paths (e.g., macropores) are of particular interest in playas because they can move water very quickly (<100 yrs). This type of recharge bypasses some or all of the soil matrix through secondary porosity, utilizing natural features including desiccation cracks, root tubes, and animal and insect burrows (Gurdak and Roe, 2009).

Studies of recharge through the dense system of SHP playas have concluded that measured playa recharge rates (60 to 120 mm yr⁻¹) are higher than diffuse recharge estimates (0.2 to 32 mm yr⁻¹) (Scanlon and Goldsmith, 1997; Wood et al., 1997; Gurdak et al., 2007; Johnson et al., 2012; Meixner et al., 2016). Additionally, it is estimated that macropore recharge, including through playas, accounts for a large percentage (84%) of the total average regional recharge in the SHP (11 mm yr⁻¹) (Wood et al., 1997).

Although playas are also abundant (>22,000) in Kansas (Figure), the possibility for recharge through Kansas playas to the HPA has not been investigated (Bowen, 2011). This is addressed in this research by first documenting and interpreting the soils and stratigraphy and then determining water fluxes through a Kansas playa and interplaya, identifying time periods of downward fluid flux during playa inundation, and quantifying travel times to the HPA. Water flux and travel times through the vadose zone are determined using the Chloride Mass Balance

(CMB), with additional information on fluid flow obtained from vadose zone anion depth profiles and matric potential (MP), groundwater chemistry, and water level changes.

Playas are internally-drained (closed basin) ephemeral lakes with varying periods of inundation. For an individual playa, inundation events, which depend on soil type and the frequency and duration of rain events, may only occur once every few years (Hillel, 2004; Gurdak and Roe, 2009). The amount of time an individual playa remains inundated is known as the hydroperiod (Gurdak and Roe, 2009). Water budget inputs to each playa basin include precipitation and runoff from surrounding topography, with outputs through either evapotranspiration or percolation downward through the playa base.

Recharge rates through playas can be controlled by rain flux, infiltration rate, K_{sat} and macropore fluid flux. At the beginning of rain events, the playa basin is dry, macropore flow (desiccation cracks) dominates, and the infiltration rate is controlled by the precipitation rate (Gurdak and Roe, 2009). During this period, macropores are open and can accept water at the precipitation rate as long as it doesn't exceed the soil infiltration rate (Gurdak and Roe, 2009). If rainfall is sufficient to cause the desiccation cracks to swell shut, the diffuse recharge mechanism takes over (Gurdak and Roe, 2009). Hydric soils, like those in playa basins, shrink and swell with response to changes in water content (Gurdak and Roe, 2009). A study in Senegal measured a time of 4.5 hours for desiccation cracks to close in a vertic soil, which would mark the transition from macropore to diffuse or focused recharge (Favre et al., 1997; Wilson, 2010). In instances when there is sufficient rainfall to inundate the playa with ponded water, infiltration is limited by the saturated hydraulic conductivity (K_{sat}) of the soil (Gurdak and Roe, 2009). Eventually, the ponded water will evaporate, transpire, or infiltrate, leaving a dry playa floor and allowing for desiccation cracks to reform (Gurdak and Roe, 2009).

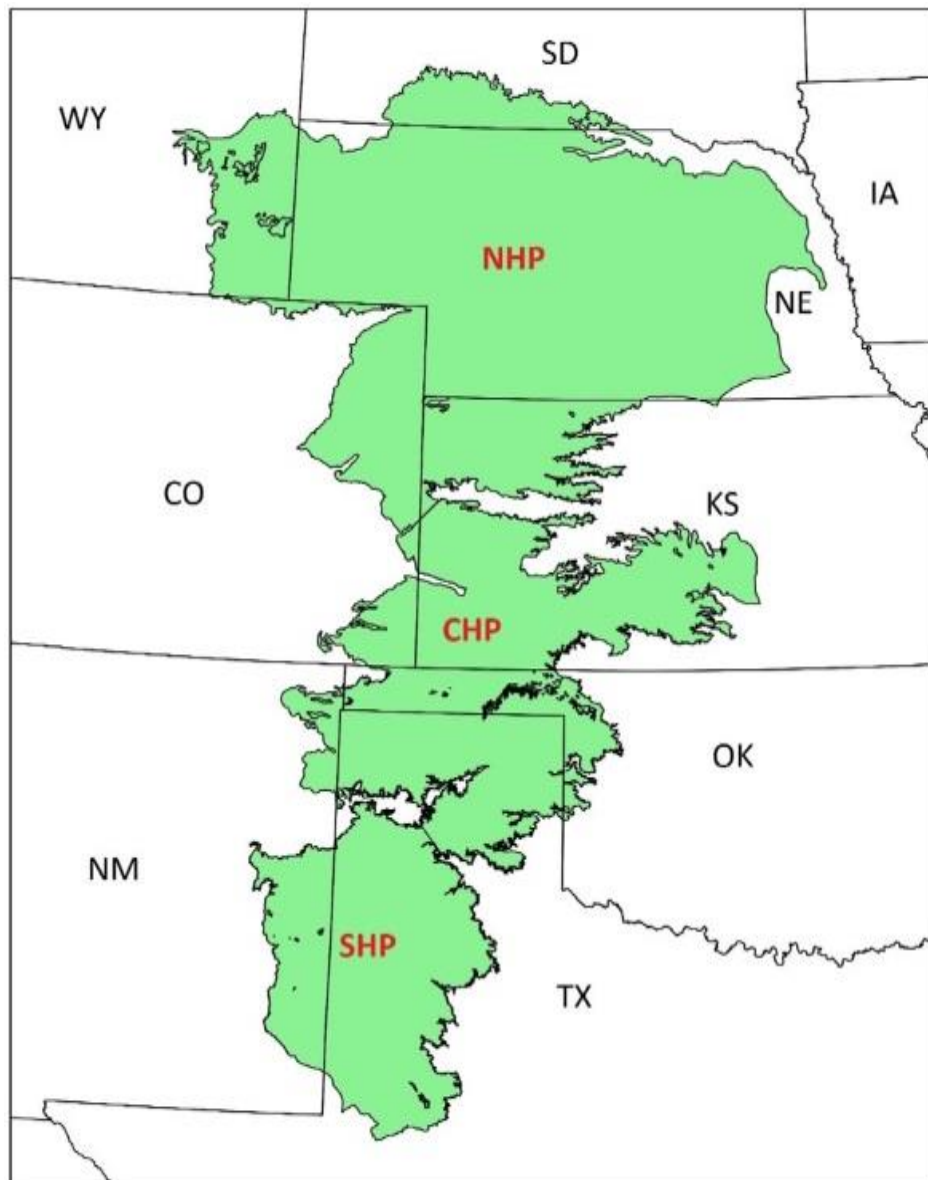


Figure 1. Aerial extent of the High Plains aquifer showing the three separate areas delineated as the Northern High Plains (NHP), Central High Plains (CHP) and Southern High Plains (SHP). (Kansas Data Access & Support Center, 2013)

ACCOMPLISHMENTS MET FOR THE GOALS, OBJECTIVES AND TASKS OF THE WORKPLAN

Goal 1. Preparation for field investigations

Action 1. Conduct final on-site evaluation of potential playas to select the study playa.

The Ehmke Playa site (38.4429, -100.6031), located on the CHP in Lane County, Kansas (Figure and 3), was selected to investigate the hydrology of playas above the HPA. This location is ideal for measuring recharge to the HPA because (1) the water table is relatively shallow (12-15 m:40-50 ft), (2) the land surface has not been affected significantly by anthropogenic modification, with rangeland surrounding the playa and little/no intensive farming or irrigation influencing the playa or run-on water, and (3) its eastward longitude within the cluster of playas in western Kansas, which, because of its higher average annual precipitation, increases the probability of precipitation events sufficient to produce runoff into the playa during the period of investigation (Figure 3). It was also advantageous because the Ehmke family, having originally settled the land, had a knowledge of its history since middle 1800s, and they were extremely cooperative and helpful logistically whenever needed. The playa watershed is approximately 429 hectares (1059 acres), with the sink (aka basin) holding up to 2 m (6 ft) of water and the inflow on the southwest end. Geomorphology of Ehmke Playa (Figure 4) consists of a suite of associated landscape elements, including the playa itself (as defined by the extent of hydric or near-hydric soils), playa sink (or basin) defined by the annulus (2 m-high rim), interplaya (upland in which this and other playas occur), bench (between the annulus and the interplaya), inflow channel and associated delta deposit, and lunette (silt dune created by deflation of the sink and bench). The 1 km (0.6 mi) elongated lunette, like several other features, occurs in association with playas elsewhere on the High Plains of Kansas (Bowen et al., 2018). Ehmke Playa frequently contains ponded water, though these hydroperiods occur at irregular intervals due to the serendipitous nature of the regional climate (Figure 5). A rare event occurred on September, 1986: “We had a huge toad strangler in the fall—in western Lane County around our farm south of Amy, we got 5 inches of rain in 2-hour period. Further west on the Lane-Scott county line, there was over 9 inches. Our playa lake stayed full of water for over a year...lots of water fowl, fairy shrimp, pelicans—you name it, they were there.” (Vance Ehmke, personal communication) (Figure 5).

The HPA underlying the study site consists of unconsolidated alluvial gravel, sand, silt and clay deposited to the east of the Rocky Mountains during the Miocene and Pliocene Epoch (Gutentag et al., 1984; Ludvigson et al., 2009). The alluvial sediments are often capped with a hard caliche layer, which is overlain by aeolian fine sand, silt, and clay (Gutentag et al., 1984; Wood and Sanford, 1995). The aerial expanse of the entire HPA is approximately 450,000 km² (173,746 mi²); the study site is located in the CHP, which encompasses approximately 125,000 km² (48.263 mi²), or about 28% the expanse of the aquifer (Meixner et al., 2016). The climate in the CHP is semiarid, with potential evapotranspiration of 2,140 mm yr⁻¹ (84 in) and average precipitation of 505 mm yr⁻¹ (20 in) (High Plains Regional Climate Center, 2017; Meixner et al., 2016). Ehmke Playa is located on the edge of the monitored portion of the HPA and is immediately adjacent to Kansas Groundwater Management District 1 (Figure 6).

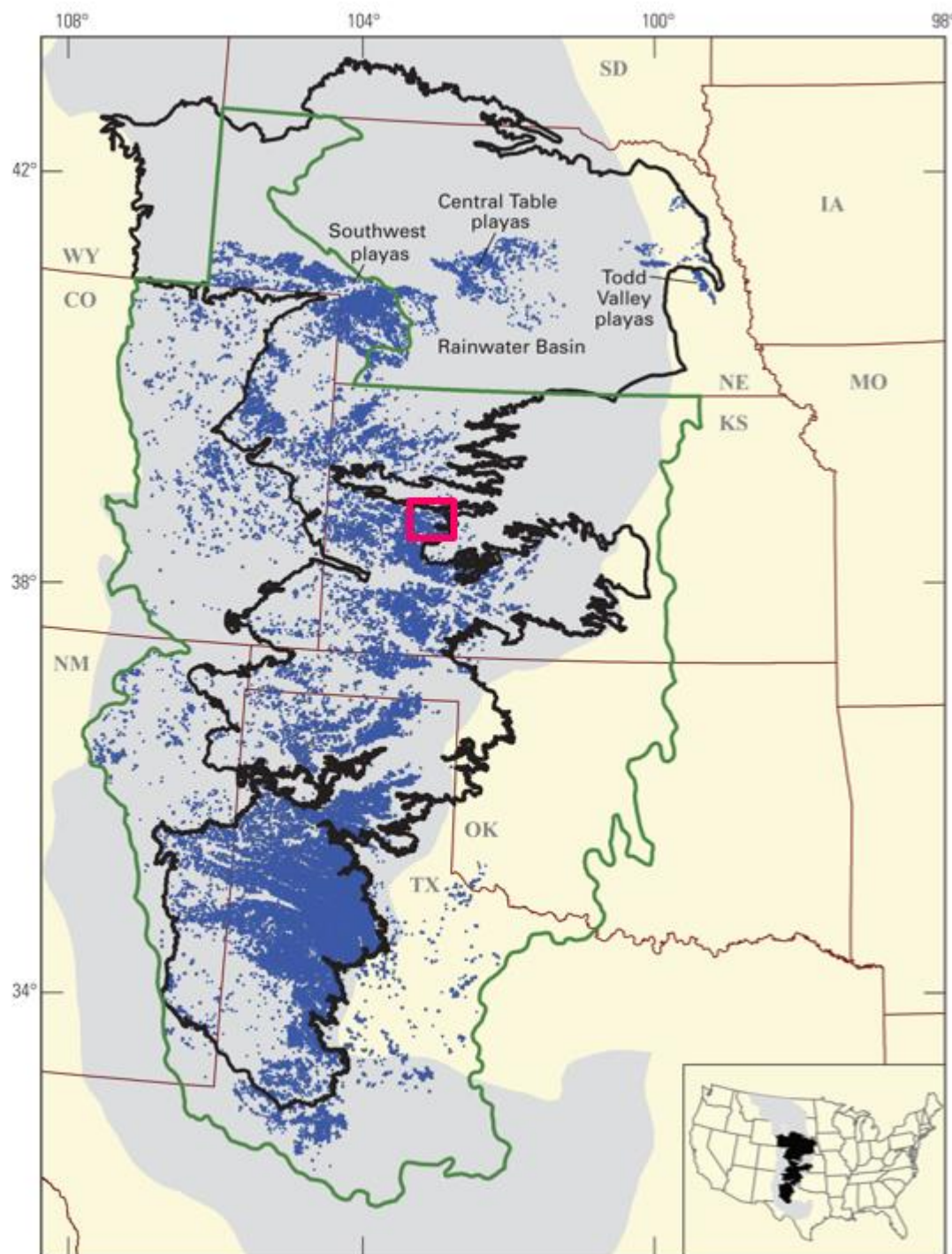


Figure 2. Distribution of playas (blue features) mapped in the Great Plains. Gray shading indicates the High Plains, black line the HPA boundary, green the Playa Lakes Joint Venture area of interest, red box Lane County, Kansas, the location of Ehmke Playa. (Playa Lakes Joint Venture)

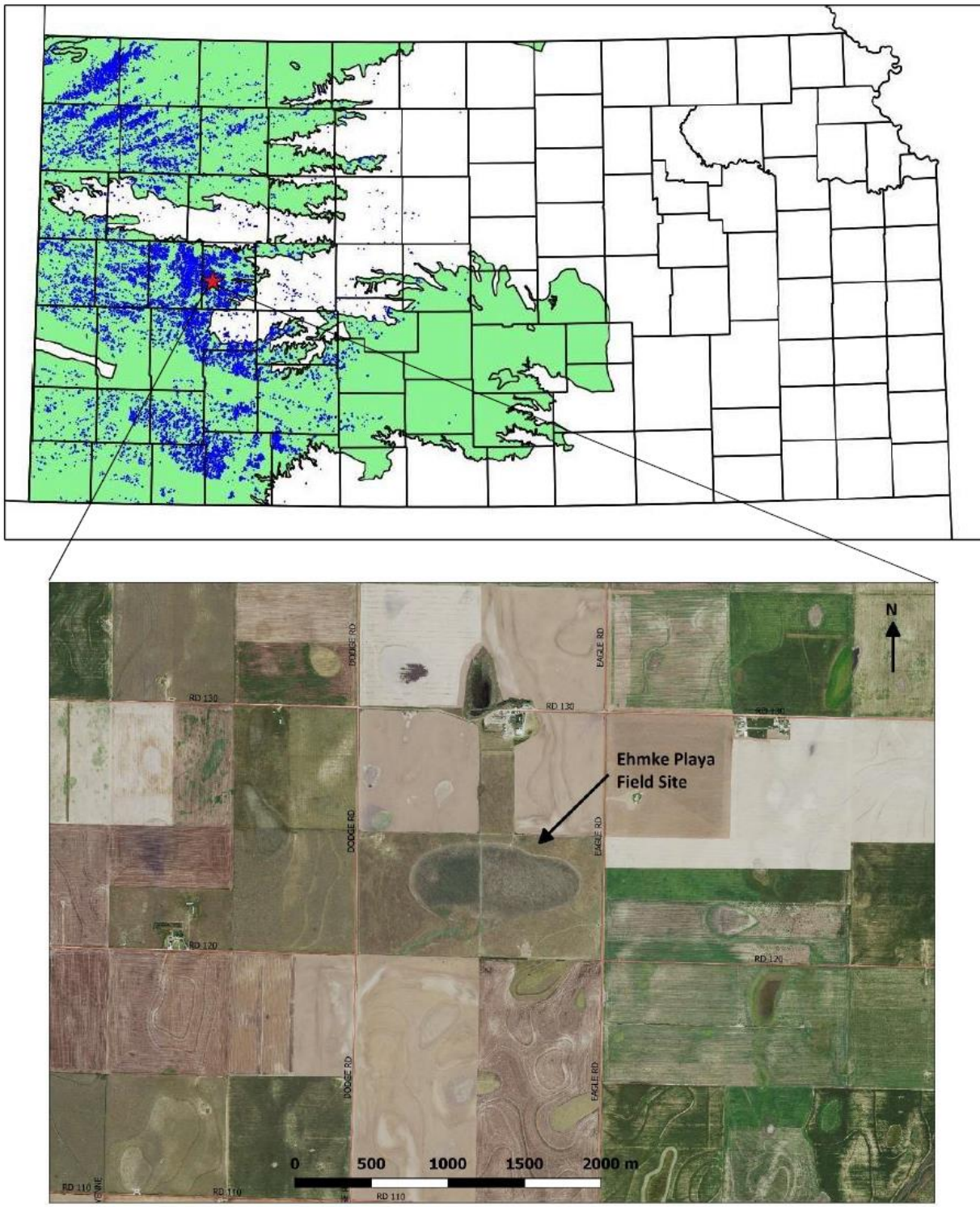


Figure 3. (U) Western Kansas with the High Plains Aquifer extent shown in green, playas shown in blue, and (L) the Ehmke Playa site field site location.

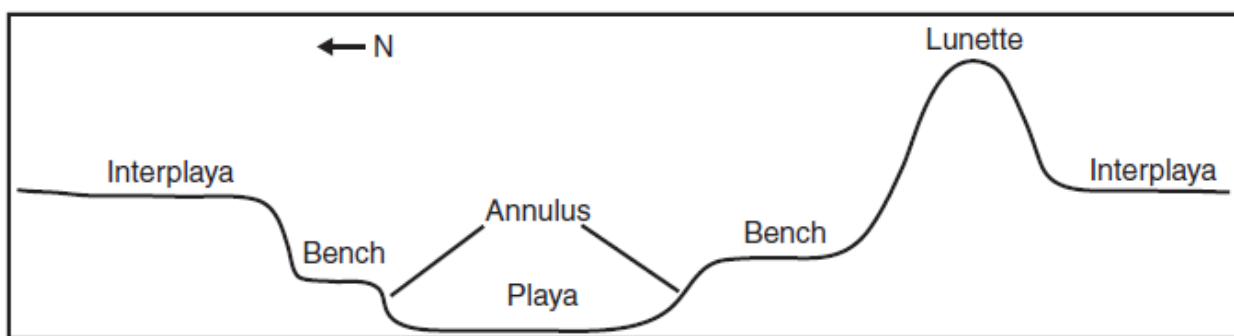
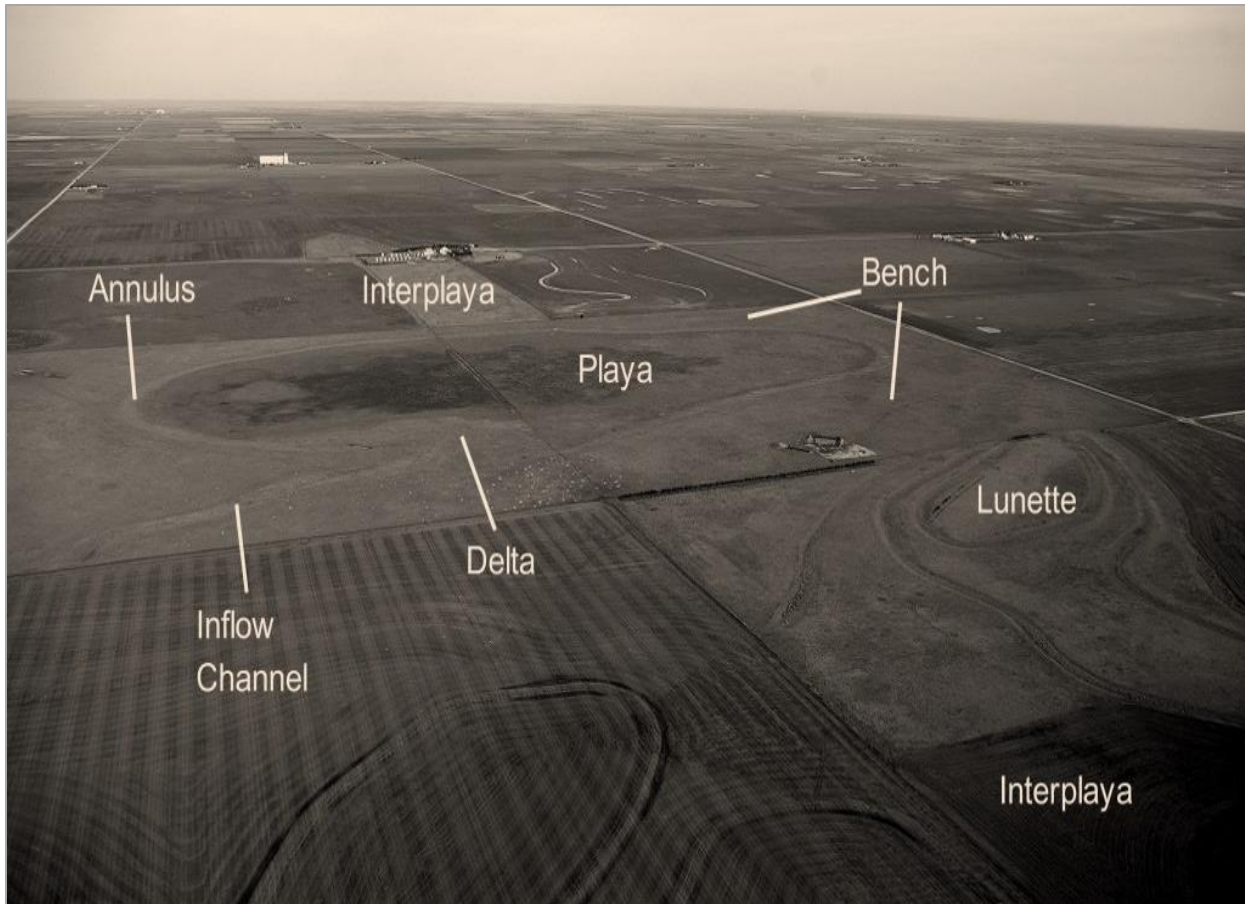


Figure 4. Aerial view north of the geomorphology of the Ehmke Playa. (U) Features include the playa—defined by the hydric soil, annulus—defines the edge of the playa sink or basin, bench—surface above the sink, interplaya—the uplands within which the playas are expressed, and the lunette—a silt dune formed by deflation of the playa basin by the northwest glacial age winds. The inflow channel and its attendant small deltaic feature occur on the south-southwest edge of the playa sink (W.C. Johnson); (L) A schematic profile north-south across Ehmke Playa. (Bowen and Johnson, 2012)



Figure 5. (UL) Cracks (macropores) developed in the hydric soil of Ehmke Playa during a dry period (W.C. Johnson); (UR) ducks, frogs, fairy shrimp and other wildlife occupying the playa during a hydroperiod resulting from several days of rain (W.C. Johnson); (L) Ehmke Playa during a hydroperiod with a maximum depth of about 2 m (6.1 ft) of water and family members on a raft made of 55-gallon drums and scrap lumber. (courtesy of Vance and Louise Ehmke).

Average 2014 - 2016 Depth to Water, Kansas High Plains Aquifer

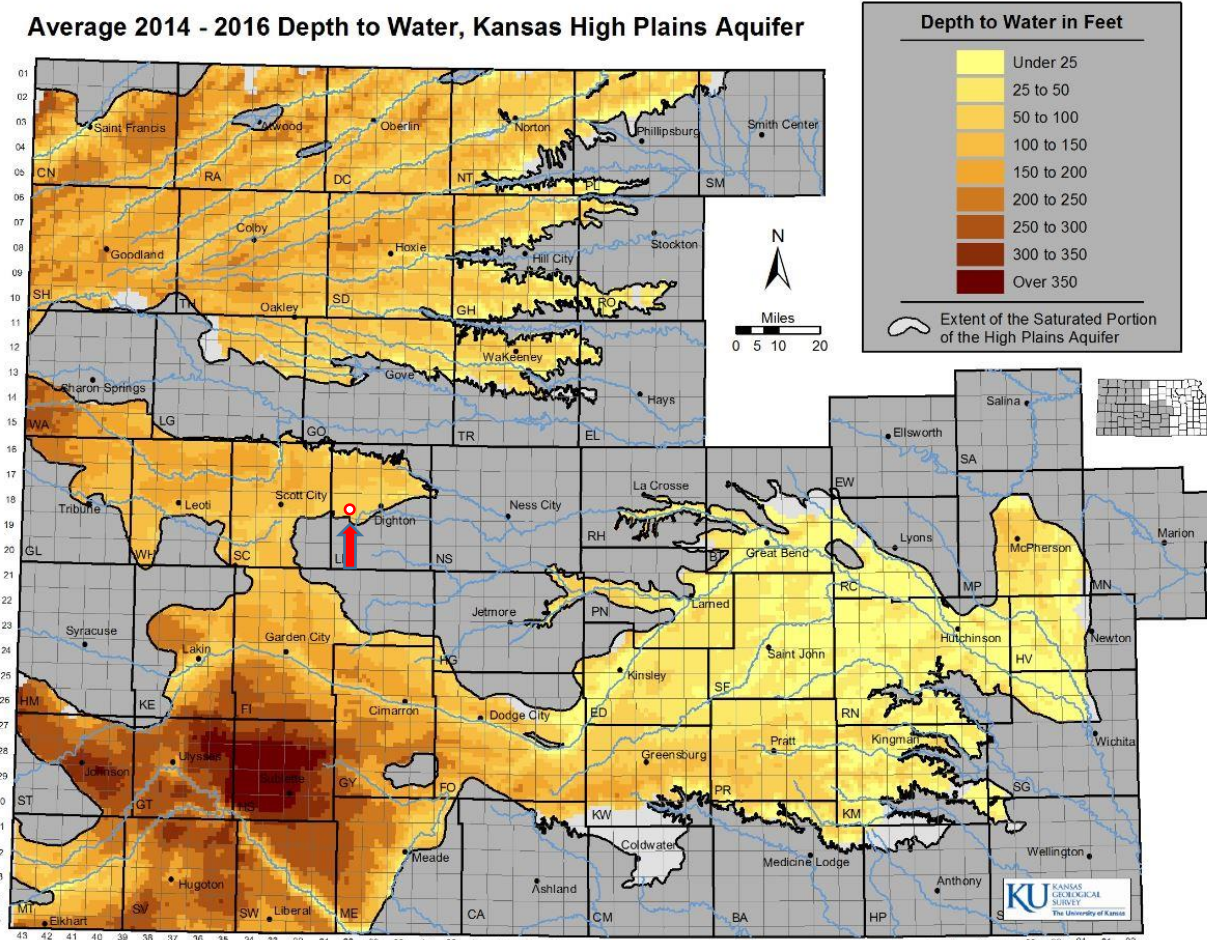


Figure 6. Average depth to the water table within the High Plains Aquifer averaged 2014-2016. The red arrow points to Ehmke Playa, which is located 12-15 m (40-50 ft) above the water table. (Kansas Geological Survey)

Action 2. Acquire supplies and assemble equipment to conduct the on-site investigations.

The University of Kansas departments of Geography and Atmospheric Science, and Geology had all equipment and supplies for routine field investigations and for most laboratory analyses. The only significant individual field equipment acquisition was a state-of-the-art Decagon infiltration measurement system. Otherwise, most acquisitions consisted of sensors and other components for assembling the above- and below-ground instrumented station in the center of the playa.

Action 3. Characterize Ehmke Playa through high-resolution rendering and detailed soil mapping.

Given that investigations were initiated prior to the availability of LiDAR imagery, a total station-based survey was done of the playa and adjacent fringe of the sink in order to establish control points to tie in core and trench locations. The playa was subsequently documented with photographic overflights using a small unmanned aerial system (sUAS), or drone (Figure 7). Images such as that depicted in Figure 8 in conjunction with ground testing permitted definition of the playa and differentiation of the playa into the well-developed hydric soils in the core or center part of the playa and the less well developed hydric soils surrounding the core. Most extensive development of desiccation cracks (macropores) occurs in the core area of the playa, though they have been observed throughout the playa. This subtle difference in the two hydric soil zones suggests that during rainfall and runoff events the macropores in the playa core enhance infiltration but following closure of the macropores infiltration may well have been greater in the outer zone through micropores. Aerial imagery was also used as a guide to selecting potential core locations and siting of the instrument station and pit.

With subsequent availability of LiDAR imagery, it was then possible to render data in greater detail and in the third dimension of the playa system in our GIS environment. Figure 9 portrays the elements of the playa and the playa catchment. The playa extent represents the hydric soil area images in Figure 8, whereas the playa sink, or basin is the area that extends to the annulus and is inundated during extreme hydroperiods such as that shown in Figure 5. The internally-drained attribute of all playas is well-illustrated by the character of the catchment, which for Ehmke Playa includes pasture and wheat fields to the southwest. In the absence of defined drainage systems flowing externally, this playa-dense landscape consist of a puzzle-like mosaic of catchments draining into playas of all sizes.

The hydrologically-filled hillshade digital elevation model (DEM) in the upper image of Figure 10 is a representation of the water surface when the playa sink is completely full. Note that the playa extends to the east side of the road and actually captures the watershed of a small playa before spilling, which is why the playa sink boundary in Figure 9 extends beyond (east of) the catchment boundary.

Application of a fill depth algorithm developed by J. Kastens to the hillshade DEM (Figure 10) adds the 3rd dimension (depth) to the filled DEM. It highlights the shallow areas around the periphery of the playa, including the incipient spillover area on the east side of the playa and the deepest water in the center of the playa, over the hydric soil area. Volumetric data extracted from the DEM indicate that the sink, with an area of (69.6 hectares: 171.9 acres), has a capacity of 668,552 m³ (542 acre ft) and the playa, with an area of (35.5 hectares: 87.6 acres), has a capacity of 32,485 m³ (26.3 acre-ft) Note that the playa area-capacity relationship (354,644 m² vs. 32,485 m³) indicates that water filling only the playa is less than a meter deep, which is a function of the playa being nearly flat—ground survey data record a maximum vertical variation of about 60 cm (2 ft). When filled to the bench surface at the annulus, water depth in the center of the playa would average 1.8 m (6 ft), with a maximum of about 2 m (6.6 ft).



Figure 7. Examples of approaching the field-based characterization of Ehmke Playa. (L) Mark Bowen and Dakota Burt (inset) employing a total station system to establish a datum and map the playa via a series of intersecting transects. (M.W. Bowen); (R) Dakota Burt preparing to launch one of our research sUAS for a photographic mission.(W.C. Johnson)

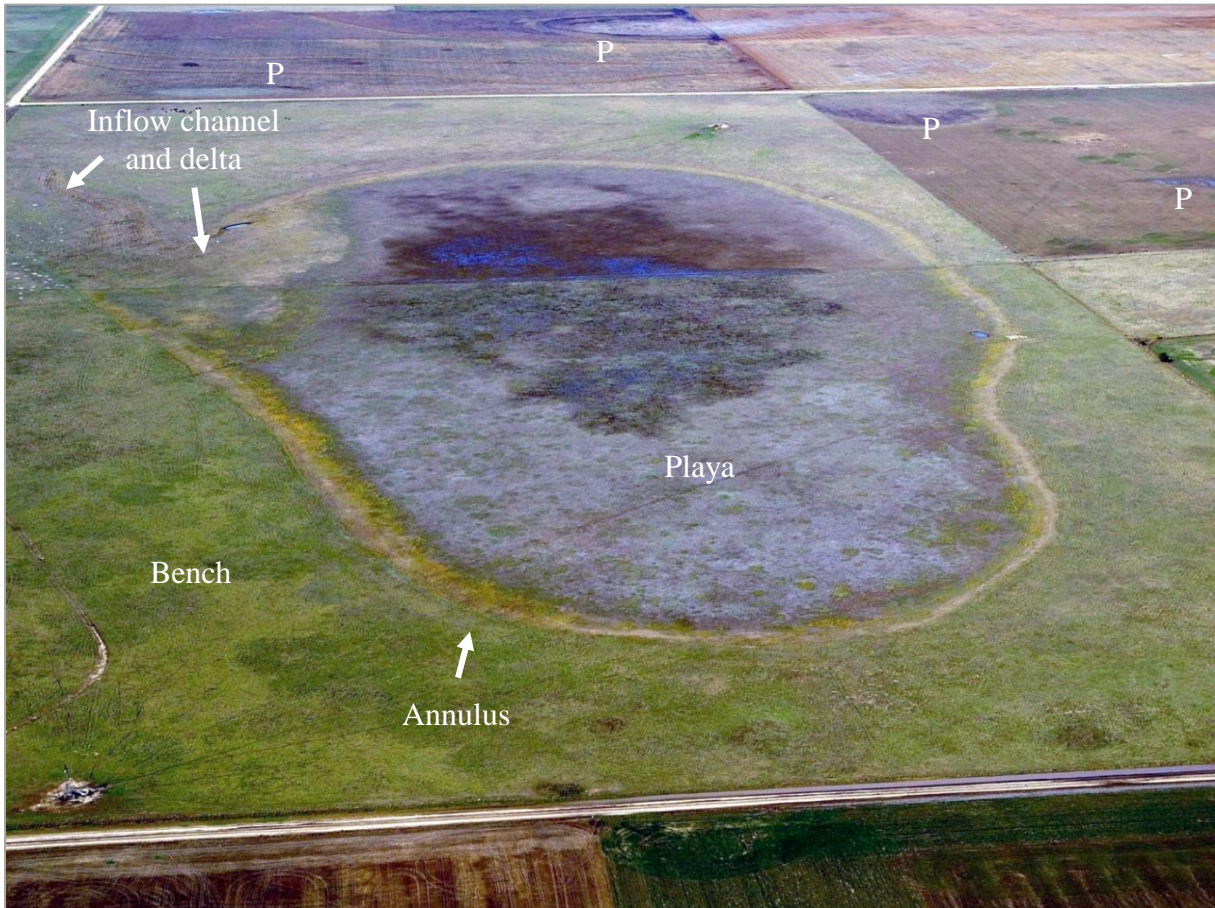


Figure 8. A low oblique view westward of Ehmke Playa during the waning of a hydroperiod. The “bathtub ring,” accentuated by flotsam, clearly defines the playa through its hydric soil zone. Best-developed hydric soils are revealed by the dark (wet) core and the less well developed hydric soils around the core and approaching the annulus especially to the southeast. Small playas are visible along the top of the image (P). (W.C. Johnson)

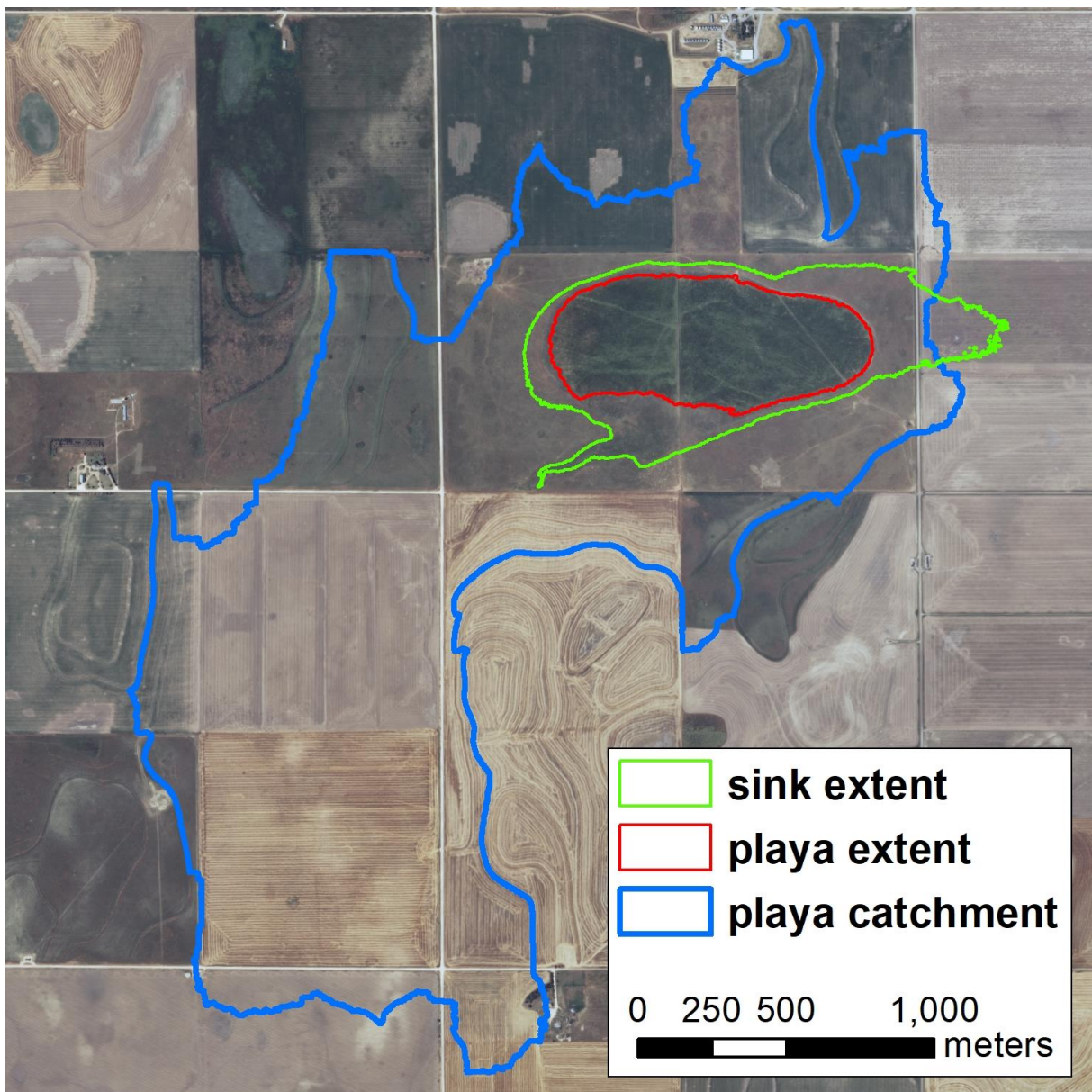


Figure 9. Ehmke Playa catchment (1059 acres: 429 hectares), playa sink (basin defined by the annulus) (69.6 hectares: 171.9 acres), and playa extent of hydric soil development (35.5 hectares: 87.6 acres).

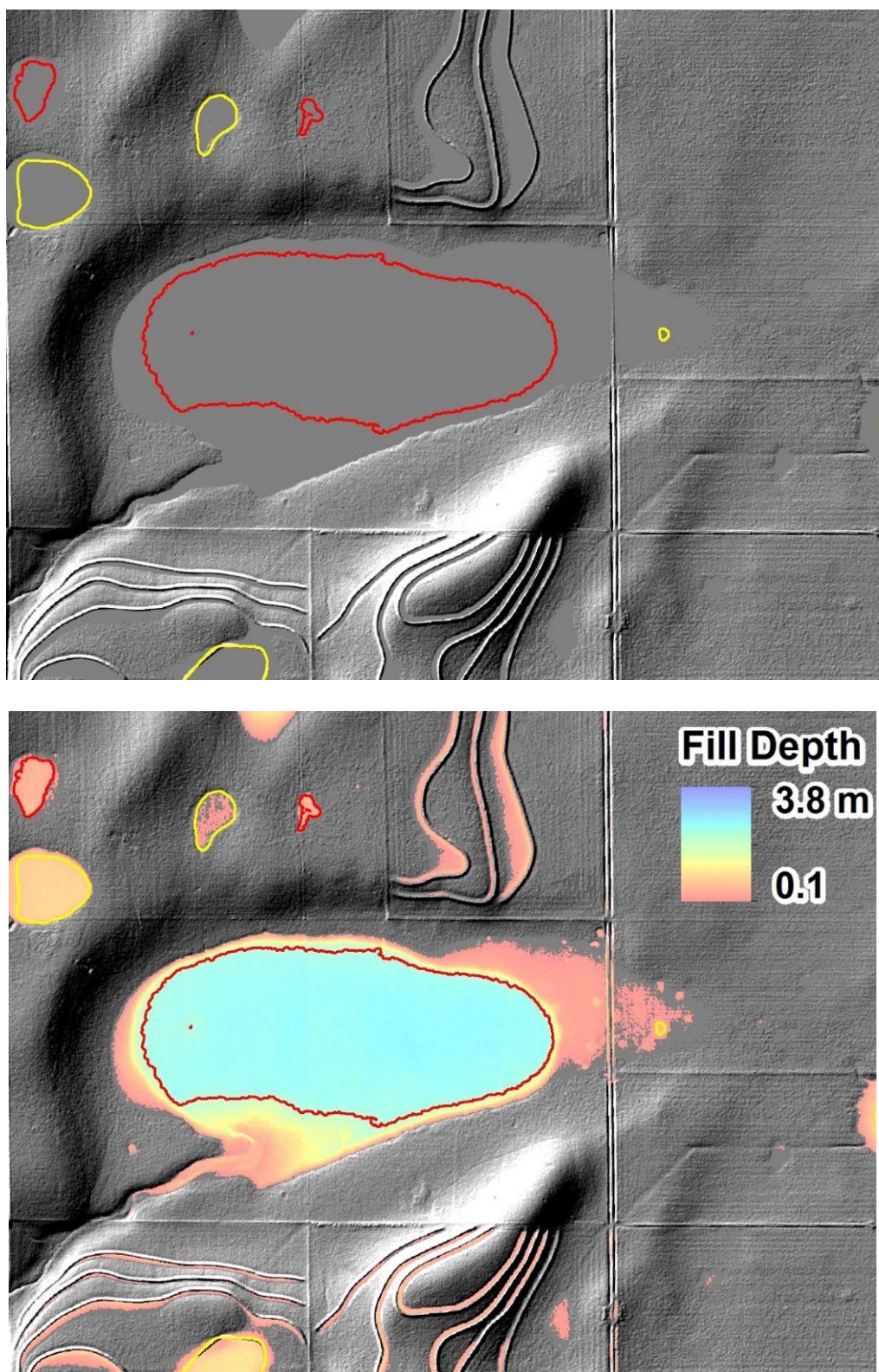


Figure 10. (U) The filled hillshade DEM (flat featureless surface) of the playa sink (or topographic basin) and outline (red) of the playa hydric soil area (Fig. 8); (L) Fill depth (maximum water depth at overflow), the level at which the volumetric capacity is $668,552 \text{ m}^3$ (542 acre ft).

Goal 2. Initiate on-site investigations and monitoring

A compilation of major data collection sites is presented in Figure 11. Three groundwater monitoring wells were installed: southwest (#3) and southeast (#2) of the playa and in the playa center (#1). The existing windmill well north of well 2 was used for water sampling only. Location of cores 5 m (16 ft) or more were labeled as the EPC series—EPC 1-5 were extracted with a Giddings trailer-mounted rig and EPC5 and 7 were obtained with the large Kansas Geological Survey drill rig. The instrument station and infiltration sites are also indicated.

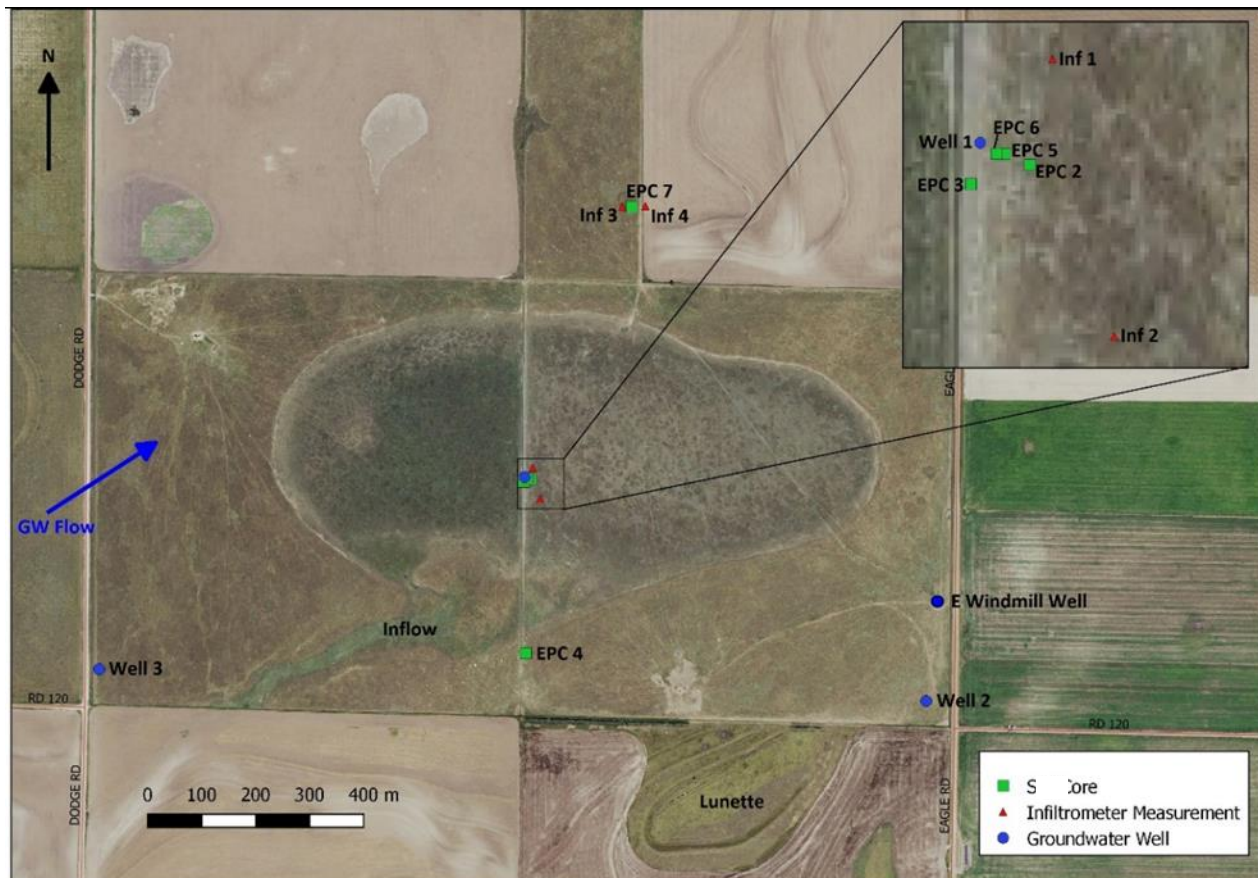


Figure 11. Locations of deep cores (vs. soil cores) (EPC series), groundwater monitoring wells 1-3 and monitored windmill well, and infiltration sites (Inf 1-4). Note the ascertained northeastward direction of groundwater flow.

Action 1. Install in-ground sensors and meteorological station.

1.1 Above- and below-ground instrumentation

The instrument group consisted of a 3.1 m (10 ft) instrument tower, sufficiently high to be unaffected by high water levels and protective enclosing cattle panels, and an array of sensors; primary sensors included an automated rain gauge, camera programmed to take two photographs each day, and automated sonic water level recorder and ground target (Figure 12). Likewise, the logger and other electronics, battery, and solar cells were mounted above the maximum potential water surface. Subsurface sensors to detect moisture flux were emplaced in a pit excavated adjacent to the power and electronics stand (Figure 13). The supplier of the instrument station tower and sensors, Campbell Scientific (<https://www.campbellsci.com/>) was contracted to write the code for all sensors due to the complexity introduced by the deployment of sensors from various manufacturers. Also within the cattle panel enclosed instrument area is groundwater monitoring well 1, with a standpipe (white pvc) extending to above the potential maximum water level to avoid surface-water contamination of the groundwater. Figure 14 provides examples of an instrument station camera image and a ground photograph taken during two spring 2017 runoff events sufficient to pond water in the playa.



Figure 12. UAS views northwestward of the above-ground instrument array and of the below-ground sensors in the pit prior to backfilling. (D.J. Burt)



Figure 13. Below-ground sensor installation. (L) soil-water potential sensors emplaced (W.C. Johnson); (R) Dakota Burt (cap) and Randy Stotler installing water content reflectometers. (W.C. Johnson)



Figure 14. Hydroperiods recorded at Ehmke Playa during the period of investigation. (L) Eastward facing morning photograph taken by the instrument station camera on May 2, 2017; (R) Southeastward view of Ehmke playa on April 12, 2017 when water covered most of the playa hydric soil area. The red arrow indicates the instrument station in the center of the playa. (W.C. Johnson)

1.2 Groundwater monitoring wells

Three monitoring wells were installed at the study site in June 2016 (Figures 15 and 16) (Table 1), including:

- Well 1 (EP-1) in the playa center within the fenced instrumentation area within the playa, drilled to a total depth of 31.5 m (103.4 ft) (all depths are reported as below ground surface unless otherwise noted),
- Well 2 (EP-2) adjacent to the road in the southeastern corner of the section, on the southeast side of the playa basin, and at the toe of the lunette, drilled to a total depth of 30.1 m (98.8 ft).
- Well 3 (EP-3) to the southwestern corner of the section and adjacent to the southwestern corner of the playa near the inflow drilled to a total depth of 30.0 m (98.3 ft).

Surface elevations were extracted from LIDAR using coordinates and are 867.8 m (2,847.2 ft) above mean sea level (amsl), 871.6 m (2,859.6 ft) amsl, and 874.2 m (2,868.0 ft) amsl at wells 1, 2, and 3, respectively. Each well was instrumented with a Solinst Levellogger pressure transducer, allowing for hourly water level measurements. A Solinst Barologger was placed in well 1 at 6.4 m (21 ft) below top of casing for barometric pressure corrections.

Table 1. Well construction data.

Well ID	Latitude	Longitude	Surface Elevation (m AMSL)	Well Depth (m BGS)	Height of Pipe above Surface (m)
EP 1	38.44240°N	100.60301°W	867.8	31.5	2.010
EP 2	38.43879°N	100.59441°W	871.6	30.1	0.355
EP 3	38.43908°N	100.61197°W	874.2	30.0	0.485



Figure 15. Kansas Geological Survey Explorations Section drill crew installing one of the three groundwater monitoring wells. (W.C. Johnson)

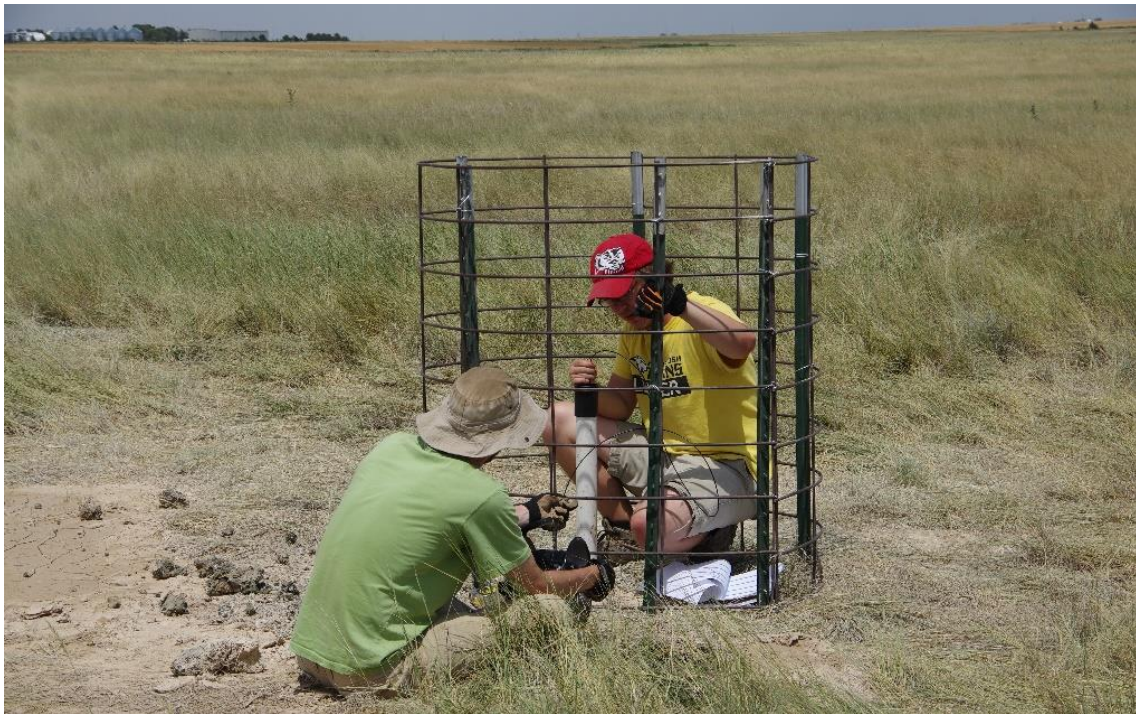


Figure 16. Nate Schlagel (L) and Dakota Burt (R) making well and water-level depth measurements at one of the three groundwater monitoring wells. All three wells were protected from cattle disturbance with heavy wire mesh and several supporting steel T-posts. (W.C. Johnson)

Action 2. Conduct subsurface investigations via machine coring and trenching.

Subsurface explorations were conducted by various means (Figure 17). Reconnaissance soil survey was conducted with spade, soil probe, bucket auger, and small Dirt Master backhoe.

Trenching, while limited due to cost, was carried out using a backhoe and operator contracted from a local oil well service company. Core extraction was accomplished using one of two approaches. For depths 5-8 m, the zone above sub-surface carbonate lentils, a trailer-mounted Giddings coring machine was used, but for deeper coring (to the water table and below), the Kansas Geological Survey's Exploration Services section drill crew using a hollow-stem auger system was brought into service. In addition to the above, a suite of cores were collected first, using the Giddings rig, outside the playa to document the soil and stratigraphy of the sink, bench and interplaya areas (Figure 18). All cores were captured in transparent PTEG plastic core-tube liners, which were capped and sealed to prevent contamination, stabilize for transportation back to the University of Kansas, and facilitate archiving.



Figure 17. Sub-surface investigations. Trenching was conducted using a locally contracted backhoe and operator (UL), and shallow soil-inspection pits were excavated with a small towable backhoe by Nate Schlagel, as well as by soil probing and hand bucket auguring (UR). Extraction of cores was conducted by the Kansas Geological Survey's Exploration Services section drill crew using a hollow-stem auger system (LL; Kait Salley pictured logging cores), and by using a trailer-mounted Giddings coring machine (LR). (W.C. Johnson)



Figure 18. Locations of soil cores extracted from the edge of the playa, sink, and bench, i.e., on the edge and outside the playa hydric soil area. The collection of representative cores was conducted during the first phase of the study. Of the nearly 50 cores collected, these were selected for characterization. (Google Earth)

Actions 3. Conduct infiltration studies.

A Decagon Devices DualHead Infiltrometer was used to measure the K_{sat} of the surface soil at four locations. Two measurements were collected at the playa center (Inf 1 and 2) near EPC 1 and two measurements were collected at the interplaya (Inf 3 and 4) near EPC 7 (Figure 11). The infiltrometer uses an encased pressurized chamber filled with water to maintain a constant pressure head through a series of high and low pressure cycles. A soak time of 25 minutes was chosen to properly wet the soil, followed by three pressure cycles using a high-pressure head of 15 cm and a low-pressure head of 5 cm. Following the pressure cycles, K_{sat} is calculated by averaging the result of the three cycles (Figure 19).

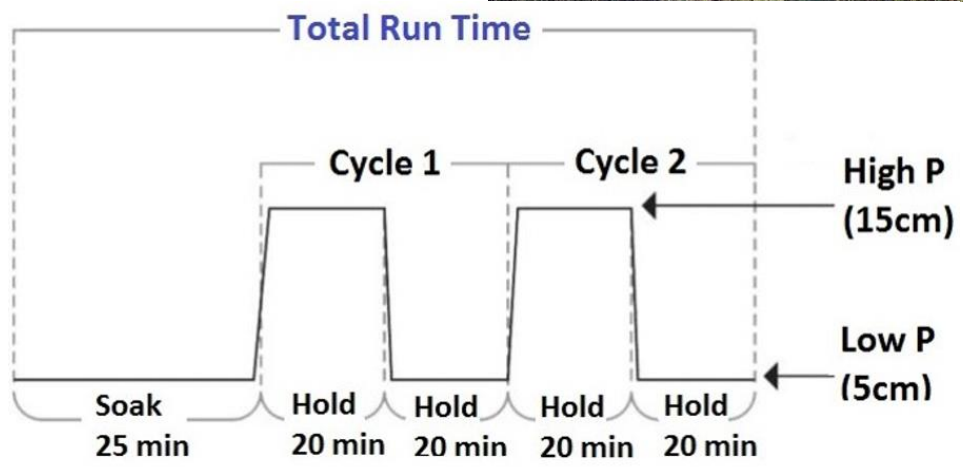


Figure 19. Kait Salley setting up and running the dual-head infiltrometer tests. The tests were conducted on both the playa floor and the interplaya near cores locations EPC5 and EPC7 (W.C. Johnson); Data were obtained using the operational cycle as illustrated. (W.C. Johnson)

Goal 3. Laboratory analyses of core and trench samples

Action 1. Prepare and analyze geochemical tracer samples.

Pore water chemistry was analyzed from four cores, including every 0.5 m from EPC 1 and 2, and every 1 m from EPC 5, and 7 (Figure 20). Approximately 120 g of soil/sediment was used for each sample, or between 3 and 5 cm length from a 6 cm diameter core. A 20 g aliquot was separated from each sample for measurement of field gravimetric water content ($\theta_{G\text{field}}$), by oven drying at 105°C for 24 hrs. The volumetric water content ($\theta_{V\text{field}}$) was estimated based on the volume of soil/sediment removed from the core and assuming a water density of 1 g mL⁻¹. The remaining 100 g of soil from each sample was air-dried in the controlled lab environment for 7 days and then re-weighed. Dried samples were softly ground using mortar and pestle to dis-aggregate clays. A saturated paste was then created using the air-dry soil and adding deionized (DI) water at a 1:1 ratio (Lindau and Spalding, 1984; Herbell and Spalding, 1993). Samples were then agitated for one minute, covered, and left for 24 hrs to ensure precipitated ions from pore water dissolved completely. Just before extraction, an aliquot of soil was removed for a second gravimetric water content ($\theta_{G\text{paste}}$) measurement. Samples were then placed into extraction cups lined with two pieces of 2.7 µm filter paper (9.0 and 4.25 cm diameter), and placed onto a Model 24VE programmable vacuum extractor. Samples were left on the vacuum for 24 hours, resulting in extraction of 60 to 80 mL of pore water. The extracted pore water was then filtered using a syringe attached to a 0.45 µm attachable filter to remove sand and coarse silt from the sample. Afterwards, the specific conductance was measured using a Hach Waterproof Handheld meter to ensure the TDS was low enough to analyze using an Ion Chromatograph (IC). The meter was calibrated using solutions of 10 and 100 ppm. In instances of high TDS water, the sample was diluted with DI water prior to IC analysis. A 5 mL aliquot of each pore water sample was analyzed on the IC for fluoride, chloride, bromide, nitrate, and sulfate.

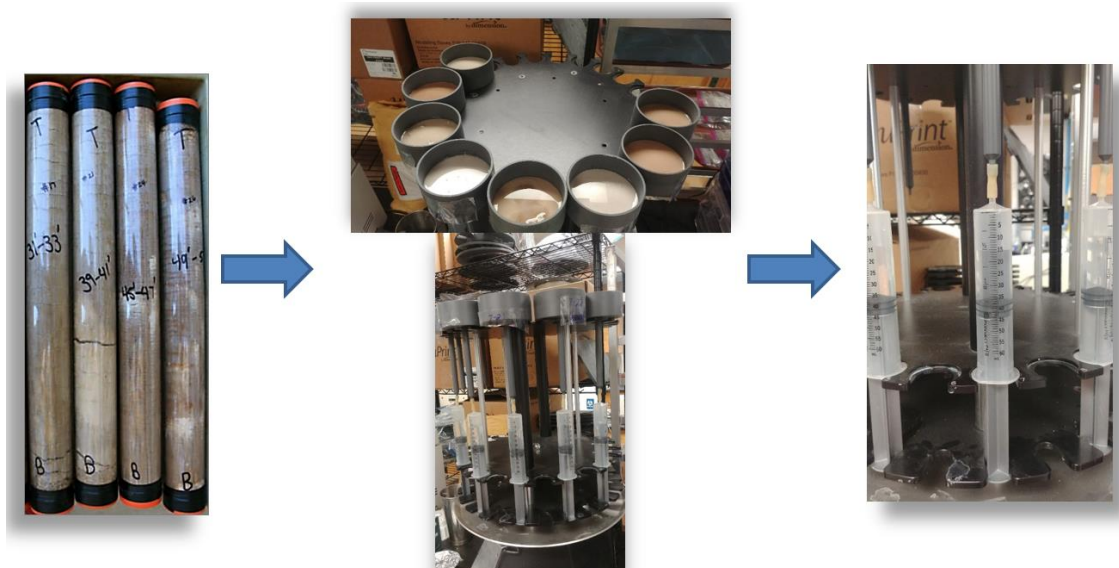


Figure 20. Extraction of pore water from saturated pastes. (K. Salley)

Instrument quantification limits (IQLs) were calculated using calibration curves with two high and two low standards for each anion. Two IC runs were completed, one in July 2017 and a second in August 2017. Calibration curves with plotted per anion per run using detector response as area under the curve along the x-axis and standard concentration along the y-axis. A best-fit line was drawn on each of the calibration curves and the y-intercept, slope, and R^2 values calculated for each (Corley, 2003). The y-intercept and slope were then used to calculate the root mean square error (RMSE) and the R^2 value used to gauge validity of the best-fit line (Corley, 2003). The final IQLs were calculated as $10 \times RMSE$ divided by the slope (Corley, 2003). Then, the IQLs and R^2 values for both runs were averaged together. Results were output from the IC in mg L^{-1} (ppm). This value was converted to mg Kg^{-1} of dry soil using the following equation:

$$\frac{\text{anion}}{\text{extracted water}} \left(\frac{\text{mg}}{\text{L}} \right) \times \theta_{\text{Gpaste}} \left(\frac{\text{g}}{\text{g}} \right) \times \frac{1}{\rho_{\text{water}}} \left(\frac{\text{mL}}{\text{g}} \right) = \frac{\text{anion}}{\text{soil}} \left(\frac{\text{mg}}{\text{Kg}} \right) \quad [1]$$

where θ_{Gpaste} is the gravimetric water content of the saturated paste described above and the density of water (ρ_{water}) is assumed 1 g mL^{-1} . The mg kg^{-1} concentration was then converted to mg L^{-1} of pore water:

$$\frac{\text{anion}}{\text{soil}} \left(\frac{\text{mg}}{\text{kg}} \right) \times \frac{1}{\theta_{\text{Gfield}}} \left(\frac{\text{g}}{\text{g}} \right) = \frac{\text{anion}}{\text{pore water}} \left(\frac{\text{mg}}{\text{L}} \right) \quad [2]$$

where $\theta_{\text{Gfield}}^{-1}$ is the inverse of the field gravimetric water content discussed above.

Action 2. Prepare and analyze soil and sediment samples.

Analysis of soil and sediment samples was carried out first on the cores collected around the playa (Figure 18) and subsequently from cores (EPC 3, 4, 5, 7) (Figure 11), with the exception of the sensor pit at the center of the playa, where samples were collected from a prepared face. Cores were transported to the Soils and Geomorphology Laboratory at the University of Kansas for examination and sampling (Figure 21). Samples were collected typically every 2 to 5 cm. Each sample was packed into 8 cm^3 plastic cubes and dried for 48 hrs at 60°C . The samples in the cubes were then used for magnetic susceptibility, particle size (texture), spectral color, and stable isotope ($\delta^{13}\text{C}$, $\delta^{15}\text{N}$) analyses.

Rock magnetic analyses of soil and sediment have been used to gauge soil development and weathering with loess through magnetic grain mineralogy, size, and concentration (e.g., Singer and Verosub, 2007; Geiss et al., 2008; Maher, 2016). Low-field magnetic susceptibility (χ), a proxy for the total abundance of magnetic minerals (Singer and Fine, 1989), was measured using a Bartington MS2B sensor, which reports values as mass-normalized SI (International System of Units)-values. Though not displayed herein, frequency-dependent susceptibility (χ_{fd}), a measure of the abundance of ultra-fine magnetic grains that straddle the superparamagnetic (SP) – single domain (SD) boundary ($\sim 0.01 \mu\text{m}$ for magnetite) which become more abundant during soil formation due to neoformation (Maher and Thompson 1991; Geiss and Zanner, 2006; Maher, 2016), was measured at 470 Hz (χ_{lf}) and 4.7 kHz (χ_{hf}) using a Bartington MS3 susceptibility meter equipped with a MS2B dual-frequency sensor. To estimate the error of the χ_{fd}

measurements, low- and high-frequency measurements were repeated five times for each sample. Data are reported as $\chi_{\text{fd}} = \chi_{\text{lf}} - \chi_{\text{hf}}$ and $\chi_{\text{fd}}(\%) = (\chi_{\text{lf}} - \chi_{\text{hf}}) / \chi_{\text{lf}} \times 100$.

Carbonate concentration was derived using a couleometer, an instrument that measures the amount, in this instance, of inorganic carbon transformed during electrolysis. Samples were assayed after acid treatment and again following combustion.

Particle size analysis was used to characterize texture. After drying, Rootlets were removed from samples, which were then soaked in 20 mL of 25% H₂O₂ for 48 hours at 60°C to remove organics (Mason et al., 2003; Sandström et al., 2005). Samples were then decanted and sonicated in deionized water for 3 minutes prior to analysis using a Malvern Mastersizer 2000 laser diffraction particle size analyzer. Malvern analysis reported each sample texture as a percentage of clay, silt and sand.

Soil color can be used to approximate melanization and rubification within soils and can be a proxy for gauging soil organic carbon levels (Wills et al., 2007). Both CIELAB color space and traditional Munsell color data were determined using a Konica Minolta CM-700 handheld spectrophotometer on moist soils cores and on dried samples within 8 cm³ plastic cubes extracted from RLCS1. CIELAB color parameters, reported herein, include the values L^* , a^* , and b^* , where lightness, L^* , represents the darkest black at $L^* = 0$, and the brightest white at $L^* = 100$. The color channels, a^* and b^* , indicate true neutral gray values at $a^* = 0$ and $b^* = 0$. The red/green opponent colors are represented with green at negative a^* values and red at positive a^* values, whereas the yellow/blue opponent colors are represented with blue at negative b^* values and yellow at positive b^* values. Color data were recorded on air-dried samples following white-standard calibration.

Samples were analyzed at the University of Kansas Keck Paleoenvironmental and Environmental Stable Isotope Laboratory (KPESIL) for δ¹³C, δ¹⁵N, total N, and total organic C. Samples were oven dried at 60°C, pulverized, picked for roots, and decarbonated with 10 mL of 0.5 M HCl, repeated as necessary until samples were no longer reactive. After drying, pulverizing and loading, samples were combusted at 1060°C in a Costech Elemental Analyzer and transferred to a ThermoFinnigan MAT 253 mass spectrometer for assay, along with specified standards. Stable carbon isotopes (δ¹³C) from plant material distinguish plants based on whether they use the C₃ or C₄ photosynthetic pathway (O'Leary, 1981). C₃ (cool season grasses, shrubs, most trees) typically have δ¹³C values between -32‰ and -20‰ (Ode et al., 1980), whereas C₄ plants (predominately warm season grasses) have δ¹³C values between -17‰ and -10‰ (O'Leary, 1988). Further, pairing organic C and total N values provides a C:N ratio which not only distinguishes terrestrial and aquatic environments, but also serves as a metric for relative soil activity (Stevenson and Cole, 1999).

To determine the approximate numerical chronology of accumulation within the upper non-gleyed (reduced) hydric soil of the playa floor and buried soils in cores, accelerated mass spectrometry radiocarbon (AMS ¹⁴C) dating was applied to bulk samples extracted from the instrument pit face and cores EPC3 and EPC4. Samples were dried, picked for rootlets, pulverized and submitted to either Beta Analytic, Inc. or the National Ocean Science Accelerator

Mass Spectrometry (NOSAMS) facility at Woods Hole Oceanographic Institution for final pre-treatment and assay.



Figure 21. Drill core analysis in the laboratory. The EPC4, the 7.25 m (23.8 ft)-long south bench core, has been opened (view down core) and dressed for description, photography, sampling, and color scanning in the University of Kansas Soils and Geomorphology Laboratory. (W.C. Johnson)

Action 3. Conduct additional field investigations and sample analyses as deemed necessary.

None

Goal 4. Research results and discussion

4.1 Soil and sediment Analyses

A thorough characterization of the playa stratigraphy in the near-surface and the full vadose zone was an essential prelude to this investigation into the connectivity of the playa basin and the watertable for the purpose of HPA recharge. Subsurface explorations by Bowen and Johnson (2012) at Ehmke Playa documented that the generalized stratigraphy consists of multiple loess units with intercalated paleosols, the oldest of which may date to 200,000 or more years ago. Underlying this sequence is a series of carbonate lentils starting at 5-7 m (16-23 ft) depth, most of which are likely within the basal Miocene-age Ogallala Formation (Figure 22). The first phase of coring was conducted to characterize the upper fine-sediment surrounding the playa, that is, from the edge of the playa up onto the interplaya. Cores were collected as in Figure 18, which did not include the lunette: lunette stratigraphy had previously been investigated (Bowen and Johnson, 2012; Bowen et al., 2018) and was not the target of this study. Cores were subsequently extracted from the playa and from the interplaya for characterization of the stratigraphy and for the use of geochemical proxies of downward water movement (Figure 11).

During the course of the investigation, numerical dating was carried out on samples from Ehmke core A3 (Figure 18) and on the sensor pit. Three AMS ^{14}C samples collected from core A3 on the bench produced calibrated (calendar) ages of 9540 years B.P. (129 cm: 4.2 ft), 11,820 years B.P. (before present: 1950) (149 cm: 4.9 ft) and 27,950 years B.P. (593 cm: 19.5 ft). These ages were readily correlated to EPC4, also on the bench and to the west of A3. Four ages were obtained from the sensor pit: at 25 cm (10 in) below the surface, the calibrated (calendar) age was 3315 years B.P.; at 47 cm (18 in), 4160 years B.P.; at 65 cm (26 in), 3765 years B.P.; and at 85 cm (34 in), 5170 years B.P. Observations include: (1) the age derived at 65 cm (3765 years B.P.) is out of stratigraphic order (appears too young) relative to the ages above and below, which is not surprising given the high amount of argiliturbation (mixing by shrink and swell of clays) occurring in the hydric soil environment; and (2) the accumulation rate has been very slow, i.e., only 85 cm of fill has accumulated over about 5200 years or about 0.16 mm/year. A fourth AMS ^{14}C age determined from a sample collected at 96 cm (lowermost part of the dark organic zone) from EPC3 produced a calibrated age of 7460 years B.P., thereby reducing the overall accumulation rate to 0.12 mm/year.

The upper 7 m (23 ft) of less of fine-grained sediment accessible above the first carbonate lentils around the playa area with the Giddings drill rig was cored (Figure 18). The resulting cores were evaluated for particle size and magnetic susceptibility, both indicators of stratigraphy and vertical change in the near-surface sediments. Though scores of cores were extracted, Figure 23 displays representative data from four cores extracted from the bench (A2, A3, A4, A7), one from the sink (A6), one from the delta (AD), one from the inflow channel (C), and one from the playa basin edge (PB2). Three graphs of particle size are presented: (1) d-Values (d₁₀, d₅₀, d₉₀), which are the most commonly used metrics when describing particle size distributions and represent the intercepts for 10%, 50% and 90% of the cumulative mass (e.g., d₁₀ is the diameter at which 10% of the sample's mass is comprised of particles with a diameter less than this value); (2) the traditional rendering of the individual percentages for sand, silt, and clay size particles; and (3) the derivative ratio metrics of coarse silt:clay and sand:clay, which track relative changes

within the fine fractions and between the extreme fractions, respectively. The fourth graph, magnetic susceptibility, can indicate different forcings (e.g., change in sediment provenance), but in the playa environment it is primarily an indication of degree of weathering (e.g., buried soil) and of reduction-versus-oxidation of iron minerals.

In Figure 23, the d10, d50, and d90 values vary little among the four bench site cores indicating that they have similar depositional and post-depositional environments and histories. Values for d90 are 50-60 um downward until they encounter the highly variable and mostly sandy particle size distributions above the contact with the upper carbonate lentil. Sand, silt and clay percentages illustrate the dominance of silt (70-75%), consisting of reworked loess, and clay in the 25-30% range, with sand (very fine grade) concentrations being extremely low. PSA ratios for the benches highlight the variations within the basic sand-silt-clay categorization. As anticipated, greatest variability occurs in the coarse silt-to-clay ratio, which is to a large extent the inverse of the clay percentage curve due to the relative constancy of the sand component, but it does show some nuances in the particle size distribution, in particular in the lower parts of the cores, where the impact of sand concentrations is crucial to the continued downward percolation of vadose water. Magnetic susceptibility varies significantly among the bench cores, though three of the four cores display the characteristic increase due to surface soil formational processes, which has resulted in neoformed magnetic grains created by pedological weather and by magnetotactic bacteria. Values below that are typically 30 SI units or less due primarily to the reduction of the iron minerals. Increased susceptibility (bumps) at depths varying between 200cm and 400 cm are a result of brief surface stability during which sedimentation was extremely slow or even soil formation occurred. For the west bench site (A4), the constancy of the low values throughout is due to slope wash from the windward flank of the lunette and to recent human disturbance.

Ehmke Playa sink east core (A6) also displays a d90 value of about 50 um due to the influence of silt and to a lesser extent clay. Between 100 cm (39 in) and 250 cm (98 in), a silt percent bulge is prominent at the expense of clay and appears to represent a series of inundations with large silts loads; this is reflected both in the sand:clay ratio and the decreased susceptibility. The sink area, situated between the annulus and the playa has likely been relatively dynamic due to impact by only the extreme hydroperiods; its stratigraphic variability is, however, surpassed by that of the delta and inflow channel cores.

The deltaic area (AD) displays considerable down-core variation in all particle size parameters because of the dynamic nature of inflow volume and sediment load and caliber, and to the function—alluvial fan-like or a true delta. The shift in parameters between about 250 cm (98 in) and 400 cm (158 in) may be related to the event recorded in the core from the sink (A6). Magnetic susceptibility increases at this time, probably due to the increase in silt, with its characteristic magnetite component. Particle size data from core C collected within the inflow channel show considerable variability expected in the dynamic channel environment, such as the sand spikes, though the increase in the coarse silt within the central part of the core appears as in some of the other cores.

Core PB from the south-southeastmost edge of the playa was collected to gage the level of sedimentary variability that has occurred along the fringe of the playa, which was presumed to be

somewhat dynamic due to wave action and marked water-level fluctuation. Also, this is the zone of weakest hydric soil development, thereby experiencing less of the homogenization resulting from argiluturbation. While the upper meter displays episodes of silt and clay interaction and the PSA fine-fraction ratio drops, a coarse silt bulge is again apparent in midcore. The lower two meters are highly variable with zones of increased very fine sand.

In summary, these cores indicate (1) silt as the dominant particle size (loess-sourced), (2) increases in sand above the contact with the carbonate zone (transition to the upper Ogallala Formation), (3) a coarse silt bulge in the middle of many of the cores from above the lentils (a period of increased sediment input), and (4) relative slow sedimentation in the upper one-to-two meters. Though no numerical ages were obtained from below the upper zone of slow accumulation except for core A3/EPC3 (bench), it is suggested that the mid-core zone of rapid accumulation occurred during the more mesic environment of past glacial period.

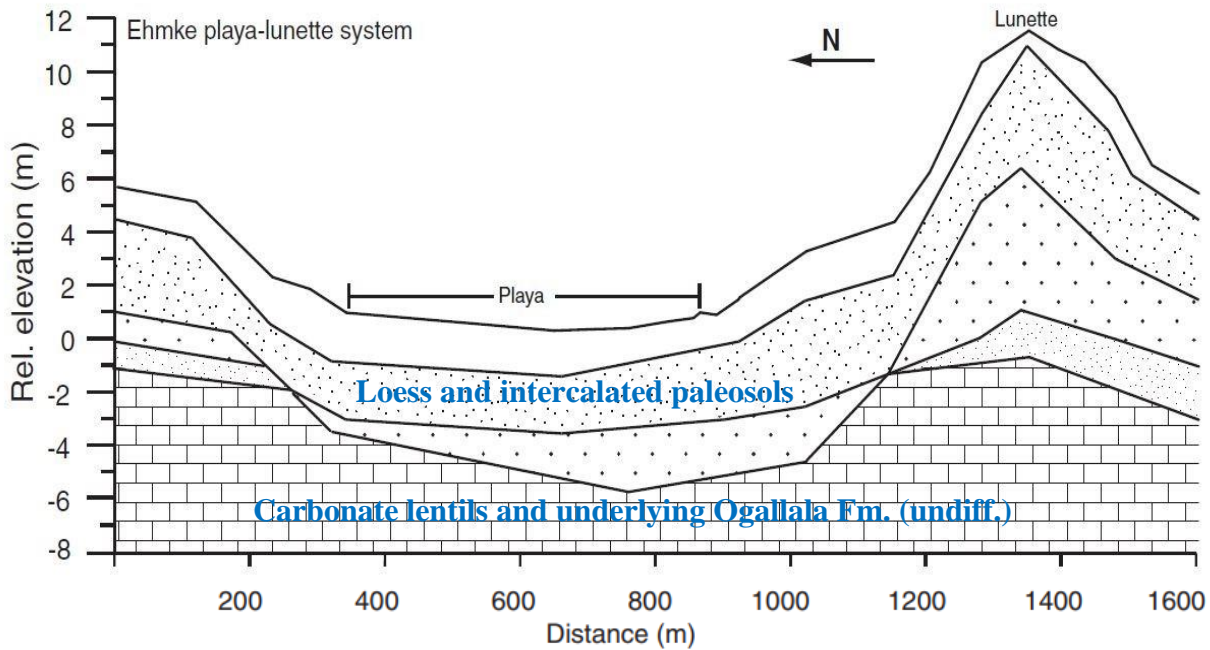
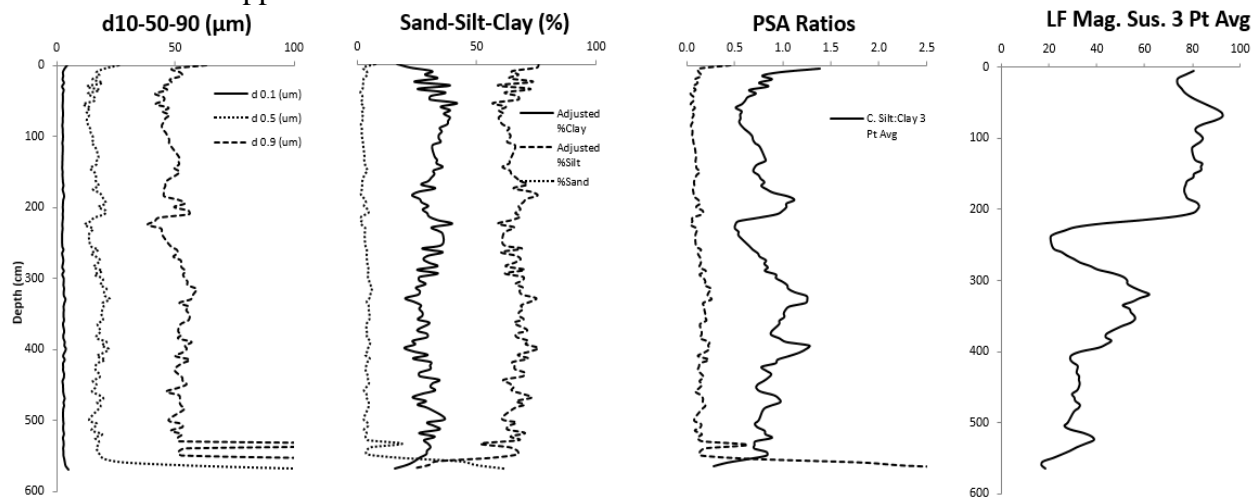
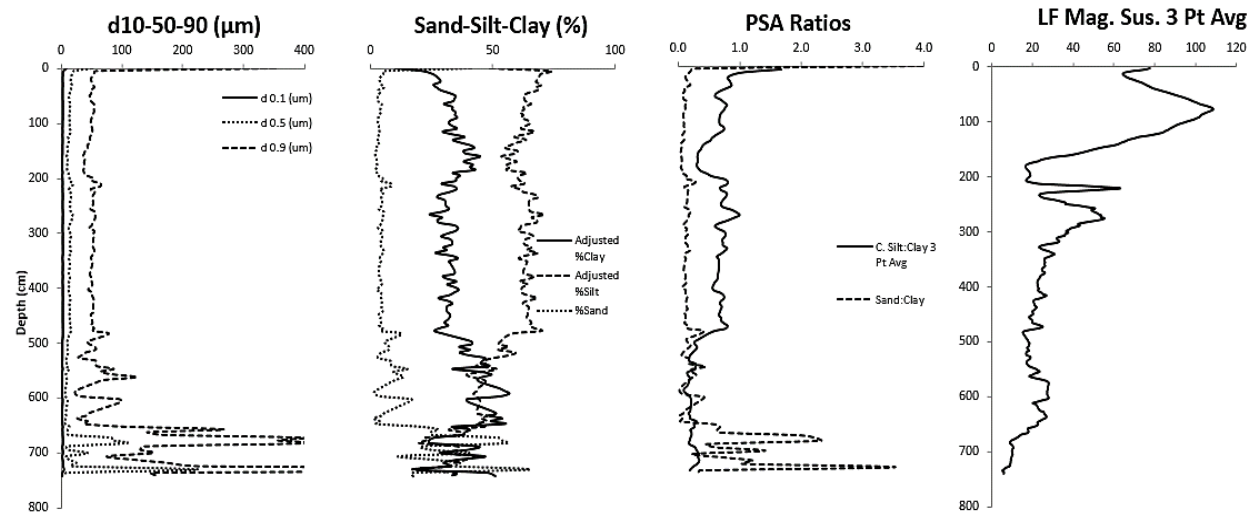


Figure 22. Generalized cross section and stratigraphy at Ehmke Playa. A sequence of loess units with intercalated paleosols overlies the zone of carbonate lentils, mostly within the underlying Ogallala Formation. The water table would be at about -13 m (-43 ft) on the y axis. (Bowen and Johnson, 2012)

Core A2 Ehmke upper bench south



Core A3 Ehmke bench south



Core A4 Ehmke bench west

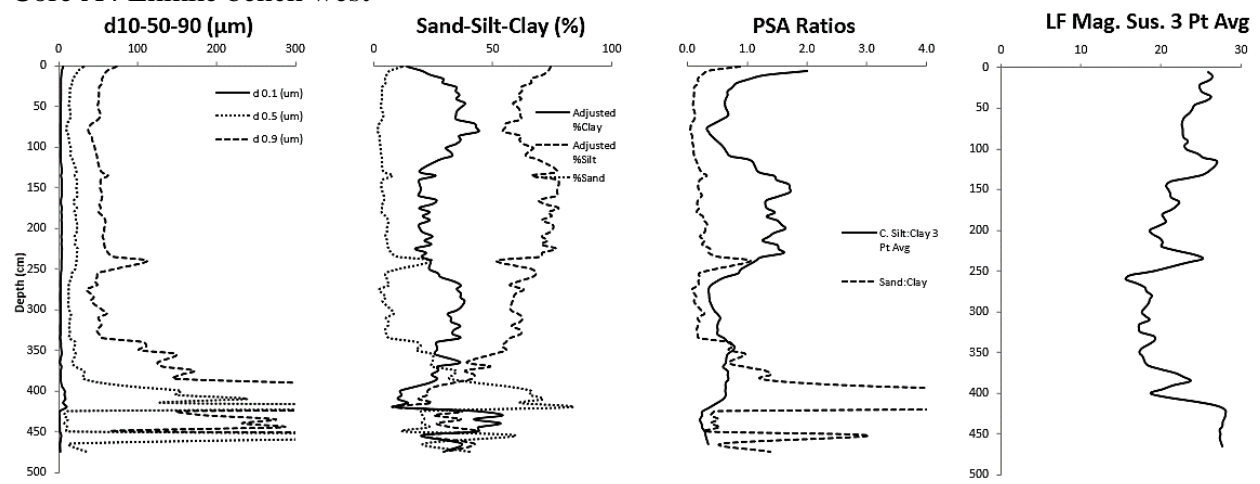
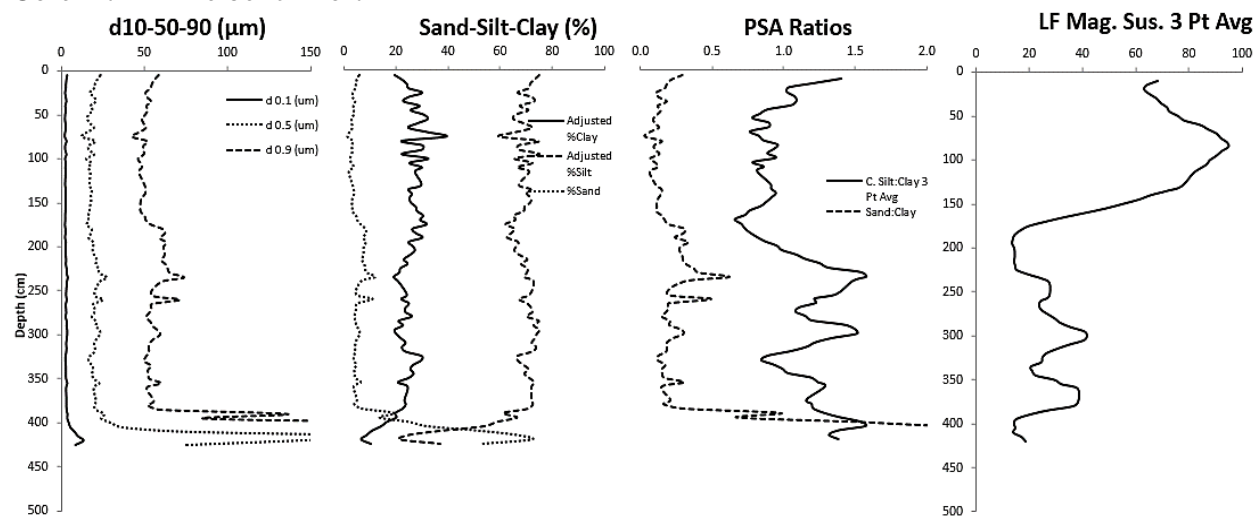
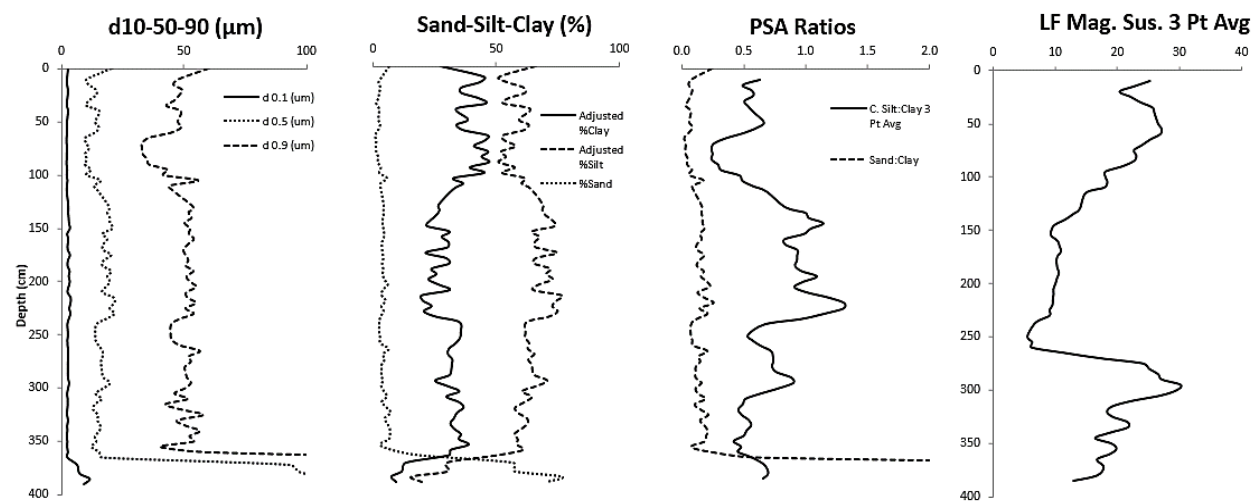


Figure 23. Representative data from cores extracted from the edge of the playa edge, sink, bench, delta, and inflow channel. Locations of cores are indicated in Figure 18. (Continued)

Core A7 Ehmke bench north



Core A6 Ehmke sink east



Core AD Ehmke delta

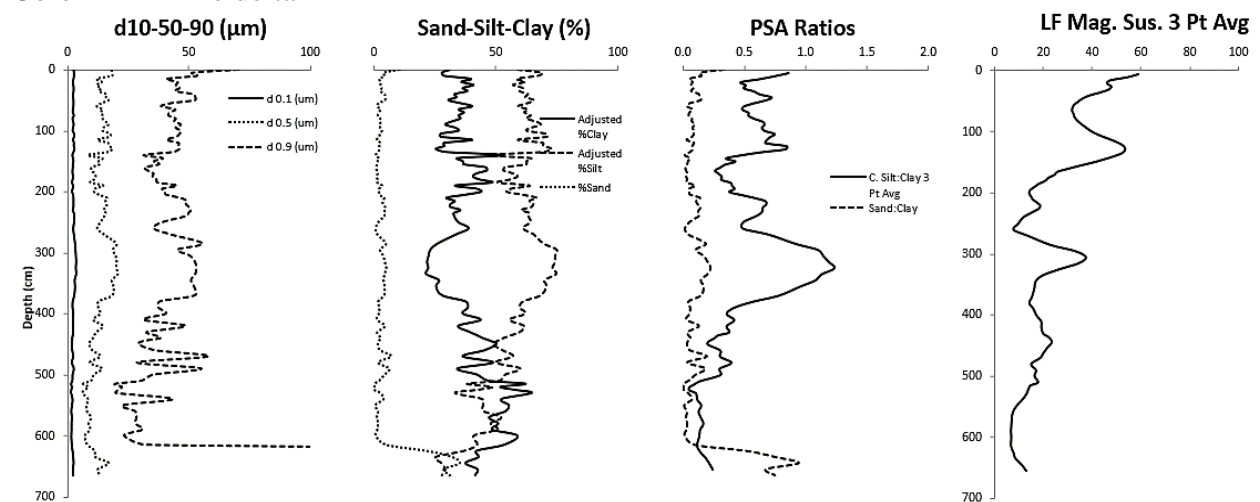
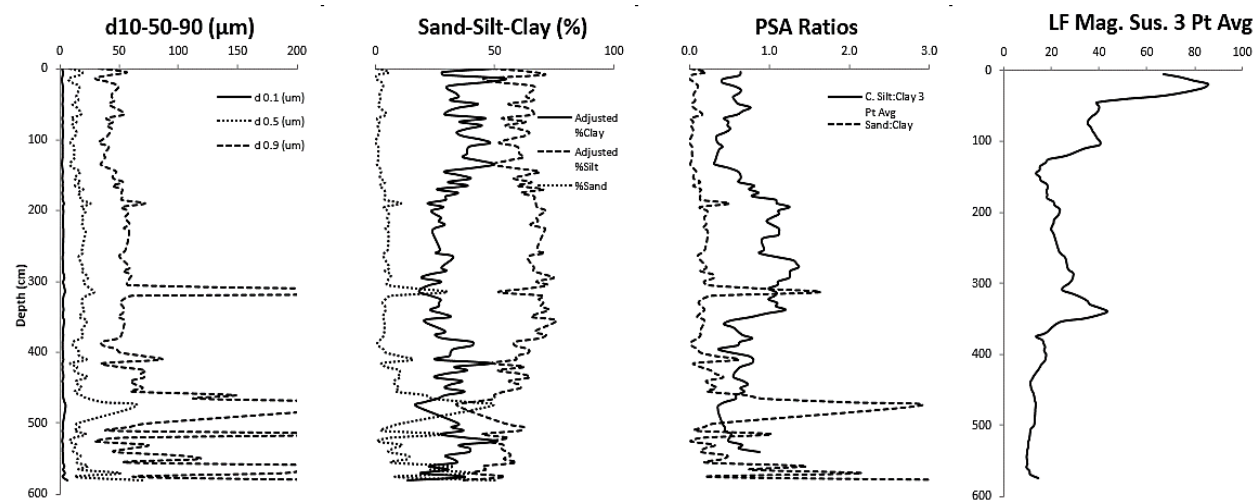


Figure 23. Representative data from cores extracted from the edge of the playa edge, sink, bench, delta, and inflow channel. Locations of cores are indicated in Figure 18. (Continued)

Core C Ehmke inflow channel



Core PB2 Ehmke playa basin edge south

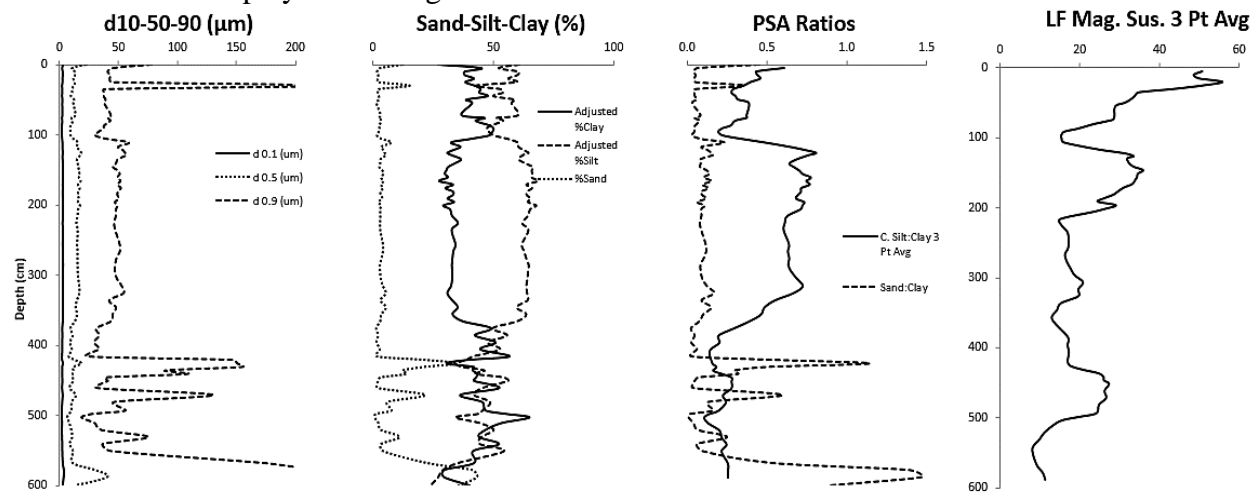


Figure 23. Representative data from cores extracted from the edge of the playa edge, sink, bench, delta, and inflow channel. Locations of cores are indicated in Figure 18.

The second phase of coring and installation of the sensor pit (Figure 11), focusing on the playa and adjacent interplaya, was conducted to collect cores for geochemical analyses and to characterize and compare the stratigraphy. Color is one of the primary features of a core or profile, and herein we used the CIELAB color, rather than the traditional Munsell systems due to its interpretability and ease in graphic representation. Color data from the sensor pit wall (Figure 24) show the obvious first-order shift from the upper hydric soil to the lower gray-brown zone: lightness increases, slightly decreases and yellow increases downward from the contact. Color is not, however, static: the spectrophotometer detected subtle changes often not seen by the eye. For example, an increase in variance of b^* values below the contact is due to the presence of redoximorphic features.

Figure 25 displays the CIELAB colors for cores EPC3, adjacent to the sensor pit; EPC5, the vadose zone core from the playa center; EPC4, bench location south of the sensor pit; and EPC7, interplaya north of the playa center. EPC3 displays the same color pattern as the adjacent sensor pit and the relative constancy of color to the upper carbonate lentil. While much lower resolution, jumps in colors from EPC5 indicate the approximate locations of lentils and lacustrine silt zones, expressed as increases in L^* and a^* and b^* particularly below 7 m (23 ft). EPC4, from the south bench, shows the same basic pattern as EPC3 to where it encountered the lentil, which was at 7 m (23 ft) because the bench is about 2 m (6.6 ft) higher than the playa. EPC7, from the interplaya and also of low resolution data, was somewhat more variable in color throughout given a higher interstitial carbonate content and multiple buried soils (peaks in a^* and b^*) than EPC5 in the playa center.

Basic sand-silt-clay percentages (Figure 26) were derived from the sensor pit, EPC5, EPC4, and EPC7. Little variation in the distribution of fines occurs, with silt dominating (>80%), clay minor at 5-10%, and very little sand showing a slight increase downward. Noting the depth scale difference from the previous graph, EPC5, playa center, shows the low-resolution pattern—more variation in clay compared to the sensor pit and a dramatic change in all three size fractions at about 6 m (20 ft), where silt and clay give way to sand within the carbonate-rich Ogallala formation. EPC4, south bench, displays the increase in sand in the transition to the lentil. EPC7, interplaya, exhibits the jumps between sandy carbonate zones and siltier buried soils and an increase in overall sand content down core.

Magnetic susceptibility (Figure 27) for these same sites provide insight to processes and events. The sensor pit displays relatively consistent susceptibility in the hydric soil zone, but shows an excursion within the upper gleyed zone, which is interpreted as increased redoximorphic activity immediately below the transition. The lower resolution EPC5 playa core indicates an increase in variability below about 7 m (23 ft) with an overall increasing trend—the values should drop due to carbonate dilution of the magnetic signal, but the smallest magnetic mineral grains ('superparamagnetic') detected with frequency dependence of susceptibility data (not shown) were translocated downward with the increase in sand texture, which implies the downward movement of water. The curve for the south bench, EPC4, portrays a gradually decreasing susceptibility punctuated by increases due to soil formation, and from about 3 m (9.8 ft) downward it is relatively low but yet shows evidence of periodic stability (soil formation), three of which have been ^{14}C -dated. Note that the upper meter or so represents about the last 10,000 years. The interplaya, EPC7, has relatively high susceptibility down to about 8 m (26 ft), though

the signal in this reach is highly variable due to episodic carbonate dilution (decrease) and soil formation (increase). The decrease in the lower 7 m (23 ft) is due primarily to carbonate dilution of the signal and a lower concentration of magnetic minerals (domination by quartz sand).

Stable C and N, along with their respective concentrations were derived for the playa, EPC3 and EPC5, and the interplaya, EPC7 (Figure 28). EPC3 $\delta^{13}\text{C}$ values obtained from the lower meter or two suggest that this was a drier period in that the values approach the C₄ grass threshold, but the middle segment of the core suggests a prolonged mesic period when the playa was dominated by the C₃ lacustrine plants, likely the more mesic and cooler last glacial period. The upper meter or so, the post glacial period, reflects the prevailing increased warmth and drier environment. The deeper but lower resolution EPC5 playa core shows a similar pattern with presumed increased climate variability at depth. Values from the interplaya core display the strong C₄ upland grass signal of the last several thousand years, whereas the interpreted last glacial drop to C₃ grasses appears. Another warmer, drier period occurs mid-core, but is preceded by a cooler more mesic period. These $\delta^{13}\text{C}$ data indicate the obvious, that climate variations through time have impacted playas and consequently the role of playas as point sources of recharge to the HPA has varied.

Organic C remains in the stratigraphic record of the playa and interplaya (Figure 29). Despite its dark, nearly black appearance, the hydric soil of the playa does not contain a large concentration of organic C, with much of the dark color coming from the clay content, iron oxides and perhaps manganese oxides. Organic C content decreases downward, being partially preserved only in buried soils, which can be identified in both playa cores and especially in the interplaya core. Very little has been preserved below 6 or 7 m (19.7-23 ft).

With the N and organic C data derived from the isotope analyses, the C:N ratio was derived for each of the two playa cores for the interplaya core as a metric for gaging which periods are more aquatic versus more terrestrial (Figure 30). Terrestrially-derived organic matter typically has C:N ratios 14-20 and higher, whereas aquatically-derived biomass typically yields a C:N ration of 4-10 (Meyers and Teranes, 2001). C:N ratios for both playa cores were highest in the hydric soil zone lower in the 4 m below and then increase a bit farther down in EPC5, indicating that mesic conditions of the presumed last glacial period left a clear aquatic biomass signal. Data from the interplay core are, however, puzzling given the low ratios and cannot be explained at this time.

Given that carbonate concentration, as a matrix in the sediments, can impede downward flux of water, concentrations were measured in the EPC3 core (playa center). Concentrations in the above-lentil fine sediments (hydric soil zone) are minimal, with concentrations of <0.01% in the 105 cm (41 in), at which point it jumps to 1.5% and shows an overall increasing trend up to about 4.5% at 5.23 m (17.16 ft), the depth at which the first carbonate lentil was encountered. The abrupt increase at 105 cm indicates the rapid transition from the upper heavily melanized hydric soil zone to the underlying carbonate-rich gleyed zone below. This lack of significant carbonate in the hydric soils zone suggest that downward water movement through macro- and micropores is not impeded by interstitial carbonate.

Historical sedimentation and degradation of the playa recharge function

Anthropically accelerated sediment accumulations within playas, a major cause of the degradation of playa function, is the greatest threat to playas (Smith, 2003) and will continue to

result in the total disappearance of many playas from the landscape. Bowen and Johnson (2017), in a study of 64 playas distributed throughout the High Plains of Kansas, found that without grass buffers, playas within cultivated watersheds accumulated an average of about 9 cm (3.5 in) of recent sedimentation and lost 30% of their storage capacity. In contrast, those playas with significant grass buffers reduced sedimentation on average to 2.3 cm (<1 in) or less.

During past runoff events Ehmke Playa has received substantial inflow, which gradually produced a delta-like feature, which again has actually functioned more like a fine-grained alluvial fan given that it is inundated only during the largest runoff events (Figure 10). Ehmke Playa has apparently been unaffected by historical sedimentation due to very good land stewardship—the playa and sink, being completely surrounded by pasture, benefit from the grasses capturing sediment being transported from the adjacent wheat fields. Further, the inflow channel, while flowing through cultivated fields southwest of the playa, enters the playa only after traversing a 625 m-long grass waterway. Though no historical sediment accumulation was detected within the sink or playa, a small area of historical sedimentation (very fine sand and coarse silt) less than 5 cm in thickness was found on the delta feature, indicating that the deltaic feature formed during prehistory. Bowen and Johnson (Johnson et al., 2016) have used ^{210}Pb (half-life ≈ 22.2 years) to date historical playa sediments in Lane and other western Kansas counties. Even though Ehmke Playa was not dated, the chronology of sedimentation at the other playa sites started about 1920 and accelerated around 1940, perhaps at least a partial response to the demand for wheat during the two world wars. The regional sedimentation chronology combined with established melanization of the historical sediments suggests that the minor extent of historical sedimentation in Ehmke Playa may date to many decades ago.

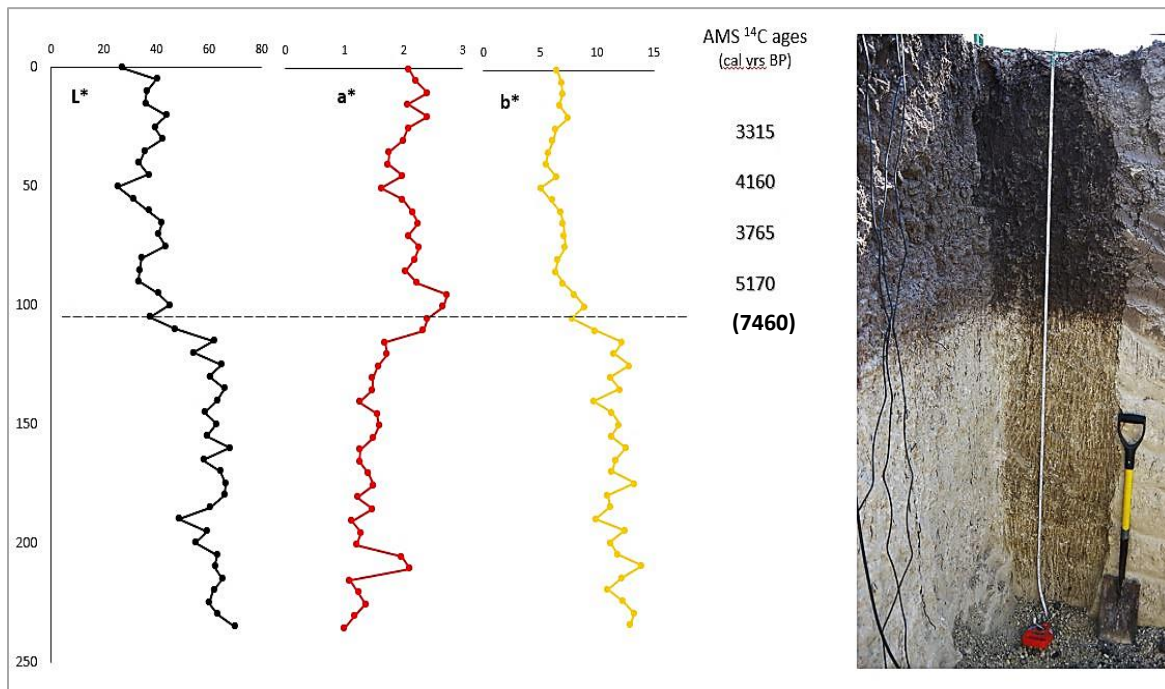


Figure 24. CIELAB colors, AMS ^{14}C ages, and sensor pit image. The dashed line represents the approximate color boundary, and the ^{14}C age of 7460 years B.P. in parentheses was from a sample collected at the lowermost boundary of the upper melanized zone from adjacent core EPC3.

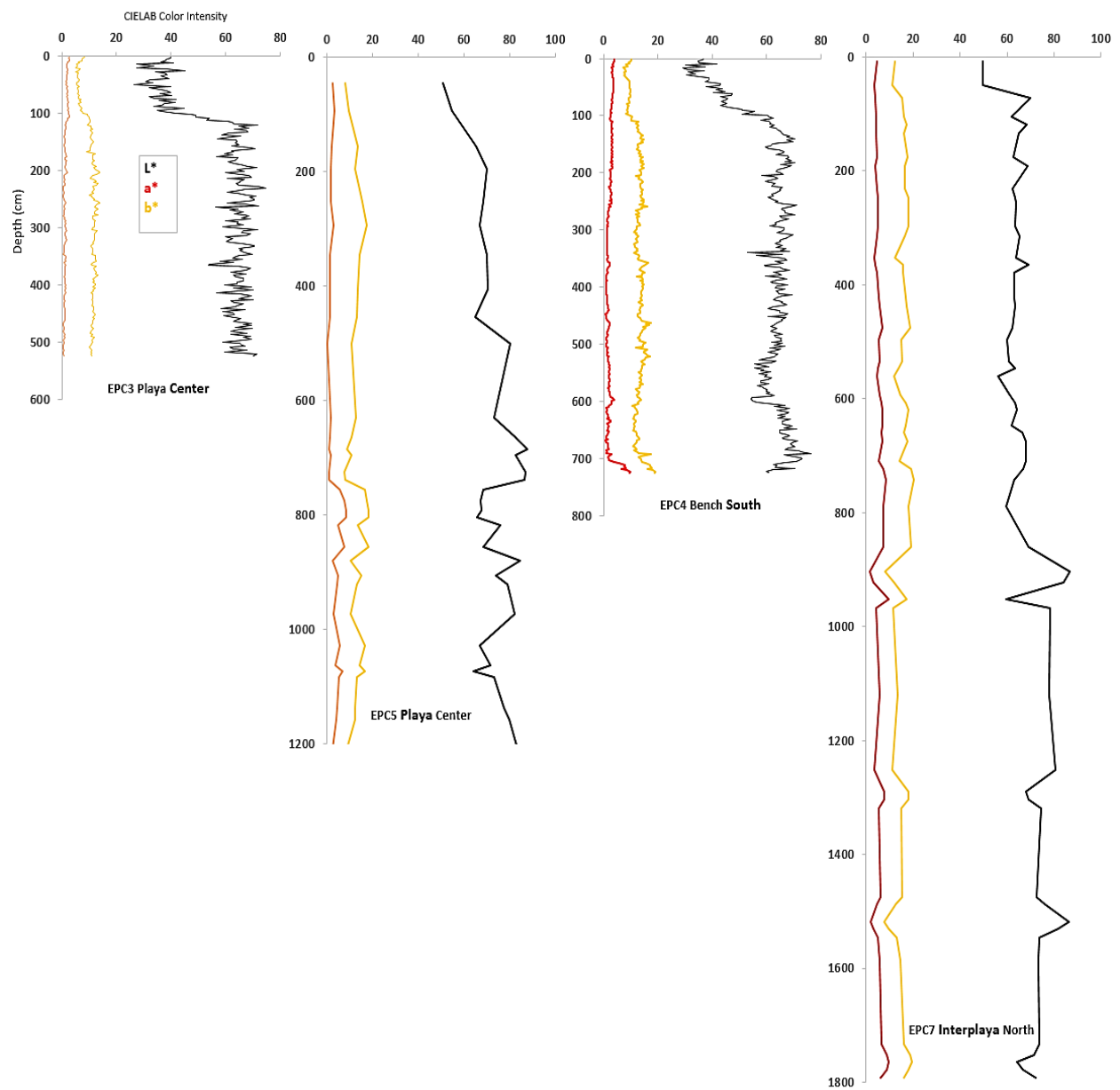


Figure 25. CIELAB colors for cores EPC3 (playa center), EPC5 playa center), EPC4 (bench south), and EPC7 (interplaya north). Cores EPC3 and 4 were extracted with the Giddings rig, and EPC5 and 7 by the Kansas Geological Survey hollow-stem rig.

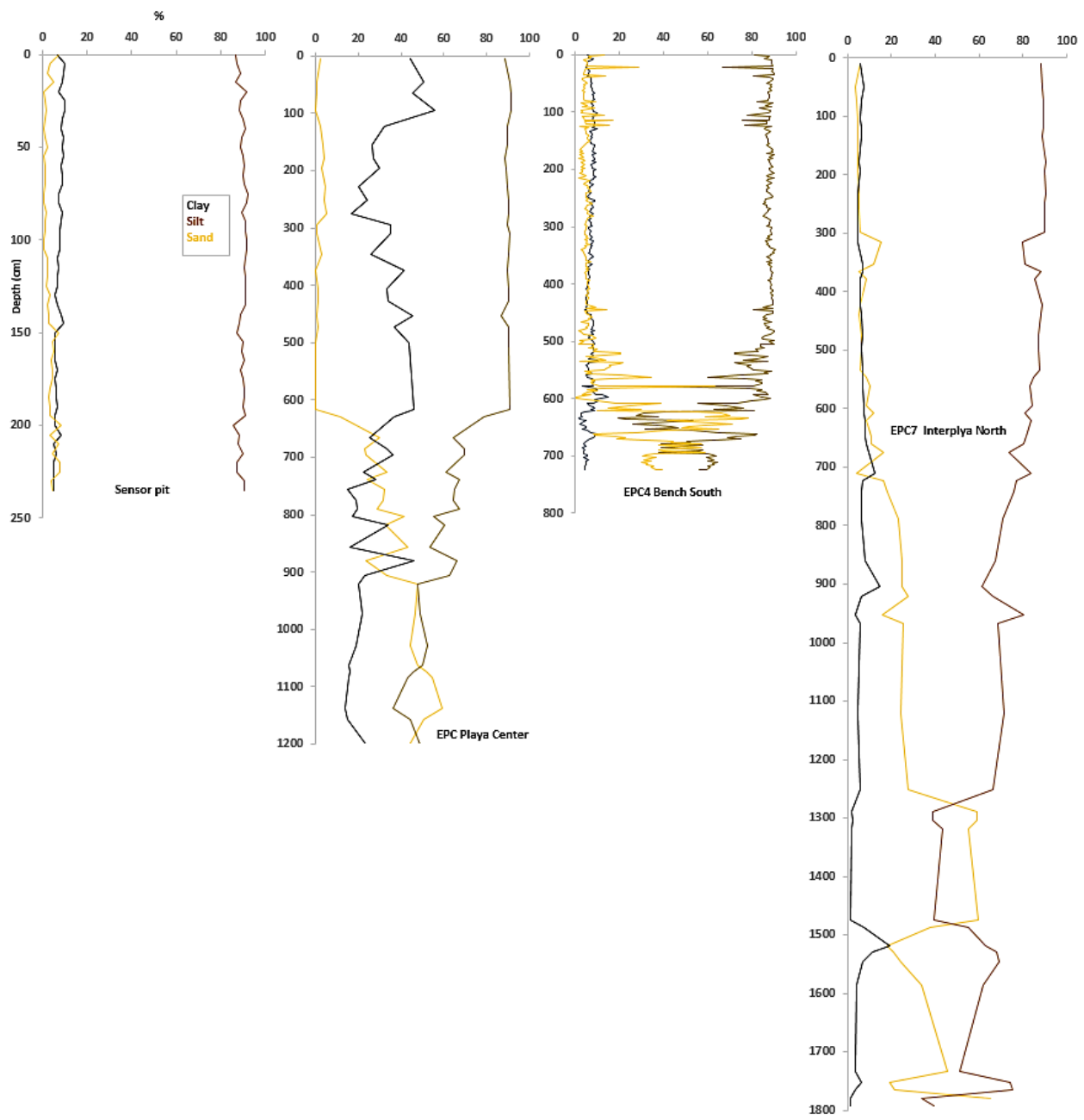


Figure 26. Particle size distribution for the sensor pit and cores EPC4 (bench south), EPC5 (playa center), and EPC7 (interplaya north). Note the change in scale for the sensor pit.

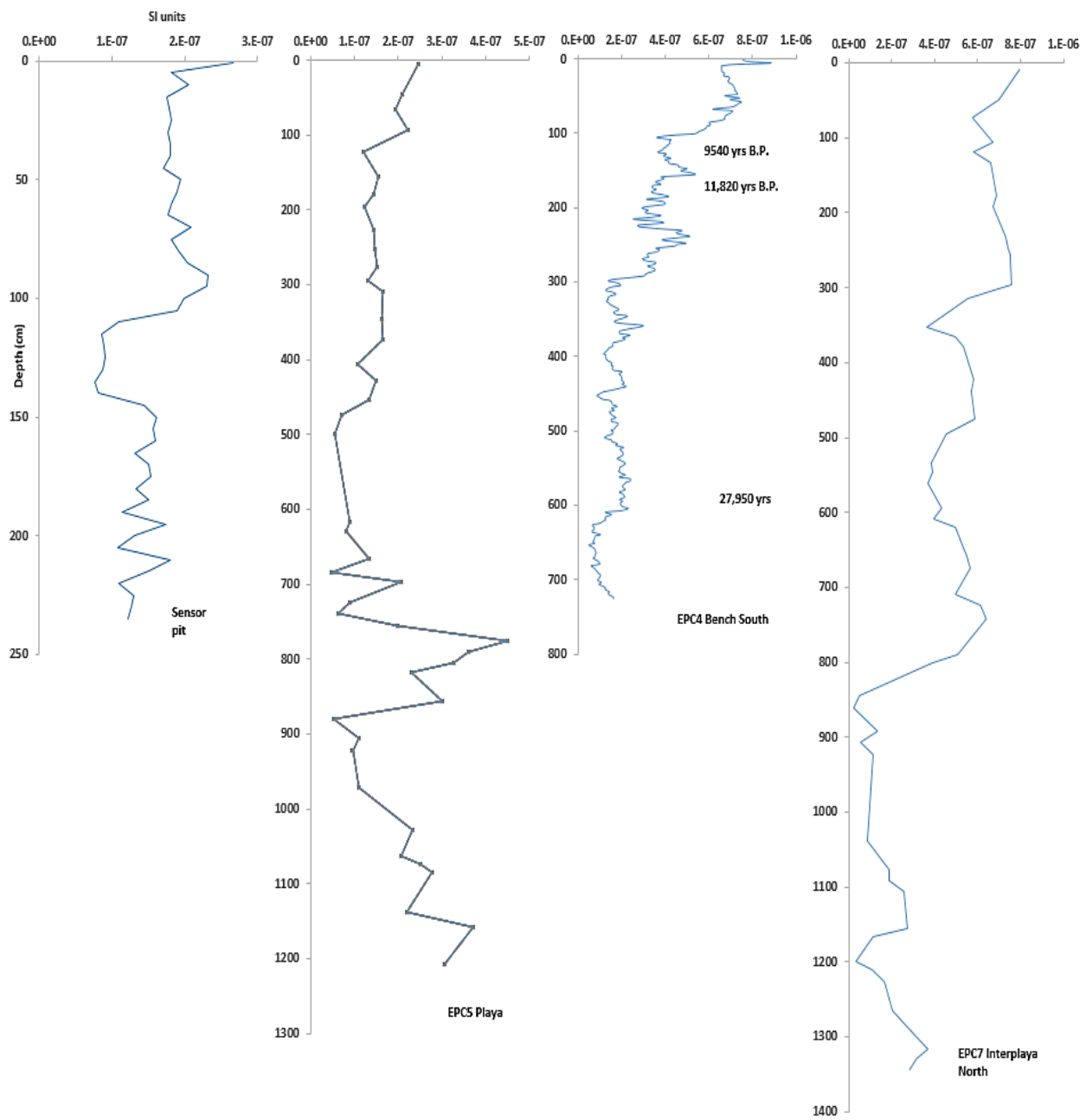


Figure 27. Magnetic susceptibility for the sensor pit and cores EPC4 (bench south), EPC5 (playa center), and EPC7 (interplaya north). Note the difference in depth scale for the sensor pit.

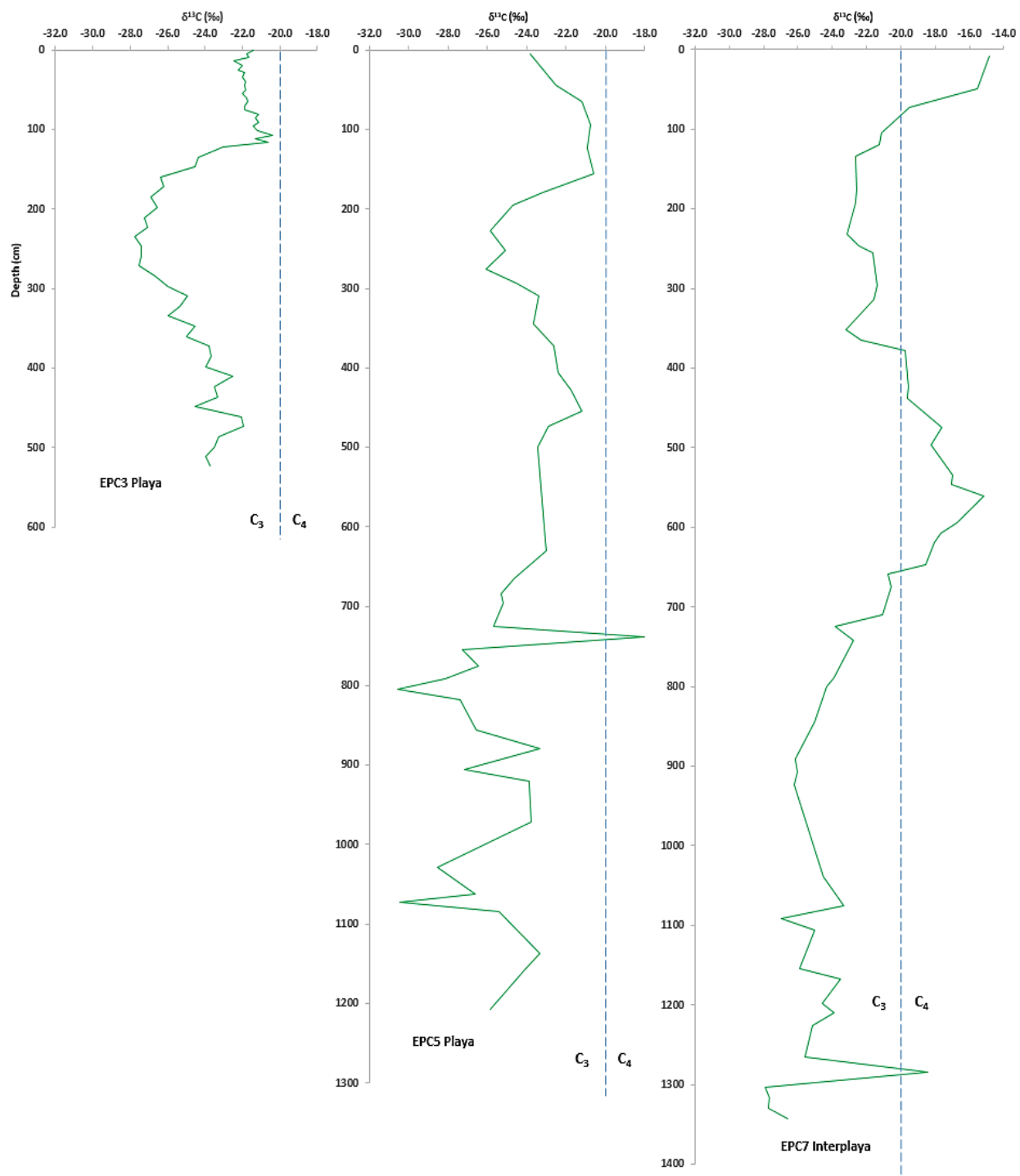


Figure 28. Stable C isotope data ($\delta^{13}\text{C}$) from cores EPC3 (playa center), EPC5 (playa center), and EPC7 (interplaya north). The vertical dashed line indicates the approximate value (-20‰) where C_3 and C_4 plants are mixed more or less equally.

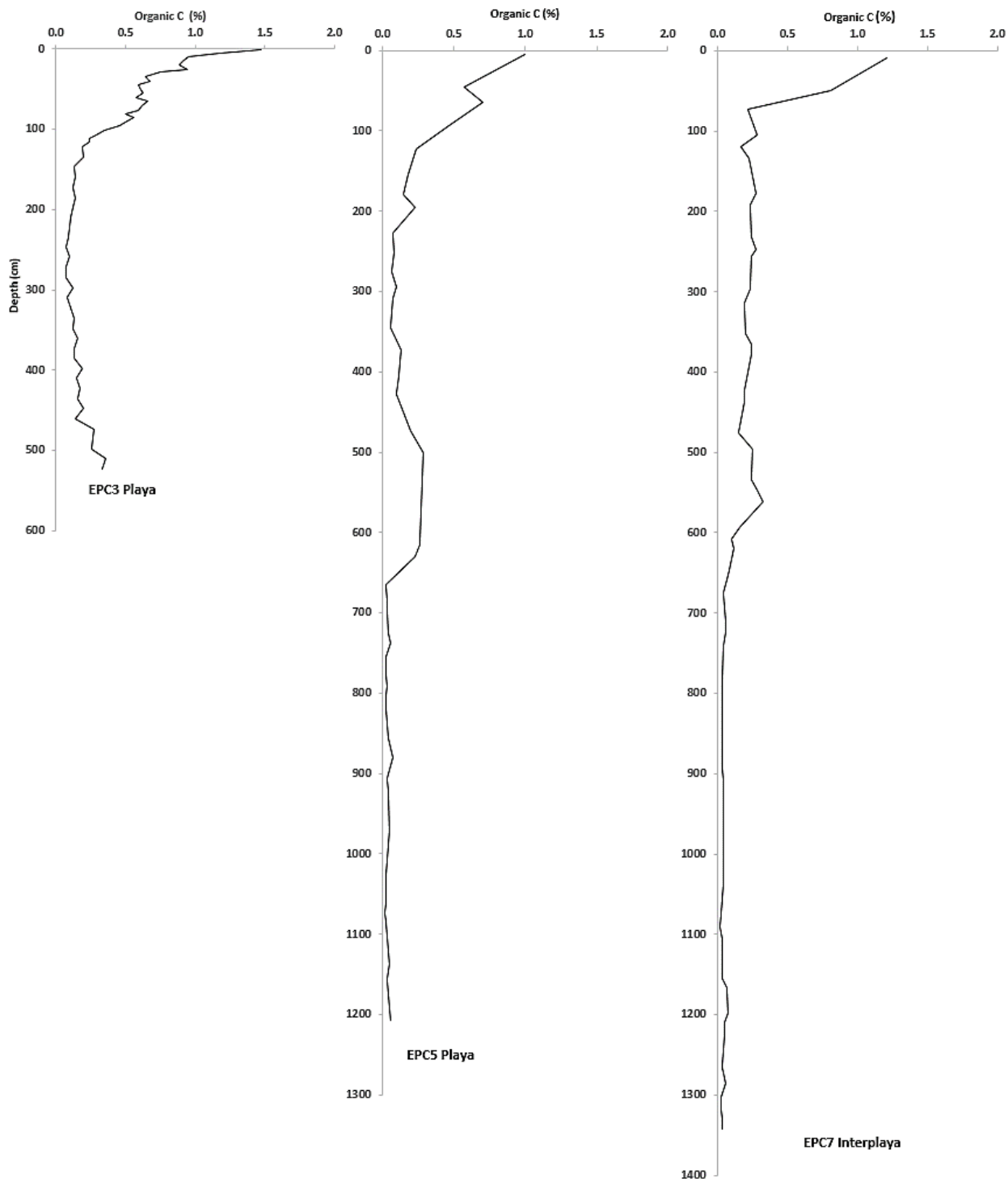


Figure 29. Organic C (%) data from cores EPC3 (playa center), EPC5 (playa center), and EPC7 (interplaya north).

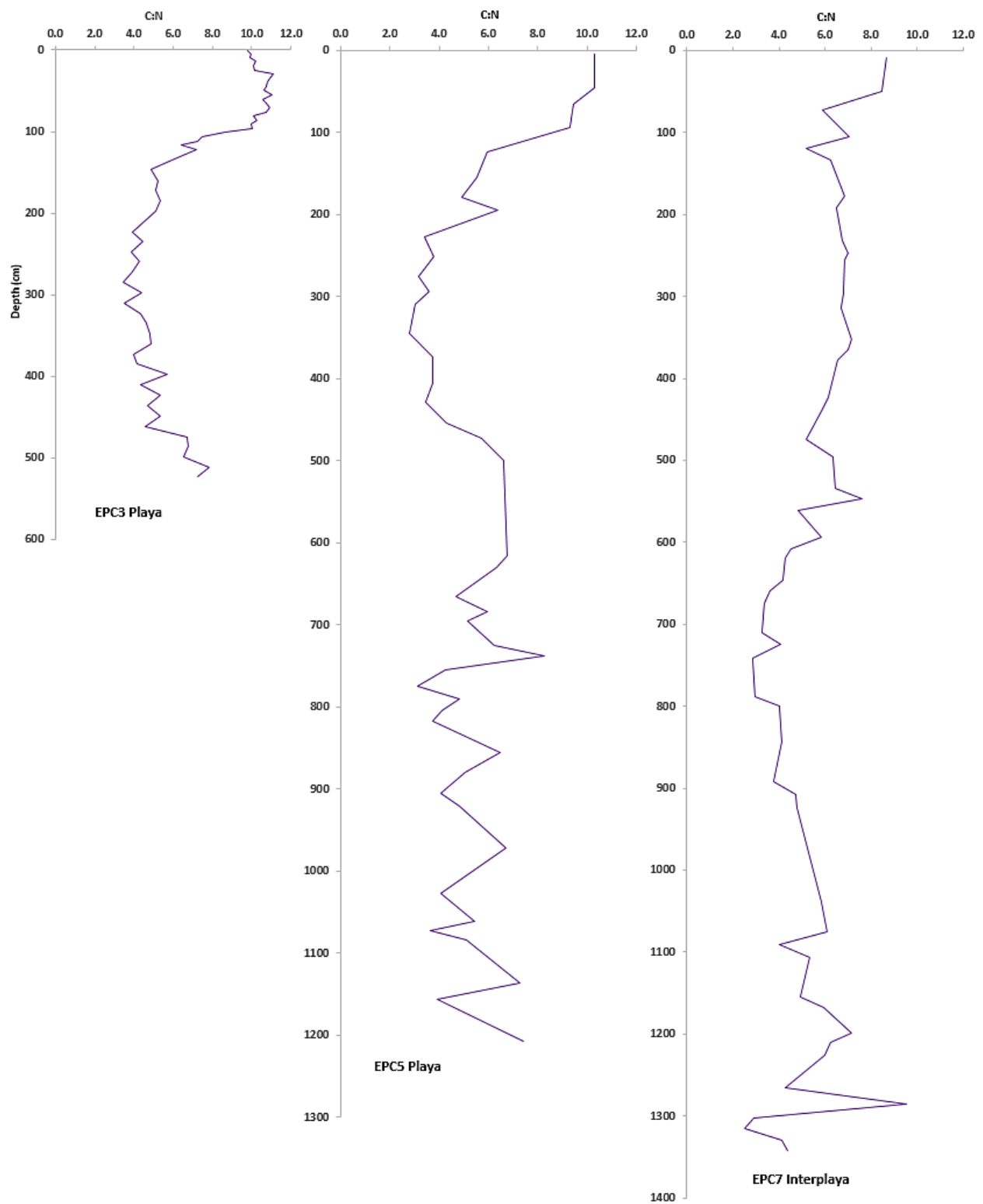


Figure 30. C:N data from cores EPC3 (playa center), EPC5 (playa center), and EPC7 (interplaya north).

4.2 Inundation and Subsurface Pressure Response

Matric Potential and Hydrus 1D Model

Matric Potential (MP) was measured at four soil depths from December 2016 to June 2017. During the winter months, MP was very negative (<-6,000 kPa) throughout all installed depths (12, 47, 96, and 152 cm) (Figure 31). Beginning on February 19, MP values at sensor 1 (12 cm) began to increase, remaining quite negative until March 29. During this time, the MP increased through a series of pulses nineteen times. Individual pulses lasted for 10 hrs to 6.8 days, with MP increasing from -7,999 kPa to a range between -6,413 kPa and -1,524. On March 29 at 11:30 AM, the MP increased above field capacity (FC), remaining at this higher potential throughout the remainder of the observation period (June 12). This final increase in MP is attributed to rain, which totaled 56.9 mm between March 23 at 8:00 PM and March 29 at 11:30 AM. The most significant rain events occurred on March 23 (12.5 mm), March 28 (35.8 mm) and March 29 (7.9 mm). These were the first significant precipitation events of the study, with only a total of 19.05 mm of rain falling between December 26 at 11:20 AM and March 23 at 8:00 PM.

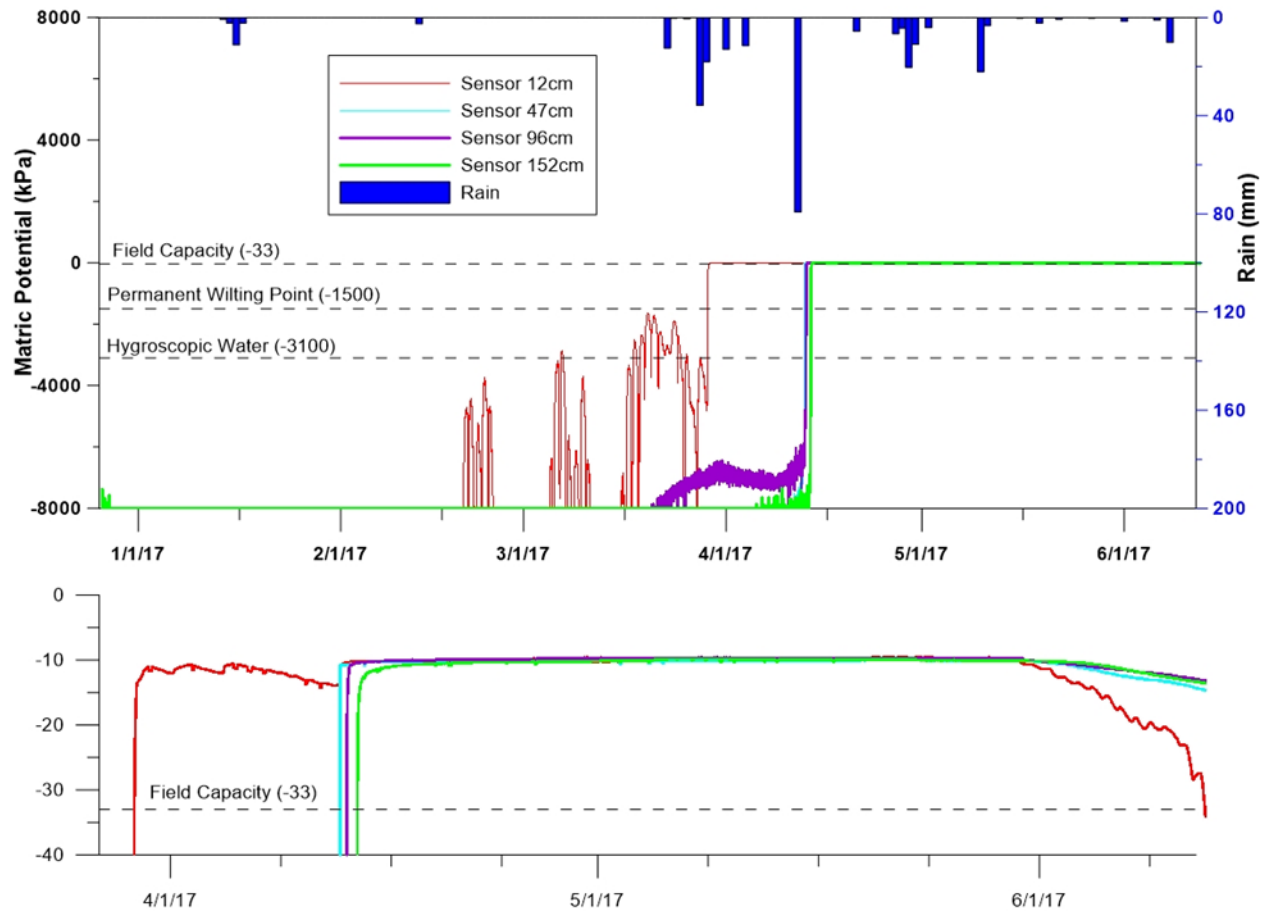


Figure 31. Upper graph: matric potential (kPa) from 12/26/16 to 6/12/17 and daily rainfall (mm). Lower graph: zoom of 3/30/17 to 6/12/17 when field capacity is exceeded and gravity drainage is underway, which corresponds to a playa inundation from April 13 to May 16.

The second sensor (47 cm) recorded very negative MP (-7,999 kPa) until April 11 at 11:20 AM, when the MP began to pulse upwards for short time periods (10 to 30 mins), increasing to between -7,500 and -7,966 kPa, and then decreasing back to -7,999 kPa (Figure 31). Two pulses lasting 1 to 7.5 hrs were observed on April 12 between 3:10 AM and 1:00 PM, increasing MP to between -7,310 and -6,914 kPa before decreasing back to -7,999 kPa. Starting April 12 at 3:10 PM, sensor 2 recorded a final pulse of water, until MP exceeded FC at 10:30 PM, likely a result of the heavy rain event that day (79.3 mm). After reaching FC, the 47 cm sensor remained above -33 kPa through the end of the sampling period (June 12). Prior smaller rain events on April 1 (13 mm) and April 4 (11.4 mm) appear to have had no effect on MP at sensor 2.

Sensor 3 (96 cm) recorded small (10 min to 1.8 hr) pulses of water starting on March 20 at 2:50 PM, with MP increasing from -7,999 kPa to a maximum of -7,606 kPa. On March 22 at 11:50 AM, the pulses become longer (20 to 26 hrs) and reach a maximum of -7,024 kPa. Beginning March 25 at 6:00 PM, MP increases above -7,999 kPa for 15 days (through April 10 at 11:50 AM), reaching a maximum of -6,460 kPa (Figure 31). Finally on April 10 at 1:00 PM, a pulse of water begins at sensor 3, resulting in MP exceeding FC on April 13 at 9:20 AM. MP then remained above FC through June 12.

Beginning on April 5 at 3:20 PM, sensor 4 at 152 cm begins to record small pulses (10 to 80 min) of water, with MP increasing from -7,999 kPa to a maximum value of -7,273 kPa (Figure 31). On April 13 at 6:00 PM, the final pulse begins, with MP exceeding FC on April 14 at 3:20 AM. The MP in this zone also remains above FC until the end of the monitoring period (June 12). Thus, it appears the 79.3 mm of rain on April 12, which influenced the 47 cm and 96 cm sensors, also pushed the wetting front beyond the 152 cm sensor.

Between March 20 and April 12, the 96 cm sensor recorded a higher MP than the 47 cm sensor. During this time, matric potentials indicate water is moving downward from 12 to 47 cm, upward from 96 to 47 cm, and downward from 96 to 152 cm (Figure 31). The probable reason for higher MP at 96 cm is desiccation cracks that contribute preferential flow to this depth (e.g., Nimmo, 2010). For the 24 days that this condition persists, the sensor at 96 cm is a zero flux plane (ZFP), where upward fluid capillarity in the vadose zone is separated by downward fluid flux. The soil color changes near this depth, from a dark-colored horizon to a light-colored horizon. This change around 1 m depth (Figures 13 and 24) likely implies that the majority of macropore activity causing bioturbation from constant shrinking and swelling of smectite clays occurs in this upper portion of the soil. A typical pedon in the Ness clay is characterized by an A horizon extending from the surface to 10 cm, a B horizon from 10 to 94 cm, and a C horizon below 94 cm (USDA Natural Resources Conservation Service, 2018). Additional evidence for preferential flow to around 96 cm includes high gravimetric water contents in cores (0.14 to 0.21) and low chloride concentrations (15.7 to 34.5 mg L⁻¹). Water that is below the ZFP and outside of the influence of evapotranspiration, will likely become recharge water. After April 12, the MP at 47 cm increases above the MP at 96 cm, the zero flux plane no longer exists at the 96 cm depth, and fluid flux is downward to at least 152 cm (and likely deeper).

In summary, on April 12, a 79.3 mm precipitation event resulted in inundation of the playa the following day. Prior to this, the 12 cm sensor had already exceeded FC (March 29); but

MP was not measured above FC in deeper intervals until April 12 (47 cm), April 13 (96 cm), and April 14 (152 cm) (Figure 31). The playa remained inundated through May 16, but all soil depths remained above FC through the end of the monitoring period (June 12). This suggests that gravity drainage is controlled by playa inundation, although downward water flux was occurring to a smaller degree in the 24 days prior to playa inundation, as evidence by the ZFP through capillarity.

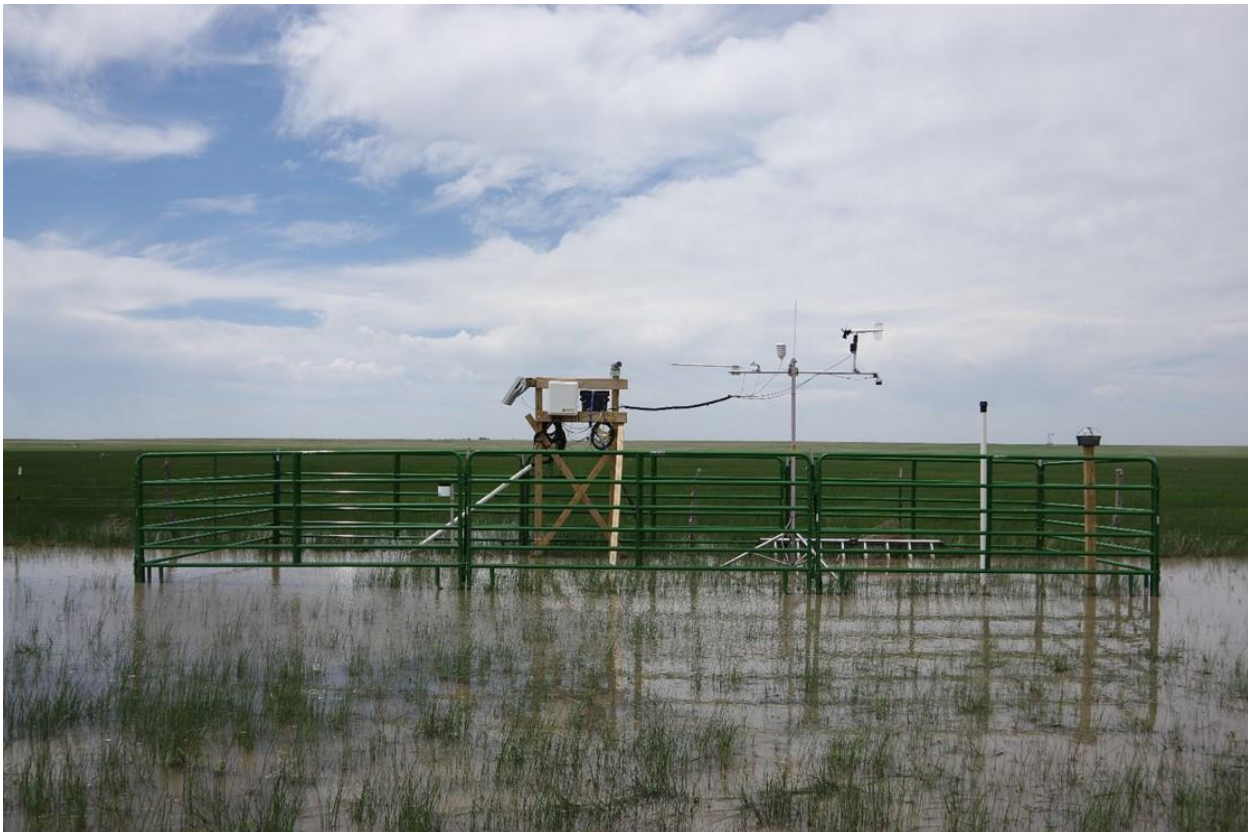


Figure 32. About 1 ft (30 cm) of water at the instrument station, in the center of the playa. (W.C. Johnson)

A fluid flux can be calculated based on the gravity drainage wetting front, which represents fluxes for time periods during playa inundation. The gravity drainage wetting front took 14.5 days to advance from 12 to 47 cm, 10.8 hrs to move from 47 to 96 cm, and 18 hours to travel from 96 to 152 cm. From this, the calculated inundation fluid flux rate ranges from 8,800 to 400,000 mm yr⁻¹ (Table 2). This equates to a travel time of 10 days to 1.3 yrs through the 11.5 m vadose zone. It is possible that these fast fluid fluxes equate to movement through the soil during the beginning of inundation events and rates may decrease as the soil wets and inundation persists.

Table 2. Fluid fluxes calculated from the date and time that each sensor reached field capacity (-33 kPa).

Sensor Depth (cm)	Date Field Capacity was Reached at Sensor	Time Elapsed Between Reaching Field Capacity (days)	Fluid Flux (mm yr ⁻¹)
12	3/29/17 11:30 AM	NA	NA
47	4/12/17 10:30 PM	14.46	8,800
96	4/13/17 9:20 AM	0.45	400,000
152	4/14/17 3:20 AM	0.75	270,000

The Hydrus-1D Software Package was utilized to constrain fluid flux rates in the vadose zone calculated both via CMB method and MP measurements (Šimůnek et al., 2009). The model was run for 169 days based on the precipitation data from December 2016 through June 2017. The upper boundary condition is the measured precipitation at the site and the lower boundary condition is a constant pressure head (11.5 m) to represent the water table. Texture from EPC 4 was input into the model, and an initial condition for MP was input as -8,000 kPa. Four nodes (0.4, 1.6, 5.1, and 11.5 m) were placed through the depth of the model for estimation of fluxes through time.

Results from the model indicate downward water movement in the upper soil during spring rain, but do not suggest recharge reaching the water table during the 169 days (December 26 to June 12, 2017) of the model run. The 39 cm node exceeds FC on day 94 (March 29), which is the same day that the shallow MP sensor (12 cm) reported above FC. The shallow model node (39 cm) fluid flux reaches a maximum (9,600 mm yr⁻¹) around day 110 (April 14), shortly after the large rain event on April 12 that resulted in inundation (Table 3). The 160 cm node exceeded FC on day 141 (May 15) and reaches a maximum of 470 mm yr⁻¹ on day 152 (May 26). Deeper nodes at 510 cm and the water table (1,150 cm) remain at very low matric potentials (-8,000 kPa) and low fluxes (2.9×10^{-6} mm yr⁻¹) through the entirety of the model run. By day 169 (June 12), fluid fluxes at shallow nodes (39 and 160 cm) had decreased to between 340 and 370 mm yr⁻¹. Although the modeled shallow node (39 cm) wetting aligns well with the MP measurements, the deeper nodes have delayed (160 cm) or no fluid travel (510 and 1150 cm). This discrepancy could be due to the lack of macropores in the model calculation, and/or the short time timeframe of the model run (169 days). Although the model did not anticipate recharge in the 169 days, the anion profiles suggest flushing to 5 and/or 9 m after playa ponding. Fluid fluxes estimated by the model suggest rapid travel times (<50 yr to 11.5 m) through the playa in the upper profile after the large rain event on April 12, and slow travel times (>10,000 yrs to 11.5 m) at deeper nodes. The maximum fluid flux in the model is within the range estimated from MP measurements during inundation (8,800 to 400,000 mm yr⁻¹). The model does support the theory that the majority of percolation beneath the playa occurs during large rain events and during inundation.

Table 3. Maximum Fluid Flux calculated by the Hydrus 1D model at each of the four nodes.

Node (cm)	Max Flux (mm yr ⁻¹)
Surface	28,900
39	9,600
160	470
510	2.9E-06
1150	2.9E-06

Groundwater Response

Water level measurements were downloaded on a biannual basis in June and July of 2016 and June and August of 2017 and range from 11.47 to 11.55 m (37.6 to 37.9 ft) in the playa and 15.97 to 16.50 m (52.4 to 54.1 ft) in the interplaya (all depths are reported as below ground surface, unless otherwise stated). Groundwater elevations were calculated at the site from the August 2017 sampling event in well 1 (856.4 m amsl, 2,809.6 ft amsl), well 2 (855.6 m amsl, 2,807.0 ft amsl) and well 3 (857.7 m amsl, 2,814.0 ft amsl) (Figure 33). Using the HydrogeoEstimatorXL tool (Devlin and Schillig, 2017), groundwater at the Ehmke Playa site is flowing under a hydraulic gradient of 0.0016 towards north 66° east.

Over the course of the study, a total variation in hydraulic head of ~10 cm (~4 inches) was observed in the wells. Daily fluctuations were greater beneath the playa than the downgradient interplaya well.



Figure 33. Isolines of the water table (top of the saturated zone) were interpolated using water level data from the three groundwater monitoring wells; values indicate the elevation of the water table above mean sea level in meters. Locally groundwater is flowing west to east (high to low hydraulic head), which is consistent with regional groundwater flow.

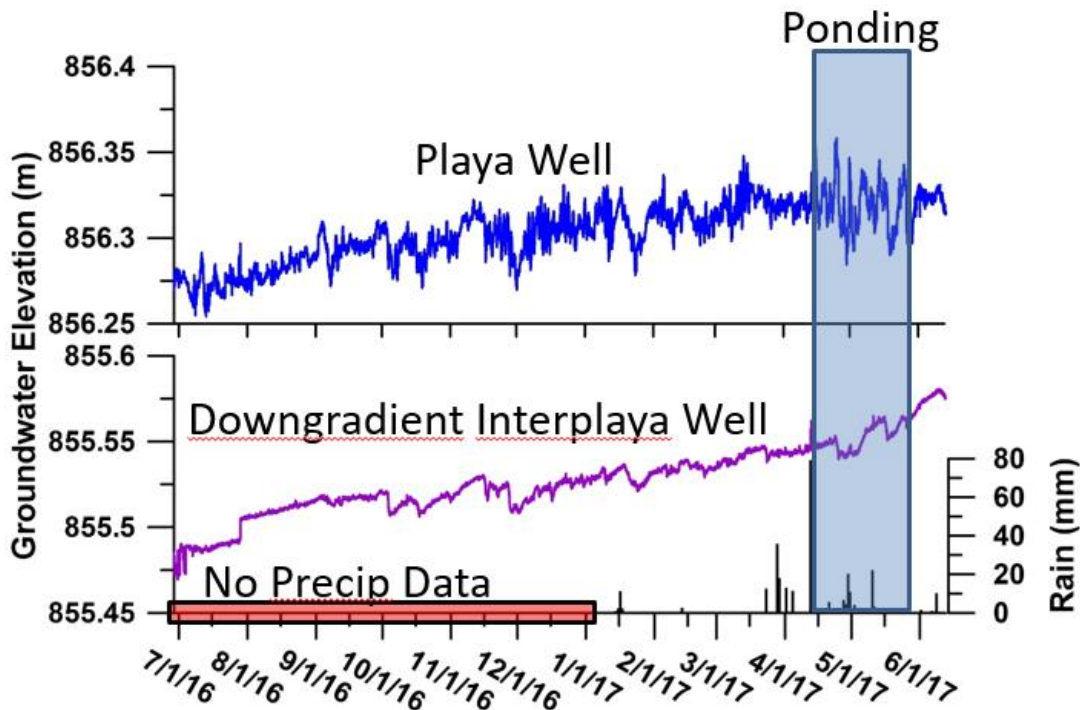


Figure 34. Hydrographs for Well 1 (Playa Well) and Well 2 (Downgradient Well) with precipitation data.

4.3 Core geochemistry

Pore Geochemistry

The gravimetric water content in the playa (EPC 1, 2 and 5) ranges from 0.05 to 0.24 g g⁻¹. In the interplaya vadose zone (EPC 7) the gravimetric water content was between 0.11 and 0.16 g g⁻¹ (Figure 35). Volumetric water contents were similar in both the playa (0.10 to 0.33) and the interplaya (0.15 to 0.34) (Tables 4 and 5).

Table 4. Playa anion concentrations in pore water (mg L⁻¹) and field water contents for EPC 1, 2, and 5.

Core Sample	Average Depth (m)	Chloride (mg L ⁻¹)	Bromide (mg L ⁻¹)	Nitrate-N (mg L ⁻¹)	Sulfate (mg L ⁻¹)	Fluoride (mg L ⁻¹)	θ_G	θ_V
EPC 1-1	0.025	81	5.4	<0.2	450	6.9	0.13	0.14
EPC 1-1	0.775	22	4.5	<0.2	170	14	0.14	0.17
EPC 1-2	1.695	42	4.2	<0.2	220	5.3	0.08	0.09
EPC 1-2	1.995	140	<0.1	<0.2	360	14	0.05	0.06
EPC 1-3	2.575	25	3.2	<0.2	170	4.2	0.10	0.16
EPC 1-3	3.025	16	<0.1	<0.2	130	<0.2	0.15	0.17
EPC 1-3	3.325	14	1.9	<0.2	110	2.7	0.18	0.21
EPC 1-4	4.085	16	1.7	<0.2	200	10	0.19	0.19
EPC 1-4	4.685	31	1.7	<0.2	190	14	0.19	0.20
EPC 1-5	5.125	60	1.7	0.83	270	8.0	0.24	0.30
EPC 2-1	0.025	96	6.5	<0.2	370	8.8	0.12	0.14
EPC 2-1	0.765	16	3.2	<0.2	120	1.3	0.15	0.15
EPC 2-2	1.715	21	3.0	<0.2	150	16	0.12	0.16
EPC 2-2	2.015	25	<0.1	<0.2	130	12	0.12	0.18
EPC 2-3	2.615	19	2.7	<0.2	170	8.2	0.12	0.14
EPC 2-3	3.075	14	<0.1	<0.2	150	9.7	0.16	0.16
EPC 2-3	3.365	12	2.0	<0.2	190	10	0.18	0.19
EPC 2-4	4.115	15	2.0	<0.2	220	16	0.18	0.22
EPC 2-4	4.725	37	2.0	<0.2	210	11	0.18	0.18
EPC 2-5	5.185	78	1.8	<0.2	310	9.5	0.22	0.25
EPC 5-2	0.515	51	<0.1	<0.2	110	2.8	0.18	0.31
EPC 5-3	1.015	35	<0.1	<0.2	83	3.4	0.21	0.29
EPC 5-4	2.015	37	<0.1	<0.2	110	5.3	0.16	0.26
EPC 5-6	3.015	27	<0.1	<0.2	180	7.0	0.19	0.29
EPC 5-8	4.015	29	<0.1	<0.2	190	13	0.21	0.25
EPC 5-9	5.015	46	<0.1	<0.2	330	18	0.24	0.31
EPC 5-11	6.015	19	<0.1	<0.2	82	17	0.16	0.26
EPC 5-12	7.015	34	<0.1	1.5	120	29	0.23	0.34
EPC 5-14	8.015	37	<0.1	2.4	78	40	0.11	0.18
EPC 5-15	9.015	72	<0.1	3.4	120	60	0.06	0.10

EPC 5-16	10.015	63	<0.1	2.4	58	47	0.10	0.16
EPC 5-18	11.015	55	<0.1	2.1	63	27	0.19	0.33
EPC 5-19	11.685	34	<0.1	<0.2	82	17	0.21	0.28

Table 5. Interplaya anion concentrations in pore water (mg L^{-1}) and field water contents for EPC 7.

Core Sample	Average Depth (m)	Chloride (mg L^{-1})	Bromide (mg L^{-1})	Nitrate-N (mg L^{-1})	Sulfate (mg L^{-1})	Fluoride (mg L^{-1})	θG	θV
EPC 7-2	0.515	59	<0.1	<0.2	59	11	0.13	0.22
EPC 7-3	1.015	220	0.91	<0.2	1100	44	0.15	0.18
EPC 7-4	2.015	3900	18	<0.2	2600	4.0	0.13	0.17
EPC 7-6	3.015	1400	6.5	3.5	1200	15	0.13	0.17
EPC 7-8	4.015	860	5.0	4.7	850	30	0.13	0.20
EPC 7-9	5.015	640	3.0	7.6	500	48	0.16	0.20
EPC 7-11	6.015	450	2.6	7.1	380	63	0.16	0.25
EPC 7-12	7.015	340	1.5	<0.2	360	66	0.12	0.23
EPC 7-14	7.905	260	1.0	<0.2	270	43	0.11	0.21
EPC 7-15	9.015	270	1.1	<0.2	230	35	0.12	0.21
EPC 7-16	10.675	85	<0.1	<0.2	130	21	0.22	0.30
EPC 7-17	11.415	58	<0.1	<0.2	140	29	0.09	0.18
EPC 7-18	12.655	31	<0.1	<0.2	94	22	0.13	0.20
EPC 7-19	14.065	41	<0.1	<0.2	140	38	0.11	0.15
EPC 7-21	15.515	46	<0.1	<0.2	220	56	0.11	0.22
EPC 7-22	16.015	45	<0.1	<0.2	83	32	0.12	0.20
EPC 7-23	16.745	42	<0.1	<0.2	69	25	0.28	0.34

Concentrations of the anions, including chloride, bromide, sulfate, fluoride, and nitrate, have similar patterns through the vadose zone. All anion concentrations have a higher maximum in the interplaya than the playa, indicating fluid flux through the playa is higher, with longer ion residence times beneath the interplaya. Water-extractable chloride concentrations ranged from 12 to 140 mg L^{-1} in the three playa cores (EPC 1, 2, and 5), and from 301 to 3,900 mg L^{-1} in the interplaya (EPC 7) (Tables 4 and 5). The playa chloride profile has several small peaks at 2, 5, and 9 m; each peak has a different magnitude in each core. For example, the 2 m peak is smaller in core 2 (25 mg L^{-1}) and core 5 (37 mg L^{-1}) than it is in core 1 (140 mg L^{-1}) (Figure 35). The interplaya core exhibits one maximum peak at 2 m (3,900 mg L^{-1}), and then gradually decreases in concentration to around 34 mg L^{-1} to the water table (16.7 m).

Bromide concentrations ranged from <0.1 to 6.5 mg L^{-1} in the playa and from <0.1 to 18 mg L^{-1} in the interplaya (Tables 4 and 5). Although all were completed in the playa center, EPC 5 did

not contain bromide at concentrations above the IQL, whereas EPC 1 (5.4 mg L^{-1}) and 2 (6.5 mg L^{-1}) contained detectable bromide with a maximum peak occurring at the surface (Figure 35).

Nitrate-N concentrations ranged from <0.2 to 3.4 mg L^{-1} in the playa, and from <0.2 to 7.6 mg L^{-1} in the interplaya. Sulfate concentrations ranged from 58 to 450 mg L^{-1} in the playa and from 59 to $2,600 \text{ mg L}^{-1}$ in the interplaya. Fluoride concentrations ranged from <0.2 to 60 mg L^{-1} in the playa, and from 4.0 to 66 mg L^{-1} in the interplaya.

Vadose zone water-extractable anion concentrations and field gravimetric contents show trends for evapoconcentration due to plant transpiration in the root zone. Bromide, sulfate, and chloride are all expected to peak at the base of the root zone due to long term evapoconcentration of salts in the root zone via transpiration by plants. Corresponding to a dip in gravimetric water content at 2 m beneath the surface in the interplaya and 2016 playa core (0.05 to 0.16 g g^{-1} in playa, 0.13 g g^{-1} in interplaya), are peaks in chloride (140 mg L^{-1} in playa, $3,900 \text{ mg L}^{-1}$ in interplaya), bromide (18 mg L^{-1} in interplaya), and sulfate ($2,600 \text{ mg L}^{-1}$ in interplaya) concentrations. In the interplaya core, fluoride exhibits a minima (4.0 mg L^{-1} in interplaya) and nitrate ($<0.2 \text{ mg L}^{-1}$ in interplaya) a low value (Figure 35). However, with the exception of chloride, anion depth profiles in the playa core are more variable, with some concentration peaks at 2 m, but others at the surface or deeper in the profile. The only playa core that exhibits a large sulfate peak at 2 m is EPC 1 (360 mg L^{-1}), whereas EPC 2 (130 mg L^{-1}) and 5 (110 mg L^{-1}) exhibit smaller peaks at this depth. Sulfate concentration maxima in EPC 1, 2, and 5 occur at 0.25 m (450 mg L^{-1}), 0.25 m (370 mg L^{-1}), and 5 m (330 mg L^{-1}), respectively. A high concentration of sulfate may also exist at 0.25 m in EPC 5, but the first sample was collected at 0.5 m (110 mg L^{-1}). Peak bromide concentrations in both EPC 1 and 2 (5.4 mg L^{-1} and 6.5 mg L^{-1} , respectively) were observed at the surface, and all bromide concentrations for EPC 5 were $<0.1 \text{ mg L}^{-1}$. Fluoride concentrations in the playa peak at 0.77 m, 2 m and 4.7 m in EPC 1 (14 mg L^{-1}), 1.7 m and 4.1 m in EPC 2 (16 mg L^{-1}), and 9 m in EPC 5 (60 mg L^{-1}). Nitrate concentrations are below the IQL in EPC 1, peak at 5 m in EPC 1 (0.83 mg L^{-1}), and at 9 m in EPC 5 (3.4 mg L^{-1}) (Figure 35).

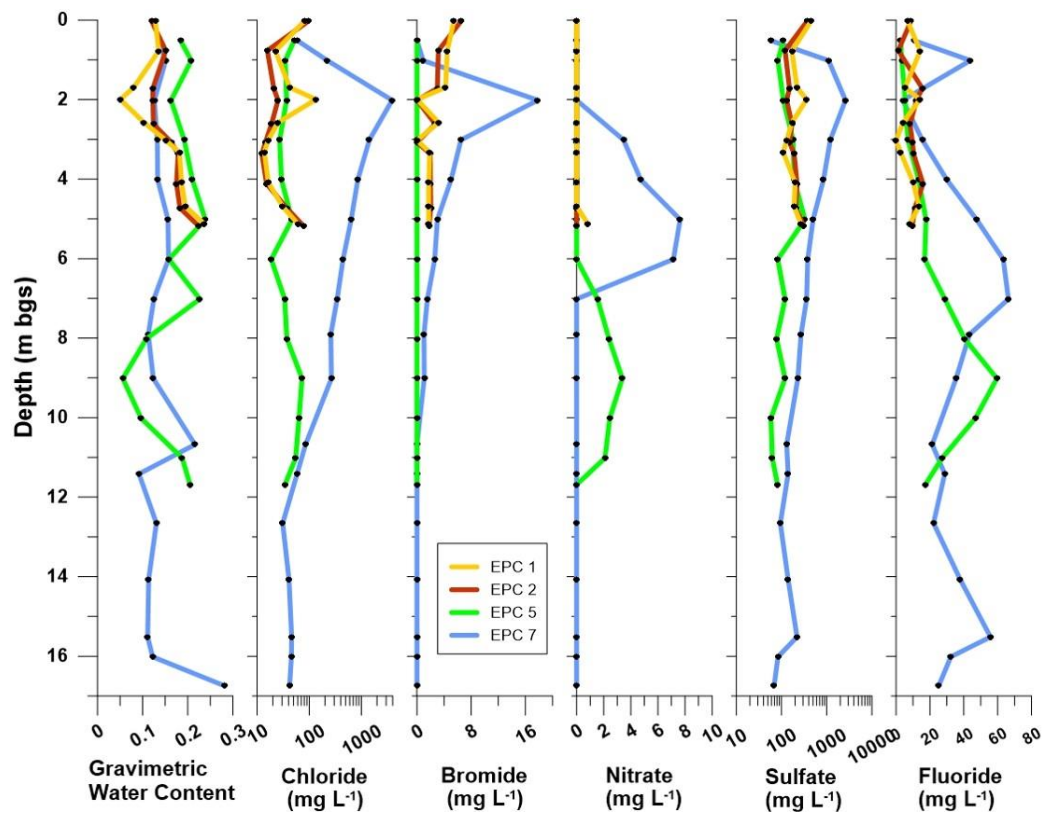


Figure 35: Gravimetric water content and anion depth profiles for playa (EPC 1, 2, 5) and interplaya (EPC 7) cores. Anion concentrations are reported as mg L^{-1} of pore water.

These data suggest a root depth of 2 m in both the playa and interplaya, with evapoconcentration affecting interplaya chloride, sulfate, and bromide concentrations, playa chloride, sulfate, and fluoride concentrations in EPC 1 and chloride concentrations in EPC 2. Contrarily, EPC 5 does not contain any anion maxima at the 2 m depth; instead they occur deeper in the profile at 5 or 9 m. EPC 1 (0.05 to 0.24 g g^{-1}) and 2 (0.12 to 0.22 g g^{-1}) have lower gravimetric water contents than EPC 5 (0.16 to 0.24 g g^{-1}) in the upper 5 m, which indicates water movement through the profile between 2016 and 2017. The lowest gravimetric water content in EPC 5 (0.06 g g^{-1}) is at 9 m, which may represent the depth of flushing or could be due to textural changes. This then is indicative of recharge due to the April-May 2017 inundation event infiltrating beyond the root zone and flushing the salts downward. It is suggested that the low values of nitrate and fluoride in the interplaya at this depth could be due to plant uptake of these nutrients; although fluoride is not an essential plant nutrient, it is still utilized by plants (Scanlon et al., 2009).

Although chloride concentrations peak at 2 m in the playa (EPC 1) and interplaya (EPC 7) cores, the magnitude is vastly different. The appreciably higher interplaya concentration is evidence that water is traveling more slowly, allowing for accumulation of chloride over a long period of time. Although evapoconcentration is also evident in the playa, the smaller magnitude implies a shorter timeframe for chloride accrual. Salt concentration at the base of the root zone is common in semiarid regions due to transpiration by plants (Scanlon, 1991). In addition, the shape of the interplaya chloride profile could have implications for long-term climate variations (Allison and Barnes, 1985; Scanlon, 1991). Over long time periods, the transition from a wetter climate

during the early Holocene (high fluid flux) to a drier climate in the middle and late Holocene (low fluid flux) could result in lower chloride concentrations in the lower profile and higher chloride concentrations in the upper profile (Scanlon, 1991).

Vadose zone ratios for bromide/chloride, nitrate/chloride, sulfate/chloride, and fluoride/chloride range from 0.023 to 0.20, 0.014 to 0.064, 0.92 to 16, and 0 to 1.1, respectively in the playa and from 0.004 to 0.0059, 0.0024 to 0.016, 0.67 to 4.9, and 0.0010 to 1.2, respectively in the interplaya (Tables 6 and 7, and Figure 36). Sulfate is the only anion measured with concentrations up to 15 times higher than chloride concentrations, a relationship observed only in the playa. It is possible that sulfate accumulates relative to chloride beneath the playa due to preferential chloride flushing and sorption of sulfate.

Table 6. Playa anion vadose zone ratios from pore water (mass ratio, mg L⁻¹) for EPC 1, 2, and 5. Some ratios are reported as not-applicable (NA) due to certain measurements of bromide and nitrate that are below the instrument quantification limit.

Core Sample	Average Depth (m)	Bromide/ Chloride	Nitrate/ Chloride	Sulfate/ Chloride	Fluoride/ Chloride
EPC 1-1	0.025	0.068	NA	5.6	0.085
EPC 1-1	0.775	0.20	NA	7.6	0.64
EPC 1-2	1.695	0.099	NA	5.2	0.13
EPC 1-2	1.995	NA	NA	2.7	0.10
EPC 1-3	2.575	0.13	NA	6.9	0.17
EPC 1-3	3.025	NA	NA	8.3	0
EPC 1-3	3.325	0.14	NA	8.0	0.20
EPC 1-4	4.085	0.11	NA	12	0.62
EPC 1-4	4.685	0.056	NA	6.2	0.44
EPC 1-5	5.125	0.029	0.014	4.4	0.13
EPC 2-1	0.025	0.068	NA	3.8	0.091
EPC 2-1	0.765	0.20	NA	7.8	0.084
EPC 2-2	1.715	0.14	NA	7.1	0.74
EPC 2-2	2.015	NA	NA	5.2	0.48
EPC 2-3	2.615	0.14	NA	9.3	0.44
EPC 2-3	3.075	NA	NA	10	0.67
EPC 2-3	3.365	0.16	NA	16	0.84
EPC 2-4	4.115	0.13	NA	15	1.1
EPC 2-4	4.725	0.055	NA	5.7	0.30
EPC 2-5	5.185	0.023	NA	4.0	0.12
EPC 5-2	0.515	NA	NA	2.2	0.054
EPC 5-3	1.015	NA	NA	2.4	0.099
EPC 5-4	2.015	NA	NA	2.9	0.15
EPC 5-6	3.015	NA	NA	6.8	0.26
EPC 5-8	4.015	NA	NA	6.6	0.46
EPC 5-9	5.015	NA	NA	7.1	0.38

EPC 5-11	6.015	NA	NA	4.4	0.91
EPC 5-12	7.015	NA	0.046	3.7	0.85
EPC 5-14	8.015	NA	0.064	2.1	1.1
EPC 5-15	9.015	NA	0.047	1.6	0.82
EPC 5-16	10.015	NA	0.039	0.92	0.74
EPC 5-18	11.015	NA	0.038	1.1	0.50
EPC 5-19	11.685	NA	NA	2.4	0.51

Table 7. Interplaya anion vadose zone ratios from pore water (mass ratio, mg L⁻¹) for EPC 7. Some ratios are reported as not-applicable (NA) due to certain measurements of bromide and nitrate that are below the instrument quantification limit.

Core Sample	Average Depth (m)	Bromide/ Chloride	Nitrate/ Chloride	Sulfate/ Chloride	Fluoride/ Chloride
EPC 7-2	0.515	NA	NA	0.99	0.18
EPC 7-3	1.015	0.0041	NA	4.7	0.20
EPC 7-4	2.015	0.0046	NA	0.67	0.0010
EPC 7-6	3.015	0.0046	0.0024	0.83	0.01
EPC 7-8	4.015	0.0059	0.0055	1.00	0.04
EPC 7-9	5.015	0.0047	0.012	0.78	0.07
EPC 7-11	6.015	0.0059	0.016	0.85	0.14
EPC 7-12	7.015	0.0045	NA	1.1	0.19
EPC 7-14	7.905	0.0040	NA	1.0	0.17
EPC 7-15	9.015	0.0040	NA	0.86	0.13
EPC 7-16	10.675	NA	NA	1.6	0.25
EPC 7-17	11.415	NA	NA	2.5	0.49
EPC 7-18	12.655	NA	NA	3.1	0.72
EPC 7-19	14.065	NA	NA	3.6	0.93
EPC 7-21	15.515	NA	NA	4.9	1.2
EPC 7-22	16.015	NA	NA	1.8	0.71
EPC 7-23	16.745	NA	NA	1.6	0.60

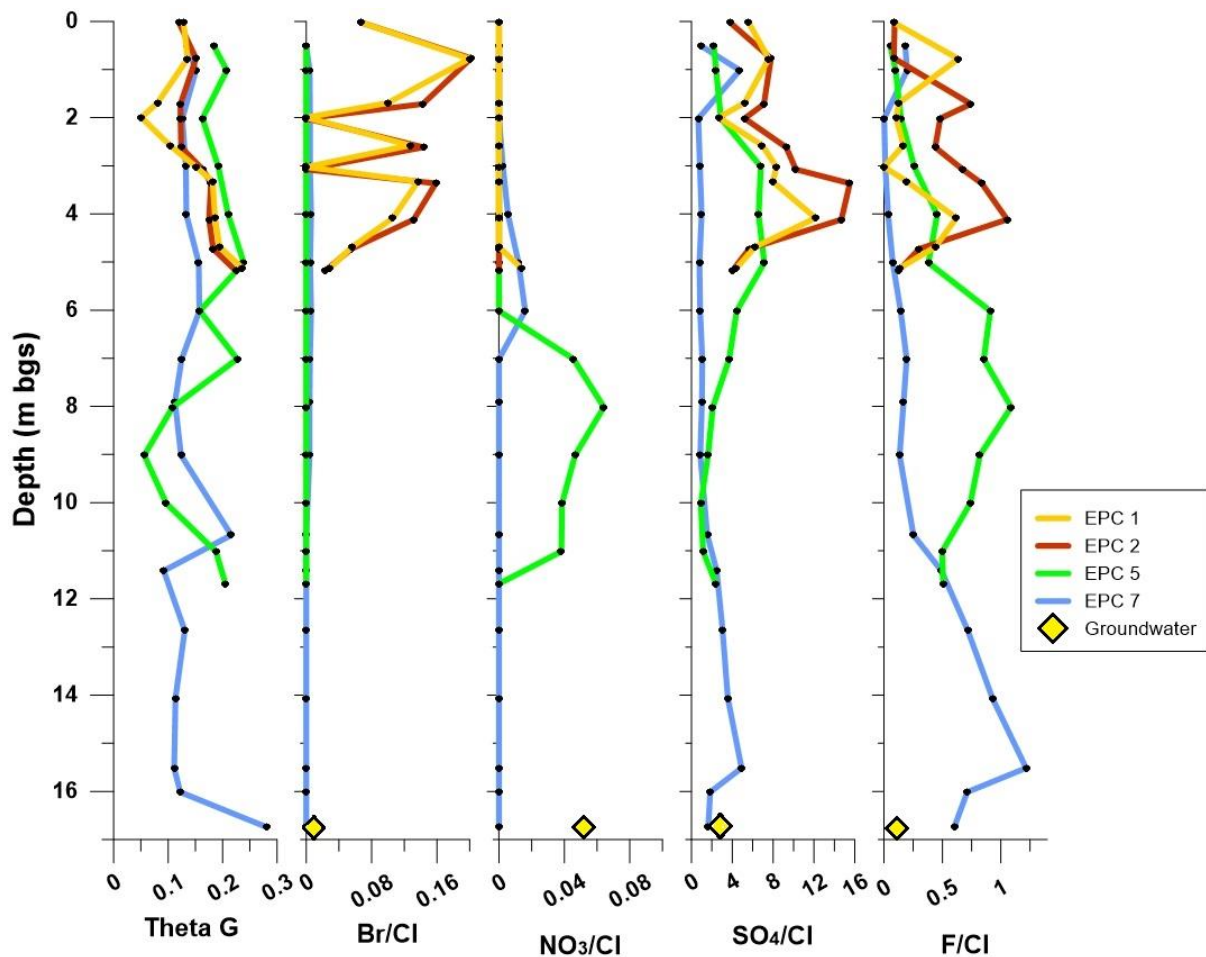


Figure 36. Vadose zone anion ratios (mass ratio, mg L^{-1}) for playa (EPC 1, 2, and 5) and interplaya (EPC 7) cores. Yellow diamonds represent groundwater concentrations in the four sampled wells. Depth location of groundwater marker does not reflect actual groundwater level.

When anion mass ratios (mg L^{-1}) are compared with chloride concentration (mg L^{-1}), conclusions can be drawn about the sources of salinity (e.g., Figure 37). Interestingly, the EPC 7 samples have nearly constant ratios at high chloride concentrations, implying evapoconcentration is occurring causing mineral precipitation (e.g., Whittemore, 1995). As the interplaya vadose zone becomes increasingly dry from evapotranspiration, it is possible that halite and gypsum may be precipitating in the root zone and subsequently re-dissolving when rain events saturate the upper soil. Ratios are higher and chloride concentrations are lower in the playa than the interplaya suggesting more frequent flushing in the playa.

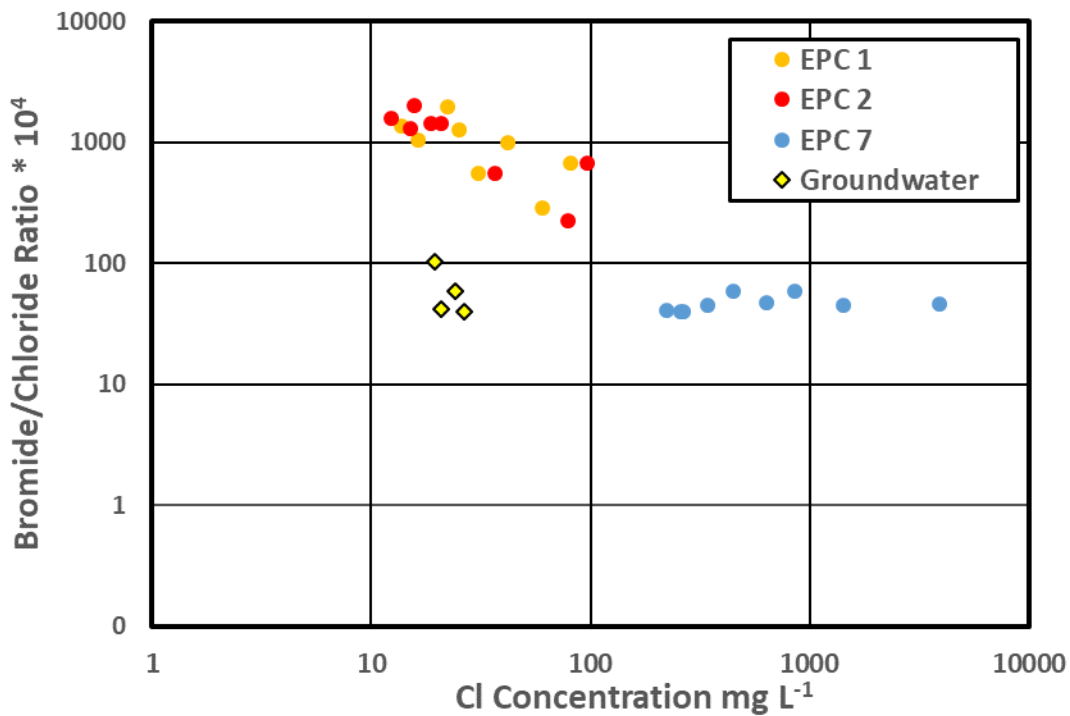


Figure 37: Bromide/chloride mass ratios (multiplied by 10^4) are plotted against chloride concentration.

Linear regression analysis provides insight into relationships among anion concentrations in the playa and interplaya. In EPC 1 and 2, the only anions that appear somewhat positively correlated are sulfate and chloride with an R^2 value of 0.65 and 0.81, respectively (Figure 38). In EPC 5 this trend is not repeated, sulfate and chloride have an R^2 value of 0.01, and the best-fit line has a slightly negative slope (Figure 38). This temporal change between the 2016 and 2017 cores supports the idea of preferential chloride flushing during the 2017 inundation event, changing the sulfate/chloride ratios and resulting in the slightly negative slope of the best-fit line. Anions in the interplaya are better correlated than those in the playa, with R^2 values of 0.99 for bromide and chloride, 0.90 for sulfate and chloride, and 0.90 for sulfate and bromide (Figure 38). Possible reasons for high correlations in these three anions is the nature of interplaya recharge flux. Interplaya recharge occurs during rain events and consists of small plugs of water moving through the vadose zone. These smaller events do not result in a significant subsurface pulse, rarely resulting in infiltration beyond the root zone, providing the ions a longer timeframe to equilibrate with the concentration of ions already present in the vadose zone. With playa recharge events happening largely through focused flow and macropore recharge, more conservative ions (chloride, bromide) are preferentially flushed, reducing the correlation and lowering R^2 values (lower correlations).

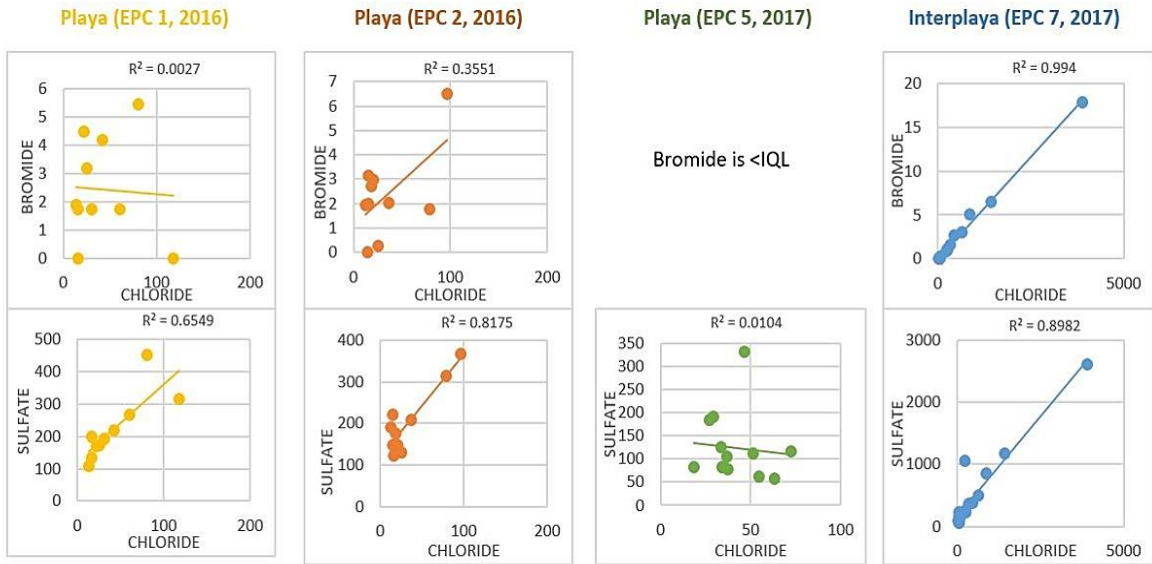


Figure 38: Linear regression of vadose zone bromide and sulfate vs. chloride concentrations for all four cores. The best-fit line is also shown, as is the calculated correlation coefficient (R^2).

Recharge rate calculations-Chloride Mass Balance (CMB)

The Chloride Mass Balance (CMB) method approximates recharge rates by comparing the concentration of chloride in the vadose zone system with the concentration of chloride input to the surface, with chloride assumed to move through the soil matrix at the same rate as infiltrating water. Chloride can be used as a conservative environmental tracer because it is non-volatile and undergoes very little sorption or plant uptake (Scanlon, 1991). Sources of chloride are mainly from atmospherically transported material originating from the oceans, whereas inland areas likely have a more terrestrial source from weathering and erosion of clastic sediment (Davis et al., 1998). The CMB method is preferred over water balance calculations when measuring fluid recharge flux to aquifers in semiarid regions, where large evapotranspiration rates and inter-annual variations in precipitation result in a large error when calculating the typically small ($<100 \text{ mm yr}^{-1}$) recharge rates (Scanlon, 1991). Inherent assumptions with the CMB method include constant rates of chloride deposition through time and a lack of horizontal flow in the vadose zone (Scanlon, 1991).

Four separate equations make up the CMB calculation. First, Equation 3 is used to determine the chloride wet and dry deposition at the land surface (q_{cl}) by multiplying the annual precipitation rate (P) by the chloride concentration in precipitation (Cl_p) (Allison and Hughes, 1978; Scanlon and Goldsmith, 1997):

$$q_{cl} = P \times Cl_p \quad [3]$$

The average (1952-2017) annual precipitation (505 mm) for the study site was obtained from a National Weather Service monitoring station in Scott City, Kansas, located approximately 26.8 km (16.7 mi) west of the study area (High Plains Regional Climate Center, CLIMOD, 2018). The concentration of chloride in precipitation (wet and dry) was measured in the SHP of Texas

and New Mexico as 0.6 g m^{-3} (Nativ and Riggio, 1990) and utilized in subsequent CMB calculations in two Texas studies (Wood and Sanford, 1995; Scanlon and Goldsmith, 1997). The annual rainfall rates for the two Texas studies (485 mm, Wood and Sanford, 1995; 500 mm, Scanlon and Goldsmith, 1997) are similar to that at the Ehmke Playa site (505 mm) and the value of 0.6 g m^{-3} for Cl_p is assumed reasonable for the study site. Using Equation 3, the q_{cl} is calculated as 0.3 g m^{-2} . A recent study in northwest Kansas with similar average annual precipitation (485 mm) also used a q_{cl} value of 0.3 g m^{-2} for CMB calculations (Katz et al., 2016).

CMB – Fluid Flux Calculations

Next, the fluid flux rate through the vadose zone (q) is calculated by dividing the q_{cl} from Equation 4 by the chloride concentration in the unsaturated zone (Cl_{uz}) (Allison and Hughes, 1978; Scanlon and Goldsmith, 1997):

$$q_1 = q_{cl}/Cl_{uz} \quad [4]$$

Equation 4 assumes that the only source of chloride deposition is from wet and dry precipitation into the playa; however, playas are closed basins and will often have additional chloride mass from run-off water in the surrounding watershed. By underrepresenting the total amount of chloride deposition in the playa basin, Equation 4 underestimates the fluid flux. To account for chloride in run-off water into a playa, the following equation was developed (Wood and Sanford, 1995; Scanlon and Goldsmith, 1997):

$$q_2 = \frac{P \times Cl_p}{Cl_{uz}} + R \frac{A_b \times Cl_r}{A_f \times Cl_{uz}} \quad [5]$$

where R is runoff, A_b is the area of the watershed (14 km^2), A_f is the area of the playa (0.51 km^2), and Cl_r is the concentration of chloride in the run-off water. The Cl_r is assumed the same as Cl_p at this site, or 0.6 g m^{-3} because there are not sufficient quantities of chloride sources in surficial sediments to alter the concentration in run-off water.

If chloride vadose zone profiles are collected in differing years, the fluid flux can be estimated based on the chloride peak displacement depth and time elapsed between the two measurements. This third flux equation is shown below (Stonestrom et al., 2003; McMahon et al., 2006; Gurdak et al., 2007):

$$q_3 = \frac{\theta_{Vfield}(z_2 - z_1)}{(t_2 - t_1)} \quad [6]$$

where θ_{Vfield} is the volumetric water content of the specified core between the two chloride peaks, z_2 and z_1 are the depths of chloride peaks, and t_2 and t_1 are the corresponding times of measurement.

The three different equations (Equations 4, 5, and 6) are used to constrain fluid flux rates through the vadose zone (Table 8). The first method (Equation 4) assumes the only input of chloride to the system is via wet and dry deposition, giving depth-weighted flux rates of 4 mm yr^{-1} in the interplaya and between 8 and 15 mm yr^{-1} in the playa. However, fluid flux through the playa is greatly underestimated using this method because the additional chloride mass from watershed run-off is ignored (e.g., Flint et al., 2002). Thus, Equation 5 is used to calculate fluid flux through the playa, as it compensates for the chloride mass from the surrounding runoff. As values for runoff (R) are not available, fluid flux was calculated using Equation 5 with values for R of 5% (25.3 mm yr^{-1}), 10% (50.1 mm yr^{-1}), and 20% (101 mm yr^{-1}) of annual precipitation.

Fluid fluxes calculated for the playa at R values of 5%, 10%, and 20% of annual precipitation, range from 20 to 37 mm yr⁻¹, 31 to 58 mm yr⁻¹, and 54 to 100 mm yr⁻¹, respectively (Table 8).

Table 81. Ehmke Playa site fluid flux ranges.

Location	Depth (m)	Depth-Wt. Fluid Flux		Depth-Wt. Fluid Flux Eq. 5 (q_2 , mm yr ⁻¹)			Depth-Wt. Fluid Flux Eq. 6 (q_3 , mm yr ⁻¹)	
		Eq. 4 (q_1 , mm yr ⁻¹)	R as 5% of P	R as 10% of P	R as 20% of P		2016 Core	2017 Core
EPC 1	5.1	12	28	45	78	78 to 118	NA	
EPC 2	5.2	15	37	58	100	NA	NA	
EPC 5	11.5	8	20	31	54	NA	1700	
EPC 7	16.7	4	NA	NA	NA	NA	NA	

Since cores were collected from the playa center in successive years before (EPC 1, June 2016) and after (EPC 5, August 2017) an inundation flushing event (April 13 to May 16, 2017), Equation 6 can also be used to estimate fluid flux through the playa. Chloride peaks for EPC 1 and EPC5 were at 2 m and 9 m, respectively; thus, the single inundation flushing event resulted in a chloride displacement of 7 m after only 1.17 years. With a depth-weighted average θ_{vfield} of 0.28 measured between 2 and 9 m in EPC5, the fluid flux was calculated across this 1.17 year sample interval as 1,700 mm yr⁻¹. Assuming a 3.0 year gap between inundation events and the formation of the chloride peak at 2 m depth, this fluid flux slows to 650 mm/yr.

In summary, fluid flux estimates beneath the playa range between 8 and 1,700 mm/yr, and 4 mm/yr beneath the interplaya. However, because the playa receives a considerable amount of extra chloride from the surrounding watershed during inundation events, fluid flux calculations using Eq. 4 are not considered valid. At values of R of 10% and 20%, Eq. 5 provides recharge values similar to those observed beneath irrigated fields and some playas elsewhere in the High Plains region (e.g., Gurdak and Roe, 2009; Katz et al., 2016). Scanlon and Goldsmith (1997) estimated that run-off water to basins in the SHP accounted for approximately 10% of annual precipitation in a watershed of fine-grained texture, which is modified from Wood and Sanford (1995) who used a R value of 5% in a coarse-textured soil. The 10% value for R is likely the most representative of this study area because the watershed surface soil is silty clay loam and the annual precipitation (505 mm) is similar to that used in by Scanlon and Goldsmith (1997) (500 mm). However, the CHP experiences inter-annual variations in precipitation (370 to 845 mm) and higher values for R may be more representative of wetter years; further study of inundation events in this particular watershed is needed to improve confidence in the selection of R=10%. Finally, estimates obtained using Eq. 6 are informative as they provide the only estimate across the inundation event. However, with the information available, it is not possible to identify whether estimates from Eq. 5 or Eq. 6 are more representative of long-term conditions. Regardless, it is clear that fluid flux rates are at least one order of magnitude higher beneath the playa than the interplaya, and possibly as much as three times higher.

CMB – Travel Time Calculations

After calculating a fluid flux based on Equation 4, 5, or 6, a simple travel time through the vadose zone can be calculated by Equation 7 below:

$$tt_1 = z_{wt}/q \quad [7]$$

where z_{wt} is depth to the water table and q is the calculated fluid flux. Additionally, a second travel time calculation can be used by averaging the volumetric mass of chloride in a depth interval and dividing by the chloride land deposition (Wood and Sanford, 1995; Scanlon and Goldsmith, 1997):

$$tt_2 = \frac{\int_0^z \theta_{vfield} Cl_{uz} dz}{q_{cl}} \quad [8]$$

where the θ_{vfield} is the field volumetric water content of the sample.

A range of travel times to the water table are determined beneath the playa and interplaya (Table 9), depending on which travel time calculation (Eq. 7 or 8) is used, and which flux rate calculation (Eq. 5-R=10%, Eq. 5-R=20%, or Eq. 6) for the playa. Eq. 8 is more robust than Eq. 7, as it takes into account variations in Cl and water content within the subsurface. Beneath the playa, these estimates range from 8 to 390 years, and between 4,800 and 5,500 years beneath the interplaya. As the travel time estimates are heavily reliant on the fluid flux estimate, it is not surprising that the travel times are similarly 1-3 orders of magnitude faster beneath the playa than the interplaya, and faster *movement beneath the playa during inundation periods*.

Table 9: Ehmke playa site travel times to the end of the core (EPC 5 and 7 end at the water table).

Location	Depth (m)	Travel Times (yrs) Calculated from Eq. 7 (tt_1)						Travel time (yrs) from Eq. 8 (tt_2)
		Eq. 4	Eq 5, R=5%	Eq. 5, R=10%	Eq. 5, R=20%	Eq. 6, 2016 Core	Eq. 6, 2017 Core	
EPC 1	5.1	NA	180	110	65	100 to 150*	NA	92
EPC 2	5.2	NA	140	90	52	NA	NA	84
EPC 5	11.5	NA	580	370	210	NA	8	390
EPC 7	16.7	4800	NA	NA	NA	NA	NA	5500

CMB Discussion

Calculated fluid fluxes through the vadose zone to the HPA in the playa are higher by at least one order of magnitude than those for the interplaya, which compares well to playa studies in the SHP. In the SHP, playa and interplaya fluid fluxes range from 24 to 610 mm yr⁻¹ and from 0.1 to 32 mm yr⁻¹, respectively (Wood and Sanford, 1995; Scanlon and Goldsmith, 1997, Gurdak and Roe, 2009), compared with fluids fluxes from the Ehmke playa and interplaya of 78 to 118 mm yr⁻¹ and 0.1 to 10 mm yr⁻¹, respectively. Despite this similarity, a study by Wood et al. (1997) indicates total fluid flux through SHP playas is actually much higher (750 to 2,720 mm yr⁻¹), suggesting the CMB method measures only the interstitial fluid flux (22 to 34 mm yr⁻¹) while ignoring macropore fluid flux (Table 9). There is currently disagreement over whether the CMB method calculates interstitial recharge and ignore macropore recharge, or represents the total system recharge (Wood, 1997; Scanlon, 1999). Nonetheless, these higher recharge rates calculated by Wood et al. (1997) are similar to that calculated via Equation 6 with the 2017 core (600-1,700 mm yr⁻¹) and may represent higher playa fluid flux during inundation periods. Wood et al. (1997) also estimated that 84% of the SHP regional recharge (11 mm yr⁻¹) occurs through

playa macropores. Similarly high inundation infiltration rates were measured in the SHP by Ganesan et al. (2016) through playas surrounded by both grassland (320 to 1,700 mm yr⁻¹) and cropland (730 to 7,200 mm yr⁻¹) watersheds.

Fluid flux rates through CHP and nearby NHP rangeland (0.2 to 5 mm yr⁻¹) and irrigated cropland (39 to 138 mm yr⁻¹) (Table 10) (McMahon et al., 2006; Gurdak et al., 2007; Katz et al., 2016) compare well to study site interplaya (0.1 to 10 mm yr⁻¹) and playa (78 to 118 mm yr⁻¹). Gurdak et al., (2007) also measured total recharge (196 to 390 mm yr⁻¹) irrigated agriculture by correlating groundwater level responses to precipitation events; this is slightly elevated when compared to Equation 6 from EPC 1 (78 to 118 mm yr⁻¹), but much lower than that estimated during/ after inundation (1,700 mm yr⁻¹). Interplaya water flux rates from the study site (0.1 to 10 mm yr⁻¹) are consistent with regional recharge estimates for regional recharge from Kansas (4 to 18 mm yr⁻¹) (Katz et al., 2016; Meixner et al., 2016).

Table 10. Anion concentrations, fluid fluxes and travel times in the Northern and Central High Plains.

Publication	Site Description	Chloride	Sulfate	Bromide	Nitrate	Fluid Flux (mm yr ⁻¹)	Travel Time (yrs)	Vadose Zone Thickness (m)
*McMahon et al., 2006	CHP Rangeland	0 to 32			0 to 290	0.2 to 5	2,000	50
	CHP Irrigated Cropland	0 to 55			0 to 19	39 to 54	49 to 130	17 to 45
Gurdak et al., 2007 (flux is regional ave.)	CHP Rangeland (mg kg ⁻¹)	1 to 42			0 to 250	196 to 390		
Katz et al., 2016	NHP Irrigated Cropland (mg L ⁻¹)	24 to 387	0 to 1,900	0 to 2.7	0 to 450	27 to 138	45	35**
	NHP Irrigated Cropland (mg kg ⁻¹)	1 to 48	0 to 230	0.01 to 0.2	0 to 55			
Meixner et al., 2016	Entire CHP (regional ave.)					18		

*Unless otherwise stated, chloride reported as mg L⁻¹, nitrate reported as mg kg⁻¹

**Depth represents the predevelopment water table, actual water table is at 64 m

Vadose zone travel times calculated at the study site compared well to other studies completed beneath the NHP, CHP and SHP. In the CHP, travel times beneath rangeland and irrigated cropland to the water table (50 m and 45 m, respectively) were calculated at 2000 yrs, and between 49 to 130 yrs, respectively (Table 10) (McMahon et al., 2006; Gurdak et al., 2007). Katz et al. (2016) also measured a travel time of 45 yrs to a depth of 36 m at an irrigated site in northwestern Kansas. Travel times through the playa (100 to 150 yrs) are slightly elevated with respect to these CHP studies; however, the inundation travel time of 8 yrs is elevated when compared to CHP rangeland and irrigated cropland (Table 10). The travel times to 16.7 m measured in the interplaya (4,800 to 5,500 yrs) are elevated to those in CHP rangeland, but are within the measured range for three SHP interplaya sites (5,000 to 9,900 yrs) with 4.5 to 26.3 m thick vadose zones (Scanlon and Goldsmith, 1997).

Infiltration

K_{sat} values for playa floor and interplaya are very similar and are representative of a silt texture, which are typically between 1×10^{-6} to 1×10^{-4} cm sec $^{-1}$ (Hillel, 2004). Values in the playa center ranged from $1.6 \times 10^{-4} \pm 1.9 \times 10^{-5}$ cm sec $^{-1}$ to $7.8 \times 10^{-4} \pm 1.5 \times 10^{-4}$ cm sec $^{-1}$ (Inf 1 and 2), and in the interplaya from $2.3 \times 10^{-4} \pm 2.6 \times 10^{-4}$ cm sec $^{-1}$ to $7.2 \times 10^{-4} \pm 6.8 \times 10^{-5}$ cm sec $^{-1}$ (Inf 3 and 4) (Figure 11 and Table 11). This is consistent with USDA Web Soil Survey information, which report Ulysses silt loam in the interplaya to 79 in. (201 cm), and hydric Ness clay followed by silt loam in the playa to 31 in. (79 cm) and 60 in. (152 cm), respectively (United States Department of Agriculture, 2017).

Table 11. Results for the four Infiltrometer measurements.

Test Name	Location	K_{sat} (cm sec $^{-1}$)	K_{sat} (mm yr $^{-1}$)	K_{sat} Error (cm sec $^{-1}$)
Inf 1	Playa	7.84E-04	247,000	1.50E-04
Inf 2	Playa	1.62E-04	51,100	1.86E-05
Inf 3	Interplaya	2.33E-04	73,500	2.57E-04
Inf 4	Interplaya	7.21E-04	227,00	6.78E-05

As the K_{sat} measurement is the same in the playa and interplaya location, fluid movement rates through saturated soil is the same, in the absence of macropores (in the playa). After a large rain event, soil in the interplaya may become saturated creating quick percolation, as it is in the playa. Although, it is unlikely that saturated conditions exist for long periods of time in the interplaya, as they do in the playa, due to the absence of ponding. Additionally, macropores are known to exist in the hydric soils of the playa floor, which are not present in the interplaya location, pointing to higher infiltration and fluid flux in the playa when soils are dry or partially saturated. Interplaya recharge occurs mostly during large rain events when the soil is saturated, whereas playa recharge occurs through macropores when dry or partially saturated, during large rain events when the soil is saturated, and during inundation.

Shallow soil K_{sat} measurements indicate similar saturated soil infiltration rates in the playa and interplaya and are indicative of a silty loam. Fluid flux through the interplaya is assumed to occur only during rain events, which are sporadic, mostly in spring, and likely contribute small pulses of water downward. As the interplaya is part of the watershed, it is assumed that once the soil is saturated, the remaining water becomes overland flow and run-off to the playa. Recharge through playa floors can occur through micropores and macropores during partial saturation, and periods of inundation. Because the interplaya is not likely saturated for extended periods, the fluid flux rate (50,000 to 240,000 mm yr $^{-1}$) calculated based on K_{sat} is representative of water infiltration and percolation through the playa during saturation. These values are similar to those obtained studies in SHP playa and interplaya using infiltrometers (e.g., Gurdak and Roe 2009). These data suggest a travel time of 17 to 82 days to the water table beneath the playa (11.5 m); however, saturated conditions may not persist this long as the 2017 inundation event lasted for 34 days. This inundation timeframe is less than the maximum calculated travel time, resulting in incomplete flushing. The maximum chloride concentrations in EPC 5 at 9 m suggest flushing

occurred only to this depth during the 2017 inundation event and did not completely reach the water table.

Summary and Conclusions

This investigation consisted of two primary components: first, the development of a sound knowledge base of the playa system's underlying stratigraphy and sedimentology in order to assess the potential and identify evidence for downward movement of surface water through the entire vadose zone; and secondly, use of geochemical tracer approaches and modeling to verify that surface water from the playa is actually moving through the vadose zone. This combination of approaches was effective in demonstrating recharge to the HPA beneath Ehmke Playa using physical and chemical methods.

Results

Stratigraphy and sedimentology were documented for both the playa and the adjacent interplaya for comparative purposes. Numerical dating indicated that Ehmke playa had filled at a relatively rapid rate during the more mesic last glacial period compared to the extremely slow rate during the post-glacial period—sedimentation has been so slow in the last several thousand years that a well-developed hydric soil has developed. Sedimentological data indicate that the upper 5-7 m (16.4-23 ft) is silt-dominated and sand poor with modest clay levels, which has produced a loamy texture, which would allow infiltration, that is, the high percentage of clay assumed by many is not present in the surface hydric soil (though concentration is sufficient to produce shrink-swell cycles, which homogenize the hydric soil zone). Magnetic evidence for fine-particle downward translocation, leaching of carbonate downward and other data provide physical evidence that water moves through the vadose zone beneath the playa.

The geochemical study was in part based on data from the instrumented station. One playa inundation event was observed during the study, in April and May of 2017. After inundation, near-surface matric potentials were above field capacity to the deepest sensor location, 152 cm (60 in). Before inundation, dissolved solutes were concentrated at 2 m (6.6 ft) depth beneath both the playa and interplaya. Beneath the playa, solutes which had accumulated at the base of the root zone were flushed to a depth of 9 m (29.5 ft), approximately 7 m (23 ft) beyond the base of the root zone. In contrast, no visible change was observed beneath the interplaya, with major solute concentrations remaining at the base of the root zone after the precipitation events. Calculations of infiltration rate and fluid flux beneath the playa were fastest from physical measurements (infiltrometer and matric potential) 8,800 to 400,000 mm yr⁻¹. Chemistry-based methods used to calculate fluid fluxes provided a more constrained range beneath the playa, between 20 and 1,700 mm yr⁻¹, although the faster rates are calculated from the infiltration rate. Additional uncertainty in this estimate is due to the unknown amount of runoff from the surrounding watershed. As discussed within the text, a range of ~50 to ~650 mm/yr is reasonable. Beneath the interplaya, fluid flux rates of only 4 mm yr⁻¹ were observed. Fluid fluxes from both the interplaya and playa are consistent with studies elsewhere in the High Plains region.

These data indicate recharge is greater beneath Ehmke Playa than the nearby interplaya by several orders of magnitude. Although only one inundation event was measured during the period instrumentation, the effects on infiltration were readily apparent within the vadose zone. Solute flushing beneath the playa but not interplaya, and changes in matric potential within the playa vadose zone indicated a physical likelihood for gravity drainage of pore water due to inundation. However, if this modest inundation event effected a change in water table due to recharge, it was too slight to be noticed using the instrumentation available; the incomplete vadose zone flushing also suggests this even resulted in minimal actual recharge reaching the water table during the study period.

Recommendations

Continued study will help identify the frequency of inundation events and the types of events which can individually push water to the water table. Despite this, it is clear that with faster fluid flux rates and water infiltrating past the root zone, intact playas provide significantly greater recharge than nearby interplaya used as rangeland. At a minimum, recharge rates beneath the Ehmke playa are also equal to those beneath irrigated cropland above the HPA in Kansas, but are likely greater. These data confirm that the Ehmke Playa, and likely other Kansas playas, behave similarly to the better studied playa systems in the SHP in Texas. This conclusion should be confirmed through study of playas of varying sizes in Kansas, and also in areas where the depth to water has increased significantly due to pumping. Once confirmed, the data should be incorporated with playa and subsurface maps in a model to determine the amount of recharge playas collectively provide to the HPA. Finally, the model results could be incorporated into a decision support model (perhaps the existing PLJV decision support model) and used to identify locations where playa preservation/restoration will have the most impact for aquifer recharge.

Acknowledgements

Several individuals were essential to the success of this investigation. Nate Schlagel and Melissa Goldade assisted with fieldwork and Eric Zautner with laboratory analyses; the Kansas Geological Survey drillers Joe Anderson, Jeremy Scobee, and assistants made two multi-day on-site trips, one to install the three groundwater monitoring wells and another to extract cores from the vadose zone and upper saturated zone of the playa and interplaya; Rick Miller, chief of the Kansas Geological Survey Exploration Services section made all the drilling possible; Don Whittemore, Kansas Geological Survey hydrogeologist (emeritus), provided extremely helpful input; and Bruce Barnett, manager of the Kansas Paleoenvironmental and Environmental Stable Isotope Laboratory (KPESIL) provided stable isotope data.

References

- Allison, G.B., and C.J. Barnes. 1985. Estimation of evaporation from the normally “dry” Lake Frome in South Australia. *J. Hydrol.* 78(3–4): 229–242. doi:10.1016/0022-1694(85)90103-9
- Allison, G.B., and M.W. Hughes. 1978. The use of environmental chloride and tritium to estimate total recharge to an unconfined aquifer. *Australia J. Soil Res.* 16(2): 181–195. doi:10.1071/SR9780181
- Bowen, M.W. 2011. Spatial distribution and geomorphic evolution of playa-lunette systems on the central High Plains of Kansas. Proquest LLC.: PhD Dissertation. 86 pages. <https://search-proquest-com-www2.lib.ku.edu/docview/873786471?pq-origsite=primo> (accessed 29 April 2018).
- Bowen, M.W., and W.C. Johnson. 2012. Late quaternary environmental reconstructions of playa-lunette system evolution on the central High Plains of Kansas, United States. *Bull. Geol. Soc. Am.* 124(1–2): 146–161. doi:10.1130/B30382.1
- Bowen, M.W., W.C. Johnson, and D.A. King. 2018. Spatial distribution and geomorphology of lunette dunes on the High Plains of Western Kansas: implications for geoarchaeological and paleoenvironmental research. *Physical Geog.* 39(1): 21–37. doi:10.1080/02723646.2017.1319683
- Bowen, M.W., and Johnson, W.C., 2017. Anthropogenically accelerated sediment accumulation within playa wetlands as a result of land cover change on the High Plains of the central United States. *Geomorphology* 294: 135–145
- Buchanan, R.C., B.B. Wilson, R.R. Buddemeier, and J.J. Butler Jr. 2015. The High Plains Aquifer. Kansas Geological Survey. Public Information Circular 18. <http://www.kgs.ku.edu/Publications/pic18/index.html> (accessed 29 April 2018).
- Corley, J. 2003. Best Practices for establishing detection and quantification limits for pesticide residues in foods. *Handbook of Residue Analytical Methods for Acrochemicals*. John Wiley & Sons Ltd. 409(c): 1–18.
- Davis, S.N., D.O. Whittemore, and J. Fabryka-Martin. 1998. Uses of chloride/bromide ratios in studies of potable water. *Ground Water* 36(2): 338–350. doi:10.1111/j.1745-6584.1998.tb01099.x
- Devlin, J.F., and P.C. Schillig. 2017. HydrogeoEstimatorXL: an Excel-based tool for estimating hydraulic gradient magnitude and direction. *Hydrogeol. J.* 25(3): 867–875. doi:10.1007/s10040-016-1518-4
- Favre, F., P. Boivin, and M.C.S. Wopereis. 1997. Water movement and soil swelling in a dry, cracked vertisol. *Geoderma* 78(1–2): 113–123. doi:10.1016/S0016-7061(97)00030-X
- Flint, A.L., L.E. Flint, E.M. Kwicklis, J.T. Fabryka-martin, and G.S. Bodvarsson. 2002. Estimating recharge at Yucca Mountain, Nevada, USA: comparison of methods. *Hydrogeol. J.* 10: 180–204. doi:10.1007/s10040-01-0169-1
- Ganesan, G., K. Rainwater, D. Gitz, N. Hall, R. Zartman, W. Hudnall, and L. Smith. Comparison of infiltration flux in playa lakes in grassland and cropland basins, Southern High Plains of Texas. *Texas Water Journal* 7(1): 25–39.
- Geiss, C. E., & Zanner, C. W. (2006). How abundant is pedogenic magnetite? Abundance and grain size estimates for loessic soils based on rock magnetic analyses. *Journal of Geophysical Research: Solid Earth*, 111(12). <https://doi.org/10.1029/2006JB004564>

- Geiss, C. E., Egli, R., & Zanner, C.W., 2008. Direct estimates of pedogenic magnetite as a tool to reconstruct past climates from buried soils. *Journal of Geophysical Research-Solid Earth*, 113. <https://doi.org/10.1029/2008jb005669>
- Gurdak, J.J., M. A. Walvoord, and P.B. McMahon. 2008. Susceptibility to enhanced chemical migration from depression-focused preferential flow, High Plains aquifer. *Vadose Zo. J.* 7(4): 1218-1330. doi:10.2136/vzj2007.0145
- Gurdak, J.J., R.T. Hanson, P.B. McMahon, B.W. Bruce, J.E. McCray, G.D. Thyne, and R.C. Reedy. 2007. Climate variability controls on unsaturated water and chemical movement, High Plains aquifer, USA. *Vadose Zo. J.* 6(3): 533–547. doi:10.2136/vzj2006.0087
- Gurdak, J.J., and Roe, C.D., 2009. Recharge rates and chemistry beneath playas of the High Plains Aquifer – A literature review and synthesis. U.S. Geological Survey Circular 1333.
- Gutentag, E.D., F.J. Heimes, N.C. Krothe, R.R. Luckey, and J.B. Weeks. 1984. Geohydrology of the High Plains aquifer in parts of Colorado, Kansas, Nebraska, New Mexico, Oklahoma, South Dakota, Texas, and Wyoming. U.S. Geological Survey Prof. Pap. 1400-B. <https://pubs.usgs.gov/pp/1400b/report.pdf> (accessed 29 April 2018).
- Herbell, M.J., and R.F. Spalding. 1993. Vadose zone fertilizer-derived nitrate and $\delta^{15}\text{N}$ extracts. *Ground Water* 31(3): 376–382. doi:10.1111/j.1745-6584.1993.tb01838.x
- High Plains Regional Climate Center, CLIMOD. 2018. <http://climod.unl.edu/> (accessed 29 April 2018).
- Hillel, D. 2004. Introduction to Environmental Soil Physics. Elsevier Science (USA), San Diego, CA.
- Johnson, L.A., D.A. Haukos, L.M. Smith, and S.T. McMurry. 2012. Physical loss and modification of Southern Great Plains playas. *J. Environ. Manage.* 112: 275–283. doi:10.1016/j.jenvman.2012.07.014
- Johnson, W.C., Burt, D.J., Bowen, M.W., Stotler, R.L., and Salley, Kaitlin, 2016. An investigation into playa basins as a point source for recharge of the High Plains Aquifer, Kansas Governor's Conference on the Future of Water in Kansas, Manhattan, KS (abst)
- Kansas Data Access & Support Center. 2013. kansasgis.org/catalog (accessed 29 April 2018).
- Katz, B.S., R.L. Stotler, D. Hirmas, G. Ludvigson, J.J. Smith, and D.O. Whittemore. 2016. Geochemical recharge estimation and the effects of a declining water table. *Vadose Zo. J.* 15(10). doi:10.2136/vzj2016.04.0031
- Lindau, C.W., and R.F. Spalding. 1984. Major procedural discrepancies in soil extracted nitrate levels and nitrogen isotopic values. *Ground Water* 22(3): 273–278. doi:10.1111/j.1745-6584.1984.tb01399.x
- Ludvigson, G.A., R.S. Sawin, E.K. Franseen, W.L. Watney, R.R. West, and J.J. Smith. 2009. A Review of the Stratigraphy of the Ogallala Formation and Revision of Neogene (“Tertiary”) Nomenclature in Kansas. *Kansas Current Research in Earth Sciences, Bulletin 256 Part 2.* <http://www.kgs.ku.edu/Current/2009/Ludvigson/Bull256part2.pdf> (accessed 29 April 2018).
- Maher, B. A. 2016. Palaeoclimatic records of the loess/palaeosol sequences of the Chinese Loess Plateau. *Quaternary Science Reviews*, 154, 23–84. <https://doi.org/10.1016/j.quascirev.2016.08.004>
- Maher, B. A., and R. Thompson. 1991. Mineral magnetic record of the Chinese loess and paleosols. *Geology*, 19(1), 3–6. [https://doi.org/10.1130/0091-7613\(1991\)019<0003:MMROTC>2.3.CO;2](https://doi.org/10.1130/0091-7613(1991)019<0003:MMROTC>2.3.CO;2)

- Mason, J. A., P.M. Jacobs, R.S.B. Greene, and W.D. Nettleton. 2003. Sedimentary aggregates in the Peoria Loess of Nebraska, USA. *Catena*, 53, 377–397. [https://doi.org/10.1016/S0341-8162\(03\)00073-0](https://doi.org/10.1016/S0341-8162(03)00073-0)
- Maupin, M.A. and N.L. Barber. 2005. Estimated withdrawals from principal aquifers in the United States, 2000. U.S. Geological Survey Circular 1279. <https://pubs.usgs.gov/circ/2005/1279/pdf/circ1279.pdf> (accessed 29 April 2018).
- McGuire, V.L. (2009) Water-level changes in the High Plains aquifer, predevelopment to 2007, 2005-06, and 2006-07. U.S. Geological Survey Scientific Investigations Report 2009-5019., 9 p. available at <http://pubs.usgs.gov/sir/2009/5019/>.
- McMahon, P.B., K.F. Dennehy, B.W. Bruce, J.K. Böhlke, R.L. Michel, J.J. Gurdak, and D.B. Hurlbut. 2006. Storage and transit time of chemicals in thick unsaturated zones under rangeland and irrigated cropland, High Plains, United States. *Water Resour. Res.* 42(3). doi:10.1029/2005WR004417
- Meixner, T., A.H. Manning, D.A. Stonestrom, D.M. Allen, H. Ajami, K.W. Blasch, A.E. Brookfield, C.L. Castro, J.F. Clark, D.J. Gochis, A.L. Flint, K.L. Neff, R. Niraula, M. Rodell, B.R. Scanlon, K. Singha, and M.A. Walvoord. 2016. Implications of projected climate change for groundwater recharge in the western United States. *J. Hydrol.* 534. doi:10.1016/j.jhydrol.2015.12.027
- Meyers, P.A., and Teranes, J.L., 2001. Sediment organic matter. In: Last, W.M., and Smol, J.P. (eds.) *Tracking Environmental Changes Using Lake Sediment*, Vol. 2: Physical and Geochemical Methods. Kluwer Academic, Dordrecht, p. 239-270.
- Nativ, R. , and R. Riggio. 1990. Precipitation in the Southern High Plains: meteorologic and isotopic features. *J. of Geophysical Res.* 95(D13): 22,559-22,564. doi:10.1029/JD095iD13p22559
- Nimmo, J.R. 2010. Theory for Source-Responsive and Free-Surface Film Modeling of Unsaturated Flow. *Vadose Zo. J.* 9(2): 295-306. doi: 10.2136/vzj2009.0085
- Sandström, H., Reeder, S., Bartha, A., Birke, M., Berge, F., Davidsen, B., Grimstvedt, A., Hagel-Brunnström, M. L., Kantor, W., Kallio, E. (2005). Sample preparation and analysis. *FOREGS Geochemical Atlas of Europe, Part 1*.
- Ode, D. J., Tieszen, L. L., & Lerman, J. C. (1980). The Seasonal Contribution of C3 and C4 Plant-Species to Primary Production in a Mixed Prairie. *Ecology*, 61, 1304–1311.
- O'Leary, M. H. (1981). Carbon isotope fractionation in plants. *Phytochemistry*, 20(4), 553–567. [https://doi.org/10.1016/0031-9422\(81\)85134-5](https://doi.org/10.1016/0031-9422(81)85134-5)
- O'Leary, M. H. (1988). Carbon Isotopes in Photosynthesis. *BioScience*, 38(5), 328–336. <https://doi.org/10.2307/1310735>
- Scanlon, B.R. 1999. Reply. *Water Resour. Res.* 35(2): 603–604. doi:10.1029/1998WR900073
- Scanlon, B.R., and R.S. Goldsmith. 1997. Field study of spatial variability in unsaturated flow beneath and adjacent to playas. *Water Resour. Res.* 33(10): 2239-2252. doi:10.1029/97WR01332
- Scanlon, B.R. 1991. Evaluation of moisture flux from chloride data in desert soils. *J. Hydrol.* 128(1–4): 137–156. doi:10.1016/0022-1694(91)90135-5
- Scanlon, B.R., D.A. Stonestrom, R.C. Reedy, F.W. Leeane, J. Gates, and R.G. Cresswell (2009). Inventories and mobilization of unsaturated zone sulfate, fluoride, and chloride related to land use change in semiarid regions, southwestern United States and Australia. *Water Resources Research*, 45, doi: 10.1029/2008WR006963.
- Scanlon, B.R., C.C. Faunt, L. Longuevergne, R.C. Reedy, W.M. Alley, V.L. McGuire, and P.B.

- McMahon. 2012. Groundwater depletion and sustainability of irrigation in the US High Plains and Central Valley. Proc. Natl. Acad. Sci. 109(24): 9320–9325.
doi:10.1073/pnas.1200311109
- Šimůnek, J., M. Sejna, H. Saito, M. Sakai, and M.Th. van Genuchten. 2009. The HYDRUS-1D software package for simulating the one-dimensional movement of water, heat, and multiple solutes in variably-saturated media. Dep. of Environ. Sci., Univ. of Calif., Riverside. Version 4.08. https://www.pc-progress.com/Downloads/Pgm_hydrus1D/HYDRUS1D-4.08.pdf (accessed 29 April 2018).
- Singer, M. J., and P. Fine. 1989. Pedogenic Factors Affecting Magnetic Susceptibility of Northern California Soils. *Soil Science Society of America Journal*, 53(4), 1119–1127. <https://doi.org/10.2136/sssaj1989.03615995005300040023x>
- Singer, M. J., and K.L. Verosub. 2007. Magnetic Mineral Analysis. In *In: Elias S (ed) The encyclopedia of Quaternary sciences* (pp. 2096–2102).
- Smith, L.M., 2003. Playas of the Great Plains. University of Texas Press, Austin.
- Stevenson, F. J., & Cole, M. A. (1999). *Cycles of Soils: Carbon, Nitrogen, Phosphorus, Sulfur, Micronutrients*. John Wiley & Sons.
- Stonestrom, D.A., D.E. Prudic, R.J. Laczniak, K.C. Akstin, R.A. Boyd, and K.K. Henleman. 2003. Estimates of Deep percolation Beneath Native Vegetation, Irrigated Fields, and the Amargosa-River Channel, Amargosa Desert, Nye County, Nevada. USGS Open File Rep. 03-104: 83. https://pubs.usgs.gov/of/2003/ofr03-104/pdf/OFR-03-104_ver1.02.pdf (accessed 29 April 2018).
- United States Department of Agriculture, N.R.C.S. 2017. Web Soil Survey. <https://websoilsurvey.sc.egov.usda.gov> (accessed 29 April 2018).
- United States Dept of Agriculture. Natural Resource Conservation Service. Official Soil Series Descriptions and Series Classification. <https://soilseries.sc.egov.usda.gov/> (accessed 29 April 2018).
- Water Information Management and Analysis System, ver 5. 2018. Kansas Geological Survey. University of Kansas, Lawrence. http://hercules.kgs.ku.edu/geohydro/wimas/query_setup.cfm?CFID=10418598&CFTOKEN=59269962&jsessionid=5a30126580006d6c56d5 (accessed 29 April 2018).
- Whittemore, D.O. 1995. Geochemical differentiation of oil and gas brine from other saltwater sources contaminating water resources: Case studies from Kansas and Oklahoma. *Environ. Geosci.* 2(1): 15–31. ISSN: 1075-9565.
- Whittemore, D.O., J.J. Butler Jr., and B.B. Wilson. 2016. Assessing the major drivers of water-level declines: new insights into the future of heavily stressed aquifers. *Hydrological Sciences Journal*. 61(1): 134-145.
- Wills, S. A., Burras, C. L., & Sandor, J. A. (2007). Prediction of Soil Organic Carbon Content Using Field and Laboratory Measurements of Soil Color. *Soil Science Society of America Journal*, 71(2), 380–388. <https://doi.org/10.2136/sssaj2005.0384>
- Wilson, R.D. 2010. Evaluating hydroperiod response in the Rainwater Basin wetlands of south-central Nebraska. University of Nebraska-Lincoln. Master's Thesis. <https://digitalcommons.unl.edu/cgi/viewcontent.cgi?article=1009&context=natresdiss> (accessed 29 April 2018)
- Wood, W.W. 1997. Comment on “Field study of spatial variability in unsaturated flow beneath and adjacent to playas.” *Water Resour. Res.* 33(2): 2239–2252.
doi:10.1029/1998WR900072

Wood, W.W., and W.E. Sanford. 1995. Chemical and isotopic methods for quantifying groundwater recharge in a regional, semiarid environment. *Ground Water* 33(3): 458–468.
doi:10.1111/j.1745-6584.1995.tb00302.x

Wood, W.W., K.A. Rainwater, and D.B. Thompson. 1997. Quantifying macropore recharge: Examples from a semi-arid area. *Ground Water* 35(6): 1097–1106. doi:10.1111/j.1745-6584.1997.tb00182.x

Appendix A. Outreach

A1. Annual Field Conference 2016 for Policy Makers: West-Central Kansas—Natural Resources, Economics and Decisions for the Future (KGS Open-file Report 2016-23)

This field conference, focused mainly for state legislators, visited the Ehmke Playa site. The image below is of Bill Johnson presenting the case for playa preservation and an explanation of this project's goals and approach. (courtesy of S. Stover)



(S. Stover)

A2. Papers and posters presented at professional meetings

Salley, K., Stotler, R.L., Johnson, W.C., 2017. Investigations of playa hydrology and recharge flux to the High Plains aquifer at Ehmke Playa in western Kansas: Governor's Conference on the Future of Water in Kansas, Manhattan (KS).

Stotler, R.L., Johnson, W.C., Salley, K., 2017. Evaluating playas as sources of recharge to the High Plains Aquifer in western Kansas: Governor's Conference on the Future of Water in Kansas, Manhattan (KS).

Salley, K., Stotler, R.L., Johnson, W.C., Investigations of playa hydrology and recharge flux to the High Plains aquifer at Ehmke Playa in western Kansas: Geological Society of America, Seattle.

Stotler, R.L., Johnson, W.C., Burt, D.J., Bowen, M.W., Salley, K., 2017. Investigations of playa basins as point source recharge to the High Plains Aquifer: 22nd Annual Informational Seminar, Grand Island, NE.

Johnson, W.C., Burt, D.J., Bowen, M.W., Stotler, R.L., Salley, K., 2016. An investigation into playa basins as a point source for recharge of the High Plains Aquifer, Kansas: Governor's Conference on the Future of Water in Kansas, Manhattan (KS).

Johnson, W.C., Stotler, R., Bowen, M.W., 2016. Playa basins as a point source for recharge of the High Plains Aquifer, Central Great Plains, USA: Geological Society of America, Denver.

Stotler, R.L., Butler, J.J., Hirmas, D.R., Johnson, W.C., Katz, B., Knobbe, S.J., Layzell, A.L., Long, M.M., Ludvigson, G.A., Reboulet, E.C., Smith, J.J., Whittemore, D.O., 2016. Understanding the role of geology on recharge to and production from the High Plains Aquifer in Kansas: Geological Society of America, Denver.

Bowen, M.W., Johnson, W.C., 2016. Evaluating the effects of environmental change on High Plains playa wetlands from the Pleistocene-Holocene transition through the Anthropocene: American Quaternary Association.

Goldade, M.M., Kastens, J.H., Johnson, W.C., 2016. Playa Wetland Morphological Analyses in Western Kansas: Governor's 4th Annual Water Conference on the Future of Water in Kansas, Manhattan, KS.

Goldade, M.M., Johnson, W.C., Kastens, J.H., Bowen, M.W., 2015. A Morphometric and Spatial Perspective on Playas in the High Plains of Kansas: Association of American Geographers, San Francisco.

Johnson, W.C., 2015. The Geology and Formation of Playa Wetlands. Rainwater Basin Joint Venture Informational Seminar, Grand Island, NE.

Appendix B. Data

B1. Physical and chemical data from near-surface and vadose zone cores

Table 1. A2 (upper bench south) magnetic susceptibility*.

Sample	Depth (cm)	LF Mag. Sus. 3 Pt		LF Mag. Sus. 5 Pt		LF Mag. Sus. 3 Pt		Frequency Dep. Mag. Sus.	Frequency Dep. 3 Pt Avg	Frequency Dep. 5 Pt Avg
		Sus.	Avg	Sus.	Avg	Sus.	Avg			
A2-1	0.0		83.11					4.74		
A2-2	5.0	80.55		82.12			80.55	1.72	3.04	
A2-3	10.0	77.36		76.41	77.56	77.36		2.66	2.62	3.55
A2-4	15.0	74.18		73.57	75.88	74.18		3.47	3.76	3.27
A2-5	20.0	73.62		72.57	74.47	73.62		5.15	3.99	3.73
A2-6	25.0	74.13		74.73	74.54	74.13		3.34	4.17	4.00
A2-7	30.0	75.51		75.09	75.44	75.51		4.01	3.79	4.27
A2-8	35.0	76.63		76.73	77.08	76.63		4.02	4.28	4.00
A2-9	40.0	78.54		78.09	79.04	78.54		4.81	4.21	4.08
A2-10	45.0	81.12		80.80	81.56	81.12		3.81	4.12	3.99
A2-11	50.0	84.32		84.48	84.29	84.32		3.73	3.71	3.73
A2-12	55.0	87.53		87.69	87.44	87.53		3.59	3.34	3.30
A2-13	60.0	90.63		90.42	89.93	90.63		2.70	2.99	3.10
A2-14	65.0	92.49		93.80	91.04	92.49		2.68	2.73	3.13
A2-15	70.0	92.37		93.27	90.43	92.37		2.82	3.13	3.05
A2-16	75.0	89.32		90.05	88.14	89.32		3.89	3.30	3.14
A2-17	80.0	84.55		84.63	85.65	84.55		3.18	3.40	3.41
A2-18	85.0	81.65		78.96	83.79	81.65		3.11	3.45	3.67
A2-19	90.0	81.42		81.35	82.68	81.42		4.04	3.76	3.55
A2-20	95.0	83.27		83.96	82.68	83.27		4.12	3.82	3.63
A2-21	100.0	84.37		84.49	83.07	84.37		3.31	3.66	3.68
A2-22	105.0	83.35		84.65	82.32	83.35		3.56	3.41	3.36
A2-23	110.0	81.05		80.91	81.72	81.05		3.36	3.13	2.74
A2-24	115.0	79.82		77.60	81.74	79.82		2.45	2.28	2.74
A2-25	130.0	81.05		80.97	82.12	81.05		1.04	2.26	2.73
A2-26	135.0	84.03		84.57	81.85	84.03		3.29	2.61	2.48
A2-27	140.0	83.56		86.55	83.28	83.56		3.49	2.97	2.68
A2-28	145.0	83.62		79.57	82.64	83.62		2.13	3.03	3.39
A2-29	150.0	80.69		84.73	81.45	80.69		3.47	3.39	3.82
A2-30	155.0	80.38		77.77	79.58	80.38		4.56	4.49	3.77
A2-31	160.0	77.87		78.62	78.85	77.87		5.44	4.42	4.04
A2-32	165.0	77.25		77.20	77.30	77.25		3.25	4.05	4.22
A2-33	170.0	76.71		75.93	77.15	76.71		3.47	3.70	4.10
A2-34	175.0	76.64		76.98	76.97	76.64		4.37	3.94	3.70
A2-35	180.0	77.24		77.00	77.47	77.24		3.99	3.93	3.54
A2-36	185.0	78.15		77.75	79.78	78.15		3.44	3.29	3.36
A2-37	190.0	81.63		79.70	80.64	81.63		2.43	2.81	3.12
A2-38	195.0	82.82		87.45	80.80	82.82		2.56	2.73	2.88

A2-39	200.0	82.19	81.32	81.62	82.19	3.19	2.84	3.02
A2-40	205.0	80.32	77.81	77.64	80.32	2.75	3.37	3.22
A2-41	210.0	73.14	81.84	67.47	73.14	4.15	3.46	3.54
A2-42	215.0	59.40	59.78	57.36	59.40	3.46	3.92	3.82
A2-43	220.0	42.38	36.58	47.11	42.38	4.14	4.06	4.22
A2-44	225.0	31.31	30.78	35.21	31.31	4.58	4.50	3.91
A2-45	230.0	26.56	26.57	26.76	26.56	4.79	3.98	3.88
A2-46	235.0	22.15	22.34	23.89	22.15	2.58	3.56	3.05
A2-47	240.0	20.71	17.55	22.92	20.71	3.32	1.96	2.25
A2-48	255.0	21.89	22.23	23.13	21.89	0.00	1.30	1.87
A2-49	260.0	25.26	25.91	24.48	25.26	0.58	1.15	1.42
A2-50	265.0	27.55	27.64	27.95	27.55	2.87	1.26	1.15
A2-51	270.0	30.53	29.09	30.60	30.53	0.34	1.72	1.24
A2-52	275.0	33.16	34.86	33.79	33.16	1.95	0.92	1.36
A2-53	280.0	37.40	35.52	37.17	37.40	0.48	1.19	1.01
A2-54	285.0	40.63	41.83	42.18	40.63	1.14	0.91	1.05
A2-55	290.0	46.83	44.53	46.10	46.83	1.12	0.94	0.86
A2-56	295.0	51.05	54.15	48.92	51.05	0.55	0.89	1.24
A2-57	300.0	52.74	54.46	51.48	52.74	0.99	1.31	1.18
A2-58	305.0	52.90	49.62	54.93	52.90	2.39	1.41	1.21
A2-59	310.0	55.35	54.62	56.06	55.35	0.84	1.51	1.48
A2-60	315.0	58.74	61.81	58.04	58.74	1.29	1.34	1.60
A2-61	320.0	61.98	59.79	58.11	61.98	1.88	1.59	1.31
A2-62	325.0	58.04	64.34	57.32	58.04	1.60	1.48	1.57
A2-63	330.0	54.99	50.00	55.40	54.99	0.97	1.56	1.66
A2-64	335.0	50.96	50.64	55.07	50.96	2.12	1.61	1.69
A2-65	340.0	53.67	52.24	52.71	53.67	1.73	1.96	1.64
A2-66	345.0	54.31	58.14	54.02	54.31	2.02	1.71	1.81
A2-67	350.0	55.74	52.56	55.67	55.74	1.38	1.73	1.58
A2-68	355.0	55.99	56.52	54.58	55.99	1.79	1.38	1.56
A2-69	360.0	54.07	58.89	51.89	54.07	0.98	1.46	1.40
A2-70	365.0	50.13	46.79	49.65	50.13	1.61	1.28	1.51
A2-71	375.0	44.28	44.71	47.36	44.28	1.24	1.59	1.42
A2-72	380.0	43.71	41.32	45.98	43.71	1.92	1.50	1.59
A2-73	385.0	46.12	45.11	43.60	46.12	1.33	1.69	2.01
A2-74	390.0	43.98	51.94	41.73	43.98	1.82	2.29	2.12
A2-75	395.0	40.74	34.90	39.59	40.74	3.71	2.45	2.70
A2-76	400.0	33.64	35.37	35.19	33.64	1.81	3.44	2.47
A2-77	405.0	29.71	30.65	31.39	29.71	4.80	2.27	2.24
A2-78	410.0	28.89	23.10	31.07	28.89	0.21	1.88	1.74
A2-79	415.0	29.78	32.93	29.94	29.78	0.64	0.70	1.83
A2-80	420.0	31.98	33.31	30.35	31.98	1.25	1.38	1.25
A2-81	425.0	31.91	29.71	32.23	31.91	2.24	1.79	1.33
A2-82	430.0	31.64	32.70	32.20	31.64	1.88	1.58	1.44
A2-83	435.0	32.66	32.49	32.01	32.66	0.61	1.23	1.36
A2-84	440.0	32.55	32.77	32.79	32.55	1.21	0.89	1.10
A2-85	445.0	32.92	32.38	32.60	32.92	0.84	1.00	1.03
A2-86	450.0	32.59	33.61	32.12	32.59	0.96	1.11	0.81
A2-87	455.0	31.82	31.77	31.04	31.82	1.53	0.67	0.50
A2-88	460.0	29.73	30.08	31.47	29.73	-0.48	0.23	0.66

A2-89	465.0	30.67	27.34	31.04	30.67	-0.36	0.27	1.03
A2-90	470.0	31.12	34.57	31.26	31.12	1.66	1.37	1.04
A2-91	475.0	32.95	31.43	31.82	32.95	2.81	2.02	1.22
A2-92	480.0	32.40	32.86	31.49	32.40	1.59	1.60	1.92
A2-93	485.0	30.48	32.91	29.67	30.48	0.41	1.71	1.70
A2-94	500.0	28.02	25.68	29.08	28.02	3.14	1.36	1.52
A2-95	505.0	26.54	25.46	29.11	26.54	0.54	1.86	1.39
A2-96	510.0	28.99	28.47	30.94	28.99	1.90	1.13	1.62
A2-97	515.0	34.53	33.02	33.56	34.53	0.94	1.48	1.28
A2-98	520.0	37.95	42.08	35.59	37.95	1.59	1.31	1.74
A2-99	525.0	38.82	38.75	36.26	38.82	1.39	1.95	1.78
A2-100	530.0	35.40	35.62	35.22	35.40	2.87	2.12	1.91
A2-101	535.0	31.75	31.83	32.22	31.75	2.09	2.18	2.07
A2-102	540.0	28.92	27.80	28.79	28.92	1.57	2.03	2.13
A2-103	545.0	25.50	27.11	25.08	25.50	2.44	1.89	1.76
A2-104	550.0	21.92	21.57	21.55	21.92	1.67	1.71	1.56
A2-105	555.0	17.61	17.09	19.88	17.61	1.02	1.27	1.47
A2-106	560.0	16.90	14.16	18.87	16.90	1.12	1.08	1.18
A2-107	565.0	18.56	19.46		18.56	1.09	1.07	
A2-108	570.0		22.07			1.02		

* Low frequency (LF) and high frequency (HF) susceptibility are expressed in international standard units. Frequency dependence of susceptibility is expressed in percent (%).

Table 2. A3 (bench south) magnetic susceptibility*.

Sample	Depth (cm)	LF Mag. Sus. 3 Pt		LF Mag. Sus. 5 Pt		LF Mag. Sus. 3 Pt		Frequency Dep. Mag. Sus.	Frequency Dep. 3 Pt Avg	Frequency Dep. 5 Pt Avg
		Dep.	Avg	Dep.	Avg	Dep.	Avg			
A3-1	0.0			75.44				3.4985		
A3-2	2.6	77.55		81.77		77.55		2.0420	2.9291	
A3-3	5.2	74.66		75.42	72.72	74.66		3.2468	2.5308	2.6623
A3-4	7.8	68.79		66.79	70.57	68.79		2.3035	2.5903	2.4658
A3-5	10.4	65.22		64.16	67.04	65.22		2.2207	2.3468	2.5207
A3-6	13.0	64.33		64.70	65.16	64.33		2.5162	2.3511	2.3990
A3-7	15.6	64.95		64.13	65.37	64.95		2.3163	2.4902	2.2769
A3-8	18.2	65.99		66.00	66.22	65.99		2.6382	2.2158	2.2542
A3-9	20.8	67.43		67.84	67.79	67.43		1.6929	2.1461	2.3091
A3-10	23.4	69.60		68.44	69.60	69.60		2.1073	2.1969	2.4528
A3-11	26.0	71.38		72.51	71.36	71.38		2.7907	2.6443	2.4666
A3-12	28.6	73.51		73.19	73.12	73.51		3.0350	2.8442	2.6525
A3-13	31.2	74.87		74.82	74.88	74.87		2.7070	2.7881	2.7151
A3-14	33.8	76.23		76.61	76.24	76.23		2.6224	2.5833	2.8526
A3-15	36.4	77.72		77.27	77.71	77.72		2.4207	2.8403	2.8955
A3-16	39.0	79.04		79.29	79.65	79.04		3.4778	3.0493	2.9645
A3-17	41.6	81.45		80.57	81.57	81.45		3.2495	3.2597	3.0851
A3-18	44.2	83.77		84.49	83.81	83.77		3.0520	3.1758	3.1708

A3-19	46.8	86.39	86.24	86.08	86.39	3.2258	3.0422	3.0701
A3-20	49.4	88.44	88.43	88.56	88.44	2.8489	3.0163	2.9548
A3-21	52.0	90.69	90.65	90.76	90.69	2.9743	2.8321	3.0619
A3-22	54.6	93.04	92.99	92.89	93.04	2.6731	3.0783	2.9857
A3-23	57.2	95.12	95.47	94.96	95.12	3.5876	3.0351	3.1389
A3-24	59.8	97.06	96.90	96.75	97.06	2.8446	3.3491	3.1318
A3-25	62.4	98.43	98.80	98.73	98.43	3.6149	3.1328	3.0762
A3-26	65.0	100.43	99.60	100.25	100.43	2.9388	2.9828	2.8702
A3-27	67.6	101.85	102.89	102.28	101.85	2.3947	2.6305	2.7072
A3-28	70.2	104.33	103.05	104.48	104.33	2.5580	2.3273	2.6950
A3-29	72.8	106.63	107.04	106.09	106.63	2.0293	2.7138	2.4977
A3-30	75.4	108.17	109.80	107.06	108.17	3.5542	2.5120	2.5847
A3-31	78.0	108.41	107.67	107.51	108.41	1.9525	2.7787	2.5424
A3-32	80.6	106.90	107.75	106.58	106.90	2.8294	2.3761	2.5753
A3-33	83.2	105.15	105.29	105.22	105.15	2.3464	2.4566	2.5447
A3-34	85.8	103.57	102.40	104.00	103.57	2.1941	2.6471	2.4771
A3-35	88.4	102.32	103.00	102.67	102.32	3.4008	2.4033	2.5070
A3-36	91.0	101.89	101.56	101.30	101.89	1.6149	2.6648	2.4425
A3-37	93.6	100.37	101.12	100.14	100.37	2.9787	2.2059	2.7207
A3-38	96.2	98.71	98.43	98.31	98.71	2.0241	2.8626	2.3378
A3-39	98.8	96.29	96.58	96.43	96.29	3.5851	2.3651	2.5072
A3-40	101.4	94.20	93.85	94.15	94.20	1.4860	2.5111	2.5554
A3-41	104.0	91.91	92.16	92.23	91.91	2.4622	2.3892	2.8292
A3-42	106.6	90.23	89.73	90.63	90.23	3.2194	3.0250	2.6590
A3-43	109.2	89.05	88.81	88.93	89.05	3.3933	3.1156	2.9436
A3-44	111.8	87.58	88.60	87.70	87.58	2.7342	3.0122	2.7005
A3-45	114.4	86.65	85.33	86.46	86.65	2.9091	2.2965	2.4329
A3-46	117.0	84.97	86.02	85.10	84.97	1.2463	2.0124	2.2967
A3-47	119.6	83.85	83.56	82.75	83.85	1.8817	1.9467	2.2507
A3-48	122.2	80.80	81.97	80.31	80.80	2.7120	2.3660	2.2664
A3-49	124.8	77.32	76.86	76.57	77.32	2.5043	2.7346	2.5724
A3-50	127.4	72.44	73.12	73.78	72.44	2.9876	2.7560	2.6414
A3-51	130.0	70.01	67.34	70.30	70.01	2.7761	2.6635	2.7525
A3-52	132.6	67.17	69.58	67.54	67.17	2.2267	2.7569	2.7483
A3-53	135.2	65.75	64.59	65.63	65.75	3.2680	2.6593	2.7860
A3-54	137.8	63.74	63.08	64.19	63.74	2.4832	2.9756	2.8984
A3-55	140.4	62.27	63.54	61.46	62.27	3.1757	2.9990	3.2530
A3-56	143.0	59.88	60.17	58.70	59.88	3.3382	3.5046	3.1729
A3-57	145.6	55.62	55.92	56.16	55.62	4.0000	3.4019	3.3684
A3-58	148.2	52.36	50.77	52.94	52.36	2.8674	3.4426	3.4309
A3-59	150.8	49.53	50.40	49.60	49.53	3.4605	3.2721	3.7156
A3-60	153.4	47.10	47.43	46.93	47.10	3.4884	3.9036	3.6954
A3-61	156.0	44.50	43.47	44.43	44.50	4.7619	4.0497	3.3469
A3-62	158.6	41.43	42.59	40.84	41.43	3.8988	3.2619	2.9365
A3-63	161.2	37.76	38.24	36.11	37.76	1.1250	2.1441	2.6264
A3-64	163.8	31.50	32.45	32.77	31.50	1.4085	1.4905	2.1120
A3-65	166.4	27.68	23.80	28.90	27.68	1.9380	1.8454	1.8161
A3-66	169.0	24.60	26.78	25.15	24.60	2.1898	2.1824	1.3906
A3-67	171.6	23.17	23.22	22.24	23.17	2.4194	1.2022	1.0543
A3-68	174.2	20.20	19.50	20.80	20.20	-1.0025	0.3812	0.6123

A3-69	176.8	18.00	17.89	18.78	18.00	-0.2732	-0.5158	-0.2302
A3-70	179.4	17.05	16.62	17.58	17.05	-0.2717	-0.8560	-0.5121
A3-71	182.0	16.84	16.65	17.24	16.84	-2.0231	-0.4283	-0.1645
A3-72	184.6	17.23	17.25	17.38	17.23	1.0101	-0.0926	-0.1593
A3-73	187.2	17.87	17.79	17.89	17.87	0.7353	0.4995	-0.1049
A3-74	189.8	18.52	18.58	18.34	18.52	-0.2469	0.1628	-0.4410
A3-75	192.4	18.89	19.19	18.72	18.89	0.0000	-1.3169	-1.2696
A3-76	195.0	19.07	18.92	19.07	19.07	-3.7037	-2.2787	-1.0393
A3-77	197.6	19.19	19.11	18.80	19.19	-3.1325	-1.6498	-0.7645
A3-78	200.2	18.63	19.56	18.27	18.63	1.8868	-0.0397	-0.5931
A3-79	202.8	17.78	17.23	18.07	17.78	1.1268	1.2902	0.0343
A3-80	205.4	17.24	16.54	17.71	17.24	0.8571	0.4724	-0.3134
A3-81	208.0	17.26	17.94	18.73	17.26	-0.5666	-1.5268	-0.5059
A3-82	210.6	19.96	17.29	21.84	19.96	-4.8711	-1.5045	-0.7313
A3-83	213.2	24.91	24.66	31.83	24.91	0.9242	-1.3156	-0.5617
A3-84	215.8	41.30	32.79	40.71	41.30	0.0000	0.8764	-0.1472
A3-85	218.4	53.86	66.45	49.36	53.86	1.7050	1.0703	1.1944
A3-86	221.0	63.11	62.35	51.88	63.11	1.5060	1.6826	1.2033
A3-87	223.6	53.39	60.54	50.19	53.39	1.8369	1.4371	1.5391
A3-88	226.2	40.71	37.27	41.59	40.71	0.9685	1.4948	1.2385
A3-89	228.8	28.35	24.32	33.95	28.35	1.6791	0.9499	0.8971
A3-90	231.4	23.98	23.46	26.48	23.98	0.2020	0.5600	0.5690
A3-91	234.0	23.60	24.17	24.27	23.60	-0.2012	0.0658	0.4876
A3-92	236.6	24.53	23.16	25.39	24.53	0.1965	0.1857	0.1198
A3-93	239.2	26.44	26.25	27.88	26.44	0.5618	0.1993	0.2774
A3-94	241.8	30.69	29.91	30.13	30.69	-0.1603	0.4639	-0.2839
A3-95	244.4	33.75	35.89	33.05	33.75	0.9901	-0.7259	-0.7197
A3-96	247.0	36.36	35.45	34.97	36.36	-3.0075	-1.3334	-0.2479
A3-97	249.6	36.35	37.75	39.67	36.35	-1.9827	-0.6898	0.6957
A3-98	252.2	42.34	35.84	42.49	42.34	2.9207	1.8319	0.9817
A3-99	254.8	46.43	53.44	45.17	46.43	4.5576	3.2995	1.7559
A3-100	257.4	50.76	50.00	47.27	50.76	2.4201	2.6138	2.2829
A3-101	260.0	49.02	48.83	50.48	49.02	0.8637	1.3121	1.7863
A3-102	262.6	49.66	48.25	50.57	49.66	0.6524	0.6513	0.9289
A3-103	265.2	51.35	51.91	50.85	51.35	0.4378	0.4535	0.5740
A3-104	267.8	52.39	53.88	52.38	52.39	0.2703	0.4513	0.5141
A3-105	270.4	53.91	51.37	53.25	53.91	0.6458	0.4935	0.8599
A3-106	273.0	53.48	56.47	54.29	53.48	0.5645	1.1971	0.8039
A3-107	275.6	55.40	52.60	53.69	55.40	2.3810	1.0345	1.0606
A3-108	278.2	53.54	57.13	51.55	53.54	0.1580	1.3643	0.4924
A3-109	280.8	49.56	50.88	49.14	49.56	1.5539	-0.1612	1.7099
A3-110	283.4	45.33	40.67	47.07	45.33	-2.1954	2.0035	1.6316
A3-111	286.0	42.44	44.43	44.36	42.44	6.6519	2.1487	1.4514
A3-112	288.6	43.42	42.22	41.87	43.42	1.9895	2.6328	1.1940
A3-113	291.2	41.41	43.61	40.67	41.41	-0.7431	0.5045	0.7566
A3-114	293.8	38.90	38.41	39.92	38.90	0.2670	-1.6195	-0.8414
A3-115	296.4	37.93	34.67	38.38	37.93	-4.3825	-1.8177	-1.0378
A3-116	299.0	36.63	40.70	37.26	36.63	-1.3378	-1.5710	-0.6849
A3-117	301.6	37.74	34.51	36.76	37.74	1.0072	0.2304	-0.4809
A3-118	304.2	36.15	38.01	36.69	36.15	1.0217	1.1053	0.5830

A3-119	306.8	36.08	35.94	34.57	36.08	1.2870	1.0819	0.5271
A3-120	309.4	33.45	34.30	34.02	33.45	0.9371	0.2021	0.0931
A3-121	312.0	32.05	30.12	33.50	32.05	-1.6176	-0.6145	0.5486
A3-122	314.6	32.43	31.73	32.89	32.43	-1.1628	0.1730	0.0708
A3-123	317.2	33.35	35.43	31.81	33.35	3.2995	0.3449	0.0307
A3-124	319.8	32.39	32.88	30.35	32.39	-1.1019	0.9780	0.3542
A3-125	322.4	28.19	28.87	28.51	28.19	0.7364	-0.1219	0.3884
A3-126	325.0	24.75	22.82	26.40	24.75	0.0000	-0.0852	-0.7160
A3-127	327.6	23.42	22.56	24.86	23.42	-0.9921	-1.0714	-0.4184
A3-128	330.2	24.21	24.88	24.50	24.21	-2.2222	-0.9427	-0.6392
A3-129	332.8	25.71	25.17	26.34	25.71	0.3861	-0.7346	-0.6673
A3-130	335.4	28.08	27.06	27.74	28.08	-0.3676	-0.0407	-0.4995
A3-131	338.0	29.54	32.00	29.05	29.54	-0.1406	-0.2204	-0.1791
A3-132	340.6	31.01	29.57	29.62	31.01	-0.1529	-0.3046	-0.2251
A3-133	343.2	29.68	31.46	29.12	29.68	-0.6202	-0.2057	-0.1515
A3-134	345.8	28.02	28.02	27.93	28.02	0.1560	-0.1547	-0.2970
A3-135	348.4	26.20	24.57	27.56	26.20	0.0000	-0.2373	-0.4661
A3-136	351.0	26.11	26.02	26.14	26.11	-0.8681	-0.6221	-0.4490
A3-137	353.6	26.04	27.75	26.00	26.04	-0.9983	-0.8004	-0.8512
A3-138	356.2	26.47	24.35	26.32	26.47	-0.5348	-1.1293	-0.9211
A3-139	358.8	25.94	27.32	26.29	25.94	-1.8547	-0.9130	-0.8881
A3-140	361.4	26.46	26.14	25.97	26.46	-0.3497	-0.9691	-0.7638
A3-141	364.0	26.05	25.91	25.65	26.05	-0.7030	-0.4764	-1.7136
A3-142	366.6	24.94	26.11	25.33	24.94	-0.3766	-2.1211	-1.4192
A3-143	369.2	24.87	22.79	25.55	24.87	-5.2838	-2.0145	-1.7224
A3-144	371.8	25.25	25.71	25.55	25.25	-0.3831	-2.5109	-1.7564
A3-145	374.4	26.28	27.24	25.11	26.28	-1.8657	-1.0405	-1.7917
A3-146	377.0	25.69	25.90	25.15	25.69	-0.8726	-1.0973	-0.9266
A3-147	379.6	24.27	23.92	25.00	24.27	-0.5535	-0.7947	-0.8499
A3-148	382.2	23.95	22.98	24.12	23.95	-0.9579	-0.5038	-0.4768
A3-149	384.8	23.60	24.96	23.15	23.60	0.0000	-0.3193	-0.0031
A3-150	387.4	22.95	22.87	23.20	22.95	0.0000	0.4986	-0.0663
A3-151	390.0	22.69	21.04	23.12	22.69	1.4957	0.2087	0.2895
A3-152	392.6	22.59	24.16	22.42	22.59	-0.8696	0.4825	0.4928
A3-153	395.2	22.72	22.57	22.67	22.72	0.8214	0.3227	0.4229
A3-154	397.8	22.72	21.45	23.04	22.72	1.0163	0.4962	0.2392
A3-155	400.4	22.82	24.14	22.83	22.82	-0.3490	0.4147	0.1787
A3-156	403.0	23.38	22.89	22.88	23.38	0.5769	-0.3147	-0.0254
A3-157	405.6	22.94	23.10	23.34	22.94	-1.1719	-0.2647	-0.1036
A3-158	408.2	23.23	22.84	23.95	23.23	-0.1992	-0.2487	-0.0010
A3-159	410.8	24.59	23.74	24.38	24.59	0.6250	0.1967	-0.4188
A3-160	413.4	25.32	27.19	25.55	25.32	0.1642	-0.2409	-0.3719
A3-161	416.0	27.06	25.03	25.58	27.06	-1.5119	-0.7617	-0.2842
A3-162	418.6	25.65	28.96	24.77	25.65	-0.9375	-0.7367	-0.4995
A3-163	421.2	23.88	22.97	23.54	23.88	0.2392	-0.3832	-0.4881
A3-164	423.8	21.24	19.72	22.77	21.24	-0.4515	0.0030	-0.1857
A3-165	426.4	20.64	21.02	21.08	20.64	0.2212	-0.0767	-0.3100
A3-166	429.0	20.90	21.18	20.85	20.90	0.0000	-0.4459	-0.5873
A3-167	431.6	21.16	20.50	21.21	21.16	-1.5590	-0.9021	-0.4970
A3-168	434.2	21.29	21.81	21.70	21.29	-1.1472	-0.9021	-0.4665

A3-169	436.8	22.27	21.55	21.63	22.27	0.0000	-0.2578	-0.4256
A3-170	439.4	21.95	23.44	21.43	21.95	0.3738	0.1928	-0.4195
A3-171	442.0	21.26	20.86	21.10	21.26	0.2045	-0.3167	-0.4793
A3-172	444.6	20.17	19.47	21.08	20.17	-1.5284	-0.9234	-0.8256
A3-173	447.2	20.36	20.17	20.41	20.36	-1.4463	-1.5688	-1.1488
A3-174	449.8	20.57	21.45	19.68	20.57	-1.7316	-1.4734	-1.2900
A3-175	452.4	19.59	20.11	19.46	19.59	-1.2422	-1.1584	-1.3934
A3-176	455.0	18.57	17.23	19.70	18.57	-0.5013	-1.2630	-1.0258
A3-177	457.6	18.97	18.36	19.40	18.97	-2.0455	-0.7184	-0.5843
A3-178	460.2	19.89	21.33	19.23	19.89	0.3914	-0.3926	-0.5734
A3-179	462.8	20.19	19.98	19.99	20.19	0.4762	-0.1067	-0.6988
A3-180	465.4	20.09	19.26	21.43	20.09	-1.1876	-0.6134	-0.4634
A3-181	468.0	21.95	21.02	22.37	21.95	-1.1287	-1.0615	-0.6476
A3-182	470.6	24.21	25.58	23.19	24.21	-0.8681	-0.8423	-0.6229
A3-183	473.2	25.23	26.03	23.20	25.23	-0.5300	-0.2660	-0.5199
A3-184	475.8	23.13	24.08	21.78	23.13	0.6000	-0.2009	-0.2941
A3-185	478.4	19.10	19.27	19.71	19.10	-0.6726	-0.0242	-0.3810
A3-186	481.0	16.15	13.95	17.99	16.15	0.0000	-0.6582	-0.4801
A3-187	483.6	15.53	15.23	16.79	15.53	-1.3021	-0.7759	-0.6465
A3-188	492.0	16.92	17.41	16.59	16.92	-1.0256	-0.8532	-0.7626
A3-189	497.0	17.93	18.11	17.44	17.93	-0.2320	-0.8369	-0.8594
A3-190	499.8	18.18	18.27	18.40	18.18	-1.2531	-0.6565	-0.0423
A3-191	502.5	18.83	18.16	18.40	18.83	-0.4843	0.3488	-0.0859
A3-192	505.3	18.55	20.06	18.32	18.55	2.7837	0.3519	-0.2473
A3-193	508.0	18.40	17.42	18.19	18.40	-1.2438	0.1670	-0.0935
A3-194	510.8	17.57	17.71	18.29	17.57	-1.0390	-0.9223	0.2533
A3-195	513.5	18.00	17.59	18.14	18.00	-0.4843	-0.0911	0.4640
A3-196	516.3	18.52	18.69	17.46	18.52	1.2500	1.5342	0.6478
A3-197	519.0	17.33	19.27	17.56	17.33	3.8369	1.5874	0.5615
A3-198	521.8	17.18	14.03	18.04	17.18	-0.3247	0.6806	0.5185
A3-199	524.5	17.41	18.25	18.13	17.41	-1.4706	-0.8315	0.5762
A3-200	527.3	19.12	19.95	17.95	19.12	-0.6993	-0.2105	0.1254
A3-201	530.0	19.16	19.16	18.70	19.16	1.5385	0.8074	-0.2117
A3-202	532.8	18.43	18.38	18.36	18.43	1.5831	0.3705	0.0824
A3-203	535.5	17.56	17.75	17.87	17.56	-2.0101	-0.1423	0.1739
A3-204	538.3	17.27	16.54	17.84	17.27	0.0000	-0.7507	0.3401
A3-205	541.0	17.70	17.53	17.79	17.70	-0.2421	0.7092	-0.0230
A3-206	543.8	18.22	19.03	18.67	18.22	2.3697	0.6317	0.1395
A3-207	546.5	19.76	18.10	20.35	19.76	-0.2326	0.3132	0.2408
A3-208	549.3	21.73	22.15	21.14	21.73	-1.1976	-0.3078	0.1286
A3-209	552.0	22.85	24.96	22.26	22.85	0.5068	-0.4980	-0.4515
A3-210	554.8	23.69	21.45	22.37	23.69	-0.8032	-0.2758	-1.3162
A3-211	557.5	21.59	24.65	21.38	21.59	-0.5310	-1.9633	-1.0766
A3-212	560.3	20.17	18.66	20.42	20.17	-4.5558	-1.6956	-1.4133
A3-213	563.0	18.67	17.20	21.14	18.67	0.0000	-1.9108	-1.0479
A3-214	565.8	20.80	20.14	21.70	20.80	-1.1765	-0.0509	-0.9417
A3-215	568.5	24.21	25.06	23.62	24.21	1.0239	-0.0509	-0.2482
A3-216	571.3	26.92	27.43	25.86	26.92	0.0000	-0.0216	-0.4072
A3-217	574.0	28.04	28.28	27.36	28.04	-1.0886	-0.6279	-0.4447
A3-218	576.8	28.11	28.41	27.94	28.11	-0.7949	-1.0824	-3.2128

A3-219	579.5	27.99	27.64	27.99	27.99	-1.3636	-4.9917	-3.4057
A3-220	582.3	27.75	27.94	27.83	27.75	-12.8167	-5.0483	-3.1570
A3-221	587.3	27.71	27.67	27.53	27.71	-0.9646	-4.5422	-2.7977
A3-222	590.0	27.36	27.51	27.61	27.36	0.1548	0.0639	-2.4593
A3-223	592.8	27.48	26.89	27.46	27.48	1.0017	0.4950	0.2461
A3-224	595.5	27.37	28.04	27.50	27.37	0.3284	0.6802	0.5034
A3-225	598.3	27.70	27.20	27.83	27.70	0.7105	0.4535	0.2335
A3-226	601.0	28.08	27.87	27.79	28.08	0.3215	-0.0542	-0.2843
A3-227	603.8	27.90	29.18	26.12	27.90	-1.1945	-0.8201	-0.3028
A3-228	606.5	25.18	26.64	25.02	25.18	-1.5873	-0.8487	-0.3638
A3-229	609.3	22.68	19.70	23.36	22.68	0.2358	-0.3153	-0.6878
A3-230	612.0	20.32	21.68	22.54	20.32	0.4057	-0.2191	-0.9011
A3-231	614.8	22.12	19.58	22.47	22.12	-1.2987	-1.0513	-0.9197
A3-232	624.8	23.65	25.11	23.61	23.65	-2.2609	-1.7467	-1.2705
A3-233	627.5	25.61	26.26	24.47	25.61	-1.6807	-1.8197	-1.1552
A3-234	630.3	25.90	25.45	26.17	25.90	-1.5177	-0.7388	-0.8293
A3-235	633.0	26.49	25.98	26.57	26.49	0.9820	-0.0684	-0.3144
A3-236	635.8	27.05	28.04	26.38	27.05	0.3306	0.5422	-0.2204
A3-237	638.5	26.83	27.13	25.93	26.83	0.3140	-0.1888	-0.0330
A3-238	641.3	25.21	25.33	25.41	25.21	-1.2111	-0.4925	-0.1901
A3-239	644.0	23.96	23.16	24.05	23.96	-0.5803	-0.5318	-0.2149
A3-240	646.8	22.61	23.39	23.50	22.61	0.1961	-0.0591	-0.0630
A3-241	649.5	23.00	21.26	22.88	23.00	0.2070	0.4922	0.0662
A3-242	652.3	22.62	24.35	21.40	22.62	1.0733	0.2385	-0.0310
A3-243	655.0	20.79	22.25	19.94	20.79	-0.5650	-0.1861	-0.0158
A3-244	657.8	18.03	15.76	20.14	18.03	-1.0667	-0.4531	0.0631
A3-245	660.5	18.03	16.07	18.61	18.03	0.2725	-0.0643	0.5237
A3-246	663.3	18.34	22.28	17.07	18.34	0.6012	1.4168	1.1479
A3-247	666.0	17.84	16.68	16.61	17.84	3.3766	2.1779	1.1057
A3-248	668.8	14.90	14.57	16.14	14.90	2.5559	1.5515	0.6819
A3-249	671.5	13.91	13.45	13.94	13.91	-1.2780	-0.1894	0.4084
A3-250	674.3	12.82	13.70	12.54	12.82	-1.8462	-1.2968	-0.4393
A3-251	677.0	11.56	11.30	11.37	11.56	-0.7663	-1.1582	-1.2505
A3-252	679.8	9.90	9.69	10.62	9.90	-0.8621	-1.0428	-0.4616
A3-253	682.5	9.36	8.70	9.79	9.36	-1.5000	0.1015	0.5217
A3-254	685.3	9.32	9.69	9.88	9.32	2.6667	1.4123	2.0852
A3-255	688.0	10.34	9.57	10.08	10.34	3.0702	4.2627	2.4866
A3-256	690.8	10.67	11.76	10.38	10.67	7.0513	3.7555	4.0230
A3-257	693.5	10.88	10.66	10.44	10.88	1.1450	4.7927	4.8959
A3-258	696.3	10.29	10.23	10.60	10.29	6.1818	4.7860	4.9637
A3-259	699.0	10.19	9.98	10.35	10.19	7.0312	5.5407	3.3320
A3-260	701.8	10.29	10.34	10.38	10.29	3.4091	3.1111	2.8800
A3-261	704.5	10.56	10.55	10.22	10.56	-1.1070	0.3956	1.6436
A3-262	707.3	10.26	10.79	10.19	10.26	-1.1152	-0.7408	-0.0764
A3-263	710.0	10.02	9.44	10.08	10.02	0.0000	-0.8946	-0.9188
A3-264	712.8	9.69	9.83	9.87	9.69	-1.5686	-0.7906	-0.6974
A3-265	715.5	9.71	9.81	9.61	9.71	-0.8032	-0.7906	0.0298
A3-266	718.3	9.59	9.50	9.65	9.59	0.0000	0.5726	0.4235
A3-267	721.0	9.54	9.44	9.30	9.54	2.5210	1.4965	0.3769
A3-268	723.8	9.07	9.68	9.25	9.07	1.9685	0.8959	1.0137

A3-269	726.5	9.09	8.08	8.17	9.09	-1.8018	0.8492	2.8887
A3-270	729.3	7.24	9.52	7.37	7.24	2.3810	3.3181	1.7223
A3-271	732.0	6.35	4.11	6.82	6.35	9.3750	2.8149	0.5956
A3-272	734.8	5.50	5.44	6.51	5.50	-3.3113	0.7996	-0.1091
A3-273	737.5	6.30	6.97	5.63	6.30	-3.6649	-4.1005	0.6177
A3-274	740.3	6.19	6.50		6.19	-5.3254	-0.9918	
A3-275	743.0		5.12			6.0150		

* Low frequency (LF) and high frequency (HF) susceptibility are expressed in international standard units. Frequency dependence of susceptibility is expressed in percent (%).

Table 3. A4 (bench west) magnetic susceptibility*.

Sample	Depth (cm)	LF Mag. Sus. 3 Pt		LF Mag. Sus. 5 Pt		LF Mag. Sus. 3 Pt		Frequency Dep. Mag. Sus.	Frequency Dep. 3 Pt Avg	Frequency Dep. 5 Pt Avg
		Dep.	Avg	Dep.	Avg	Dep.	Avg			
A4-1	1.0			24.35				2.5945		
A4-2	6.0	25.94		27.32		25.94		4.1911	1.8632	
A4-3	11.0	26.46		26.14	25.97	26.46		-1.1961	1.8850	2.9072
A4-4	16.0	26.05		25.91	25.65	26.05		2.6600	2.5835	2.5678
A4-5	21.0	24.94		26.11	25.33	24.94		6.2865	3.2814	3.2381
A4-6	26.0	24.87		22.79	25.55	24.87		0.8975	4.9088	4.4670
A4-7	31.0	25.25		25.71	25.55	25.25		7.5424	4.4628	4.8115
A4-8	36.0	26.28		27.24	25.11	26.28		4.9486	5.6245	4.6250
A4-9	41.0	25.69		25.90	25.15	25.69		4.3825	4.8950	5.8970
A4-10	46.0	24.27		23.92	25.00	24.27		5.3539	5.6647	5.4633
A4-11	51.0	23.95		22.98	24.12	23.95		7.2578	5.9952	5.5881
A4-12	56.0	23.60		24.96	23.15	23.60		5.3738	6.0681	5.8065
A4-13	61.0	22.95		22.87	23.20	22.95		5.5726	5.4736	6.0042
A4-14	66.0	22.69		21.04	23.12	22.69		5.4743	5.7965	5.4802
A4-15	71.0	22.59		24.16	22.42	22.59		6.3425	5.4849	5.2406
A4-16	76.0	22.72		22.57	22.67	22.72		4.6378	5.0519	4.9678
A4-17	81.0	22.72		21.45	23.04	22.72		4.1755	4.3407	4.2259
A4-18	86.0	22.82		24.14	22.83	22.82		4.2088	3.3831	3.3691
A4-19	91.0	23.38		22.89	22.88	23.38		1.7651	2.6773	2.9004
A4-20	96.0	22.94		23.10	23.34	22.94		2.0582	2.0393	2.7157
A4-21	101.0	23.23		22.84	23.95	23.23		2.2946	2.5349	1.9275
A4-22	106.0	24.59		23.74	24.38	24.59		3.2520	1.9381	2.1678
A4-23	111.0	25.32		27.19	25.55	25.32		0.2676	2.1621	2.4608
A4-24	116.0	27.06		25.03	25.58	27.06		2.9667	2.2524	2.4872
A4-25	130.0	25.65		28.96	24.77	25.65		3.5230	2.9722	1.7300
A4-26	135.0	23.88		22.97	23.54	23.88		2.4268	1.8053	2.6813
A4-27	140.0	21.24		19.72	22.77	21.24		-0.5339	2.3057	3.0643
A4-28	145.0	20.64		21.02	21.08	20.64		5.0241	3.1239	3.2556
A4-29	150.0	20.90		21.18	20.85	20.90		4.8815	4.7950	3.7403
A4-30	155.0	21.16		20.50	21.21	21.16		4.4796	4.7371	4.6528
A4-31	160.0	21.29		21.81	21.70	21.29		4.8502	4.4528	4.6839

A4-32	165.0	22.27	21.55	21.63	22.27	4.0286	4.6862	4.7587
A4-33	170.0	21.95	23.44	21.43	21.95	5.1799	4.8212	4.5545
A4-34	175.0	21.26	20.86	21.10	21.26	5.2553	4.6313	4.0922
A4-35	180.0	20.17	19.47	21.08	20.17	3.4587	3.7509	4.1333
A4-36	185.0	20.36	20.17	20.41	20.36	2.5387	3.4104	3.8631
A4-37	190.0	20.57	21.45	19.68	20.57	4.2339	3.5339	3.7059
A4-38	195.0	19.59	20.11	19.46	19.59	3.8291	4.1774	3.5005
A4-39	200.0	18.57	17.23	19.70	18.57	4.4693	3.5767	2.9594
A4-40	205.0	18.97	18.36	19.40	18.97	2.4316	2.2447	2.7030
A4-41	210.0	19.89	21.33	19.23	19.89	-0.1667	1.7388	1.8760
A4-42	215.0	20.19	19.98	19.99	20.19	2.9516	0.8263	2.6832
A4-43	220.0	20.09	19.26	21.43	20.09	-0.3060	3.7171	3.1881
A4-44	225.0	21.95	21.02	22.37	21.95	8.5056	4.3852	4.0206
A4-45	230.0	24.21	25.58	23.19	24.21	4.9561	5.8191	4.0061
A4-46	235.0	25.23	26.03	23.20	25.23	3.9955	3.9436	5.1913
A4-47	240.0	23.13	24.08	21.78	23.13	2.8791	4.1650	4.3598
A4-48	250.0	19.10	19.27	19.71	19.10	5.6204	4.2824	3.6132
A4-49	255.0	16.15	13.95	17.99	16.15	4.3478	3.7305	2.9940
A4-50	260.0	15.53	15.23	16.79	15.53	1.2232	2.1569	3.5804
A4-51	265.0	16.92	17.41	16.59	16.92	0.8996	2.6445	3.2311
A4-52	270.0	17.93	18.11	17.44	17.93	5.8108	3.5282	2.7511
A4-53	275.0	18.18	18.27	18.40	18.18	3.8741	3.8777	2.5065
A4-54	280.0	18.83	18.16	18.40	18.83	1.9481	1.9407	2.6870
A4-55	285.0	18.55	20.06	18.32	18.55	0.0000	1.2500	2.4988
A4-56	290.0	18.40	17.42	18.19	18.40	1.8018	2.2240	1.9830
A4-57	300.0	17.57	17.71	18.29	17.57	4.8701	2.6556	1.8751
A4-58	305.0	18.00	17.59	18.14	18.00	1.2950	2.5245	2.5932
A4-59	310.0	18.52	18.69	17.46	18.52	1.4085	2.0980	2.6180
A4-60	315.0	17.33	19.27	17.56	17.33	3.5905	2.3082	2.5027
A4-61	320.0	17.18	14.03	18.04	17.18	1.9257	3.2701	3.5298
A4-62	325.0	17.41	18.25	18.13	17.41	4.2940	4.2167	4.4837
A4-63	330.0	19.12	19.95	17.95	19.12	6.4303	5.6341	3.9360
A4-64	335.0	19.16	19.16	18.70	19.16	6.1779	4.4868	3.4162
A4-65	340.0	18.43	18.38	18.36	18.43	0.8521	2.1189	2.9226
A4-66	345.0	17.56	17.75	17.87	17.56	-0.6732	0.6682	2.1347
A4-67	350.0	17.27	16.54	17.84	17.27	1.8257	1.2145	1.3389
A4-68	355.0	17.70	17.53	17.79	17.70	2.4911	2.1718	1.5595
A4-69	365.0	18.22	19.03	18.67	18.22	2.1986	2.2151	2.1929
A4-70	370.0	19.76	18.10	20.35	19.76	1.9555	2.2159	2.2447
A4-71	375.0	21.73	22.15	21.14	21.73	2.4936	2.1779	2.2824
A4-72	380.0	22.85	24.96	22.26	22.85	2.0847	2.4193	2.6158
A4-73	385.0	23.69	21.45	22.37	23.69	2.6797	2.8767	2.3236
A4-74	390.0	21.59	24.65	21.38	21.59	3.8657	2.3466	2.6925
A4-75	395.0	20.17	18.66	20.42	20.17	0.4944	2.8993	3.0421
A4-76	400.0	18.67	17.20	21.14	18.67	4.3379	2.8883	3.5855
A4-77	405.0	20.80	20.14	21.70	20.80	3.8328	4.5225	3.5834
A4-78	410.0	24.21	25.06	23.62	24.21	5.3968	4.3617	3.7633
A4-79	415.0	26.92	27.43	25.86	26.92	3.8554	3.5485	3.6649
A4-80	420.0	28.04	28.28	27.36	28.04	1.3934	3.0316	2.8764
A4-81	425.0	28.11	28.41	27.94	28.11	3.8462	1.7099	2.0180

A4-82	430.0	27.99	27.64	27.99	27.99	-0.1099	1.6137	1.2189
A4-83	435.0	27.75	27.94	27.83	27.75	1.1050	0.2849	1.8474
A4-84	440.0	27.71	27.67	27.53	27.71	-0.1403	1.8336	1.5418
A4-85	445.0	27.36	27.51	27.61	27.36	4.5361	2.2379	2.2347
A4-86	450.0	27.48	26.89	27.46	27.48	2.3179	3.4029	1.9111
A4-87	455.0	27.37	28.04	27.50	27.37	3.3548	1.7200	2.8253
A4-88	465.0	27.70	27.20		27.70	-0.5128	2.4241	
A4-89	475.0		27.87			4.4304		

* Low frequency (LF) and high frequency (HF) susceptibility are expressed in international standard units. Frequency dependence of susceptibility is expressed in percent (%).

Table 4. A7 (bench north) magnetic susceptibility*.

Sample	Depth (cm)	LF		LF		LF		Frequency Dep. Mag. Sus.	Frequency Dep. 3 Pt Avg	Frequency Dep. 5 Pt Avg
		Mag. Sus. 3 Pt	Avg	Mag. Sus.	Avg	Mag. Sus. 3 Pt	Avg			
A7-1	5.0			75.54				-0.7974		
A7-2	10.0	68.25		67.36		68.25		7.9802	3.4545	
A7-3	15.0	64.04		61.85	66.56	64.04		3.1808	5.3439	3.6187
A7-4	20.0	63.31		62.91	65.01	63.31		4.8708	3.6369	4.5003
A7-5	25.0	65.28		65.16	65.71	65.28		2.8590	3.7801	4.0983
A7-6	30.0	67.93		67.79	67.27	67.93		3.6106	4.1466	4.1304
A7-7	35.0	69.43		70.84	69.65	69.43		5.9701	4.3073	4.5764
A7-8	40.0	71.77		69.66	71.40	71.77		3.3413	5.4708	4.4396
A7-9	45.0	72.79		74.80	73.70	72.79		7.1009	4.2058	5.0373
A7-10	50.0	76.01		73.91	75.85	76.01		2.1751	5.2917	4.5807
A7-11	55.0	78.27		79.31	80.26	78.27		6.5990	4.1537	5.5730
A7-12	60.0	84.19		81.59	82.95	84.19		3.6871	6.1964	4.1617
A7-13	65.0	87.19		91.68	86.46	87.19		8.3031	4.0115	2.9762
A7-14	70.0	90.48		88.29	89.81	90.48		0.0443	1.5316	3.0441
A7-15	75.0	91.93		91.46	92.62	91.93	-3.7527	1.0768	3.7071	
A7-16	80.0	94.37		96.04	92.85	94.37		6.9388	3.3961	2.7538
A7-17	85.0	94.84		95.63	92.83	94.84		7.0021	5.8259	3.4842
A7-18	90.0	92.21		92.86	92.56	92.21		3.5367	4.7450	4.3442
A7-19	95.0	90.38		88.14	90.43	90.38		3.6961	2.5934	3.6658
A7-20	100.0	87.90		90.13	88.17	87.90	0.5474	2.5967	3.6582	
A7-21	105.0	86.62		85.41	86.04	86.62		3.5465	3.6860	3.9881
A7-22	110.0	83.98		84.33	84.09	83.98		6.9642	5.2323	3.9025
A7-23	115.0	81.64		82.19	80.24	81.64		5.1864	5.1395	4.8069
A7-24	130.0	77.15		78.39	76.42	77.15		3.2680	4.5079	5.2852
A7-25	135.0	71.87		70.87	71.50	71.87		5.0694	4.7584	4.8743
A7-26	140.0	65.64		66.34	66.56	65.64		5.9379	5.3058	4.1665
A7-27	145.0	61.18		59.73	60.52	61.18		4.9100	4.1650	3.9936
A7-28	150.0	55.13		57.48	54.54	55.13		1.6471	2.9868	4.2444
A7-29	155.0	48.89		48.18	48.21	48.89		2.4034	3.4581	3.9512

A7-30	160.0	41.28	40.99	41.15	41.28	6.3237	4.3997	3.4025
A7-31	165.0	33.36	34.67	33.61	33.36	4.4720	4.3206	4.0508
A7-32	170.0	26.30	24.41	27.16	26.30	2.1661	3.8423	4.1257
A7-33	175.0	20.04	19.82	21.91	20.04	4.8889	3.2776	3.1764
A7-34	180.0	16.83	15.90	17.65	16.83	2.7778	3.0813	2.6820
A7-35	185.0	14.68	14.77	15.53	14.68	1.5773	2.1184	3.2228
A7-36	190.0	13.98	13.36	14.38	13.98	2.0000	2.8158	2.8820
A7-37	195.0	13.74	13.82	14.33	13.74	4.8701	3.3516	2.6464
A7-38	200.0	14.51	14.04	14.27	14.51	3.1847	3.2183	3.2238
A7-39	205.0	14.72	15.65	14.42	14.72	1.6000	3.0830	3.0186
A7-40	210.0	14.74	14.46	14.62	14.74	4.4643	2.3461	2.5648
A7-41	215.0	14.47	14.12	14.95	14.47	0.9740	2.6798	2.4993
A7-42	220.0	14.89	14.85	14.99	14.89	2.6012	2.1441	3.3781
A7-43	225.0	15.45	15.70	17.62	15.45	2.8571	3.8173	2.0577
A7-44	230.0	19.72	15.82	21.16	19.72	5.9937	2.2378	2.3583
A7-45	235.0	25.09	27.64	22.96	25.09	-2.1374	2.1110	2.4667
A7-46	240.0	27.76	31.82	25.25	27.76	2.4768	1.1609	2.3707
A7-47	255.0	27.60	23.83	26.64	27.60	3.1434	2.6657	1.2996
A7-48	260.0	24.58	27.14	25.43	24.58	2.3769	2.0529	2.3507
A7-49	265.0	23.83	22.77	24.94	23.83	0.6383	2.0444	1.5215
A7-50	270.0	24.58	21.59	26.14	24.58	3.1180	0.6957	0.0713
A7-51	275.0	26.93	29.37	26.66	26.93	-1.6692	-0.8863	-1.1149
A7-52	280.0	29.65	29.84	29.23	29.65	-4.1076	-3.1103	-0.7579
A7-53	285.0	31.72	29.73	33.21	31.72	-3.5541	-1.7461	-1.7580
A7-54	290.0	35.61	35.60	36.45	35.61	2.4235	-1.0044	-1.7765
A7-55	295.0	40.89	41.50	38.14	40.89	-1.8826	-0.4069	-1.2887
A7-56	300.0	41.79	45.56	39.79	41.79	-1.7617	-1.7710	0.5471
A7-57	305.0	40.62	38.31	38.46	40.62	-1.6687	0.7316	0.4572
A7-58	310.0	35.08	37.99	34.93	35.08	5.6250	1.9767	1.0878
A7-59	315.0	30.26	28.95	31.14	30.26	1.9737	2.9564	1.0389
A7-60	320.0	26.47	23.83	28.40	26.47	1.2704	0.4126	1.6851
A7-61	325.0	25.02	26.62	25.37	25.02	-2.0062	0.2756	0.6311
A7-62	330.0	24.70	24.62	22.53	24.70	1.5625	-0.0295	-0.3058
A7-63	335.0	20.74	22.85	23.03	20.74	0.3552	-0.2644	-0.1217
A7-64	340.0	21.30	14.76	23.01	21.30	-2.7108	-0.0549	0.5494
A7-65	345.0	22.53	26.30	25.29	22.53	2.1909	0.2764	0.3967
A7-66	350.0	29.61	26.54	27.60	29.61	1.3491	1.4464	0.3504
A7-67	355.0	32.32	35.99	33.59	32.32	0.7991	0.7574	0.8139
A7-68	360.0	38.37	34.43	35.59	38.37	0.1239	0.1766	0.6529
A7-69	375.0	38.47	44.68	35.99	38.47	-0.3933	0.3721	0.3545
A7-70	380.0	36.50	36.30	31.84	36.50	1.3857	0.2831	0.3465
A7-71	385.0	26.70	28.53	28.02	26.70	-0.1431	0.6674	0.3747
A7-72	390.0	19.70	15.27	22.02	19.70	0.7595	0.2937	2.0555
A7-73	395.0	15.09	15.30	17.45	15.09	0.2646	3.0117	1.7784
A7-74	400.0	14.48	14.69	15.06	14.48	8.0110	2.7585	2.6607
A7-75	405.0	14.90	13.43	14.49	14.90	0.0000	4.0931	3.0665
A7-76	410.0	14.15	16.58	16.02	14.15	4.2683	2.3524	3.8662
A7-77	415.0	17.33	12.44	17.27	17.33	2.7888	3.7733	2.9798
A7-78	420.0	18.78	22.98		18.78	4.2629	3.5436	
A7-79	425.0		20.93			3.5789		

Table 5. A6 (sink east) magnetic susceptibility*.

Sample	Depth (cm)	LF Mag. Sus. 3 Pt	LF Mag. Sus.	LF Mag. Sus. 5 Pt	LF Mag. Sus. 3 Pt	Frequency Dep. Mag. Sus.	Frequency Dep. 3 Pt Avg	Frequency Dep. 5 Pt Avg
A6-1	0.0		29.18			1.1215		
A6-2	10.0	25.18	26.64		25.18	0.0796	0.7624	
A6-3	15.0	22.68	19.70	23.36	22.68	1.0863	1.4030	1.5615
A6-4	20.0	20.32	21.68	22.54	20.32	3.0432	2.2022	1.8031
A6-5	25.0	22.12	19.58	22.47	22.12	2.4771	2.6166	2.3748
A6-6	30.0	23.65	25.11	23.61	23.65	2.3295	2.5815	2.3968
A6-7	35.0	25.61	26.26	24.47	25.61	2.9378	2.1546	2.4984
A6-8	40.0	25.90	25.45	26.17	25.90	1.1966	2.5619	2.6858
A6-9	50.0	26.49	25.98	26.57	26.49	3.5512	2.7206	2.9078
A6-10	55.0	27.05	28.04	26.38	27.05	3.4139	3.4681	3.0111
A6-11	60.0	26.83	27.13	25.93	26.83	3.4393	3.4359	3.8898
A6-12	65.0	25.21	25.33	25.41	25.21	3.4544	4.1612	4.2144
A6-13	70.0	23.96	23.16	24.05	23.96	5.5901	4.7396	4.7385
A6-14	75.0	22.61	23.39	23.50	22.61	5.1745	5.5997	4.8015
A6-15	80.0	23.00	21.26	22.88	23.00	6.0345	4.9877	4.8853
A6-16	85.0	22.62	24.35	21.40	22.62	3.7543	4.5540	4.3525
A6-17	90.0	20.79	22.25	19.94	20.79	3.8732	3.5178	3.6534
A6-18	95.0	18.03	15.76	20.14	18.03	2.9260	2.8261	3.1023
A6-19	100.0	18.03	16.07	18.61	18.03	1.6791	2.6279	2.8069
A6-20	105.0	18.34	22.28	17.07	18.34	3.2787	2.4117	2.4489
A6-21	110.0	17.84	16.68	16.61	17.84	2.2774	2.5465	2.0900
A6-22	115.0	14.90	14.57	16.14	14.90	2.0833	1.8308	1.9040
A6-23	130.0	13.91	13.45	13.94	13.91	1.1315	1.3213	1.2483
A6-24	135.0	12.82	13.70	12.54	12.82	0.7491	0.6269	1.0069
A6-25	140.0	11.56	11.30	11.37	11.56	0.0000	0.6065	0.5399
A6-26	145.0	9.90	9.69	10.62	9.90	1.0703	0.2730	0.4236
A6-27	150.0	9.36	8.70	9.79	9.36	-0.2513	0.4563	0.1750
A6-28	155.0	9.32	9.69	9.88	9.32	0.5500	-0.0651	0.4136
A6-29	160.0	10.34	9.57	10.08	10.34	-0.4941	0.4162	0.2625
A6-30	165.0	10.67	11.76	10.38	10.67	1.1928	0.3380	0.6438
A6-31	170.0	10.88	10.66	10.44	10.88	0.3151	1.0544	0.7631
A6-32	175.0	10.29	10.23	10.60	10.29	1.6552	1.0389	0.9833
A6-33	180.0	10.19	9.98	10.35	10.19	1.1465	1.1362	1.2146
A6-34	185.0	10.29	10.34	10.38	10.29	0.6068	1.3676	1.2845
A6-35	190.0	10.56	10.55	10.22	10.56	2.3495	1.2069	1.4696
A6-36	195.0	10.26	10.79	10.19	10.26	0.6645	1.8649	1.5077
A6-37	200.0	10.02	9.44	10.08	10.02	2.5806	1.5275	1.5626
A6-38	205.0	9.69	9.83	9.87	9.69	1.3373	1.5997	1.4148
A6-39	210.0	9.71	9.81	9.61	9.71	0.8811	1.2762	1.4956
A6-40	215.0	9.59	9.50	9.65	9.59	1.6103	1.1867	0.8825
A6-41	220.0	9.54	9.44	9.30	9.54	1.0687	0.7315	0.9776
A6-42	225.0	9.07	9.68	9.25	9.07	-0.4847	0.7989	0.8663
A6-43	230.0	9.09	8.08	8.17	9.09	1.8127	0.5509	1.1027
A6-44	235.0	7.24	9.52	7.37	7.24	0.3247	1.6431	0.9120
A6-45	240.0	6.35	4.11	6.82	6.35	2.7919	1.0773	1.3770

A6-46	250.0	5.50	5.44	6.51	5.50	0.1155	1.5826	1.4172
A6-47	255.0	6.30	6.97	5.63	6.30	1.8405	1.3231	1.8850
A6-48	260.0	6.19	6.50	9.31	6.19	2.0134	2.1726	1.6241
A6-49	265.0	11.38	5.12	12.95	11.38	2.6639	2.0548	2.3247
A6-50	270.0	17.10	22.51	16.77	17.10	1.4870	2.5898	2.6057
A6-51	275.0	24.08	23.68	20.56	24.08	3.6184	2.7837	2.4632
A6-52	280.0	25.05	26.07	25.13	25.05	3.2457	2.7217	2.2924
A6-53	285.0	26.49	25.41	26.20	26.49	1.3008	2.1188	2.2741
A6-54	290.0	27.09	28.00	28.37	27.09	1.8100	1.5020	1.5737
A6-55	295.0	30.12	27.85	28.37	30.12	1.3953	1.1074	1.2007
A6-56	300.0	29.48	34.52	27.33	29.48	0.1168	0.9642	1.3796
A6-57	305.0	26.93	26.08	25.91	26.93	1.3804	1.2309	1.3699
A6-58	310.0	22.39	20.20	23.65	22.39	2.1956	1.7791	1.2743
A6-59	315.0	19.22	20.89	20.23	19.22	1.7613	1.6248	1.2960
A6-60	320.0	18.29	16.58	19.74	18.29	0.9174	0.9680	1.0199
A6-61	325.0	19.20	17.40	20.46	19.20	0.2252	0.3809	0.9034
A6-62	330.0	21.61	23.61	19.76	21.61	0.0000	0.6127	0.9330
A6-63	335.0	21.61	23.83	19.43	21.61	1.6129	1.1741	1.3457
A6-64	340.0	18.70	17.39	19.32	18.70	1.9093	2.1677	1.2533
A6-65	345.0	16.39	14.90	19.63	16.39	2.9810	1.5511	1.5244
A6-66	350.0	18.97	16.89	18.34	18.97	-0.2370	1.3667	1.3493
A6-67	355.0	19.80	25.13	17.60	19.80	1.3559	0.6187	1.0477
A6-68	360.0	18.73	17.39	18.42	18.73	0.7371	0.8315	0.5503
A6-69	365.0	16.69	13.67	19.16	16.69	0.4016	0.5442	0.7248
A6-70	372.0	17.76	19.01	16.23	17.76	0.4938	0.5103	-0.0137
A6-71	380.0	16.70	20.59	14.27	16.70	0.6356	-0.4023	-1.0472
A6-72	385.0	12.89	10.49		12.89	-2.3364	-2.0437	
A6-73	390.0		7.60			-4.4304		

* Low frequency (LF) and high frequency (HF) susceptibility are expressed in international standard units. Frequency dependence of susceptibility is expressed in percent (%).

Table 6. AD (delta) magnetic susceptibility*.

Sample	Depth (cm)	LF		LF		LF		Frequency Dep. Mag. Sus.	Frequency Dep. 3 Pt Avg	Frequency Dep. 5 Pt Avg
		Mag. Sus.	Sus. 3 Pt Avg	Mag. Sus.	Sus. 5 Pt Avg	Mag. Sus.	Avg			
AD-1	0.0		56.94					1.6569		
AD-2	5.0	58.89		66.98		58.89		1.6981	1.5282	
AD-3	10.0	54.42		52.77	53.25	54.42		1.2295	0.8790	0.9866
AD-4	15.0	47.45		43.51	51.55	47.45		-0.2907	0.5260	0.8931
AD-5	20.0	46.00		46.09	47.98	46.00		0.6393	0.5126	1.1681
AD-6	25.0	47.87		48.42	46.01	47.87		1.1893	1.6339	1.4991
AD-7	30.0	46.82		49.10	44.84	46.82		3.0731	2.3823	2.2431
AD-8	35.0	43.23		42.94	42.79	43.23		2.8846	3.1290	2.3064
AD-9	40.0	38.81		37.64	40.01	38.81		3.4292	2.4232	2.4283
AD-10	45.0	36.00		35.86	36.68	36.00		0.9558	2.0612	1.7906

AD-11	50.0	34.27	34.49	34.30	34.27	1.7986	0.8797	1.1160
AD-12	55.0	32.67	32.46	33.24	32.67	-0.1152	0.3983	0.7863
AD-13	60.0	31.94	31.07	32.45	31.94	-0.4884	0.3924	1.2056
AD-14	65.0	31.76	32.30	32.12	31.76	1.7808	1.4482	1.1211
AD-15	70.0	32.36	31.91	32.31	32.36	3.0523	2.0698	1.5049
AD-16	75.0	32.73	32.88	33.04	32.73	1.3761	2.0774	2.1524
AD-17	80.0	33.67	33.40	33.95	33.67	1.8038	1.9762	2.1632
AD-18	85.0	34.98	34.73	35.26	34.98	2.7487	2.1291	2.2040
AD-19	90.0	36.67	36.82	36.63	36.67	1.8349	2.6133	2.7287
AD-20	95.0	38.34	38.45	38.48	38.34	3.2563	3.0304	2.9717
AD-21	100.0	40.28	39.74	40.82	40.28	4.0000	3.4251	2.8491
AD-22	105.0	42.93	42.64	43.33	42.93	3.0189	3.0515	3.1116
AD-23	110.0	46.16	46.42	46.09	46.16	2.1356	2.7672	3.1981
AD-24	115.0	49.35	49.42	49.00	49.35	3.1471	2.9905	3.0520
AD-25	120.0	51.97	52.22	51.18	51.97	3.6889	3.3684	2.8678
AD-26	125.0	53.35	54.28	52.42	53.35	3.2694	3.0187	3.0388
AD-27	130.0	53.48	53.54	52.46	53.48	2.0979	2.7860	2.8588
AD-28	135.0	51.93	52.62	50.68	51.93	2.9908	2.4453	2.8199
AD-29	140.0	48.53	49.64	47.94	48.53	2.2472	2.9108	2.9007
AD-30	145.0	44.51	43.32	44.51	44.51	3.4943	3.1383	3.3093
AD-31	150.0	40.10	40.56	39.51	40.10	3.6735	3.7694	3.4641
AD-32	155.0	34.86	36.43	34.85	34.86	4.1405	3.8597	3.7398
AD-33	160.0	30.13	27.60	30.83	30.13	3.7651	3.8437	3.4695
AD-34	165.0	25.72	26.35	27.51	25.72	3.6254	3.1778	3.2217
AD-35	170.0	24.51	23.22	23.98	24.51	2.1429	2.7343	2.9881
AD-36	175.0	21.99	23.96	22.29	21.99	2.4348	2.5167	2.7190
AD-37	180.0	20.62	18.78	20.25	20.62	2.9724	2.6088	2.2072
AD-38	185.0	18.02	19.14	18.31	18.02	2.4194	2.1528	1.7180
AD-39	190.0	16.27	16.15	16.31	16.27	1.0667	1.0610	1.7325
AD-40	195.0	14.54	13.54	15.54	14.54	-0.3030	1.0902	1.3452
AD-41	200.0	14.14	13.94	14.87	14.14	2.5070	1.0801	3.2240
AD-42	205.0	14.89	14.94	14.87	14.89	1.0363	5.1188	3.5762
AD-43	210.0	15.63	15.80	16.10	15.63	11.8132	5.2257	4.1889
AD-44	215.0	17.21	16.15	17.35	17.21	2.8278	5.8003	3.7696
AD-45	220.0	18.68	19.69	17.34	18.68	2.7601	1.9995	4.1194
AD-46	225.0	18.24	20.19	16.77	18.24	0.4107	1.9854	2.5102
AD-47	230.0	16.01	14.85	16.17	16.01	2.7855	2.3211	2.4429
AD-48	235.0	13.66	12.99	14.01	13.66	3.7671	3.0146	2.6644
AD-49	240.0	11.66	13.16	11.35	11.66	2.4911	3.3752	3.4646
AD-50	250.0	9.63	8.85	9.91	9.63	3.8674	3.5901	2.7840
AD-51	260.0	7.80	6.90	12.63	7.80	4.4118	2.5540	2.1325
AD-52	270.0	13.71	7.66	16.95	13.71	-0.6173	1.4346	1.7687
AD-53	285.0	23.00	26.58	22.74	23.00	0.5093	0.1880	1.1601
AD-54	295.0	33.05	34.77	29.33	33.05	0.6720	0.6686	0.3009
AD-55	305.0	37.47	37.80	32.89	37.47	0.8245	0.5375	0.4244
AD-56	315.0	34.37	39.84	30.31	34.37	0.1159	0.3135	1.0655
AD-57	325.0	26.33	25.48	27.29	26.33	0.0000	1.2770	1.4716
AD-58	335.0	19.60	13.66	23.14	19.60	3.7152	2.1393	1.6533
AD-59	345.0	16.80	19.66	17.64	16.80	2.7027	2.7168	2.4130
AD-60	355.0	16.35	17.06	15.86	16.35	1.7327	2.7833	3.4683

AD-61	370.0	15.32	12.32	15.88	15.32	3.9146	3.6412	3.1026
AD-62	380.0	14.22	16.58	15.44	14.22	5.2764	3.6926	3.3755
AD-63	390.0	15.94	13.74	16.05	15.94	1.8868	3.7434	4.1254
AD-64	400.0	17.11	17.49	17.50	17.11	4.0670	3.8121	3.7408
AD-65	410.0	19.05	20.09	17.76	19.05	5.4825	3.8469	3.2525
AD-66	420.0	19.19	19.58	19.42	19.19	1.9912	3.4362	3.2688
AD-67	430.0	19.84	17.90	21.04	19.84	2.8351	2.2649	2.4230
AD-68	435.0	21.84	22.03	21.36	21.84	1.9685	1.5471	1.3265
AD-69	440.0	23.10	25.60	22.05	23.10	-0.1623	0.6021	1.3387
AD-70	445.0	23.43	21.68	22.93	23.43	0.0000	0.6300	1.1631
AD-71	450.0	22.33	23.02	21.66	22.33	2.0522	1.3364	1.0305
AD-72	460.0	20.34	22.29	20.18	20.34	1.9569	1.7716	1.1100
AD-73	470.0	18.73	15.70	18.06	18.73	1.3055	1.1659	0.8774
AD-74	480.0	14.99	18.21	17.78	14.99	0.2353	0.1260	0.2239
AD-75	490.0	16.96	11.05	16.59	16.96	-1.1628	-0.7143	0.0560
AD-76	500.0	16.36	21.62	16.54	16.36	-1.2153	-0.4203	-0.1481
AD-77	510.0	17.82	16.39	15.44	17.82	1.1173	0.0623	-0.1952
AD-78	515.0	14.84	15.44	16.00	14.84	0.2849	0.4674	1.1899
AD-79	520.0	14.00	12.69	14.46	14.00	0.0000	2.0159	1.9238
AD-80	525.0	13.49	13.86	13.39	13.49	5.7627	2.7389	2.1950
AD-81	530.0	12.94	13.93	11.95	12.94	2.4540	3.5634	2.1380
AD-82	540.0	11.06	11.02	10.79	11.06	2.4735	1.6425	2.0168
AD-83	550.0	8.73	8.23	9.45	8.73	0.0000	0.6225	0.4893
AD-84	560.0	7.43	6.93	8.04	7.43	-0.6061	-0.8270	0.1336
AD-85	570.0	6.98	7.12	7.15	6.98	-1.8750	-0.6018	-1.1830
AD-86	580.0	6.86	6.90	6.82	6.86	0.6757	-1.7696	-0.4262
AD-87	590.0	6.69	6.55	6.90	6.69	-4.1096	0.1166	-0.0260
AD-88	600.0	6.84	6.63	6.74	6.84	3.7838	0.3565	1.7593
AD-89	615.0	6.75	7.32	7.25	6.75	1.3953	4.0768	1.1242
AD-90	625.0	7.69	6.30	7.92	7.69	7.0513	1.9822	1.9461
AD-91	635.0	8.55	9.46	9.34	8.55	-2.5000	1.5171	1.4109
AD-92	645.0	11.03	9.88	10.92	11.03	0.0000	-0.4640	0.7971
AD-93	655.0	12.95	13.76		12.95	1.1080	-0.1885	
AD-94	665.0		15.22			-1.6736		

Table 7. C (inflow channel) magnetic susceptibility*.

Sample	Depth (cm)	LF Mag. Sus. 3 Pt		LF Mag. Sus. 5 Pt		LF Mag. Sus. 3 Pt		Frequency Dep. Mag. Sus.	Frequency Dep. 3 Pt Avg	Frequency Dep. 5 Pt Avg
		Avg	Sus.	Avg	Sus.	Avg	Sus.			
C-1	0.0		63.54					3.1020		
C-2	5.0	66.90	65.34			66.90	2.9342	3.1484		
C-3	9.0	73.64	71.84	73.38	73.64	3.4091	3.6812	3.7987		
C-4	14.0	79.34	83.74	78.77	79.34	4.7004	4.3191	3.7516		
C-5	19.0	85.56	82.43	80.84	85.56	4.8478	4.1383	3.5180		
C-6	25.0	82.88	90.52	73.91	82.88	2.8666	3.1601	3.1253		
C-7	35.0	67.79	75.69	65.15	67.79	1.7659	2.0261	2.4692		

C-8	40.0	50.94	37.15	56.63	50.94	1.4458	1.5439	2.0237
C-9	45.0	38.98	39.97	46.54	38.98	1.4201	1.8287	1.4959
C-10	50.0	39.95	39.83	39.30	39.95	2.6201	1.4227	1.4094
C-11	55.0	39.80	40.05	39.28	39.80	0.2278	1.3937	1.2201
C-12	60.0	38.86	39.51	38.04	38.86	1.3333	0.6868	1.5850
C-13	65.0	36.78	37.01	37.22	36.78	0.4994	1.6924	1.6211
C-14	70.0	35.51	33.82	36.41	35.51	3.2445	2.1814	1.8866
C-15	75.0	35.17	35.71	36.08	35.17	2.8005	2.5335	1.9960
C-16	80.0	36.52	36.00	36.21	36.52	1.5556	2.0787	2.1234
C-17	85.0	37.18	37.86	37.28	37.18	1.8801	1.5240	1.9551
C-18	90.0	38.23	37.68	38.23	38.23	1.1364	1.8064	1.9890
C-19	95.0	39.09	39.16	39.35	39.09	2.4027	2.1698	2.2207
C-20	100.0	40.40	40.44	39.45	40.40	2.9703	2.6957	2.3627
C-21	105.0	40.13	41.62	36.18	40.13	2.7140	2.7581	2.8049
C-22	110.0	33.77	38.34	32.23	33.77	2.5901	2.8838	3.3720
C-23	120.0	26.37	21.36	27.36	26.37	3.3473	3.7252	3.5865
C-24	125.0	18.94	19.41	22.48	18.94	5.2381	4.2095	3.9528
C-25	130.0	17.57	16.06	17.36	17.57	4.0431	4.6089	3.5642
C-26	135.0	15.34	17.23	16.20	15.34	4.5455	3.0786	3.0087
C-27	140.0	15.17	12.74	14.82	15.17	0.6472	1.9208	1.6862
C-28	145.0	13.60	15.54	15.16	13.60	0.5698	-0.0525	1.5011
C-29	150.0	15.28	12.51	15.06	15.28	-1.3746	0.7709	0.6920
C-30	155.0	15.67	17.77	16.44	15.67	3.1175	0.7476	1.4908
C-31	160.0	18.05	16.74	17.16	18.05	0.5000	2.7530	1.9211
C-32	165.0	18.51	19.64	17.69	18.51	4.6414	2.6208	2.1960
C-33	170.0	17.97	19.16	18.30	17.97	2.7211	2.4541	2.0073
C-34	175.0	18.38	15.12	18.74	18.38	0.0000	1.6317	2.0446
C-35	180.0	18.30	20.86	19.40	18.30	2.1739	0.9535	1.4115
C-36	185.0	20.90	18.92	20.03	20.90	0.6865	1.4455	1.3606
C-37	190.0	21.39	22.93	22.04	21.39	1.4760	1.5431	1.5800
C-38	195.0	23.47	22.31	22.42	23.47	2.4668	1.6799	1.5328
C-39	200.0	23.42	25.18	22.70	23.42	1.0969	1.8339	1.9785
C-40	205.0	22.75	22.77	22.23	22.75	1.9380	1.9832	2.1972
C-41	210.0	21.22	20.29	22.20	21.22	2.9148	2.4741	2.0145
C-42	215.0	21.01	20.59	20.76	21.01	2.5696	2.3459	2.2044
C-43	220.0	20.25	22.14	20.19	20.25	1.5534	2.0563	2.5640
C-44	225.0	20.03	18.02	21.13	20.03	2.0460	2.4452	2.2297
C-45	230.0	20.97	19.92	22.00	20.97	3.7363	2.3419	2.3064
C-46	235.0	23.28	24.96	22.38	23.28	1.2433	2.6441	2.3914
C-47	260.0	24.65	24.95	24.57	24.65	2.9528	2.0582	2.3504
C-48	265.0	25.99	24.05	26.18	25.99	1.9784	2.2575	1.8150
C-49	280.0	27.00	28.98	27.22	27.00	1.8414	1.6263	2.1871
C-50	285.0	29.04	27.96	28.10	29.04	1.0590	2.0014	2.0664
C-51	290.0	29.16	30.17	28.60	29.16	3.1039	2.1708	2.1124
C-52	295.0	28.69	29.35	28.15	28.69	2.3495	2.5539	2.3285
C-53	300.0	27.54	26.55	27.08	27.54	2.2082	2.4933	2.7901
C-54	305.0	25.29	26.71	25.98	25.29	2.9221	2.8324	2.2628
C-55	310.0	24.66	22.60	28.06	24.66	3.3670	2.2521	2.1407
C-56	315.0	29.01	24.67	29.36	29.01	0.4673	1.8578	2.2596
C-57	320.0	32.50	39.76	30.50	32.50	1.7391	1.6697	2.2242

C-58	325.0	35.07	33.07	34.60	35.07	2.8025	2.4289	1.9013
C-59	330.0	36.19	32.39	38.76	36.19	2.7451	2.4334	2.1553
C-60	335.0	40.32	43.11	39.14	40.32	1.7526	2.0783	2.1386
C-61	340.0	43.41	45.46	38.85	43.41	1.7372	1.7151	1.7162
C-62	345.0	39.58	41.67	37.76	39.58	1.6556	1.3612	1.2472
C-63	350.0	33.41	31.62	31.50	33.41	0.6906	0.9154	1.5145
C-64	355.0	23.45	26.94	25.35	23.45	0.4000	1.3931	1.4728
C-65	370.0	17.82	11.80	19.92	17.82	3.0888	1.6726	1.2583
C-66	375.0	13.68	14.73	17.50	13.68	1.5291	1.7336	2.1424
C-67	380.0	16.25	14.51	15.39	16.25	0.5831	2.4078	2.8799
C-68	385.0	16.81	19.51	16.32	16.81	5.1111	3.2605	2.7487
C-69	390.0	17.46	16.41	17.01	17.46	4.0872	3.8771	2.8492
C-70	395.0	17.01	16.44	17.89	17.01	2.4331	2.8506	3.1646
C-71	400.0	17.85	18.17	17.19	17.85	2.0316	2.2082	2.6800
C-72	405.0	17.70	18.93	17.28	17.70	2.1598	2.2932	1.9613
C-73	410.0	17.27	15.99	16.92	17.27	2.6882	1.7806	1.7509
C-74	415.0	15.83	16.89	15.99	15.83	0.4938	1.5211	1.7127
C-75	420.0	15.01	14.62	14.97	15.01	1.3812	1.2385	1.5153
C-76	425.0	13.99	13.52	14.02	13.99	1.8405	1.4649	2.0136
C-77	430.0	12.86	13.83	12.88	12.86	1.1730	2.7309	2.7844
C-78	435.0	12.08	11.23	12.20	12.08	5.1793	3.5667	3.5912
C-79	440.0	11.22	11.19	11.90	11.22	4.3478	4.9808	4.0895
C-80	445.0	11.49	11.23	11.56	11.49	5.4152	4.6984	4.3795
C-81	450.0	11.79	12.03	12.02	11.79	4.3321	4.1234	3.7542
C-82	455.0	12.56	12.11	12.41	12.56	2.6230	3.0026	4.1749
C-83	460.0	12.93	13.52	12.69	12.93	2.0528	3.7091	4.5290
C-84	465.0	13.10	13.15	13.28	13.10	6.4516	5.2300	4.6652
C-85	470.0	13.59	12.62	13.38	13.59	7.1856	6.2168	4.4561
C-86	475.0	13.42	15.00	12.89	13.42	5.0132	4.5920	4.5438
C-87	500.0	12.89	12.63	12.45	12.89	1.5773	3.0272	4.3646
C-88	505.0	11.55	11.04	12.25	11.55	2.4911	3.2080	4.6635
C-89	510.0	11.20	10.98	11.36	11.20	5.5556	5.5757	5.0319
C-90	515.0	11.04	11.59	10.91	11.04	8.6806	7.0303	7.2164
C-91	520.0	10.85	10.56	10.72	10.85	6.8548	9.3451	9.8849
C-92	525.0	10.34	10.38	10.72	10.34	12.5000	11.7294	9.8808
C-93	530.0	10.47	10.06	10.22	10.47	15.8333	11.2895	9.8914
C-94	535.0	10.06	10.98	10.06	10.06	5.5351	10.0340	9.6411
C-95	540.0	9.94	9.14	10.04	9.94	8.7336	6.6240	9.4632
C-96	545.0	9.71	9.72	9.96	9.71	5.6034	8.6492	7.0724
C-97	550.0	9.89	10.29	9.80	9.89	11.6105	7.0311	7.3788
C-98	555.0	10.05	9.68	9.80	10.05	3.8793	7.5190	6.7065
C-99	560.0	9.67	10.19	10.58	9.67	7.0671	5.4394	7.3032
C-100	565.0	10.98	9.12	10.75	10.98	5.3719	7.0088	6.3782
C-101	570.0	11.30	13.61	12.63	11.30	8.5873	6.9815	6.1104
C-102	575.0	14.61	11.17		14.61	6.9853	6.0377	
C-103	580.0		19.04			2.5404		

* Low frequency (LF) and high frequency (HF) susceptibility are expressed in international standard units. Frequency dependence of susceptibility is expressed in percent (%).

Table 8. PB2 (playa basin edge south) magnetic susceptibility*.

Sample	Depth (cm)	LF Mag. Sus. 3 Pt Avg	LF Mag. Sus.	LF Mag. Sus. 5 Pt Avg	LF Mag. Sus. 3 Pt Avg	Frequency Dep. Mag. Sus.	Frequency Dep. 3 Pt Avg	Frequency Dep. 5 Pt Avg
PB2-1	0.0		57.43			3.8793		
PB2-2	5.0	50.74	50.73		50.74	2.8933	2.6212	
PB2-3	10.0	48.59	44.07	51.54	48.59	1.0909	3.3224	3.5705
PB2-4	15.0	49.85	50.96	52.45	49.85	5.9829	3.6933	3.8114
PB2-5	20.0	55.81	54.53	49.67	55.81	4.0060	5.0242	4.1829
PB2-6	25.0	51.10	61.93	47.37	51.10	5.0836	4.6136	6.2258
PB2-7	30.0	43.79	36.83	44.20	43.79	4.7511	7.0468	6.6402
PB2-8	35.0	34.85	32.62	40.05	34.85	11.3055	8.0371	6.8822
PB2-9	40.0	33.83	35.09	33.59	33.83	8.0545	8.1921	6.8337
PB2-10	45.0	32.84	33.79	32.32	32.84	5.2163	6.0373	6.9621
PB2-11	50.0	31.29	29.64	31.13	31.29	4.8411	5.1501	2.7154
PB2-12	55.0	28.93	30.44	29.88	28.93	5.3929	0.1021	2.0136
PB2-13	72.0	28.65	26.71	28.21	28.65	-9.9278	0.0035	1.6266
PB2-14	76.0	27.00	28.80	25.68	27.00	4.5455	-0.7003	2.4330
PB2-15	80.0	23.75	25.48	22.77	23.75	3.2815	5.5666	2.9161
PB2-16	87.0	19.45	16.97	20.60	19.45	8.8729	6.6543	6.4121
PB2-17	91.0	16.24	15.91	17.77	16.24	7.8086	8.0778	7.5558
PB2-18	96.0	15.46	15.84	15.89	15.46	7.5521	8.5415	8.0730
PB2-19	101.0	15.53	14.64	15.88	15.53	10.2639	7.8945	5.9930
PB2-20	106.0	15.88	16.11	17.87	15.88	5.8673	4.8682	4.6911
PB2-21	111.0	19.63	16.91	21.30	19.63	-1.5267	1.8798	4.7878
PB2-22	117.0	25.25	25.86	25.38	25.25	1.2987	2.6026	4.0056
PB2-23	122.0	31.29	32.97	28.69	31.29	8.0357	5.2291	4.0760
PB2-24	126.0	33.57	35.04	30.97	33.57	6.3529	6.8694	5.4385
PB2-25	129.0	32.00	32.70	32.98	32.00	6.2195	5.9527	6.0513
PB2-26	135.0	32.30	28.27	33.64	32.30	5.2857	5.2892	5.0578
PB2-27	141.0	33.48	35.93	33.74	33.48	4.3624	4.2388	4.0108
PB2-28	146.0	35.91	36.24	33.62	35.91	3.0682	2.8495	3.4164
PB2-29	151.0	34.63	35.56	35.08	34.63	1.1180	2.4779	2.4991
PB2-30	156.0	34.40	32.07	34.67	34.40	3.2476	1.6883	1.9445
PB2-31	161.0	33.84	35.57	33.44	33.84	0.6993	1.8454	2.0311
PB2-32	166.0	33.19	33.89	32.17	33.19	1.5894	1.9300	2.6684
PB2-33	171.0	31.07	30.10	31.73	31.07	3.5014	3.1317	3.2991
PB2-34	176.0	29.73	29.24	29.90	29.73	4.3042	4.7356	3.5482
PB2-35	181.0	28.50	29.84	27.63	28.50	6.4011	4.2167	3.6172
PB2-36	186.0	26.26	26.44	26.56	26.26	1.9449	3.4268	3.5883
PB2-37	191.0	24.57	22.52	28.71	24.57	1.9342	2.4120	3.5570
PB2-38	196.0	29.09	24.76	25.72	29.09	3.3569	3.1464	2.6187
PB2-39	201.0	26.56	40.00	23.32	26.56	4.1480	3.0714	3.8368
PB2-40	206.0	23.11	14.91	22.03	23.11	1.7094	4.6310	6.9259
PB2-41	216.0	15.13	14.41	20.40	15.13	8.0357	9.0416	11.1752
PB2-42	226.0	15.69	16.07	16.12	15.69	17.3797	16.6729	13.6199
PB2-43	236.0	17.09	16.61	16.41	17.09	24.6032	19.4515	17.3397
PB2-44	256.0	17.20	18.60	16.35	17.20	16.3717	20.4278	8.0703
PB2-45	266.0	16.36	16.39	17.11	16.36	20.3085	-0.5438	5.3533

PB2-46	276.0	16.78	14.10	17.63	16.78	-38.3117	-4.7362	3.1777
PB2-47	286.0	17.73	19.86	17.37	17.73	3.7946	-6.9305	-8.8256
PB2-48	296.0	18.79	19.22	19.32	18.79	13.7255	-8.7083	-4.8172
PB2-49	306.0	20.88	17.30	19.64	20.88	-43.6451	3.4771	3.8869
PB2-50	316.0	19.70	26.13	19.12	19.70	40.3509	0.6380	6.9015
PB2-51	326.0	19.69	15.69	17.88	19.69	5.2083	21.4757	5.0117
PB2-52	336.0	15.33	17.27	16.98	15.33	18.8679	9.4509	13.0650
PB2-53	346.0	14.36	13.02	14.41	14.36	4.2763	6.5886	5.1243
PB2-54	356.0	13.04	12.78	14.50	13.04	-3.3784	0.5151	4.2655
PB2-55	366.0	14.06	13.31	14.62	14.06	0.6472	-0.6055	0.5415
PB2-56	376.0	15.77	16.09	15.56	15.77	0.9146	0.6031	-0.4676
PB2-57	386.0	17.24	17.91	16.10	17.24	0.2475	0.1310	0.9202
PB2-58	396.0	17.04	17.71	17.21	17.04	-0.7692	1.0130	0.6920
PB2-59	406.0	17.35	15.49	17.37	17.35	3.5608	0.7659	1.9008
PB2-60	416.0	17.08	18.84	16.91	17.08	-0.4938	3.3419	3.6991
PB2-61	421.0	17.11	16.93	17.63	17.11	6.9588	5.2347	4.0153
PB2-62	426.0	17.95	15.57	19.72	17.95	9.2391	5.6698	3.7901
PB2-63	431.0	20.94	21.34	21.38	20.94	0.8114	4.1619	4.5614
PB2-64	436.0	24.80	25.93	22.99	24.80	2.4351	2.2030	3.8319
PB2-65	441.0	26.02	27.14	25.12	26.02	3.3626	3.0363	2.5528
PB2-66	446.0	26.11	24.98	27.07	26.11	3.3113	3.1725	9.6946
PB2-67	451.0	27.42	26.22	26.19	27.42	2.8436	14.2251	3.1005
PB2-68	461.0	26.28	31.06	26.25	26.28	36.5206	2.9428	5.2764
PB2-69	471.0	26.68	21.56	26.38	26.68	-30.5357	6.7424	4.6142
PB2-70	481.0	24.87	27.41	25.06	24.87	14.2424	-5.4311	3.7482
PB2-71	493.0	24.22	25.66	21.85	24.22	0.0000	4.2521	-3.5559
PB2-72	498.0	20.10	19.61	20.03	20.10	-1.4862	-0.4954	2.8153
PB2-73	503.0	15.70	15.04	16.97	15.70	0.0000	-0.0554	0.2380
PB2-74	511.0	13.20	12.45	13.62	13.20	1.3201	0.8920	1.2856
PB2-75	521.0	11.16	12.12	11.44	11.16	1.3559	2.6381	2.4047
PB2-76	531.0	9.90	8.90	9.92	9.90	5.2381	3.5679	1.9047
PB2-77	541.0	8.35	8.69	9.20	8.35	4.1096	2.2826	2.9899
PB2-78	551.0	8.33	7.46	9.16	8.33	-2.5000	2.7852	5.2797
PB2-79	568.0	9.40	8.85	9.72	9.40	6.7460	5.6836	5.9231
PB2-80	578.0	10.81	11.88	10.12	10.81	12.8049	9.3352	5.8758
PB2-81	588.0	11.43	11.70		11.43	8.4548	8.3776	
PB2-82	600.0		10.71			3.8732		

* Low frequency (LF) and high frequency (HF) susceptibility are expressed in international standard units. Frequency dependence of susceptibility is expressed in percent (%).

Table 9. A2 (upper bench south) particle size analysis (PSA) data.

Sample	d 0.1 (um)	d 0.5 (um)	d 0.9 (um)	%Clay	%Silt	%Sand	USDA Class	Silt:Clay 3 Pt Avg
A2-1	4.613	26.315	63.006	16.58	75.89	7.53	silt loam	
A2-2	3.318	20.151	48.639	22.19	75.21	2.60	silt loam	1.38
A2-3	2.523	16.944	51.925	31.30	64.75	3.95	silty clay loam	0.97
A2-4	2.731	18.246	52.693	28.27	67.43	4.30	silty clay loam	0.78
A2-5	2.386	15.331	47.712	33.51	63.67	2.82	silty clay loam	0.88
A2-6	3.065	19.486	48.343	23.82	73.51	2.66	silt loam	0.74
A2-7	2.165	12.934	44.365	38.84	58.76	2.40	silty clay loam	0.84
A2-8	2.954	18.252	46.478	25.16	72.56	2.28	silt loam	0.64
A2-9	2.524	13.292	41.391	36.85	61.77	1.37	silty clay loam	0.71
A2-10	2.551	15.966	44.988	30.67	67.14	2.19	silty clay loam	0.63
A2-11	2.551	16.114	45.001	30.42	67.47	2.11	silty clay loam	0.60
A2-12	2.460	11.415	41.670	41.75	56.62	1.64	silty clay	0.57
A2-13	2.441	14.380	47.107	34.87	62.19	2.94	silty clay loam	0.50
A2-14	2.578	12.649	44.567	38.79	59.23	1.98	silty clay loam	0.56
A2-15	2.657	13.903	47.391	36.22	61.20	2.58	silty clay loam	0.55
A2-16	2.432	12.970	45.739	38.73	59.18	2.09	silty clay loam	0.55
A2-17	2.507	12.981	45.154	37.97	59.77	2.26	silty clay loam	0.54
A2-18	2.266	13.600	44.222	37.61	60.81	1.58	silty clay loam	0.56
A2-19	2.495	14.417	44.619	34.45	63.61	1.93	silty clay loam	0.59
A2-20	2.489	14.514	45.887	35.34	62.62	2.04	silty clay loam	0.64
A2-21	2.596	15.365	46.680	34.05	64.09	1.86	silty clay loam	0.67
A2-22	2.554	15.580	47.395	34.09	63.72	2.19	silty clay loam	0.68
A2-23	2.302	15.002	47.299	34.81	62.77	2.42	silty clay loam	0.70
A2-24	2.498	16.431	48.311	31.32	66.12	2.56	silty clay loam	0.75
A2-25	2.354	17.841	51.589	32.28	64.65	3.08	silty clay loam	0.80
A2-26	2.334	17.007	51.279	33.37	63.67	2.96	silty clay loam	0.81
A2-27	2.297	16.894	51.492	33.11	63.62	3.27	silty clay loam	0.73
A2-28	2.196	14.287	49.522	35.68	60.77	3.55	silty clay loam	0.70
A2-29	2.424	15.892	51.781	31.84	63.84	4.32	silty clay loam	0.69
A2-30	2.346	16.784	50.222	32.24	64.51	3.25	silty clay loam	0.74
A2-31	2.465	16.678	47.566	30.94	66.45	2.61	silty clay loam	0.76
A2-32	2.589	16.828	45.766	29.60	68.23	2.16	silty clay loam	0.80
A2-33	2.845	17.932	45.757	26.72	71.19	2.09	silt loam	0.77
A2-34	2.421	15.476	45.093	32.59	65.36	2.05	silty clay loam	0.83
A2-35	2.845	18.323	45.109	25.53	72.69	1.78	silt loam	0.90
A2-36	3.160	19.349	45.371	22.84	75.48	1.69	silt loam	1.05
A2-37	2.694	20.175	51.498	25.95	70.93	3.12	silt loam	1.11
A2-38	2.575	20.840	53.941	26.90	69.42	3.68	silt loam	1.03
A2-39	2.466	17.794	49.459	29.62	67.52	2.86	silty clay loam	1.03
A2-40	2.614	20.850	55.482	27.29	68.25	4.46	silty clay loam	0.99
A2-41	2.446	20.256	55.738	29.17	66.20	4.63	silty clay loam	0.93
A2-42	2.562	16.011	42.877	30.03	68.21	1.75	silty clay loam	0.74
A2-43	2.400	14.422	41.293	33.61	64.46	1.93	silty clay loam	0.53
A2-44	2.263	12.007	38.261	39.71	58.80	1.49	silty clay loam	0.50
A2-45	2.422	15.452	43.893	31.10	65.69	3.21	silty clay loam	0.49

A2-46	2.234	14.458	44.211	33.88	62.75	3.37	silty clay loam	0.53
A2-47	2.153	13.760	44.609	35.77	61.09	3.14	silty clay loam	0.53
A2-48	2.238	14.572	47.961	35.28	61.32	3.40	silty clay loam	0.65
A2-49	2.830	17.741	50.549	27.07	68.94	3.99	silty clay loam	0.68
A2-50	2.165	14.690	50.927	35.74	60.15	4.11	silty clay loam	0.73
A2-51	2.493	16.847	49.159	29.64	66.40	3.95	silty clay loam	0.75
A2-52	2.764	18.520	52.252	27.56	68.36	4.07	silty clay loam	0.82
A2-53	2.555	17.143	52.218	29.96	65.78	4.26	silty clay loam	0.80
A2-54	2.241	15.862	52.602	33.48	62.13	4.39	silty clay loam	0.84
A2-55	2.987	19.391	54.252	24.98	70.10	4.92	silt loam	0.81
A2-56	2.245	16.132	53.219	33.74	61.77	4.49	silty clay loam	0.92
A2-57	2.925	19.437	53.952	25.98	69.52	4.49	silt loam	0.92
A2-58	2.939	19.538	55.106	25.84	69.16	4.99	silt loam	0.99
A2-59	2.819	18.672	55.121	28.53	66.22	5.26	silty clay loam	1.04
A2-60	3.112	21.207	58.827	24.49	69.31	6.21	silt loam	1.05
A2-61	2.931	20.144	58.198	26.16	67.88	5.97	silt loam	1.12
A2-62	3.025	20.484	57.086	25.40	69.09	5.51	silt loam	1.24
A2-63	3.804	22.618	56.510	19.96	74.92	5.13	silt loam	1.25
A2-64	3.241	19.535	51.660	23.61	72.37	4.01	silt loam	1.23
A2-65	2.876	19.964	55.512	26.61	68.58	4.81	silt loam	1.06
A2-66	2.988	19.422	54.516	25.82	69.47	4.71	silt loam	1.02
A2-67	2.831	18.976	55.666	27.17	67.64	5.19	silty clay loam	1.00
A2-68	2.894	19.450	56.020	27.12	67.75	5.13	silty clay loam	1.01
A2-69	3.093	19.624	55.254	25.29	69.60	5.11	silt loam	0.96
A2-70	2.589	17.375	52.175	30.20	65.67	4.13	silty clay loam	0.96
A2-71	3.166	18.703	51.133	24.99	71.18	3.83	silt loam	0.88
A2-72	2.777	17.232	52.534	29.09	66.49	4.42	silty clay loam	0.87
A2-73	2.779	17.065	51.145	29.14	66.84	4.02	silty clay loam	0.96
A2-74	3.462	21.222	56.783	23.07	71.58	5.35	silt loam	1.03
A2-75	3.235	19.234	54.050	24.12	70.53	5.34	silt loam	1.27
A2-76	3.987	22.133	54.761	19.60	75.78	4.62	silt loam	1.24
A2-77	3.305	20.149	52.927	23.46	72.31	4.23	silt loam	1.17
A2-78	2.628	17.192	49.960	29.40	67.21	3.39	silty clay loam	1.06
A2-79	3.424	20.559	55.998	23.17	71.51	5.32	silt loam	0.94
A2-80	2.619	17.295	52.951	30.76	64.93	4.31	silty clay loam	0.92
A2-81	2.690	16.559	50.525	30.36	65.82	3.82	silty clay loam	0.77
A2-82	2.633	16.677	49.662	30.51	65.99	3.50	silty clay loam	0.81
A2-83	3.127	18.083	51.092	25.90	70.21	3.88	silt loam	0.87
A2-84	3.062	18.221	52.841	26.12	69.32	4.56	silt loam	0.84
A2-85	2.360	15.415	53.103	34.30	61.17	4.53	silty clay loam	0.79
A2-86	2.569	16.965	54.622	31.39	63.67	4.95	silty clay loam	0.73
A2-87	2.639	16.337	50.873	30.58	65.46	3.96	silty clay loam	0.72
A2-88	2.688	15.096	46.145	32.50	64.65	2.85	silty clay loam	0.76
A2-89	2.993	18.111	51.416	26.74	69.36	3.90	silt loam	0.90
A2-90	3.407	19.863	51.901	23.10	73.03	3.87	silt loam	0.95
A2-91	2.846	17.235	51.701	28.70	66.55	4.75	silty clay loam	0.97
A2-92	3.147	18.733	52.434	25.14	70.00	4.85	silt loam	0.86
A2-93	2.683	17.708	53.689	29.66	65.74	4.61	silty clay loam	0.79
A2-94	2.664	13.842	47.067	36.73	60.52	2.75	silty clay loam	0.74
A2-95	2.862	17.111	52.006	29.24	66.60	4.17	silty clay loam	0.70

A2-96	2.645	16.141	52.981	32.15	63.24	4.61	silty clay loam	0.73
A2-97	2.731	15.004	48.088	34.32	62.82	2.86	silty clay loam	0.80
A2-98	3.076	19.381	52.657	25.75	70.25	4.00	silt loam	0.81
A2-99	2.547	16.387	50.954	32.39	64.09	3.52	silty clay loam	0.88
A2-100	2.869	17.977	51.497	27.88	67.72	4.40	silty clay loam	0.71
A2-101	2.943	17.662	163.719	29.59	51.61	18.80	silty clay loam	0.70
A2-102	2.676	16.955	54.140	30.58	63.62	5.80	silty clay loam	0.69
A2-103	2.833	17.726	51.132	29.09	66.99	3.92	silty clay loam	0.83
A2-104	2.822	18.574	52.511	28.77	67.18	4.05	silty clay loam	0.83
A2-105	3.193	20.279	135.695	25.90	55.98	18.12	silt loam	0.63
A2-106	3.494	29.058	301.411	23.74	32.84	43.42	loam	0.41
A2-107	3.909	63.262	301.316	20.65	30.07	49.28	loam	0.27
A2-108	5.214	116.859	340.699	15.59	23.44	60.97	sandy loam	

Table 10. A3 (bench south) particle size analysis (PSA) data.

Sample	Depth (cm)	% clay	% silt	% sand
A3-1	0	10.29	48.91	40.79
A3-3	5	21.22	73.59	5.19
A3-5	10	25.23	69.66	5.11
A3-7	15	26.96	68.93	4.12
A3-9	20	28.22	68.47	3.31
A3-11	25	28.43	67.60	3.97
A3-13	30	25.74	69.88	4.38
A3-15	35	27.09	67.52	5.40
A3-17	40	28.73	68.28	3.00
A3-19	45	32.13	64.28	3.59
A3-21	50	34.71	62.58	2.70
A3-23	55	34.26	62.84	2.90
A3-25	60	33.60	63.38	3.02
A3-27	65	29.99	65.59	4.42
A3-29	70	33.40	62.63	3.97
A3-31	75	33.41	62.69	3.90
A3-33	80	34.76	61.12	4.12
A3-35	85	34.42	62.35	3.22
A3-37	90	35.35	61.59	3.07
A3-39	95	32.67	64.30	3.02
A3-41	100	31.94	65.25	2.80
A3-43	105	33.38	63.33	3.29
A3-45	110	35.16	61.55	3.30
A3-47	115	29.46	67.04	3.50
A3-49	120	33.29	63.23	3.47
A3-51	125	38.41	58.75	2.84
A3-53	130	33.63	63.55	2.82
A3-55	135	36.50	59.91	3.59
A3-57	140	40.66	57.12	2.21

A3-59	145	42.26	54.99	2.76
A3-61	150	38.00	59.89	2.11
A3-63	155	38.76	59.41	1.83
A3-65	160	44.71	53.47	1.81
A3-67	165	41.11	56.59	2.30
A3-69	170	38.03	59.63	2.34
A3-71	175	41.74	55.73	2.53
A3-73	180	40.56	56.92	2.53
A3-75	185	42.52	55.57	1.91
A3-77	190	33.72	63.79	2.49
A3-79	195	36.52	60.76	2.72
A3-81	200	34.94	60.19	4.87
A3-83	205	34.73	61.17	4.10
A3-85	210	28.99	62.81	8.20
A3-87	215	34.32	57.47	8.21
A3-89	220	35.09	61.29	3.62
A3-91	225	32.39	62.36	5.25
A3-93	230	28.27	67.22	4.51
A3-95	235	27.25	68.47	4.28
A3-97	240	30.33	65.06	4.61
A3-99	250	30.80	64.76	4.43
A3-101	256	32.10	64.75	3.15
A3-103	261	29.20	65.55	5.25
A3-105	266	24.12	70.95	4.92
A3-107	271	29.15	65.88	4.97
A3-109	276	27.31	67.93	4.76
A3-111	281	28.00	67.75	4.25
A3-113	286	34.50	61.72	3.78
A3-115	291	35.76	61.26	2.98
A3-117	296	34.66	60.30	5.04
A3-119	301	31.31	64.72	3.97
A3-121	306	28.89	66.44	4.67
A3-123	311	32.55	63.37	4.08
A3-125	316	33.38	62.55	4.07
A3-127	321	33.00	63.10	3.89
A3-129	326	29.69	65.77	4.53
A3-131	331	31.01	63.84	5.16
A3-133	336	26.52	68.37	5.11
A3-135	341	32.99	63.19	3.82
A3-137	346	35.66	60.56	3.78
A3-139	351	32.00	63.87	4.12
A3-141	356	32.73	63.65	3.62
A3-143	373	34.36	62.45	3.19
A3-145	378	29.60	66.91	3.49
A3-147	383	31.32	64.71	3.98
A3-149	388	35.04	60.93	4.03
A3-151	393	31.35	64.23	4.42
A3-153	398	34.28	62.11	3.61
A3-155	403	35.96	61.61	2.43
A3-157	408	34.10	61.66	4.24

A3-159	413	32.02	64.10	3.88
A3-161	418	27.73	68.03	4.24
A3-163	423	31.47	63.97	4.56
A3-165	428	33.41	62.21	4.38
A3-167	433	31.19	64.40	4.41
A3-169	438	31.07	64.57	4.37
A3-171	443	31.29	63.93	4.78
A3-173	448	32.50	64.29	3.20
A3-175	453	32.32	63.74	3.94
A3-177	458	31.40	64.83	3.77
A3-179	463	30.12	65.77	4.11
A3-181	468	31.69	64.99	3.32
A3-183	473	28.16	66.98	4.85
A3-185	478	26.12	69.77	4.11
A3-187	483	29.77	57.66	12.57
A3-189	497	41.17	53.08	5.75
A3-191	502	41.27	52.33	6.40
A3-193	507	36.17	56.37	7.46
A3-195	512	40.53	52.03	7.43
A3-197	517	36.40	59.18	4.42
A3-199	522	40.03	56.78	3.19
A3-201	527	46.69	50.39	2.92
A3-203	532	45.69	46.44	7.87
A3-205	537	45.03	46.86	8.11
A3-207	542	48.23	43.08	8.69
A3-209	547	33.43	51.60	14.97
A3-211	552	44.56	46.09	9.34
A3-213	557	49.39	39.24	11.37
A3-215	562	45.24	41.45	13.32
A3-217	567	43.51	46.37	10.12
A3-219	572	45.34	46.88	7.78
A3-221	582	52.34	43.81	3.85
A3-223	587	54.62	43.48	1.91
A3-225	592	56.57	42.04	1.39
A3-227	597	52.62	43.11	4.27
A3-229	602	39.32	44.16	16.52
A3-231	607	39.81	44.80	15.39
A3-233	627	51.00	43.32	5.68
A3-235	632	48.09	47.59	4.32
A3-237	637	53.75	45.10	1.15
A3-239	642	48.93	47.47	3.60
A3-241	647	54.72	43.02	2.25
A3-243	652	33.49	46.54	19.97
A3-245	657	40.40	32.14	27.47
A3-247	662	38.59	36.85	24.56
A3-249	667	37.27	38.14	24.59
A3-251	672	26.27	21.82	51.91
A3-253	677	23.86	22.63	53.50
A3-255	682	24.16	19.83	56.01
A3-257	688	44.00	35.44	20.56

A3-259	694	39.79	35.94	24.27
A3-261	700	28.40	31.52	40.08
A3-263	706	46.72	42.04	11.24
A3-265	712	35.59	39.04	25.37
A3-267	718	29.78	33.90	36.32
A3-269	724	32.77	32.96	34.27
A3-271	730	18.39	16.86	64.75
A3-273	736	47.76	35.52	16.72
A3-275	742	50.90	31.91	17.19

Table 11. A4 (bench west) particle size analysis (PSA) data.

Sample	%Clay	%Silt	%Sand	USDA Class	d 0.1 (um)	d 0.5 (um)	d 0.9 (um)	Silt:Clay 3 Pt Avg	Silt:Clay
A4-1	13.83	74.14	12.03	silt loam	5.827	32.031	73.638		2.96
A4-2	19.89	73.21	6.90	silt loam	3.934	24.748	61.684	1.99	1.70
A4-3	23.50	70.87	5.63	silt loam	3.347	22.161	58.282	1.30	1.32
A4-4	29.09	66.01	4.90	silty clay loam	2.939	17.984	55.180	1.03	0.89
A4-5	28.85	66.02	5.13	silty clay loam	2.934	17.918	55.625	0.82	0.88
A4-6	34.44	61.82	3.75	silty clay loam	2.953	14.864	51.624	0.75	0.68
A4-7	34.21	62.19	3.60	silty clay loam	2.938	14.903	51.417	0.67	0.69
A4-8	35.82	60.53	3.65	silty clay loam	2.873	14.168	51.247	0.67	0.64
A4-9	34.61	61.79	3.60	silty clay loam	2.896	14.750	51.338	0.64	0.68
A4-10	38.20	58.48	3.32	silty clay loam	2.761	13.110	50.345	0.63	0.59
A4-11	36.46	60.33	3.21	silty clay loam	2.816	13.852	49.632	0.64	0.62
A4-12	34.72	61.50	3.78	silty clay loam	2.847	15.116	52.150	0.67	0.71
A4-13	34.36	61.38	4.27	silty clay loam	2.868	15.021	53.160	0.68	0.69
A4-14	34.56	61.73	3.71	silty clay loam	2.761	14.474	50.433	0.56	0.63
A4-15	42.13	55.37	2.50	silty clay	2.497	10.907	42.542	0.44	0.37
A4-16	42.86	55.17	1.98	silty clay	2.444	10.606	38.366	0.33	0.31
A4-17	43.77	54.32	1.90	silty clay	2.410	10.346	38.021	0.35	0.30
A4-18	35.81	61.63	2.57	silty clay loam	2.436	13.173	41.972	0.40	0.45
A4-19	36.36	61.07	2.56	silty clay loam	2.408	13.146	42.513	0.48	0.46
A4-20	34.49	62.68	2.84	silty clay loam	2.453	14.010	44.824	0.55	0.53
A4-21	30.16	66.80	3.03	silty clay loam	2.565	15.868	46.124	0.62	0.67
A4-22	32.02	64.86	3.12	silty clay loam	2.409	15.547	46.975	0.66	0.65
A4-23	32.65	63.87	3.48	silty clay loam	2.324	15.506	48.865	0.73	0.66
A4-24	27.05	69.26	3.68	silty clay loam	2.639	18.119	49.415	1.06	0.88
A4-25	18.98	76.88	4.14	silt loam	3.917	22.849	53.969	1.18	1.65
A4-26	25.82	66.04	8.14	silt loam	2.922	20.764	62.722	1.45	1.03
A4-27	19.16	76.90	3.94	silt loam	3.911	23.077	53.858	1.49	1.67
A4-28	18.99	77.62	3.39	silt loam	3.999	23.589	53.368	1.68	1.76
A4-29	19.56	77.07	3.37	silt loam	3.865	22.766	52.615	1.70	1.62
A4-30	19.36	76.79	3.85	silt loam	3.911	23.675	54.476	1.71	1.73
A4-31	18.83	76.77	4.40	silt loam	3.758	24.047	55.486	1.53	1.78
A4-32	26.05	69.41	4.54	silt loam	2.938	19.973	54.528	1.32	1.07
A4-33	24.53	71.66	3.81	silt loam	2.952	20.007	51.708	1.30	1.11
A4-34	18.92	77.47	3.61	silt loam	3.902	23.302	53.384	1.33	1.72

A4-35	23.28	73.26	3.46	silt loam	3.320	19.984	50.893	1.46	1.16
A4-36	20.39	74.53	5.08	silt loam	3.808	22.327	56.255	1.32	1.49
A4-37	23.31	70.47	6.23	silt loam	3.403	22.246	59.475	1.50	1.31
A4-38	19.06	74.80	6.14	silt loam	4.097	23.885	59.321	1.57	1.70
A4-39	19.14	75.24	5.62	silt loam	4.034	23.623	58.043	1.63	1.69
A4-40	20.63	73.64	5.73	silt loam	3.786	22.911	58.114	1.45	1.51
A4-41	24.48	70.55	4.97	silt loam	3.315	20.424	55.760	1.35	1.16
A4-42	21.19	72.90	5.91	silt loam	3.729	21.965	58.036	1.26	1.39
A4-43	23.91	70.29	5.81	silt loam	3.367	21.202	58.114	1.50	1.22
A4-44	17.18	76.44	6.38	silt loam	4.398	24.358	59.270	1.52	1.89
A4-45	21.76	70.68	7.56	silt loam	3.662	23.471	62.959	1.60	1.45
A4-46	19.93	69.96	10.11	silt loam	4.016	23.438	69.499	1.23	1.46
A4-47	23.68	51.47	24.85	silt loam	3.452	22.933	112.509	1.13	0.79
A4-48	23.11	66.12	10.77	silt loam	3.503	21.396	71.581	0.89	1.13
A4-49	26.72	68.10	5.18	silt loam	2.903	17.180	50.398	0.84	0.76
A4-50	27.97	66.45	5.59	silty clay loam	2.720	16.411	49.001	0.62	0.64
A4-51	33.20	61.03	5.77	silty clay loam	2.396	14.605	46.259	0.49	0.45
A4-52	36.37	57.09	6.53	silty clay loam	2.297	13.129	48.889	0.39	0.36
A4-53	34.70	62.83	2.47	silty clay loam	2.687	13.022	35.541	0.36	0.34
A4-54	36.49	59.69	3.83	silty clay loam	2.321	12.881	40.472	0.36	0.36
A4-55	36.20	58.59	5.22	silty clay loam	2.235	13.243	44.847	0.37	0.38
A4-56	37.98	58.14	3.88	silty clay loam	2.346	12.368	41.565	0.38	0.35
A4-57	35.28	57.28	7.45	silty clay loam	2.404	13.507	55.034	0.44	0.40
A4-58	30.91	60.50	8.59	silty clay loam	2.467	16.089	61.315	0.51	0.57
A4-59	32.33	62.35	5.32	silty clay loam	2.545	14.706	50.538	0.55	0.54
A4-60	32.33	61.39	6.28	silty clay loam	2.769	14.536	53.540	0.52	0.53
A4-61	36.13	57.78	6.09	silty clay loam	2.218	13.372	53.985	0.50	0.48
A4-62	33.55	61.49	4.96	silty clay loam	2.203	14.200	48.527	0.51	0.49
A4-63	32.98	61.63	5.39	silty clay loam	2.378	14.623	51.474	0.50	0.55
A4-64	36.11	57.26	6.63	silty clay loam	1.838	13.552	55.310	0.62	0.46
A4-65	26.23	55.47	18.30	silt loam	2.810	21.563	107.292	0.68	0.84
A4-66	26.30	53.83	19.87	silt loam	2.924	20.308	111.452	0.79	0.75
A4-67	26.33	55.58	18.09	silt loam	3.389	19.539	102.676	0.75	0.77
A4-68	25.52	49.82	24.66	loam	3.612	21.710	149.593	0.66	0.73
A4-69	36.16	39.05	24.78	clay loam	1.671	17.588	125.664	0.64	0.49
A4-70	26.58	48.94	24.48	loam	3.586	21.067	131.263	0.59	0.70
A4-71	26.92	38.47	34.61	loam	2.661	31.598	171.864	0.67	0.59
A4-72	24.18	42.18	33.64	loam	2.837	32.834	155.791	0.67	0.72
A4-73	26.46	41.59	31.95	loam	2.585	31.299	145.776	0.68	0.70
A4-74	23.44	33.68	42.88	loam	3.074	52.967	301.681	0.64	0.63
A4-75	17.17	25.62	57.21	sandy loam	4.481	95.997	479.759	0.64	0.58
A4-76	11.06	22.68	66.26	sandy loam	7.798	155.183	601.404	0.63	0.70
A4-77	11.60	22.77	65.64	sandy loam	7.419	149.133	533.310	0.64	0.61
A4-78	9.96	18.80	71.24	sandy loam	8.749	238.821	705.907	0.59	0.61
A4-79	14.21	24.13	61.66	sandy loam	5.633	138.494	708.837	0.48	0.55
A4-80	9.14	7.96	82.90	loamy sand	10.404	742.776	1445.802	0.37	0.29
A4-81	42.97	36.88	20.15	clay	1.367	11.751	151.453	0.25	0.27
A4-82	54.00	25.37	20.63	clay	0.978	7.061	184.313	0.24	0.19
A4-83	41.93	36.69	21.38	clay	1.521	12.301	275.078	0.21	0.27
A4-84	53.11	26.41	20.48	clay	1.067	7.503	232.516	0.24	0.17

A4-85	43.52	33.24	23.25	clay	1.637	11.734	282.499	0.25	0.27
A4-86	43.76	43.40	12.84	silty clay	1.494	11.120	86.108	0.30	0.31
A4-87	19.74	20.45	59.80	sandy loam	3.253	540.218	1454.567	0.31	0.31
A4-88	36.79	42.20	21.01	clay loam	1.733	14.860	348.699	0.35	0.31
A4-89	29.21	30.44	40.35	clay loam	2.057	36.233	698.510		0.43

Table 12. A7 (bench north) particle size analysis (PSA) data.

Sample	%Clay	%Silt	%Sand	USDA Class	d 0.1 (um)	d 0.5 (um)	d 0.9 (um)	Silt:Clay 3 Pt Avg	Silt:Clay
A7-1	19.47	74.85	5.68	silt loam	3.917	23.658	58.337		1.67
A7-2	22.15	73.07	4.78	silt loam	3.420	21.802	55.844	1.40	1.37
A7-3	24.17	71.40	4.43	silt loam	3.192	20.387	54.280	1.21	1.17
A7-4	24.82	70.99	4.19	silt loam	3.120	19.886	53.389	1.03	1.11
A7-5	30.11	66.63	3.26	silty clay loam	2.632	17.250	50.495	1.02	0.83
A7-6	24.77	72.13	3.11	silt loam	3.076	19.908	51.251	1.07	1.13
A7-7	22.87	72.98	4.15	silt loam	3.392	20.893	53.801	1.09	1.27
A7-8	29.05	67.49	3.46	silty clay loam	2.743	17.696	51.063	1.06	0.87
A7-9	25.62	70.75	3.64	silt loam	3.073	19.059	51.817	0.89	1.03
A7-10	30.58	65.86	3.56	silty clay loam	2.695	16.506	50.196	0.83	0.76
A7-11	32.22	64.96	2.83	silty clay loam	2.572	15.800	48.289	0.78	0.71
A7-12	28.13	69.05	2.81	silty clay loam	2.888	17.595	49.338	0.90	0.88
A7-13	24.74	72.13	3.13	silt loam	3.099	19.683	50.661	0.90	1.10
A7-14	32.14	65.85	2.01	silty clay loam	2.695	15.609	46.563	0.77	0.71
A7-15	39.33	59.47	1.20	silty clay loam	2.498	12.536	42.255	0.83	0.49
A7-16	22.14	74.59	3.27	silt loam	3.485	20.633	51.432	0.86	1.28
A7-17	30.22	66.94	2.85	silty clay loam	2.686	16.716	49.250	0.96	0.80
A7-18	29.92	67.10	2.99	silty clay loam	2.732	16.694	49.131	0.93	0.79
A7-19	22.18	74.93	2.89	silt loam	3.439	19.915	49.391	0.89	1.20
A7-20	32.41	65.43	2.15	silty clay loam	2.639	15.207	45.866	0.94	0.67
A7-21	25.06	72.30	2.64	silt loam	3.088	18.298	47.606	0.78	0.97
A7-22	29.92	66.48	3.60	silty clay loam	2.786	16.372	48.183	0.86	0.72
A7-23	27.26	71.04	1.70	silty clay loam	2.935	17.644	46.405	0.81	0.90
A7-24	29.72	67.13	3.15	silty clay loam	2.695	17.110	49.912	0.91	0.82
A7-25	24.77	71.62	3.61	silt loam	3.137	18.634	50.510	0.91	1.01
A7-26	26.09	70.15	3.76	silt loam	3.029	17.905	50.135	0.95	0.91
A7-27	25.19	71.68	3.13	silt loam	3.103	18.088	47.973	0.92	0.93
A7-28	25.61	71.55	2.85	silt loam	3.064	18.060	47.351	0.88	0.91
A7-29	27.58	69.28	3.14	silty clay loam	2.896	17.141	47.376	0.84	0.80
A7-30	28.09	68.90	3.01	silty clay loam	2.838	17.200	47.491	0.76	0.80
A7-31	30.43	65.08	4.49	silty clay loam	2.702	16.185	49.879	0.73	0.68
A7-32	29.31	65.78	4.90	silty clay loam	2.764	16.564	50.663	0.66	0.71
A7-33	31.80	61.97	6.24	silty clay loam	2.593	15.351	53.944	0.70	0.59
A7-34	26.34	65.57	8.09	silt loam	2.875	18.376	60.913	0.73	0.82
A7-35	27.56	64.15	8.29	silty clay loam	2.864	17.891	62.121	0.76	0.78
A7-36	30.16	62.59	7.25	silty clay loam	2.644	16.660	58.950	0.81	0.70
A7-37	24.88	66.84	8.28	silt loam	3.153	19.526	62.898	0.87	0.96
A7-38	26.49	66.09	7.42	silt loam	2.862	19.208	61.208	0.95	0.95

A7-39	27.19	65.42	7.39	silty clay loam	2.973	19.004	61.719	0.99	0.94
A7-40	25.26	67.41	7.33	silt loam	3.111	20.132	61.780	1.08	1.07
A7-41	22.94	70.33	6.73	silt loam	3.278	21.545	59.945	1.15	1.24
A7-42	24.36	68.02	7.62	silt loam	3.161	20.904	62.567	1.25	1.14
A7-43	21.65	70.35	8.00	silt loam	3.511	22.700	63.770	1.31	1.37
A7-44	21.22	70.23	8.55	silt loam	3.618	23.051	65.326	1.53	1.42
A7-45	19.04	69.18	11.78	silt loam	4.158	27.661	73.532	1.58	1.81
A7-46	20.81	72.81	6.38	silt loam	3.709	23.020	59.800	1.48	1.50
A7-47	24.13	71.30	4.58	silt loam	3.224	20.071	54.075	1.37	1.13
A7-48	22.03	67.12	10.85	silt loam	3.602	25.305	71.169	1.22	1.47
A7-49	24.91	70.25	4.84	silt loam	3.109	19.356	54.045	1.22	1.04
A7-50	23.60	71.79	4.60	silt loam	3.207	20.200	54.072	1.11	1.16
A7-51	23.57	72.24	4.19	silt loam	3.320	19.953	52.609	1.08	1.14
A7-52	26.00	70.16	3.84	silt loam	3.023	18.586	50.839	1.15	0.95
A7-53	20.99	74.74	4.28	silt loam	3.648	21.327	53.379	1.19	1.37
A7-54	22.67	72.74	4.58	silt loam	3.481	20.919	54.606	1.42	1.26
A7-55	19.49	74.92	5.59	silt loam	3.926	23.413	57.986	1.50	1.64
A7-56	20.09	73.95	5.96	silt loam	3.892	23.208	59.213	1.51	1.58
A7-57	21.94	73.18	4.88	silt loam	3.550	21.228	55.028	1.34	1.30
A7-58	23.66	72.05	4.29	silt loam	3.284	19.952	52.760	1.22	1.13
A7-59	22.18	73.75	4.07	silt loam	3.491	20.427	52.383	1.16	1.23
A7-60	23.64	72.18	4.19	silt loam	3.321	19.828	52.499	1.05	1.12
A7-61	29.90	66.46	3.64	silty clay loam	2.864	16.870	50.583	0.89	0.79
A7-62	29.72	66.70	3.57	silty clay loam	2.865	16.666	49.592	0.84	0.76
A7-63	26.66	68.74	4.60	silt loam	3.140	18.823	53.824	0.93	0.97
A7-64	25.48	70.80	3.72	silt loam	3.157	19.242	51.887	0.99	1.04
A7-65	26.77	69.21	4.03	silt loam	3.127	18.588	52.271	1.03	0.96
A7-66	24.79	71.12	4.09	silt loam	3.253	19.734	52.777	1.19	1.09
A7-67	20.69	73.02	6.28	silt loam	3.965	23.008	59.852	1.23	1.52
A7-68	24.46	71.98	3.57	silt loam	3.274	19.615	51.215	1.29	1.09
A7-69	23.20	71.98	4.82	silt loam	3.438	21.049	55.427	1.16	1.25
A7-70	23.72	72.45	3.83	silt loam	3.368	19.901	51.863	1.20	1.13
A7-71	22.52	70.65	6.83	silt loam	3.539	21.071	58.947	1.20	1.20
A7-72	19.63	61.13	19.23	silt loam	4.042	25.981	136.201	1.28	1.28
A7-73	20.04	66.43	13.52	silt loam	3.917	24.162	85.923	1.39	1.35
A7-74	16.45	58.74	24.81	silt loam	4.824	30.197	213.481	1.53	1.53
A7-75	14.21	53.92	31.87	silt loam	5.685	36.471	226.736	1.57	1.71
A7-76	10.73	37.79	51.48	loam	8.077	74.942	502.005	1.38	1.47
A7-77	8.70	24.91	66.39	sandy loam	10.022	194.278	552.918	1.31	0.97
A7-78	6.53	21.41	72.06	sandy loam	13.191	142.186	505.512	1.38	1.51
A7-79	10.20	36.95	52.85	sandy loam	8.536	75.572	345.700		1.67

Table 13. A6 (sink east) particle size analysis (PSA) data.

Sample	%Clay	%Silt	%Sand	USDA Class	d 0.1 (um)	d 0.5 (um)	d 0.9 (um)	Silt:Clay 3 Pt Avg	Silt:Clay
A6-1	27.37	66.00	6.64	silty clay loam	2.758	20.480	59.835		1.04
A6-2	45.03	51.33	3.64	silty clay	2.377	10.334	47.683	0.63	0.40
A6-3	43.26	54.49	2.25	silty clay	2.394	10.962	45.512	0.49	0.44
A6-4	35.87	61.19	2.94	silty clay loam	2.705	14.027	49.108	0.57	0.63
A6-5	35.73	61.77	2.50	silty clay loam	2.646	14.069	47.885	0.58	0.63
A6-6	42.74	55.09	2.17	silty clay	2.409	11.298	45.946	0.51	0.48
A6-7	45.66	53.01	1.33	silty clay	2.332	10.155	42.661	0.54	0.41
A6-8	33.66	63.91	2.43	silty clay loam	2.749	15.447	48.533	0.58	0.72
A6-9	38.47	59.33	2.20	silty clay loam	2.374	13.671	47.344	0.66	0.60
A6-10	33.81	63.34	2.85	silty clay loam	2.326	15.217	48.803	0.61	0.67
A6-11	36.62	61.28	2.10	silty clay loam	2.352	13.734	44.927	0.50	0.56
A6-12	46.55	52.61	0.84	silty clay	2.163	9.680	35.563	0.36	0.28
A6-13	45.01	53.66	1.33	silty clay	2.171	10.018	32.711	0.26	0.23
A6-14	40.89	58.01	1.10	silty clay	2.420	11.160	32.705	0.24	0.27
A6-15	46.60	52.09	1.30	silty clay	2.198	9.609	32.929	0.25	0.23
A6-16	43.99	53.95	2.06	silty clay	2.206	10.360	34.846	0.24	0.25
A6-17	47.05	51.03	1.92	silty clay	2.155	9.493	35.476	0.30	0.24
A6-18	39.20	57.63	3.17	silty clay loam	2.436	12.025	43.245	0.32	0.39
A6-19	45.05	52.37	2.58	silty clay	2.210	10.154	41.434	0.47	0.32
A6-20	32.59	61.76	5.64	silty clay loam	2.545	15.931	55.640	0.49	0.69
A6-21	36.51	60.43	3.06	silty clay loam	2.302	13.206	43.929	0.57	0.46
A6-22	32.75	64.09	3.16	silty clay loam	2.257	14.925	45.544	0.68	0.58
A6-23	26.60	69.07	4.33	silt loam	2.908	19.421	53.573	0.84	1.01
				silt loam/silty clay					
A6-24	27.00	68.74	4.25	loam	2.837	18.664	51.691	1.00	0.92
A6-25	25.58	70.20	4.22	silt loam	3.011	19.650	52.918	1.03	1.05
A6-26	23.14	73.05	3.81	silt loam	3.138	19.773	50.139	1.14	1.10
A6-27	21.95	74.04	4.00	silt loam	3.552	20.845	52.308	1.04	1.27
A6-28	30.92	64.63	4.45	silty clay loam	2.456	16.778	51.855	0.99	0.75
A6-29	27.90	67.64	4.45	silty clay loam	2.870	18.590	53.844	0.83	0.94
A6-30	30.63	65.73	3.65	silty clay loam	2.613	17.072	51.447	0.84	0.80
A6-31	30.16	66.22	3.62	silty clay loam	2.644	16.866	49.638	0.93	0.77
A6-32	21.32	74.86	3.83	silt loam	3.550	20.244	50.449	0.93	1.23
A6-33	29.61	66.20	4.19	silty clay loam	2.732	17.195	51.620	0.93	0.80
A6-34	30.99	65.34	3.67	silty clay loam	2.559	16.696	50.509	0.91	0.76
A6-35	23.79	72.08	4.14	silt loam	3.403	20.267	53.675	0.97	1.18
A6-36	25.71	70.36	3.93	silt loam	3.042	18.630	50.857	1.09	0.96
A6-37	22.55	72.90	4.55	silt loam	3.496	19.699	52.332	0.98	1.13
A6-38	26.76	67.26	5.98	silt loam	2.955	18.082	54.836	0.91	0.85
A6-39	31.00	65.08	3.91	silty clay loam	2.567	16.627	50.819	1.01	0.75
A6-40	19.77	76.69	3.54	silt loam	3.848	21.246	51.281	1.19	1.43
A6-41	20.25	74.60	5.15	silt loam	3.795	21.541	54.734	1.31	1.39
A6-42	23.75	72.84	3.41	silt loam	3.289	19.676	50.476	1.31	1.11
A6-43	20.69	75.05	4.26	silt loam	3.719	21.629	53.753	1.15	1.42
A6-44	25.58	71.38	3.05	silt loam	3.070	18.201	48.092	0.96	0.93
A6-45	34.96	62.49	2.55	silty clay loam	2.538	14.191	44.623	0.67	0.55

A6-46	35.49	61.99	2.52	silty clay loam	2.711	13.787	44.394	0.54	0.53
A6-47	35.25	61.83	2.92	silty clay loam	2.511	13.885	45.003	0.57	0.52
A6-48	33.48	63.51	3.01	silty clay loam	2.596	15.101	48.472	0.63	0.65
A6-49	30.81	62.86	6.33	silty clay loam	2.824	16.740	56.312	0.72	0.73
A6-50	30.35	65.59	4.07	silty clay loam	2.827	16.749	51.811	0.74	0.78
A6-51	32.15	63.13	4.72	silty clay loam	2.701	16.060	52.643	0.74	0.70
A6-52	31.91	64.58	3.52	silty clay loam	2.670	16.265	50.211	0.73	0.73
A6-53	31.74	64.74	3.52	silty clay loam	2.644	16.528	50.544	0.77	0.75
A6-54	30.85	65.78	3.37	silty clay loam	2.725	17.044	51.030	0.88	0.81
A6-55	25.20	70.85	3.94	silt loam	3.185	19.756	52.677	0.90	1.09
A6-56	30.10	66.59	3.31	silty clay loam	2.794	17.108	50.281	0.79	0.81
A6-57	34.94	60.59	4.48	silty clay loam	2.403	13.872	46.013	0.64	0.47
A6-58	29.80	64.54	5.65	silty clay loam	2.603	16.431	51.326	0.52	0.65
A6-59	34.72	61.73	3.55	silty clay loam	2.643	13.595	42.299	0.49	0.44
A6-60	36.71	57.82	5.47	silty clay loam	2.462	12.891	48.827	0.46	0.40
A6-61	34.08	58.73	7.19	silty clay loam	2.384	14.832	57.662	0.48	0.54
A6-62	32.86	62.37	4.77	silty clay loam	2.740	14.583	47.115	0.54	0.51
A6-63	31.39	62.93	5.67	silty clay loam	2.452	15.749	50.366	0.56	0.58
A6-64	32.77	60.44	6.79	silty clay loam	2.505	15.512	56.300	0.52	0.60
A6-65	35.59	57.51	6.91	silty clay loam	2.313	13.630	52.096	0.50	0.40
A6-66	34.84	58.82	6.34	silty clay loam	2.503	14.175	53.728	0.42	0.50
A6-67	38.73	58.43	2.84	silty clay loam	2.418	12.212	40.113	0.48	0.36
A6-68	31.41	60.95	7.64	silty clay loam	2.697	15.515	59.448	0.45	0.58
A6-69	30.71	50.44	18.84	silty clay loam	2.523	16.608	153.842	0.56	0.42
A6-70	13.38	29.73	56.88	sandy loam	6.501	93.543	292.155	0.66	0.69
A6-71	11.79	30.75	57.46	sandy loam	7.436	99.344	343.453	0.70	0.88
A6-72	7.55	15.75	76.70	sandy loam	11.595	268.702	782.596	0.66	0.52
A6-73	9.44	19.77	70.79	sandy loam	9.231	192.449	542.240	0.57	

Table 14. AD (delta/alluvial fan) particle size analysis (PSA) data.

Sample	%Clay	%Silt	%Sand	USDA Class	d 0.1 (um)	d 0.5 (um)	d 0.9 (um)	Silt:Clay 3 Pt Avg	Silt:Clay
AD-1	30.99	58.67	10.35	silty clay loam	2.651	18.110	70.588		0.74
AD-2	27.57	68.70	3.73	silty clay loam	2.720	18.290	51.377	0.86	0.92
AD-3	28.52	67.24	4.24	silty clay loam	2.751	18.266	53.537	0.75	0.92
AD-4	39.46	58.53	2.00	silty clay loam	2.599	11.997	40.900	0.62	0.41
AD-5	35.57	61.77	2.66	silty clay loam	2.389	14.002	45.398	0.47	0.55
AD-6	40.61	56.87	2.52	silty clay	2.516	11.841	44.675	0.51	0.45
AD-7	36.14	60.89	2.97	silty clay loam	2.630	13.691	46.267	0.49	0.54
AD-8	38.06	59.56	2.38	silty clay loam	2.611	12.828	44.500	0.58	0.49
AD-9	32.85	63.00	4.15	silty clay loam	2.438	15.886	51.612	0.62	0.69
AD-10	33.66	61.94	4.39	silty clay loam	2.385	15.763	52.748	0.72	0.69
AD-11	30.26	65.49	4.26	silty clay loam	2.587	16.852	52.556	0.67	0.78
AD-12	35.32	62.85	1.83	silty clay loam	2.576	13.890	42.712	0.57	0.53
AD-13	39.98	58.94	1.08	silty clay loam	2.527	11.948	38.627	0.49	0.40
AD-14	34.47	62.97	2.56	silty clay loam	2.304	14.445	44.479	0.48	0.55

AD-15	36.67	61.53	1.79	silty clay loam	2.324	13.528	42.145	0.53	0.50
AD-16	34.41	64.13	1.46	silty clay loam	2.710	14.354	41.690	0.53	0.55
AD-17	35.21	62.37	2.43	silty clay loam	2.175	14.335	44.614	0.58	0.55
AD-18	31.61	66.21	2.18	silty clay loam	2.444	15.569	44.069	0.65	0.64
AD-19	29.01	68.25	2.74	silty clay loam	2.650	16.877	46.774	0.66	0.76
AD-20	32.98	64.64	2.38	silty clay loam	2.408	14.758	44.616	0.64	0.59
AD-21	34.44	62.50	3.06	silty clay loam	2.244	14.435	46.755	0.67	0.57
AD-22	27.19	70.50	2.31	silty clay loam	2.810	17.434	46.252	0.75	0.84
AD-23	27.24	70.84	1.93	silty clay loam	2.744	17.442	44.858	0.71	0.83
AD-24	40.08	58.90	1.02	silty clay	2.424	12.190	40.844	0.68	0.45
AD-25	28.40	69.16	2.44	silty clay loam	2.722	16.589	45.819	0.67	0.76
AD-26	28.66	69.30	2.05	silty clay loam	2.658	17.232	45.754	0.84	0.80
AD-27	25.11	72.89	2.00	silt loam	2.954	18.456	46.184	0.83	0.97
AD-28	29.42	68.99	1.59	silty clay loam	2.567	16.493	43.445	0.63	0.73
AD-29	52.15	47.36	0.49	silty clay	2.127	8.194	31.420	0.47	0.20
AD-30	33.93	64.23	1.84	silty clay loam	2.377	14.195	39.327	0.35	0.48
AD-31	36.25	62.41	1.33	silty clay loam	2.556	12.745	35.655	0.43	0.37
AD-32	36.53	62.37	1.10	silty clay loam	2.303	13.195	37.836	0.34	0.43
AD-33	45.51	53.81	0.68	silty clay	2.294	9.877	31.969	0.30	0.23
AD-34	46.07	53.02	0.90	silty clay	2.199	9.759	33.008	0.26	0.24
AD-35	41.89	56.79	1.32	silty clay	2.191	11.025	35.464	0.29	0.30
AD-36	40.34	58.77	0.89	silty clay	2.416	11.492	35.138	0.32	0.33
AD-37	43.01	55.71	1.28	silty clay	2.222	10.827	36.770	0.31	0.32
AD-38	48.14	50.69	1.17	silty clay	2.025	9.274	37.083	0.39	0.29
AD-39	33.03	63.78	3.18	silty clay loam	2.403	14.669	45.190	0.40	0.56
AD-40	41.75	56.33	1.92	silty clay	2.238	11.269	39.226	0.42	0.35
AD-41	43.80	54.24	1.96	silty clay	2.012	10.727	40.177	0.38	0.35
AD-42	37.21	60.71	2.08	silty clay loam	2.444	12.845	40.727	0.48	0.43
AD-43	29.49	66.54	3.97	silty clay loam	2.572	16.174	46.447	0.59	0.65
AD-44	32.88	63.67	3.46	silty clay loam	2.590	15.606	49.119	0.67	0.68
AD-45	31.19	65.29	3.52	silty clay loam	2.576	15.940	48.769	0.68	0.69
AD-46	31.10	64.51	4.39	silty clay loam	2.567	16.038	50.020	0.65	0.67
AD-47	35.17	60.38	4.44	silty clay loam	2.276	14.742	50.929	0.65	0.59
AD-48	32.52	63.62	3.85	silty clay loam	2.703	15.658	49.945	0.63	0.68
AD-49	32.68	63.22	4.10	silty clay loam	2.798	15.120	48.912	0.59	0.62
AD-50	34.29	64.08	1.63	silty clay loam	2.789	13.497	39.087	0.49	0.47
AD-51	38.58	60.93	0.49	silty clay loam	2.467	12.078	35.532	0.49	0.37
AD-52	33.43	65.38	1.19	silty clay loam	2.691	14.891	42.529	0.70	0.62
AD-53	25.88	69.38	4.74	silt loam	3.149	20.117	55.690	0.92	1.11
AD-54	22.94	74.76	2.30	silt loam	3.332	18.679	45.426	1.10	1.02
AD-55	22.18	74.19	3.62	silt loam	3.476	19.782	50.546	1.14	1.17
AD-56	21.53	74.21	4.25	silt loam	3.606	20.272	52.579	1.19	1.24
AD-57	22.05	73.06	4.89	silt loam	3.446	20.021	53.148	1.23	1.16
AD-58	21.20	74.61	4.19	silt loam	3.612	20.720	52.700	1.13	1.30
AD-59	26.42	69.81	3.77	silt loam	2.990	18.233	50.910	1.08	0.93
AD-60	25.24	70.63	4.13	silt loam	3.151	18.866	52.147	0.95	1.00
AD-61	27.73	68.25	4.02	silty clay loam	2.873	18.453	52.440	0.78	0.93
AD-62	37.36	61.11	1.53	silty clay loam	2.264	12.716	38.015	0.57	0.40
AD-63	38.26	59.66	2.08	silty clay loam	2.191	12.566	37.566	0.41	0.37
AD-64	36.18	62.02	1.80	silty clay loam	2.515	13.418	40.505	0.36	0.47

AD-65	43.55	55.42	1.03	silty clay	2.348	10.436	31.413	0.42	0.23
AD-66	34.30	61.37	4.33	silty clay loam	2.415	14.512	48.723	0.35	0.55
AD-67	38.99	59.77	1.24	silty clay loam	2.379	11.797	32.837	0.38	0.28
AD-68	41.84	56.51	1.65	silty clay	2.286	10.981	35.789	0.29	0.29
AD-69	44.35	53.03	2.62	silty clay	2.071	10.345	38.338	0.25	0.28
AD-70	47.77	50.45	1.78	silty clay	2.067	9.283	31.223	0.21	0.19
AD-71	49.91	48.63	1.45	silty clay	1.954	8.731	29.324	0.20	0.16
AD-72	45.05	52.62	2.32	silty clay	2.078	10.095	36.225	0.30	0.26
AD-73	36.13	56.95	6.92	silty clay loam	2.473	13.423	58.327	0.30	0.50
AD-74	48.65	49.85	1.51	silty clay	1.924	9.044	28.638	0.39	0.15
AD-75	33.96	59.91	6.13	silty clay loam	2.685	14.098	55.196	0.30	0.53
AD-76	42.10	53.70	4.20	silty clay	2.219	10.733	35.459	0.30	0.21
AD-77	46.79	51.25	1.96	silty clay	2.127	9.513	30.510	0.14	0.18
AD-78	61.95	38.05	0.00	clay	1.622	6.290	19.686	0.09	0.04
AD-79	51.57	48.43	0.00	silty clay	1.931	8.370	22.517	0.05	0.07
AD-80	57.87	42.13	0.00	silty clay	1.741	7.073	20.962	0.05	0.05
AD-81	64.44	33.13	2.43	clay	1.642	5.942	20.006	0.10	0.03
AD-82	51.96	44.29	3.75	silty clay	2.213	8.256	43.501	0.11	0.23
AD-83	55.07	44.60	0.34	silty clay	1.999	7.685	23.041	0.15	0.08
AD-84	53.67	44.83	1.50	silty clay	1.702	7.820	28.004	0.13	0.13
AD-85	46.91	52.09	1.01	silty clay	1.954	9.499	28.502	0.14	0.16
AD-86	50.71	47.77	1.52	silty clay	1.789	8.534	28.014	0.16	0.14
AD-87	48.22	50.56	1.21	silty clay	1.843	9.189	30.943	0.14	0.19
AD-88	58.55	40.90	0.55	silty clay	1.726	6.955	23.293	0.13	0.08
AD-89	53.10	42.21	4.69	silty clay	1.899	8.018	32.755	0.11	0.12
AD-90	41.70	36.81	21.49	clay	2.216	11.142	333.841	0.14	0.14
AD-91	42.63	25.30	32.06	clay	2.484	11.350	229.653	0.18	0.15
AD-92	37.23	27.56	35.21	clay loam	2.607	16.856	261.442	0.21	0.25
AD-93	42.22	29.16	28.62	clay	2.407	12.401	229.600	0.24	0.24
AD-94	41.24	27.77	30.99	clay	2.387	13.144	221.181		0.23

Table 15. C (inflow channel) particle size analysis (PSA) data.

Sample	%Clay	%Silt	%Sand	USDA Class	d 0.1 (um)	d 0.5 (um)	d 0.9 (um)	Silt:Clay 3 Pt Avg	Silt:Clay
C-1	50.30	48.93	0.77	silty clay	2.138	8.635	32.544		0.22
C-2	28.03	66.12	5.86	silty clay loam	2.679	19.376	56.037	0.64	0.93
C-3	28.40	70.61	0.99	silty clay loam	2.625	16.935	42.473	0.62	0.77
C-4	54.20	45.58	0.22	silty clay	2.022	7.770	29.351	0.42	0.17
C-5	46.80	50.56	2.64	silty clay	2.103	9.671	40.678	0.41	0.31
C-6	30.20	66.40	3.40	silty clay loam	2.610	16.722	49.094	0.56	0.76
C-7	33.79	64.17	2.04	silty clay loam	2.519	15.144	43.965	0.64	0.62
C-8	34.92	63.08	2.00	silty clay loam	2.539	14.206	43.338	0.62	0.55
C-9	31.54	66.10	2.36	silty clay loam	2.640	15.928	45.862	0.54	0.69
C-10	43.05	55.55	1.40	silty clay	2.348	10.928	41.000	0.57	0.39
C-11	35.02	63.07	1.91	silty clay loam	2.595	14.831	45.531	0.61	0.63
C-12	30.48	65.81	3.72	silty clay loam	2.661	17.252	51.471	0.76	0.81

C-13	29.21	66.07	4.72	silty clay loam	2.788	17.903	53.570	0.67	0.85
C-14	46.18	52.91	0.92	silty clay	2.239	9.880	38.849	0.60	0.34
C-15	35.23	62.95	1.82	silty clay loam	2.691	14.386	44.558	0.43	0.60
C-16	44.65	54.35	1.00	silty clay	2.299	10.384	39.331	0.49	0.36
C-17	38.24	59.95	1.80	silty clay loam	2.539	13.042	43.454	0.47	0.51
C-18	34.02	64.39	1.60	silty clay loam	2.547	14.423	41.873	0.51	0.55
C-19	36.54	62.27	1.19	silty clay loam	2.708	13.158	39.775	0.45	0.47
C-20	44.16	55.32	0.52	silty clay	2.391	10.417	35.752	0.34	0.32
C-21	48.04	51.72	0.24	silty clay	2.298	9.218	32.573	0.34	0.24
C-22	39.34	59.28	1.39	silty clay loam	2.506	12.402	40.915	0.36	0.45
C-23	38.37	60.24	1.39	silty clay loam	2.499	12.294	36.966	0.41	0.37
C-24	36.72	61.92	1.37	silty clay loam	2.462	13.045	37.758	0.37	0.42
C-25	43.99	54.79	1.23	silty clay	2.200	10.513	36.411	0.32	0.31
C-26	49.82	49.41	0.77	silty clay	2.011	8.757	34.040	0.31	0.24
C-27	40.74	57.31	1.95	silty clay	2.299	11.796	40.171	0.49	0.39
C-28	28.83	68.63	2.54	silty clay loam	2.627	17.593	47.237	0.60	0.83
C-29	34.97	63.00	2.03	silty clay loam	2.388	14.791	44.389	0.64	0.59
C-30	39.94	57.77	2.28	silty clay loam	2.221	12.618	44.873	0.64	0.49
C-31	30.42	65.34	4.24	silty clay loam	2.579	17.777	53.005	0.61	0.84
C-32	38.72	59.36	1.92	silty clay loam	2.396	13.097	44.161	0.81	0.52
C-33	25.82	70.40	3.77	silt loam	2.811	20.016	52.127	0.74	1.07
C-34	34.64	61.02	4.34	silty clay loam	2.253	15.494	51.540	0.86	0.65
C-35	29.38	66.48	4.15	silty clay loam	2.591	18.189	52.788	0.78	0.87
C-36	29.46	66.36	4.19	silty clay loam	2.520	17.746	51.840	1.08	0.83
C-37	21.83	67.16	11.01	silt loam	3.561	26.292	71.503	1.09	1.54
C-38	28.49	67.57	3.94	silty clay loam	2.589	18.492	51.998	1.25	0.90
C-39	23.50	71.33	5.17	silt loam	3.174	22.113	56.939	1.11	1.31
C-40	24.93	69.36	5.71	silt loam	3.043	20.756	56.954	1.12	1.13
C-41	27.52	67.33	5.15	silty clay loam	2.747	18.743	54.371	1.03	0.92
C-42	26.53	67.94	5.53	silt loam	2.835	20.084	56.869	0.96	1.04
C-43	29.03	64.87	6.10	silty clay loam	2.649	19.080	58.272	1.03	0.92
C-44	24.80	70.89	4.31	silt loam	3.040	20.238	53.752	1.11	1.12
C-45	23.85	70.56	5.59	silt loam	3.157	22.085	58.172	1.12	1.29
C-46	27.05	67.61	5.34	silty clay loam	2.867	19.007	55.107	1.10	0.95
C-47	25.34	70.80	3.86	silt loam	2.999	19.716	52.136	0.91	1.07
C-48	32.70	63.76	3.54	silty clay loam	2.415	16.134	50.013	0.93	0.71
C-49	27.71	66.32	5.98	silty clay loam	2.916	19.945	58.538	0.87	1.02
C-50	29.71	66.12	4.17	silty clay loam	2.639	18.438	53.062	1.07	0.89
C-51	22.64	70.62	6.74	silt loam	3.433	22.137	59.808	1.29	1.30
C-52	19.38	74.63	5.98	silt loam	3.913	24.107	58.793	1.34	1.69
C-53	27.62	67.30	5.09	silty clay loam	2.883	19.913	56.450	1.36	1.03
C-54	22.67	72.16	5.17	silt loam	3.423	22.316	57.165	1.26	1.37
C-55	19.26	63.32	17.42	silt loam	4.119	26.046	220.915	1.26	1.38
C-56	18.46	51.39	30.15	silt loam	4.387	29.254	608.668	1.24	1.02
C-57	23.17	70.16	6.67	silt loam	3.326	22.615	60.520	1.11	1.33
C-58	27.28	68.30	4.42	silty clay loam	2.859	19.250	53.379	1.10	0.97
C-59	26.62	70.28	3.10	silt loam	2.920	19.075	50.488	0.99	1.00
C-60	26.53	69.23	4.24	silt loam	2.931	19.134	52.778	1.09	0.99
C-61	22.98	72.65	4.37	silt loam	3.277	21.271	53.964	1.07	1.27
C-62	27.99	68.11	3.90	silty clay loam	2.690	18.914	52.324	0.99	0.95

C-63	31.36	65.46	3.18	silty clay loam	2.583	16.770	48.904	1.10	0.75
C-64	20.33	75.77	3.90	silt loam	3.641	23.122	54.150	1.08	1.59
C-65	29.21	66.85	3.93	silty clay loam	2.731	18.419	52.515	1.20	0.90
C-66	24.98	71.41	3.61	silt loam	3.083	20.083	51.553	0.96	1.10
C-67	28.23	68.68	3.08	silty clay loam	2.752	18.202	49.291	0.77	0.89
C-68	40.70	58.11	1.19	silty clay	2.482	11.387	35.030	0.51	0.31
C-69	40.62	58.20	1.18	silty clay	2.497	11.522	36.028	0.43	0.34
C-70	32.87	63.75	3.38	silty clay loam	2.470	15.653	47.419	0.55	0.64
C-71	31.46	64.14	4.41	silty clay loam	2.648	16.109	50.351	0.66	0.68
C-72	31.00	58.77	10.23	silty clay loam	2.602	16.856	70.121	0.79	0.65
C-73	25.38	58.80	15.82	silt loam	3.175	22.713	84.850	0.63	1.03
C-74	48.46	48.69	2.85	silty clay	2.241	9.087	35.729	0.60	0.21
C-75	33.30	62.27	4.42	silty clay loam	2.506	14.822	48.778	0.36	0.57
C-76	38.50	51.19	10.31	silty clay loam	2.349	12.496	71.468	0.52	0.31
C-77	29.23	61.07	9.70	silty clay loam	3.037	16.905	67.959	0.74	0.68
C-78	24.85	64.57	10.57	silt loam	3.130	23.724	70.589	0.80	1.24
C-79	36.30	55.85	7.85	silty clay loam	2.217	14.112	59.489	0.78	0.48
C-80	31.52	60.08	8.40	silty clay loam	2.869	15.663	63.418	0.64	0.62
C-81	29.29	60.60	10.11	silty clay loam	2.669	18.834	69.527	0.59	0.83
C-82	37.40	53.84	8.76	silty clay loam	2.542	12.710	60.149	0.56	0.32
C-83	29.44	49.53	21.03	clay loam	2.722	18.154	147.638	0.55	0.52
C-84	25.93	49.87	24.20	loam	3.180	24.280	114.829	0.67	0.82
C-85	20.34	39.85	39.80	loam	4.030	37.493	270.309	0.73	0.66
C-86	16.97	34.31	48.72	loam	4.963	65.190	271.425	0.64	0.70
C-87	34.86	54.24	10.90	silty clay loam	2.771	14.589	72.409	0.69	0.55
C-88	31.80	62.18	6.02	silty clay loam	2.890	16.987	58.303	0.58	0.80
C-89	36.90	60.46	2.64	silty clay loam	2.365	12.732	39.672	0.58	0.39
C-90	27.29	44.47	28.24	clay loam	2.717	22.198	253.997	0.43	0.54
C-91	38.24	55.63	6.13	silty clay loam	2.508	12.364	51.170	0.36	0.37
C-92	51.14	48.00	0.86	silty clay	2.138	8.454	29.014	0.36	0.16
C-93	35.32	53.47	11.21	silty clay loam	2.734	14.332	73.509	0.36	0.53
C-94	39.65	52.63	7.72	silty clay loam	2.482	12.165	58.977	0.41	0.39
C-95	39.34	54.85	5.81	silty clay loam	2.517	11.882	46.083	0.44	0.31
C-96	29.47	56.57	13.96	silty clay loam	2.650	17.894	100.034	0.45	0.62
C-97	32.53	53.68	13.79	silty clay loam	2.766	15.209	117.628	0.52	0.41
C-98	34.17	58.66	7.17	silty clay loam	2.724	14.636	57.921	0.50	0.54
C-99	22.34	44.97	32.69	loam	3.936	24.194	272.763	0.49	0.55
C-100	30.70	46.12	23.18	clay loam	2.923	16.767	210.441	0.66	0.38
C-101	18.88	40.41	40.71	loam	4.367	51.355	186.519	0.62	1.06
C-102	37.64	54.02	8.34	silty clay loam	2.407	12.979	61.734	0.87	0.41
C-103	13.46	35.28	51.26	loam	6.361	72.574	250.384		1.15

Table 16. PB2 (playa sink) particle size analysis (PSA) data.

Sample	%Clay	%Silt	%Sand	USDA Class	d 0.1 (um)	d 0.5 (um)	d 0.9 (um)	Silt:Clay 3 Pt Avg	Silt:Clay
PB2-1	27.17	60.63	12.20	silty clay loam	2.885	22.136	77.632		0.99
PB2-2	45.04	52.15	2.81	silty clay	2.130	10.424	44.358	0.61	0.39
PB2-3	38.08	60.33	1.59	silty clay loam	2.532	12.561	40.314	0.43	0.44
PB2-4	38.18	59.78	2.03	silty clay loam	2.514	12.680	42.765	0.44	0.47
PB2-5	41.99	56.11	1.90	silty clay	2.397	11.329	42.147	0.46	0.41
PB2-6	38.39	59.58	2.04	silty clay loam	2.451	12.821	43.428	0.39	0.49
PB2-7	42.28	42.56	15.16	silty clay	2.065	11.676	225.875	0.35	0.29
PB2-8	44.79	53.07	2.15	silty clay	2.167	10.179	37.226	0.29	0.28
PB2-9	44.16	53.88	1.96	silty clay	2.177	10.358	37.248	0.27	0.29
PB2-10	47.64	50.04	2.32	silty clay	2.072	9.354	37.018	0.30	0.25
PB2-11	38.82	58.82	2.36	silty clay loam	2.378	12.066	38.571	0.32	0.36
PB2-12	41.24	57.42	1.35	silty clay	2.255	11.369	37.472	0.38	0.34
PB2-13	36.75	60.16	3.09	silty clay loam	2.364	13.257	43.078	0.37	0.45
PB2-14	46.46	51.34	2.20	silty clay	2.033	9.783	40.510	0.37	0.31
PB2-15	42.60	54.03	3.37	silty clay	2.194	11.049	42.584	0.30	0.34
PB2-16	48.72	48.89	2.39	silty clay	2.015	9.050	37.214	0.27	0.24
PB2-17	50.14	47.28	2.58	silty clay	1.921	8.673	36.918	0.21	0.22
PB2-18	49.60	48.20	2.19	silty clay	1.972	8.810	32.478	0.19	0.18
PB2-19	48.32	50.15	1.52	silty clay	1.962	9.136	29.660	0.22	0.17
PB2-20	40.57	55.92	3.51	silty clay	2.160	11.537	39.731	0.34	0.30
PB2-21	32.45	59.96	7.59	silty clay loam	2.370	15.341	58.459	0.48	0.55
PB2-22	36.37	60.26	3.36	silty clay loam	2.488	14.165	49.286	0.63	0.60
PB2-23	33.27	62.42	4.32	silty clay loam	2.500	16.688	53.465	0.74	0.76
PB2-24	30.90	64.40	4.70	silty clay loam	2.608	18.084	55.182	0.81	0.87
PB2-25	32.62	62.13	5.26	silty clay loam	2.466	17.367	56.310	0.76	0.80
PB2-26	36.59	60.39	3.03	silty clay loam	2.467	14.418	49.059	0.69	0.62
PB2-27	33.89	63.23	2.89	silty clay loam	2.635	15.061	47.387	0.64	0.64
PB2-28	31.25	66.21	2.54	silty clay loam	2.765	15.671	44.750	0.67	0.65
PB2-29	30.49	65.72	3.79	silty clay loam	2.628	16.205	49.004	0.70	0.71
PB2-30	29.87	65.95	4.18	silty clay loam	2.650	16.568	50.660	0.72	0.74
PB2-31	31.07	65.69	3.24	silty clay loam	2.795	16.074	48.527	0.77	0.72
PB2-32	27.48	68.29	4.23	silty clay loam	2.950	17.658	51.341	0.75	0.86
PB2-33	33.26	63.57	3.16	silty clay loam	2.498	15.388	48.439	0.77	0.66
PB2-34	30.09	65.84	4.07	silty clay loam	2.703	16.790	51.664	0.71	0.78
PB2-35	33.28	63.79	2.93	silty clay loam	2.478	15.653	49.114	0.71	0.70
PB2-36	33.19	63.66	3.15	silty clay loam	2.550	15.152	48.631	0.69	0.65
PB2-37	31.03	65.26	3.71	silty clay loam	2.654	16.130	49.948	0.68	0.72
PB2-38	33.68	64.19	2.13	silty clay loam	2.679	15.216	46.503	0.73	0.67
PB2-39	29.20	67.57	3.22	silty clay loam	2.968	17.013	48.871	0.72	0.81
PB2-40	31.95	65.20	2.86	silty clay loam	2.754	15.621	47.514	0.71	0.69
PB2-41	32.93	64.10	2.96	silty clay loam	2.850	14.862	47.299	0.62	0.64
PB2-42	35.32	61.85	2.82	silty clay loam	2.439	13.970	45.836	0.61	0.55
PB2-43	32.72	64.37	2.91	silty clay loam	2.826	15.125	46.829	0.60	0.64
PB2-44	34.29	61.73	3.98	silty clay loam	2.563	14.623	50.550	0.64	0.62
PB2-45	33.41	62.58	4.01	silty clay loam	2.744	15.012	50.779	0.63	0.65
PB2-46	33.07	63.48	3.45	silty clay loam	2.766	14.934	47.905	0.64	0.62

PB2-47	32.77	64.49	2.73	silty clay loam	2.985	14.982	46.630	0.63	0.64
PB2-48	32.95	64.19	2.86	silty clay loam	2.738	15.096	46.548	0.65	0.63
PB2-49	32.90	63.95	3.15	silty clay loam	2.868	15.647	48.457	0.69	0.69
PB2-50	32.45	63.49	4.06	silty clay loam	2.584	16.506	52.424	0.72	0.75
PB2-51	30.91	63.85	5.24	silty clay loam	2.730	16.426	53.746	0.66	0.73
PB2-52	32.97	64.05	2.98	silty clay loam	2.752	14.433	41.608	0.55	0.50
PB2-53	35.20	59.46	5.34	silty clay loam	2.697	13.303	47.323	0.48	0.41
PB2-54	33.09	63.54	3.37	silty clay loam	2.637	14.525	44.614	0.46	0.53
PB2-55	37.34	59.75	2.90	silty clay loam	2.572	12.686	43.220	0.38	0.43
PB2-56	49.19	49.62	1.19	silty clay	2.216	8.904	30.685	0.29	0.19
PB2-57	42.40	55.59	2.00	silty clay	2.285	10.756	33.277	0.19	0.24
PB2-58	50.98	47.67	1.35	silty clay	2.196	8.489	28.748	0.20	0.15
PB2-59	44.59	52.66	2.75	silty clay	2.266	10.084	33.139	0.14	0.20
PB2-60	56.84	41.66	1.50	silty clay	2.028	7.368	22.917	0.14	0.07
PB2-61	39.54	38.95	21.51	clay loam	2.081	12.376	146.760	0.15	0.14
PB2-62	30.53	34.61	34.86	clay loam	2.727	18.289	150.469	0.16	0.23
PB2-63	41.92	36.96	21.12	clay	2.150	11.285	155.034	0.18	0.09
PB2-64	41.45	46.23	12.32	silty clay	2.171	11.357	89.796	0.16	0.22
PB2-65	43.42	42.75	13.83	silty clay	2.112	10.698	107.880	0.22	0.17
PB2-66	42.84	54.08	3.09	silty clay	2.220	10.756	38.279	0.28	0.28
PB2-67	42.08	55.92	2.00	silty clay	2.376	11.235	40.656	0.27	0.38
PB2-68	52.53	45.50	1.97	silty clay	2.064	8.131	31.156	0.27	0.16
PB2-69	36.31	41.97	21.71	clay loam	2.546	13.585	130.324	0.22	0.28
PB2-70	45.39	48.64	5.97	silty clay	2.205	9.944	45.851	0.24	0.22
PB2-71	46.79	45.55	7.65	silty clay	1.896	9.636	55.611	0.19	0.22
PB2-72	55.18	43.73	1.09	silty clay	2.044	7.625	27.368	0.13	0.13
PB2-73	65.05	34.35	0.60	clay	1.929	6.239	18.222	0.10	0.04
PB2-74	53.54	44.32	2.13	silty clay	2.123	7.951	29.261	0.13	0.14
PB2-75	46.69	50.10	3.21	silty clay	1.882	9.669	35.151	0.20	0.21
PB2-76	44.12	44.85	11.04	silty clay	2.052	10.429	74.984	0.21	0.25
PB2-77	52.42	44.38	3.21	silty clay	2.208	8.183	35.948	0.24	0.18
PB2-78	41.62	54.33	4.05	silty clay	2.247	11.062	43.136	0.21	0.30
PB2-79	42.09	35.51	22.40	clay	2.607	10.897	172.807	0.25	0.15
PB2-80	29.65	29.17	41.17	clay loam	3.606	30.110	227.529	0.25	0.30
PB2-81	29.45	27.30	43.25	clay loam	3.398	40.295	416.030	0.25	0.31
PB2-82	40.16	24.16	35.68	clay	2.712	13.274	264.032		0.15

Table 17. Sensor pit (playa center) color data (CIELAB only).

sample	depth (cm)	L*	a*	b*
1	235	69.61	1	12.99
2	230	63.17	1.17	13.29
3	225	60.03	1.36	12.31
4	220	61.59	1.24	10.94
5	215	64.95	1.09	12.17

6	210	61.93	2.11	13.95
7	205	63.29	1.96	11.78
8	200	54.94	1.2	11.17
9	195	59.29	1.28	12.46
10	190	48.37	1.12	9.88
11	185	60.44	1.48	11.19
12	180	65.74	1.22	10.95
13	175	66.16	1.49	13.32
14	170	64.15	1.4	11.3
15	165	57.65	1.25	11.6
16	160	67.9	1.26	12.54
17	155	59.19	1.49	11.25
18	150	62.63	1.59	11.97
19	145	58.34	1.55	11.31
20	140	63.03	1.25	9.7
21	135	65.82	1.47	12.01
22	130	60.14	1.47	11.19
23	125	64.66	1.57	12.86
24	120	53.9	1.72	11.49
25	115	61.55	1.68	12.22
26	110	46.93	2.33	9.81
27	105	37.49	2.4	7.81
28	100	44.88	2.67	8.86
29	95	40.6	2.73	8.03
30	90	33.39	2.23	7.01
31	85	33.55	2.04	6.34
32	80	34.19	2.18	6.55
33	75	43.52	2.27	7.19
34	70	40.64	2.08	7.1
35	65	42.08	2.24	7.04
36	60	36.78	2.15	6.76
37	55	30.96	1.98	5.99
38	50	25.44	1.62	4.99
39	45	36.8	1.98	6.41
40	40	33.46	1.74	5.51
41	35	35.4	1.75	5.71
42	30	42.26	1.99	6.09
43	25	39.28	2.08	6.39
44	20	43.69	2.41	7.47
45	15	35.72	2.07	6.68
46	10	36.31	2.4	6.92
47	5	40.02	2.2	6.87
48	0	26.92	2.09	6.46

Table 18. EPC3 (playa center) color data (CIELAB and Munsell).

Sample	depth (cm)	L*	a*	b*	Munsell Hue	Munsell Value	Munsell Chroma
EPC3-1	1	39.78	2.93	8.37	9.9YR	3.89	1.31
EPC3-2	3	39.76	2.59	7.63	10.0YR	3.89	1.19
EPC3-3	5	38.48	2.7	7.45	9.8YR	3.76	1.18
EPC3-4	8	37.54	2.75	7.41	9.8YR	3.67	1.18
EPC3-5	10	36.29	2.08	6.14	0.3Y	3.55	0.97
EPC3-6	12	40.74	2.18	6.29	9.9YR	3.98	0.98
EPC3-7	14	27.38	1.82	5.27	0.8Y	2.69	0.9
EPC3-8	17	33.76	1.9	5.78	0.6Y	3.31	0.92
EPC3-9	20	27.27	1.77	5.13	0.8Y	2.68	0.87
EPC3-10	22	37.76	2.25	6.75	0.2Y	3.69	1.06
EPC3-11	25	44.96	2.06	6.15	9.9YR	4.38	0.97
EPC3-12	27	34.37	1.77	5.13	0.4Y	3.36	0.82
EPC3-13	29	37.45	2.07	6.14	0.2Y	3.66	0.96
EPC3-14	32	38.61	1.76	5.74	0.5Y	3.77	0.88
EPC3-15	35	36.18	1.71	5.8	0.9Y	3.54	0.9
EPC3-16	37	38.17	1.9	5.83	0.3Y	3.73	0.91
EPC3-17	40	39.33	1.88	6.1	0.4Y	3.84	0.94
EPC3-18	42	32.28	1.72	6.27	1.4Y	3.16	0.99
EPC3-19	45	30.78	1.6	5.95	1.6Y	3.02	0.95
EPC3-20	47	33.22	1.76	5.33	0.7Y	3.25	0.86
EPC3-21	50	26.52	1.56	5.47	1.6Y	2.6	0.92
EPC3-22	53	39.73	2.01	6.41	0.3Y	3.88	0.98
EPC3-23	55	32	1.67	5.65	1.2Y	3.14	0.9
EPC3-24	57	33.81	1.75	5.8	1.0Y	3.31	0.92
EPC3-25	60	38.25	2.02	6.19	0.3Y	3.74	0.96
EPC3-26	63	39.94	1.97	6.16	0.2Y	3.9	0.95
EPC3-27	65	35.79	1.93	5.87	0.5Y	3.5	0.93
EPC3-28	68	40.2	2.07	6.43	0.2Y	3.93	0.99
EPC3-29	71	31.84	1.87	6.16	1.0Y	3.12	0.99
EPC3-30	74	33.86	1.98	5.92	0.5Y	3.32	0.95
EPC3-31	76	41.84	2.09	6.98	0.5Y	4.08	1.06
EPC3-32	78	35.46	2.11	6.38	0.5Y	3.47	1.01
EPC3-33	81	41.39	2.33	7.07	10.0YR	4.04	1.09
EPC3-34	83	37.49	2.02	6.15	0.3Y	3.66	0.96
EPC3-35	86	36.43	2.05	6.36	0.5Y	3.56	1
EPC3-36	88	33.64	2.1	6.66	0.9Y	3.3	1.06
EPC3-37	91	44.69	2.34	7.32	0.1Y	4.36	1.14
EPC3-38	94	35.07	2.19	6.67	0.5Y	3.43	1.06
EPC3-39	96	36.53	2.38	7.46	0.6Y	3.58	1.17

EPC3-40	99	41.7	2.44	7.65	0.2Y	4.07	1.17
EPC3-41	101	47.04	2.44	9.45	1.2Y	4.59	1.45
EPC3-42	104	49.08	2.73	9.4	0.6Y	4.79	1.48
EPC3-43	107	49.05	2.77	9.93	0.8Y	4.79	1.55
EPC3-44	109	53.91	2.13	10.16	1.7Y	5.26	1.53
EPC3-45	112	52.92	2.16	10.44	1.9Y	5.17	1.58
EPC3-46	114	60.65	1.94	10.33	1.6Y	5.93	1.51
EPC3-47	116	62.31	1.52	10.32	2.1Y	6.1	1.48
EPC3-48	118	63.32	1.61	9.56	1.7Y	6.2	1.38
EPC3-49	120	71.54	1.2	9.45	1.9Y	7.03	1.33
EPC3-50	122	64.8	1.58	10.61	1.9Y	6.35	1.52
EPC3-51	125	68.54	1.63	10.81	1.8Y	6.73	1.55
EPC3-52	127	63.14	1.53	11.16	2.2Y	6.19	1.59
EPC3-53	129	67.28	1.18	10.48	2.4Y	6.6	1.47
EPC3-54	132	68.2	1.15	11.05	2.5Y	6.7	1.54
EPC3-55	135	61.18	1.06	11.15	3.1Y	5.99	1.56
EPC3-56	137	58.44	1.07	10.51	3.1Y	5.71	1.48
EPC3-57	139	65.44	0.93	10.62	2.9Y	6.42	1.47
EPC3-58	142	61.54	0.79	10.29	3.4Y	6.02	1.42
EPC3-59	144	56.89	1.03	10.66	3.4Y	5.56	1.51
EPC3-60	147	63.96	1.03	10.93	2.9Y	6.27	1.52
EPC3-61	150	64.06	1.17	11.61	2.9Y	6.28	1.62
EPC3-62	152	63.5	1.01	11.15	3.1Y	6.22	1.55
EPC3-63	155	64.95	0.95	10.69	3.0Y	6.37	1.48
EPC3-64	157	62.02	0.94	10.71	3.1Y	6.07	1.49
EPC3-65	160	68.97	1.02	10.17	2.5Y	6.77	1.41
EPC3-66	162	70.68	1.09	10.43	2.3Y	6.94	1.46
EPC3-67	165	62.12	1.03	10.39	2.9Y	6.08	1.45
EPC3-68	167	62.89	1.26	9.03	2.2Y	6.15	1.28
EPC3-69	170	59.7	1.43	12.2	2.8Y	5.84	1.73
EPC3-70	172	62.48	1.42	11.46	2.5Y	6.12	1.62
EPC3-71	175	56.66	1.67	11.29	2.5Y	5.54	1.64
EPC3-72	178	64.42	1.16	11.34	2.7Y	6.31	1.58
EPC3-73	180	63.85	1.17	11.33	2.8Y	6.26	1.58
EPC3-74	182	63.32	1.7	11.95	2.2Y	6.21	1.71
EPC3-75	185	60.94	1.53	11.45	2.4Y	5.96	1.63
EPC3-76	188	63.25	1.52	11.1	2.2Y	6.2	1.58
EPC3-77	190	65.59	1.37	11.36	2.3Y	6.43	1.6
EPC3-78	193	68.17	1.05	12.54	3.0Y	6.7	1.74
EPC3-79	195	71.33	1.1	11.72	2.5Y	7.01	1.63
EPC3-80	198	64.05	1.47	12.33	2.5Y	6.28	1.74
EPC3-81	201	66.68	1.73	13.53	2.3Y	6.55	1.92
EPC3-82	203	59.92	2.01	13.82	2.4Y	5.87	1.99

EPC3-83	206	65.57	1.28	12.7	2.8Y	6.43	1.78
EPC3-84	208	68.46	0.94	11.42	2.9Y	6.72	1.58
EPC3-85	211	69.48	0.9	10.72	2.8Y	6.82	1.48
EPC3-86	213	60.69	0.95	10.31	3.2Y	5.93	1.44
EPC3-87	216	66.64	1.29	11.54	2.4Y	6.54	1.62
EPC3-88	218	65.29	0.87	12.5	3.5Y	6.41	1.72
EPC3-89	221	65.28	0.83	11.69	3.4Y	6.4	1.61
EPC3-90	223	63.87	1.04	13.18	3.3Y	6.26	1.83
EPC3-91	226	64.79	1.05	12.73	3.2Y	6.35	1.77
EPC3-92	228	71.86	0.6	11.18	3.4Y	7.07	1.52
EPC3-93	231	74.5	0.58	11.51	3.3Y	7.34	1.55
EPC3-94	233	66.96	0.54	11.85	3.8Y	6.57	1.61
EPC3-95	235	65.49	0.59	11.71	3.8Y	6.42	1.6
EPC3-96	238	60.59	0.66	11.03	3.8Y	5.93	1.52
EPC3-97	240	64.08	0.68	11.6	3.7Y	6.28	1.59
EPC3-98	242	67.83	0.4	10.16	3.8Y	6.65	1.37
EPC3-99	245	71.09	0.46	10.94	3.6Y	6.99	1.48
EPC3-100	247	68.75	0.6	11.11	3.5Y	6.75	1.51
EPC3-101	249	70.46	0.81	12.11	3.2Y	6.93	1.66
EPC3-102	252	70.28	0.67	11.58	3.4Y	6.91	1.58
EPC3-103	254	68.06	1.02	12.99	3.1Y	6.69	1.79
EPC3-104	257	60.49	1.52	13.98	3.0Y	5.93	1.97
EPC3-105	259	66.87	1.02	12.89	3.1Y	6.57	1.78
EPC3-106	262	72.04	0.67	12.41	3.4Y	7.09	1.69
EPC3-107	264	56.21	0.91	12.13	3.8Y	5.49	1.71
EPC3-108	267	64.39	1.17	13.44	3.1Y	6.32	1.87
EPC3-109	269	61.57	0.81	12.51	3.7Y	6.03	1.72
EPC3-110	272	66.48	0.76	11.98	3.5Y	6.52	1.64
EPC3-111	275	63.28	0.76	11.84	3.6Y	6.2	1.63
EPC3-112	277	66.84	0.72	13.28	3.7Y	6.56	1.82
EPC3-113	279	68.48	0.47	11.15	3.8Y	6.72	1.51
EPC3-114	282	65.82	1.02	11.37	2.9Y	6.46	1.58
EPC3-115	285	68.96	0.92	11.28	2.9Y	6.77	1.56
EPC3-116	288	59.86	1.33	12.41	3.0Y	5.86	1.75
EPC3-117	290	64.46	1.2	11.86	2.8Y	6.32	1.66
EPC3-118	292	63.99	1.33	12.06	2.7Y	6.27	1.69
EPC3-119	295	66.5	1.16	11.82	2.7Y	6.52	1.65
EPC3-120	298	59.03	1.27	11.81	3.0Y	5.78	1.67
EPC3-121	300	62.57	1.32	11.3	2.6Y	6.13	1.59
EPC3-122	303	71.85	1.32	10.88	2.0Y	7.06	1.53
EPC3-123	305	66.43	1.8	12.92	2.1Y	6.52	1.84
EPC3-124	308	65.63	1.24	12.18	2.7Y	6.44	1.7
EPC3-125	310	68.93	1.13	11.82	2.6Y	6.77	1.64

EPC3-126	313	67.29	1.17	12.01	2.7Y	6.61	1.67
EPC3-127	315	59.9	1.31	11.87	2.9Y	5.86	1.68
EPC3-128	318	62.41	1.38	11.95	2.6Y	6.11	1.68
EPC3-129	320	61.41	1.72	12.01	2.2Y	6.01	1.72
EPC3-130	323	60.18	1.48	11.68	2.6Y	5.89	1.66
EPC3-131	326	62.11	1.16	11.36	2.9Y	6.08	1.59
EPC3-132	328	65.67	1.16	11.61	2.7Y	6.44	1.62
EPC3-133	330	70.53	0.73	10.74	3.0Y	6.93	1.47
EPC3-134	333	70.43	0.7	10.65	3.1Y	6.92	1.46
EPC3-135	335	64.89	0.92	11.3	3.2Y	6.36	1.56
EPC3-136	337	66.09	0.66	11.21	3.5Y	6.48	1.53
EPC3-137	340	65.05	0.78	11.47	3.4Y	6.38	1.58
EPC3-138	343	66.85	0.66	11.35	3.5Y	6.56	1.55
EPC3-139	346	69.65	0.55	10.91	3.5Y	6.84	1.48
EPC3-140	348	65.11	1.04	12.32	3.1Y	6.39	1.71
EPC3-141	350	63.7	1.33	12.41	2.7Y	6.24	1.74
EPC3-142	353	62.44	1.47	12.26	2.5Y	6.12	1.73
EPC3-143	355	66.06	1.17	12.45	2.9Y	6.48	1.73
EPC3-144	358	57.76	1.31	12.73	3.3Y	5.65	1.8
EPC3-145	360	62.78	0.97	11.76	3.2Y	6.15	1.63
EPC3-146	363	54.09	1.12	10.63	3.4Y	5.28	1.53
EPC3-147	365	53.64	1.41	11.05	3.1Y	5.24	1.6
EPC3-148	367	64.54	1.26	12.53	2.8Y	6.33	1.75
EPC3-149	370	69.08	1.09	11.73	2.7Y	6.79	1.63
EPC3-150	373	67.27	1.19	12.11	2.7Y	6.6	1.69
EPC3-151	375	64.77	1.2	12.33	2.9Y	6.35	1.72
EPC3-152	378	61.72	1.14	12.54	3.2Y	6.04	1.75
EPC3-153	380	67.41	1.22	12.44	2.7Y	6.62	1.73
EPC3-154	383	62.71	1.3	13.33	3.0Y	6.15	1.87
EPC3-155	385	63.72	0.85	12.35	3.5Y	6.25	1.7
EPC3-156	388	66.46	1.11	12.06	2.8Y	6.52	1.68
EPC3-157	390	66.36	1.21	11.2	2.5Y	6.51	1.57
EPC3-158	392	66.47	1.2	12.08	2.7Y	6.52	1.69
EPC3-159	395	64.15	1.2	11.4	2.7Y	6.29	1.59
EPC3-160	398	64.11	1.3	12.15	2.7Y	6.28	1.7
EPC3-161	400	59.56	1.55	12.41	2.7Y	5.83	1.77
EPC3-162	403	69.49	1.06	11.47	2.6Y	6.83	1.59
EPC3-163	405	62.91	1.52	12.18	2.5Y	6.16	1.73
EPC3-164	408	70.12	1.09	11.22	2.5Y	6.89	1.56
EPC3-165	410	65.13	1.28	11.74	2.6Y	6.39	1.65
EPC3-166	413	56.53	1.31	10.55	2.9Y	5.52	1.51
EPC3-167	415	65.08	1.04	11.19	2.8Y	6.38	1.55
EPC3-168	418	69.51	0.93	11.18	2.8Y	6.83	1.54

EPC3-169	420	67.56	0.95	11.43	2.9Y	6.63	1.58
EPC3-170	423	64.67	0.84	11.18	3.2Y	6.34	1.54
EPC3-171	425	69.91	0.89	10.84	2.7Y	6.87	1.5
EPC3-172	428	61.92	1.02	11.17	3.1Y	6.06	1.55
EPC3-173	430	63.12	0.94	11.31	3.1Y	6.18	1.57
EPC3-174	433	66.35	0.94	11.2	3.0Y	6.51	1.55
EPC3-175	436	64.29	0.85	11.1	3.2Y	6.3	1.53
EPC3-176	438	63.42	0.94	11.61	3.2Y	6.21	1.61
EPC3-177	441	58.3	1.19	11.58	3.1Y	5.7	1.64
EPC3-178	443	67.01	1.04	11.73	2.8Y	6.58	1.63
EPC3-179	446	58.84	1.18	11.29	3.1Y	5.75	1.59
EPC3-180	448	62.4	0.99	11.72	3.2Y	6.11	1.63
EPC3-181	451	63.04	1.24	12.32	2.9Y	6.18	1.73
EPC3-182	453	59.25	1.19	12	3.1Y	5.8	1.69
EPC3-183	456	63.31	0.99	11.19	3.0Y	6.2	1.55
EPC3-184	458	65.55	1.16	11.85	2.7Y	6.43	1.65
EPC3-185	461	63.34	1.05	11.3	3.0Y	6.2	1.57
EPC3-186	463	62.99	0.93	11.39	3.2Y	6.17	1.58
EPC3-187	466	69.42	0.63	11.35	3.4Y	6.82	1.55
EPC3-188	469	66.36	0.56	11.05	3.6Y	6.51	1.5
EPC3-189	471	69.43	0.53	10.81	3.5Y	6.82	1.47
EPC3-190	474	63.41	0.73	10.92	3.5Y	6.21	1.5
EPC3-191	476	69.61	0.67	11.49	3.3Y	6.84	1.57
EPC3-192	478	65.28	0.78	11.34	3.4Y	6.4	1.56
EPC3-193	481	61.97	0.56	10.51	3.7Y	6.06	1.43
EPC3-194	484	67.83	0.79	10.48	3.0Y	6.66	1.44
EPC3-195	486	61.94	1.17	11.15	2.8Y	6.06	1.56
EPC3-196	489	68.96	0.82	10.68	2.9Y	6.77	1.47
EPC3-197	491	66.46	1.1	11.86	2.8Y	6.52	1.65
EPC3-198	494	69.41	0.8	11.41	3.1Y	6.82	1.57
EPC3-199	496	66.3	0.59	10.96	3.6Y	6.5	1.49
EPC3-200	499	59.01	0.78	11.22	3.6Y	5.77	1.56
EPC3-201	502	65.11	0.78	10.86	3.3Y	6.38	1.49
EPC3-202	504	65.67	0.62	10.75	3.5Y	6.44	1.47
EPC3-203	506	66.97	0.55	10.37	3.5Y	6.57	1.41
EPC3-204	509	61.52	0.43	10.15	3.9Y	6.02	1.38
EPC3-205	511	62.99	0.64	10.82	3.6Y	6.17	1.48
EPC3-206	513	67.68	0.7	10.98	3.3Y	6.64	1.5
EPC3-207	516	59.6	0.58	10.59	3.8Y	5.83	1.46
EPC3-208	519	65.78	0.57	11.06	3.6Y	6.45	1.51
EPC3-209	521	71.26	0.52	10.61	3.3Y	7	1.44
EPC3-210	523	69.94	0.66	11.14	3.2Y	6.87	1.52

Table 19. EPC5 (playa center) color data (CIELAB and Munsell).

Sample	depth (cm)	L*	a*	b*	Munsell Hue	Munsell Value	Munsell Chroma
EPC5 2	45	50.82	2.37	8.15	0.5Y	4.95	1.29
EPC5 4	94	54.53	3.11	9.71	9.9YR	5.33	1.57
EPC5 6	155	65.2	2.18	13.66	2.0Y	6.4	1.97
EPC5 8	195	70.14	1.66	12.49	2.1Y	6.9	1.77
EPC5 10	252	68.65	1.8	15.51	2.7Y	6.76	2.19
EPC5 12	294	66.97	2.98	17.41	2.0Y	6.59	2.55
EPC5 14	345	69.94	1.45	14.14	2.7Y	6.88	1.97
EPC5 16	406	70.43	1.2	13.55	2.9Y	6.93	1.88
EPC5 18	454	64.91	1.3	12.92	2.9Y	6.37	1.81
EPC5 20	500	80.1	0.29	10.6	3.6Y	7.91	1.37
EPC5 22	630	73	1.56	12.81	2.1Y	7.19	1.8
EPC5 23	665	82.43	1.46	10.81	1.5Y	8.15	1.51
EPC5 24	684	87.66	0.94	8.97	1.7Y	8.68	1.19
EPC5 25	696	82.76	1.58	10.82	1.3Y	8.18	1.52
EPC5 26	725	86.93	0.79	7.77	1.7Y	8.6	1.02
EPC5 27	738	86.37	1.02	8.01	1.3Y	8.54	1.08
EPC5 28	755	68.49	5.72	16.7	9.2YR	6.75	2.75
EPC5 29	775	67.19	7.6	17.28	8.0YR	6.62	3.07
EPC5 30	791	67.59	8.26	18.09	7.8YR	6.67	3.26
EPC5 31	804	65.77	8.27	18.16	7.9YR	6.48	3.26
EPC5 32	818	75.91	4.92	13.43	8.5YR	7.49	2.27
EPC5 33	856	68.41	7.72	18.39	8.2YR	6.75	3.22
EPC5 34	880	84.43	2.61	10.41	9.5YR	8.35	1.59
EPC5 35	906	74.09	4.82	14.97	9.2YR	7.31	2.44
EPC5 36	921	79.11	4.36	13.01	8.7YR	7.82	2.16
EPC5 37	972	82.11	2.72	10.19	9.4YR	8.11	1.59
EPC5 38	1028	67.08	5.6	16.53	9.3YR	6.6	2.71
EPC5 39	1062	71.67	3.73	14.15	0.2Y	7.06	2.2
EPC5 40	1073	64	7	16.72	8.4YR	6.3	2.91
EPC5 41	1084	73.25	5.38	13.13	8.1YR	7.22	2.28
EPC5 42	1137	77.32	4.34	12.43	8.6YR	7.63	2.08
EPC5 43	1157	79.68	4.06	12.44	8.8YR	7.88	2.05
EPC5 44	1207	83.38	2.42	8.78	9.2YR	8.24	1.37

Table 20. EPC4 (playa center) color data (CIELAB and Munsell).

Sample	Depth (cm)	L*	a*	b*	Munsell Hue	Munsell Value	Munsell Chroma
1	1	36.61	3.87	10.16	9.8YR	3.59	1.65
2	3	36.54	4.04	10.26	9.7YR	3.59	1.68
3	5	34.71	3.9	9.97	9.8YR	3.41	1.64
4	7	35.2	3.53	9.35	9.9YR	3.46	1.52
5	9	41.83	3.71	9.69	9.5YR	4.09	1.55
6	11	30.15	3.23	8.19	10.0YR	2.97	1.39
7	14	37.37	3.59	8.98	9.5YR	3.66	1.46
8	16	29.02	2.94	7.23	9.9YR	2.85	1.24
9	19	31.3	3.27	7.9	9.7YR	3.08	1.34
10	22	37.01	3.33	8.35	9.6YR	3.63	1.36
11	24	31.2	3.11	7.71	9.9YR	3.07	1.3
12	27	33.64	3.17	7.81	9.7YR	3.3	1.3
13	29	30.35	3.15	7.73	9.9YR	2.99	1.31
14	32	35.36	3.41	8.35	9.6YR	3.47	1.38
15	34	38.81	3.54	8.7	9.4YR	3.8	1.41
16	37	38.72	3.56	9.1	9.6YR	3.79	1.47
17	39	38.44	3.78	9.63	9.6YR	3.77	1.56
18	41	37.57	3.72	9.45	9.6YR	3.68	1.53
19	44	42.9	3.68	9.44	9.5YR	4.2	1.52
20	47	42.85	3.64	9.42	9.5YR	4.19	1.51
21	49	37.85	3.6	9.48	9.8YR	3.71	1.52
22	52	43.68	3.58	9.56	9.6YR	4.27	1.53
23	54	41.33	3.6	9.91	9.8YR	4.05	1.55
24	57	44.69	3.61	10.03	9.8YR	4.37	1.6
25	59	40.36	3.58	9.9	9.9YR	3.95	1.55
26	62	47.28	3.31	9.49	9.9YR	4.62	1.53
27	64	46.98	3.39	9.88	10.0YR	4.59	1.58
28	67	43.02	3.42	9.97	10.0YR	4.21	1.56
29	69	45.74	3.22	9.32	9.9YR	4.47	1.48
30	72	45.44	3.09	9.08	10.0YR	4.44	1.44
31	75	43.24	3.15	9.58	0.2Y	4.23	1.49
32	78	45.21	3.14	9.47	0.1Y	4.42	1.49
33	80	44.32	2.88	8.62	0.1Y	4.33	1.35
34	82	43.14	3.1	9.29	0.2Y	4.22	1.45
35	85	45.87	2.94	8.86	0.1Y	4.48	1.4
36	88	51	2.84	9.05	0.3Y	4.97	1.46
37	90	50.93	2.66	8.58	0.3Y	4.97	1.38
38	93	55.58	2.65	8.89	0.3Y	5.43	1.41
39	95	52.94	2.89	8.94	10.0YR	5.17	1.44

40	97	51.08	2.73	8.34	0.1Y	4.98	1.35
41	100	60.29	2.7	10	0.5Y	5.9	1.54
42	102	61.23	2.72	10.4	0.6Y	5.99	1.59
43	105	62.63	2.3	10.09	1.0Y	6.13	1.51
44	108	57.73	2.7	10.36	0.8Y	5.64	1.6
45	110	60.85	3.37	12.88	0.7Y	5.96	1.98
46	113	61.38	2.97	11.74	0.7Y	6.01	1.79
47	115	61.07	2.91	12.44	1.0Y	5.98	1.88
48	117	62.75	3.09	12.79	0.8Y	6.15	1.94
49	120	61.07	3.07	12.19	0.8Y	5.98	1.86
50	122	63.63	3.14	12.59	0.7Y	6.24	1.92
51	125	63.97	3.09	12.79	0.8Y	6.28	1.95
52	127	65.1	2.91	12.53	0.9Y	6.39	1.89
53	130	65.38	3.07	13.29	0.9Y	6.42	2.01
54	133	66.45	3.15	13.81	0.9Y	6.53	2.09
55	135	68.29	3.14	14.42	1.0Y	6.72	2.17
56	137	67.36	3.03	13.7	0.9Y	6.62	2.06
57	140	70.44	2.84	13.37	0.9Y	6.93	2
58	142	67.45	3.29	14.68	0.9Y	6.63	2.22
59	145	69.8	2.81	13.9	1.1Y	6.87	2.07
60	147	65.2	3.14	14.65	1.2Y	6.41	2.2
61	150	62.14	3.1	12.53	0.8Y	6.09	1.91
62	152	61.39	3.03	12.49	0.9Y	6.01	1.9
63	155	59.42	3.24	12.71	0.8Y	5.82	1.95
64	158	60.74	3.12	12.23	0.7Y	5.95	1.87
65	160	64.31	3.06	12.89	0.8Y	6.31	1.95
66	163	66.37	3.14	13.52	0.8Y	6.52	2.05
67	165	65.97	2.99	12.84	0.8Y	6.48	1.94
68	168	63.53	3.26	13.74	0.9Y	6.23	2.09
69	170	67.63	2.89	13.05	0.9Y	6.65	1.96
70	173	68.17	3.15	14.51	1.0Y	6.71	2.18
71	175	67.23	3	13.82	1.0Y	6.61	2.07
72	178	69.06	2.81	13.52	1.1Y	6.79	2.02
73	180	66.62	3.26	14.57	1.0Y	6.55	2.2
74	182	70.41	2.64	13.67	1.2Y	6.93	2.02
75	185	65.24	3.22	14.67	1.1Y	6.41	2.21
76	188	69.09	2.98	13.94	1.0Y	6.8	2.09
77	190	67.1	3.13	14.33	1.0Y	6.6	2.15
78	192	65.9	3.13	14.71	1.2Y	6.48	2.21
79	195	64.27	2.45	13.11	1.6Y	6.31	1.92
80	198	63.32	2.75	13.82	1.4Y	6.21	2.05
81	200	64.76	2.65	13.79	1.5Y	6.36	2.03
82	203	66.01	2.56	14	1.6Y	6.49	2.05

83	205	58.04	2.61	12.01	1.4Y	5.68	1.8
84	207	62.51	2.6	13.34	1.5Y	6.13	1.97
85	210	64.07	2.33	12.96	1.7Y	6.29	1.9
86	213	61.18	2.6	13.85	1.7Y	6	2.04
87	215	59.47	2.95	14.5	1.6Y	5.83	2.17
88	218	63.2	2.58	14.03	1.7Y	6.2	2.06
89	220	62.42	2.61	13.67	1.6Y	6.12	2.01
90	223	61.85	2.69	13.66	1.6Y	6.06	2.02
91	225	65.62	1.86	13.44	2.2Y	6.44	1.92
92	228	64.62	2.25	13.78	1.9Y	6.34	1.99
93	230	65.06	2.74	14.39	1.5Y	6.39	2.12
94	233	64.49	2.62	13.71	1.5Y	6.33	2.02
95	235	63.17	2.86	14.12	1.4Y	6.2	2.1
96	238	61.68	3.12	14.02	1.2Y	6.05	2.11
97	240	62.35	2.72	13.63	1.5Y	6.11	2.02
98	243	60.49	2.69	13.72	1.6Y	5.93	2.03
99	247	62.81	2.9	14.67	1.5Y	6.16	2.18
100	249	64.08	2.42	13.89	1.8Y	6.29	2.03
101	251	63.13	2.83	14.84	1.6Y	6.2	2.19
102	254	66.48	2.86	14.54	1.4Y	6.53	2.16
103	256	71.19	2.06	13.11	1.7Y	7.01	1.89
104	259	68.34	2.62	16.03	1.9Y	6.73	2.33
105	261	65.95	2.11	13.86	2.0Y	6.48	1.99
106	263	65.28	2.12	14.29	2.1Y	6.41	2.05
107	266	66.72	1.99	11.91	1.7Y	6.55	1.73
108	268	66.69	1.74	12.54	2.1Y	6.55	1.79
109	271	66.91	1.78	13.26	2.2Y	6.57	1.89
110	273	70.54	1.58	11.97	2.0Y	6.94	1.7
111	276	64.92	1.81	13.05	2.2Y	6.37	1.86
112	278	65.7	1.5	12.28	2.4Y	6.45	1.73
113	281	67.92	1.47	12.38	2.3Y	6.67	1.74
114	284	65.16	1.45	12.44	2.5Y	6.39	1.75
115	286	64.07	1.5	12.65	2.5Y	6.28	1.79
116	288	63.1	1.5	13.21	2.7Y	6.19	1.86
117	291	63.53	1.43	13.38	2.8Y	6.23	1.88
118	293	61.08	1.51	12.09	2.6Y	5.98	1.71
119	296	66.46	1.38	12.22	2.5Y	6.52	1.72
120	298	66.33	1.23	12.2	2.7Y	6.51	1.7
121	301	65.95	1.17	11.86	2.8Y	6.47	1.65
122	304	63.9	1.21	11.1	2.6Y	6.26	1.55
123	306	66.45	1.32	12.2	2.5Y	6.52	1.71
124	308	69.66	1.46	12.02	2.2Y	6.85	1.7
125	311	67.93	1.35	12.75	2.6Y	6.67	1.79

126	313	67.77	1.3	12.38	2.5Y	6.66	1.73
127	316	65.45	1.2	11.78	2.7Y	6.42	1.64
128	318	64.64	1.31	12.24	2.7Y	6.34	1.72
129	321	65.13	1.36	12.55	2.6Y	6.39	1.76
130	323	63.01	1.16	11.85	2.9Y	6.17	1.65
131	325	64.35	1.3	11.28	2.5Y	6.31	1.59
132	328	65.9	1.19	11.63	2.7Y	6.47	1.62
133	330	63.58	1.35	11.63	2.6Y	6.23	1.64
134	333	66.95	1.24	12.53	2.7Y	6.57	1.75
135	335	65.08	1.3	12.13	2.7Y	6.38	1.7
136	337	68.43	1.31	12.64	2.6Y	6.72	1.77
137	340	52.88	1.43	11.31	3.2Y	5.16	1.65
138	343	65.87	1.41	12.9	2.6Y	6.47	1.81
139	345	56.17	1.75	13.02	2.8Y	5.5	1.88
140	348	63.55	1.48	12.98	2.7Y	6.23	1.83
141	350	66.43	1.31	12.68	2.7Y	6.52	1.77
142	353	67.46	1.43	13	2.5Y	6.63	1.82
143	355	63.08	1.77	15.15	2.8Y	6.19	2.15
144	358	66.12	2.17	16.52	2.5Y	6.5	2.36
145	362	59.14	2.26	14.81	2.4Y	5.8	2.15
146	364	59.56	1.88	14.17	2.7Y	5.84	2.03
147	366	64.73	1.71	13.77	2.5Y	6.35	1.95
148	369	66.17	1.38	13.18	2.7Y	6.5	1.84
149	371	68.54	1.4	13.8	2.7Y	6.74	1.93
150	374	62.37	1.6	15.06	3.0Y	6.12	2.12
151	376	64.14	1.29	14.29	3.2Y	6.29	1.99
152	379	65.29	1.13	14.08	3.3Y	6.41	1.95
153	381	59.55	1.06	12.19	3.4Y	5.83	1.71
154	383	63.9	1.13	14.17	3.4Y	6.27	1.97
155	386	67.56	1.02	14.34	3.4Y	6.64	1.98
156	388	63.81	1.32	13.64	3.0Y	6.26	1.91
157	391	61.6	1.13	14.37	3.5Y	6.04	2
158	393	62.52	1.02	14.18	3.6Y	6.13	1.96
159	396	67.67	0.93	14.68	3.6Y	6.65	2.02
160	398	63.67	1.03	14.19	3.5Y	6.25	1.96
161	401	63.18	1.14	14.44	3.4Y	6.2	2
162	403	66.85	1.02	14.57	3.5Y	6.57	2.01
163	406	63.44	1.13	14.24	3.4Y	6.22	1.98
164	408	64.05	0.99	13.76	3.5Y	6.28	1.9
165	411	64.48	1	13.73	3.5Y	6.33	1.9
166	413	69.3	0.87	13.82	3.5Y	6.81	1.9
167	415	65.84	1.16	14.22	3.2Y	6.47	1.97
168	418	63.45	1.15	13.74	3.3Y	6.22	1.91

169	420	63.08	1.15	13.43	3.2Y	6.18	1.87
170	423	62.58	1.25	14.05	3.2Y	6.14	1.96
171	425	65.7	1.16	13.47	3.1Y	6.45	1.87
172	427	65.53	1.36	12.76	2.7Y	6.43	1.79
173	430	67.27	1.45	14.09	2.7Y	6.61	1.97
174	432	65.34	1.72	14.53	2.6Y	6.42	2.05
175	435	62.55	1.65	13.66	2.6Y	6.13	1.93
176	437	60.42	1.67	13.47	2.7Y	5.92	1.91
177	440	62.5	1.81	13.26	2.3Y	6.13	1.89
178	442	64.63	1.48	13.49	2.7Y	6.34	1.9
179	445	64.72	1.17	13.6	3.2Y	6.35	1.89
180	447	67.68	0.69	12.57	3.6Y	6.65	1.72
181	450	66.43	0.83	12.37	3.4Y	6.52	1.7
182	452	60.46	0.86	12.69	3.7Y	5.92	1.76
183	454	67.18	0.96	13.43	3.3Y	6.6	1.85
184	457	65.45	1.26	13.75	3.0Y	6.42	1.92
185	459	65.63	1.79	14.12	2.4Y	6.44	2
186	462	64	2.31	17.42	2.6Y	6.29	2.5
187	464	63.47	2.36	15.5	2.2Y	6.23	2.24
188	467	62.5	2.32	16.66	2.4Y	6.14	2.4
189	469	61.41	1.86	14.42	2.5Y	6.02	2.06
190	472	63.73	1.81	15.59	2.7Y	6.26	2.21
191	474	62.68	1.75	14.64	2.6Y	6.15	2.08
192	477	61.56	1.48	14.18	3.0Y	6.03	1.99
193	479	62.85	1.41	14.05	3.0Y	6.16	1.97
194	482	65.64	1.37	13.5	2.8Y	6.44	1.89
195	484	62.65	1.53	13.44	2.7Y	6.14	1.9
196	487	63.52	1.28	13.3	3.0Y	6.23	1.86
197	489	65.58	1.14	12.64	3.0Y	6.43	1.76
198	492	65.26	1.13	13.51	3.2Y	6.4	1.88
199	494	65.48	1.15	13.15	3.1Y	6.43	1.83
200	497	61.92	1.29	15.33	3.4Y	6.07	2.14
201	499	65.75	0.99	14.68	3.5Y	6.46	2.03
202	501	62.66	1.04	14.43	3.6Y	6.14	2
203	504	66.79	0.95	14.65	3.6Y	6.56	2.02
204	506	61.19	1.56	11.77	2.4Y	5.99	1.67
205	509	64.97	1.32	16.06	3.4Y	6.38	2.24
206	512	62.33	1.4	14.77	3.2Y	6.11	2.07
207	514	60.48	1.52	14.98	3.2Y	5.93	2.11
208	517	64.16	1.32	15.64	3.3Y	6.3	2.18
209	519	63.4	1.3	16.21	3.5Y	6.23	2.27
210	522	62.79	2.04	16.99	2.8Y	6.17	2.42
211	524	60.39	1.68	15.57	3.1Y	5.92	2.21

212	527	57.15	1.79	15.06	3.1Y	5.6	2.16
213	530	63.57	1.58	13.94	2.7Y	6.24	1.97
214	532	61.39	1.81	14.03	2.5Y	6.02	2
215	535	55.39	2.05	15.14	2.9Y	5.42	2.19
216	537	57.31	2.18	14.24	2.4Y	5.61	2.07
217	540	60.75	2.11	14.1	2.2Y	5.95	2.03
218	542	55.45	2.18	14.01	2.5Y	5.43	2.05
219	544	59	2.21	14	2.2Y	5.78	2.03
220	547	58.01	1.93	13.83	2.6Y	5.68	1.99
221	549	61.37	1.85	12.7	2.2Y	6.01	1.82
222	552	57.29	2.2	13.88	2.3Y	5.61	2.02
223	554	60.27	1.95	14.03	2.4Y	5.9	2.01
224	557	59.06	2.02	13.63	2.3Y	5.78	1.97
225	559	61.98	1.93	13.23	2.2Y	6.07	1.9
226	562	60.66	2.33	13.84	1.9Y	5.94	2.02
227	564	57.94	2.2	13.9	2.3Y	5.67	2.02
228	567	57.78	2.08	13.1	2.2Y	5.66	1.91
229	569	60.84	2.09	14.63	2.3Y	5.96	2.11
230	572	56.63	1.98	13.34	2.5Y	5.54	1.94
231	574	58.16	2.18	13.45	2.2Y	5.69	1.96
232	577	59.26	1.77	13.03	2.5Y	5.8	1.87
233	579	60.17	2	11.86	1.9Y	5.89	1.73
234	582	59.97	2.03	12.45	2.0Y	5.87	1.81
235	584	61.04	2.18	13.22	1.9Y	5.98	1.92
236	587	59.99	2.41	12.84	1.7Y	5.87	1.89
237	589	62.91	2.35	12.26	1.4Y	6.17	1.81
238	592	60.91	2.7	12.67	1.2Y	5.97	1.89
239	594	54.64	3.28	13.14	1.1Y	5.35	2.03
240	597	54.34	3.92	13.81	0.6Y	5.32	2.18
241	600	55.35	3.05	13.14	1.3Y	5.42	2
242	602	56.68	3.05	12.62	1.1Y	5.55	1.93
243	604	59.69	2.8	12.97	1.3Y	5.85	1.94
244	607	66.65	1.84	10.69	1.5Y	6.54	1.55
245	609	62.74	2.13	11.4	1.5Y	6.15	1.67
246	612	68.57	1.08	11.55	2.6Y	6.73	1.61
247	614	66.36	1.21	12.03	2.7Y	6.51	1.68
248	616	63.96	1.23	12.23	2.8Y	6.27	1.71
249	619	68.13	1.03	12.51	2.9Y	6.69	1.73
250	621	67.81	1.15	12.37	2.7Y	6.66	1.72
251	624	64.2	1.49	11.58	2.3Y	6.29	1.64
252	626	66.75	1.77	11.05	1.7Y	6.55	1.59
253	629	63.98	2.06	11.33	1.6Y	6.27	1.65
254	631	68.67	1.42	10.87	2.1Y	6.74	1.54

255	634	65.72	2.77	11.98	0.8Y	6.45	1.81
256	636	65.66	2.59	11.96	1.0Y	6.44	1.79
257	639	65.68	1.33	11.22	2.4Y	6.44	1.58
258	641	67.67	1.56	11.21	2.0Y	6.64	1.6
259	644	69.52	2.02	11.57	1.4Y	6.83	1.69
260	646	66.44	1.65	11.31	2.0Y	6.52	1.62
261	649	70.92	1.68	11.11	1.7Y	6.97	1.6
262	651	64.88	1.46	10.8	2.2Y	6.36	1.53
263	653	64.74	1.97	11.97	1.8Y	6.35	1.73
264	656	64.76	1.52	12.17	2.4Y	6.35	1.72
265	659	67.81	1.19	12.03	2.6Y	6.66	1.68
266	661	68.26	0.94	12.66	3.1Y	6.7	1.75
267	664	65.88	1.08	13.28	3.2Y	6.47	1.84
268	666	66.26	1.57	13.15	2.4Y	6.51	1.86
269	669	71.48	0.75	12.08	3.2Y	7.03	1.65
270	671	70.21	1.09	12.1	2.7Y	6.9	1.68
271	674	68.88	1.68	11.79	1.9Y	6.77	1.68
272	676	69.14	1.77	11.59	1.7Y	6.79	1.67
273	679	70.24	1.72	10.95	1.6Y	6.9	1.58
274	681	68.11	1.68	11.62	1.9Y	6.69	1.66
275	684	66.83	1.95	12.34	1.8Y	6.56	1.78
276	686	72.05	0.91	11.06	2.6Y	7.08	1.52
277	689	72.5	1.3	12.55	2.3Y	7.14	1.75
278	691	76.47	0.98	12.93	2.8Y	7.54	1.76
279	693	66.36	2.88	17.45	2.0Y	6.53	2.55
280	696	70.17	1.92	13.94	2.0Y	6.9	1.99
281	698	72.38	1.57	12.82	2.1Y	7.12	1.81
282	701	72.94	2.06	13.7	1.7Y	7.18	1.97
283	703	71.66	2.06	13.88	1.8Y	7.06	1.99
284	706	70.7	3.83	14.28	0.1Y	6.96	2.23
285	708	66.92	5.66	15.34	8.9YR	6.59	2.57
286	711	62.4	7.96	17.1	7.9YR	6.14	3.08
287	713	63.95	7.45	17.14	8.2YR	6.29	3.02
288	716	63.03	8.26	17.65	7.8YR	6.2	3.19
289	718	70.37	6.74	16.02	8.1YR	6.94	2.8
290	720	62.41	8.48	18.25	7.9YR	6.14	3.29
291	723	60	9.77	19.08	7.3YR	5.9	3.56
292	725	60.92	9.62	18.69	7.2YR	5.99	3.5

Table 21. EPC7 (interplaya north) color data (CIELAB and Munsell).

Sample	depth (cm)	L*	a*	b*	Munsell Hue	Munsell Value	Munsell Chroma
EPC7 1	9	49.51	4.48	12.33	9.6YR	4.84	2.04
EPC7 2	49	49.61	3.41	11.23	0.5Y	4.85	1.78
EPC7 3	73	70.09	3.76	15.34	0.6Y	6.9	2.35
EPC7 4	105	61.85	4.06	15.9	0.8Y	6.07	2.45
EPC7 5	119	68.48	4.31	17.27	0.7Y	6.75	2.66
EPC7 6	134	65.13	4.11	16.02	0.7Y	6.41	2.48
EPC7 7	177	62.84	4.75	17.66	0.6Y	6.18	2.76
EPC7 8	192	68.77	3.93	16.3	0.8Y	6.77	2.5
EPC7 9	232	62.27	4.57	16.57	0.5Y	6.12	2.6
EPC7 10	247	63.46	4.93	17.92	0.5Y	6.24	2.81
EPC7 11	256	63.62	5.09	18.07	0.4Y	6.26	2.85
EPC7 12	297	63.56	5.07	17.87	0.3Y	6.25	2.82
EPC7 13	314	65.39	4.66	16.28	0.2Y	6.43	2.57
EPC7 14	352	63.9	3.39	12.43	0.4Y	6.27	1.93
EPC7 15	365	69.06	3.99	15.72	0.5Y	6.8	2.43
EPC7 16	378	62.96	4.52	15.51	0.2Y	6.19	2.45
EPC7 17	423	63.19	5.34	16.95	9.8YR	6.21	2.73
EPC7 18	438	63.28	5.61	17.04	9.6YR	6.22	2.78
EPC7 19	475	62.32	7.01	18.71	9.1YR	6.13	3.16
EPC7 20	496	59.96	5.29	14.88	9.4YR	5.88	2.46
EPC7 21	534	60.64	5.62	15.27	9.2YR	5.95	2.55
EPC7 22	547	63.3	4.99	13.79	9.1YR	6.21	2.29
EPC7 23	561	56.26	4.6	11.78	9.0YR	5.51	1.99
EPC7 24	594	61.22	5.75	14.59	8.8YR	6.01	2.48
EPC7 25	608	63.34	6.47	16.85	8.9YR	6.23	2.86
EPC7 26	619	64.23	6.81	17.9	8.9YR	6.32	3.03
EPC7 27	647	61.75	6.8	16.93	8.8YR	6.07	2.9
EPC7 28	659	66.35	6.45	16.24	8.7YR	6.53	2.77
EPC7 29	675	68.19	6.76	17.67	8.8YR	6.72	2.99
EPC7 30	710	67.95	5.21	13.97	8.9YR	6.69	2.34
EPC7 31	724	66.92	7.23	19.18	8.9YR	6.6	3.24
EPC7 32	742	63.21	8.25	20.38	8.7YR	6.23	3.52
EPC7 33	789	59.75	7.37	18.07	8.7YR	5.87	3.11
EPC7 34	860	69	7.4	19.28	8.7YR	6.81	3.28
EPC7 35	904	86.54	1.65	8.13	9.9YR	8.56	1.18
EPC7 36	922	83.96	3.09	11.67	9.4YR	8.31	1.81
EPC7 37	952	59.78	9.44	17.14	6.7YR	5.88	3.29

EPC7 38	967	78.44	4.33	11.36	8.1YR	7.74	1.96
EPC7 39	1120	78.03	5.58	13.36	7.7YR	7.71	2.38
EPC7 40	1252	80.56	3.35	11	9.0YR	7.96	1.79
EPC7 41	1289	67.88	7.51	17.93	8.3YR	6.69	3.13
EPC7 42	1304	69	7.51	18	8.3YR	6.81	3.14
EPC7 43	1319	74.54	5.53	14.75	8.5YR	7.36	2.5
EPC7 44	1475	72.55	6.01	15.36	8.4YR	7.16	2.63
EPC7 45	1487	75.85	4.47	12.58	8.6YR	7.48	2.11
EPC7 46	1519	86.44	1.95	7.59	9.2YR	8.55	1.16
EPC7 47	1530	81.64	3.24	9.43	8.4YR	8.06	1.59
EPC7 48	1546	73.91	4.92	12.84	8.4YR	7.29	2.19
EPC7 49	1586	73.29	5.73	14.35	8.3YR	7.23	2.48
EPC7 50	1734	73.68	6.4	15.91	8.2YR	7.28	2.76
EPC7 51	1752	71.31	8.93	18.58	7.3YR	7.04	3.42
EPC7 52	1765	64.18	9.7	19.56	7.4YR	6.33	3.62
EPC7 53	1779	67.04	8.78	18.05	7.4YR	6.61	3.32
EPC7 54	1792	72.32	6.18	16.14	8.6YR	7.14	2.75

Table 22. Sensor pit (playa center) particle size analysis (PSA) data.

sample	depth (cm)	%clay	% silt	% sand
48	0	26.70	86.49	7.01
47	5	42.48	87.12	3.10
46	10	38.60	88.78	2.07
45	15	42.21	86.40	4.73
44	20	39.76	91.72	0.81
43	25	40.01	89.05	1.26
42	30	41.50	88.47	1.47
41	35	39.39	90.00	1.39
40	40	41.48	91.32	0.51
39	45	41.33	89.46	0.94
38	50	39.56	88.83	2.18
37	55	41.44	89.94	0.80
36	60	40.07	90.69	0.88
35	65	41.25	90.08	1.07
34	70	40.96	90.42	0.93
33	75	42.60	92.03	0.49
32	80	41.80	91.87	0.65

31	85	38.18	89.37	1.95
30	90	37.89	90.89	0.87
29	95	35.66	91.15	1.03
28	100	35.29	91.43	0.76
27	105	35.76	91.36	0.79
26	110	25.60	91.23	2.15
25	115	27.28	90.39	2.40
24	120	25.64	91.02	2.15
23	125	26.21	91.24	1.95
22	130	21.52	91.19	3.10
21	135	25.30	90.89	2.47
20	140	30.73	88.86	2.65
19	145	33.23	88.05	2.67
18	150	20.47	87.33	7.21
17	155	20.75	89.89	4.56
16	160	20.10	89.62	5.07
15	165	21.36	90.45	4.01
14	170	25.24	89.11	4.41
13	175	21.42	90.10	4.42
12	180	24.92	90.55	3.11
11	185	24.79	90.72	2.92
10	190	25.41	90.14	3.23
9	195	23.34	90.98	3.39
8	200	22.29	85.75	8.44
7	205	29.81	88.24	3.44
6	210	20.17	87.68	7.17
5	215	22.74	89.90	4.20
4	220	20.50	87.32	7.54
3	225	19.74	87.06	7.97
2	230	20.17	90.68	4.13
1	235	19.34	90.58	4.58

Table 23. EPC4 (playa center) particle size analysis (PSA) data.

sample	depth (cm)	% clay	% silt	% sand
1	1	5.57	81.38	13.05
2	3	6.34	87.80	5.85
3	5	5.83	87.11	7.07
4	7	8.20	85.75	6.04
5	9	7.51	88.85	3.65
6	11	5.90	88.93	5.17
7	14	5.55	89.22	5.23
8	16	5.35	89.18	5.47
9	19	5.53	89.54	4.93
10	22	4.75	66.58	28.67
11	24	5.50	89.81	4.69
12	27	5.90	89.49	4.62
13	29	6.75	89.03	4.22
14	32	5.94	90.20	3.86
15	34	6.02	90.02	3.96
16	37	5.67	80.60	13.74
17	39	7.21	88.08	4.71
18	41	6.88	89.59	3.52
19	44	7.27	89.36	3.37
20	47	7.12	88.06	4.82
21	49	7.50	87.02	5.49
22	52	7.39	89.01	3.60
23	54	7.27	88.20	4.53
24	57	7.14	89.21	3.65
25	59	7.64	88.13	4.23
26	62	7.58	89.02	3.40
27	64	8.21	87.57	4.22
28	67	8.65	87.41	3.94
29	69	7.92	88.07	4.01
30	72	8.27	87.66	4.07
31	75	8.24	87.74	4.02
32	78	8.96	87.15	3.88
33	80	7.76	87.63	4.61
34	82	8.35	82.11	9.54
35	85	7.39	89.77	2.84
36	88	8.33	86.43	5.25
37	90	7.70	89.29	3.01

38	93	7.70	83.70	8.60
39	95	7.54	86.50	5.96
40	97	8.53	88.56	2.90
41	100	8.47	88.26	3.27
42	102	9.75	87.31	2.93
43	105	9.29	77.62	13.09
44	108	7.94	88.59	3.47
45	110	8.15	87.85	4.00
46	113	7.52	87.90	4.58
47	115	6.95	75.63	17.42
48	117	9.03	86.80	4.17
49	120	8.73	86.62	4.65
50	122	8.05	76.52	15.42
51	125	8.72	89.26	2.02
52	127	7.70	86.22	6.08
53	130	9.68	85.90	4.42
54	133	6.71	88.30	4.99
55	135	7.18	88.00	4.82
56	137	7.98	87.00	5.02
57	140	7.51	86.45	6.04
58	142	7.00	86.83	6.18
59	145	7.48	86.83	5.69
60	147	6.92	87.62	5.45
61	150	6.47	87.12	6.42
62	152	7.19	87.28	5.53
63	155	7.27	87.79	4.95
64	158	8.70	87.06	4.24
65	160	8.97	87.19	3.84
66	163	8.34	88.89	2.78
67	165	8.50	89.57	1.93
68	168	7.80	88.93	3.27
69	170	8.22	89.54	2.24
70	173	9.23	86.98	3.79
71	175	7.71	89.89	2.40
72	178	8.42	88.01	3.58
73	180	8.72	89.63	1.64
74	182	8.77	87.18	4.05
75	185	7.73	87.74	4.53
76	188	9.33	88.12	2.54
77	190	8.04	88.62	3.34
78	192	7.18	88.35	4.47

79	195	7.75	89.33	2.92
80	198	7.75	88.14	4.11
81	200	9.59	87.97	2.44
82	203	8.20	88.39	3.41
83	205	7.99	88.77	3.24
84	207	8.07	90.02	1.91
85	210	8.53	86.69	4.78
86	213	9.15	87.18	3.67
87	215	8.24	90.12	1.64
88	218	8.33	87.45	4.22
89	220	6.73	86.89	6.38
90	223	6.44	89.05	4.51
91	225	8.08	87.96	3.95
92	228	7.55	86.91	5.54
93	230	6.62	87.20	6.18
94	233	6.77	87.75	5.48
95	235	6.83	86.79	6.38
96	238	6.12	86.93	6.95
97	240	6.98	88.15	4.87
98	243	6.54	88.58	4.88
99	247	5.34	89.80	4.86
100	249	6.29	88.76	4.95
101	251	7.39	86.47	6.14
102	254	8.98	86.12	4.91
103	256	8.88	85.84	5.28
104	259	6.45	86.36	7.19
105	261	7.26	85.06	7.68
106	263	7.76	86.87	5.37
107	266	8.02	86.86	5.12
108	268	7.41	88.21	4.38
109	271	7.13	87.54	5.34
110	273	6.85	87.35	5.80
111	276	7.35	86.95	5.70
112	278	8.01	86.52	5.47
113	281	6.56	85.02	8.42
114	284	6.74	86.99	6.27
115	286	7.21	87.54	5.24
116	288	6.22	88.20	5.58
117	291	6.60	88.31	5.09
118	293	7.17	88.06	4.77
119	296	7.38	88.00	4.62

120	298	7.53	87.03	5.44
121	301	5.87	89.29	4.84
122	304	6.09	88.96	4.95
123	306	6.45	88.46	5.09
124	308	7.14	88.59	4.28
125	311	6.60	88.98	4.42
126	313	6.43	89.17	4.40
127	316	7.21	87.52	5.27
128	318	7.53	87.75	4.72
129	321	7.23	86.74	6.03
130	323	6.85	89.03	4.12
131	325	8.29	86.06	5.65
132	328	7.89	87.41	4.70
133	330	6.61	86.87	6.53
134	333	7.58	87.78	4.63
135	335	6.90	88.01	5.10
136	337	7.00	88.85	4.15
137	340	6.57	90.49	2.94
138	343	6.56	89.76	3.68
139	345	6.00	90.28	3.72
140	348	6.99	88.70	4.31
141	350	7.43	88.44	4.12
142	353	8.44	86.84	4.72
143	355	6.97	88.11	4.92
144	358	6.21	88.82	4.97
145	362	6.24	86.66	7.11
146	364	6.24	88.79	4.97
147	366	7.62	87.48	4.90
148	369	6.07	89.14	4.79
149	371	5.42	88.36	6.22
150	374	6.58	88.61	4.81
151	376	5.77	88.47	5.76
152	379	6.16	88.90	4.94
153	381	6.23	89.55	4.21
154	383	6.10	88.92	4.98
155	386	6.39	88.83	4.78
156	388	6.41	88.71	4.88
157	391	6.01	88.81	5.18
158	393	6.19	87.31	6.50
159	396	6.24	88.54	5.22
160	398	5.97	88.52	5.51

161	401	5.54	88.87	5.59
162	403	5.27	88.56	6.16
163	406	5.23	88.69	6.08
164	408	4.98	88.67	6.35
165	411	5.41	89.37	5.22
166	413	5.28	89.33	5.38
167	415	5.77	88.24	5.98
168	418	5.71	88.94	5.34
169	420	5.61	89.48	4.91
170	423	5.04	89.11	5.85
171	425	4.76	89.24	6.00
172	427	4.83	89.43	5.74
173	430	5.36	89.85	4.78
174	432	5.71	89.57	4.73
175	435	5.35	89.79	4.86
176	437	5.26	89.53	5.21
177	440	5.14	85.29	9.57
178	442	5.68	89.48	4.84
179	445	4.61	80.83	14.57
180	447	5.57	89.80	4.63
181	450	5.36	89.84	4.79
182	452	5.53	89.35	5.12
183	454	7.12	86.64	6.24
184	457	7.07	85.35	7.58
185	459	7.05	86.97	5.98
186	462	7.75	85.39	6.86
187	464	7.99	87.01	5.00
188	467	8.27	88.99	2.74
189	469	8.03	85.91	6.06
190	472	8.00	86.20	5.80
191	474	7.45	87.74	4.81
192	477	7.43	87.00	5.57
193	479	7.40	88.65	3.95
194	482	8.54	89.89	1.57
195	484	7.12	90.06	2.82
196	487	8.06	88.29	3.65
197	489	6.17	86.38	7.45
198	492	6.45	85.03	8.52
199	494	6.27	84.59	9.14
200	497	6.89	85.41	7.71
201	499	7.57	90.12	2.31

202	501	8.04	88.08	3.89
203	504	8.73	89.96	1.31
204	506	7.50	84.02	8.49
205	509	7.59	83.94	8.47
206	512	8.10	85.81	6.09
207	514	8.25	82.01	9.74
208	517	8.81	83.06	8.12
209	519	7.61	72.07	20.32
210	522	7.31	72.45	20.25
211	524	8.08	78.78	13.15
212	527	7.76	87.42	4.82
213	530	6.30	82.30	11.40
214	532	10.10	76.14	13.76
215	535	10.29	87.34	2.37
216	537	5.95	72.40	21.64
217	540	5.90	74.33	19.76
218	542	4.89	79.33	15.77
219	544	5.64	78.04	16.33
220	547	5.85	80.29	13.85
221	549	6.19	80.49	13.32
222	552	6.23	89.20	4.57
223	554	6.90	85.93	7.17
224	557	7.88	87.20	4.92
225	559	4.89	75.41	19.71
226	562	5.65	59.90	34.46
227	564	7.64	76.57	15.79
228	567	8.45	84.45	7.10
229	569	9.03	81.97	8.99
230	572	8.52	84.30	7.18
231	574	7.72	84.38	7.90
232	577	8.48	80.41	11.11
233	579	3.02	33.36	63.63
234	582	9.23	78.81	11.96
235	584	10.12	84.67	5.21
236	587	7.55	82.44	10.01
237	589	8.38	86.15	5.46
238	592	9.11	87.51	3.38
239	594	12.11	80.90	7.00
240	597	14.70	84.70	0.60
241	600	11.46	88.22	0.31
242	602	8.93	85.91	5.16

243	604	10.24	79.85	9.91
244	607	8.08	73.44	18.49
245	609	5.61	55.67	38.72
246	612	6.82	68.24	24.94
247	614	8.27	71.84	19.89
248	616	8.84	76.11	15.05
249	619	6.92	62.93	30.15
250	621	8.70	81.17	10.13
251	624	4.14	40.59	55.27
252	626	2.61	31.10	66.28
253	629	2.52	27.49	69.99
254	631	3.43	37.79	58.78
255	634	1.84	19.55	78.61
256	636	2.17	22.87	74.96
257	639	4.88	53.46	41.66
258	641	3.96	44.41	51.63
259	644	2.39	26.34	71.27
260	646	3.89	37.03	59.09
261	649	4.88	43.49	51.63
262	651	4.90	46.70	48.40
263	653	3.28	31.41	65.31
264	656	5.33	52.97	41.70
265	659	7.36	64.99	27.64
266	661	9.73	82.13	8.14
267	664	9.02	81.47	9.51
268	666	8.75	72.71	18.55
269	669	8.06	69.19	22.75
270	671	6.44	74.98	18.58
271	674	4.93	50.56	44.51
272	676	4.35	52.36	43.29
273	679	3.62	39.02	57.36
274	681	4.35	58.04	37.61
275	684	4.87	49.88	45.24
276	686	3.48	39.10	57.42
277	689	4.32	57.75	37.93
278	691	4.07	56.08	39.85
279	693	3.57	37.68	58.76
280	696	3.66	60.30	36.04
281	698	5.68	62.11	32.21
282	701	5.52	64.20	30.29
283	703	3.64	59.74	36.62

284	706	6.08	62.93	30.99
285	708	5.17	60.34	34.50
286	711	5.19	64.63	30.18
287	713	5.08	62.26	32.66
288	716	4.97	62.64	32.39
289	718	4.34	60.10	35.57
290	720	4.30	61.30	34.40
291	723	4.14	59.38	36.49
292	725	4.22	56.07	39.71

Table 24. EPC5 (playa center) particle size analysis (PSA) data.

sample	depth (cm)	% clay	% silt	% sand
EPC5-1	5	9.295638	88.53	2.17
EPC5-2	45	8.714699	90.78	0.51
EPC5-3	65	7.993017	91.40	0.61
EPC5-4	94	8.027709	91.69	0.28
EPC5-5	123	8.376193	89.46	2.16
EPC5-6	155	7.049994	89.69	3.26
EPC5-7	179	7.072583	88.73	4.20
EPC5-8	195	8.164166	89.16	2.68
EPC5-9	227	5.398431	89.91	4.70
EPC5-10	252	5.946044	90.24	3.81
EPC5-11	276	4.652046	90.13	5.22
EPC5-12	294	9.61619	89.62	0.76
EPC5-13	309	8.434341	90.81	0.76
EPC5-14	345	6.528984	90.55	2.93
EPC5-15	373	10.241347	89.68	0.08
EPC5-16	406	8.754463	90.19	1.05
EPC5-17	428	8.405899	90.33	1.26
EPC5-18	454	12.509641	86.81	0.68
EPC5-19	473	8.353191	90.49	1.15
EPC5-20	500	9.634094	90.29	0.07
EPC5-21	616	8.924692	90.95	0.12
EPC5-22	630	9.477457	78.84	11.68
EPC5-23	665	5.385497	64.58	30.04
EPC5-24	684	7.460667	69.52	23.02
EPC5-25	696	6.518644	69.85	23.63
EPC5-26	725	5.627097	60.75	33.62

EPC5-27	738	8.049622	67.52	24.43
EPC5-28	755	3.046922	64.83	32.12
EPC5-29	775	3.776909	64.44	31.78
EPC5-30	791	3.95083	67.04	29.01
EPC5-31	804	3.086834	55.23	41.68
EPC5-32	818	7.158343	60.31	32.53
EPC5-33	856	3.195098	53.57	43.23
EPC5-34	880	10.227297	66.39	23.39
EPC5-35	906	4.319922	62.46	33.22
EPC5-36	921	4.200734	47.94	47.86
EPC5-37	972	4.579007	48.90	46.52
EPC5-38	1028	3.17063	52.36	44.47
EPC5-39	1062	2.411435	50.00	47.59
EPC5-40	1073	2.527949	45.81	51.66
EPC5-41	1084	2.566332	43.03	54.41
EPC5-42	1137	4.076517	36.50	59.42
EPC5-43	1157	4.995934	44.51	50.50
EPC5-44	1207	7.520756	49.30	43.18

Table 25. EPC7 (interplaya north) particle size analysis (PSA) data.

sample	depth (cm)	% clay	% silt	% sand
1	9	5.99	88.13	5.88
2	49	7.66	88.73	3.61
3	73	6.34	89.43	4.22
4	105	6.00	89.27	4.73
5	119	6.12	89.35	4.54
6	134	6.49	88.83	4.67
7	177	4.90	90.47	4.63
8	192	5.58	89.91	4.52
9	232	4.72	90.37	4.91
10	247	4.75	90.05	5.19
11	256	4.69	89.99	5.32
12	297	4.62	89.92	5.47
13	314	4.63	80.05	15.32
14	352	6.84	81.11	12.05
15	365	6.58	88.19	5.23
16	378	5.77	85.66	8.57

17	423	5.52	88.84	5.65
18	438	6.42	88.47	5.11
19	475	6.66	87.33	6.01
20	496	6.34	87.12	6.54
21	534	7.03	87.45	5.52
22	547	6.74	84.66	8.59
23	561	6.74	82.93	10.33
24	594	7.30	84.03	8.67
25	608	7.42	80.66	11.92
26	619	7.71	83.98	8.32
27	647	7.79	81.54	10.67
28	659	8.72	80.49	10.79
29	675	9.61	73.84	16.55
30	710	12.43	83.64	3.93
31	724	6.91	76.74	16.36
32	742	6.09	75.67	18.24
33	789	6.29	70.64	23.07
34	860	7.99	67.28	24.74
35	904	14.43	61.04	24.54
36	922	6.32	66.29	27.39
37	952	3.68	80.39	15.92
38	967	5.82	68.74	25.45
39	1120	4.61	71.11	24.28
40	1252	6.00	66.56	27.44
41	1289	1.92	38.96	59.12
42	1304	2.25	38.69	59.06
43	1319	1.96	43.17	54.87
44	1475	1.09	39.44	59.47
45	1487	7.25	55.30	37.45
46	1519	18.95	62.81	18.24
47	1530	11.52	67.77	20.71
48	1546	6.91	68.94	24.14
49	1586	4.12	62.01	33.87
50	1734	3.31	51.06	45.62
51	1752	6.52	74.29	19.19
52	1765	3.35	75.15	21.51
53	1779	1.18	33.69	65.12
54	1792	1.27	39.45	59.28

Table 26. Sensor pit (playa center) magnetic susceptibility*.

Sample	depth (cm)	LF Mag. Sus.	Frequency Dep.
EP-48	1	2.67E-07	2.7526
EP-47	5	1.82E-07	1.6954
EP-46	10	2.05E-07	1.6436
EP-45	15	1.75E-07	1.20E-01
EP-44	20	1.79E-07	1.1969
EP-43	25	1.82E-07	2.3708
EP-42	30	1.77E-07	5.6354
EP-41	35	1.81E-07	1.6596
EP-40	40	1.79E-07	1.1959
EP-39	45	1.71E-07	1.5681
EP-38	50	1.94E-07	1.0815
EP-37	55	1.89E-07	6.10E-01
EP-36	60	1.81E-07	5.92E-01
EP-35	65	1.78E-07	1.4825
EP-34	70	2.09E-07	1.6967
EP-33	75	1.81E-07	2.62E-01
EP-32	80	1.91E-07	0.00E+00
EP-31	85	2.03E-07	1.472
EP-30	90	2.32E-07	5.7708
EP-29	95	2.30E-07	2.076
EP-28	100	1.99E-07	1.4375
EP-27	105	1.90E-07	1.9375
EP-26	110	1.09E-07	3.5505
EP-25	115	8.60E-08	1.1888
EP-24	120	8.87E-08	2.3813
EP-23	125	9.06E-08	3.1718
EP-22	130	8.72E-08	2.1333
EP-21	135	7.68E-08	1.0396
EP-20	140	8.06E-08	2.2775
EP-19	145	1.45E-07	2.4983
EP-18	150	1.62E-07	2.2218
EP-17	155	1.57E-07	4.92E-01
EP-16	160	1.60E-07	7.70E-01
EP-15	165	1.32E-07	1.4501
EP-14	170	1.51E-07	4.92E-01
EP-13	175	1.53E-07	1.00E+00
EP-12	180	1.34E-07	9.65E-01
EP-11	185	1.50E-07	7.8378
EP-10	190	1.14E-07	2.8876

EP-9	195	1.73E-07	8.22E-01
EP-8	200	1.32E-07	2.292
EP-7	205	1.07E-07	0
EP-6	210	1.80E-07	9.12E-01
EP-5	215	1.50E-07	1.7856
EP-4	220	1.09E-07	1.7059
EP-3	225	1.30E-07	9.71E-01
EP-2	230	1.26E-07	2.06E-01
EP-1	235	1.22E-07	2.1268

* Low frequency (LF) and high frequency (HF) susceptibility are expressed in international standard units. Frequency dependence of susceptibility is expressed in percent (%).

Table 27. EPC3 (playa center) magnetic susceptibility*.

Sample & magnetic parameter	depth (cm)	Mag. Sus.
EPC3-1(LF)	1	2.81E-07
EPC3-1(HF)	1	2.78E-07
EPC3-1 FD %	1	1.0846
EPC3-2(LF)	3	2.19E-07
EPC3-2(HF)	3	2.19E-07
EPC3-2 FD %	3	-8.27E-02
EPC3-3(LF)	5	2.05E-07
EPC3-3(HF)	5	2.03E-07
EPC3-3 FD %	5	8.53E-01
EPC3-4(LF)	8	2.05E-07
EPC3-4(HF)	8	2.05E-07
EPC3-4 FD %	8	2.12E-01
EPC3-5(LF)	10	1.94E-07
EPC3-5(HF)	10	1.92E-07
EPC3-5 FD %	10	1.1567
EPC3-6(LF)	12	1.81E-07
EPC3-6(HF)	12	1.79E-07
EPC3-6 FD %	12	1.0914
EPC3-7(LF)	14	1.76E-07
EPC3-7(HF)	14	1.77E-07
EPC3-7 FD %	14	-1.45E-01
EPC3-8(LF)	17	1.79E-07
EPC3-8(HF)	17	1.77E-07

EPC3-8 FD %	17	1.1075
EPC3-9(LF)	20	1.81E-07
EPC3-9(HF)	20	1.80E-07
EPC3-9 FD %	20	7.43E-01
EPC3-10(LF)	22	1.78E-07
EPC3-10(HF)	22	1.74E-07
EPC3-10 FD %	22	1.7362
EPC3-11(LF)	25	1.70E-07
EPC3-11(HF)	25	1.68E-07
EPC3-11 FD %	25	9.67E-01
EPC3-12(LF)	27	1.69E-07
EPC3-12(HF)	27	1.68E-07
EPC3-12 FD %	27	7.61E-01
EPC3-13(LF)	29	1.66E-07
EPC3-13(HF)	29	1.66E-07
EPC3-13 FD %	29	1.81E-01
EPC3-14(LF)	32	1.66E-07
EPC3-14(HF)	32	1.65E-07
EPC3-14 FD %	32	6.71E-01
EPC3-15(LF)	35	1.69E-07
EPC3-15(HF)	35	1.67E-07
EPC3-15 FD %	35	1.1999
EPC3-16(LF)	37	1.71E-07
EPC3-16(HF)	37	1.69E-07
EPC3-16 FD %	37	1.1185
EPC3-17(LF)	40	1.67E-07
EPC3-17(HF)	40	1.66E-07
EPC3-17 FD %	40	7.37E-01
EPC3-18(LF)	42	1.73E-07
EPC3-18(HF)	42	1.70E-07
EPC3-18 FD %	42	1.3592
EPC3-19(LF)	45	1.73E-07
EPC3-19(HF)	45	1.68E-07
EPC3-19 FD %	45	2.5508
EPC3-20(LF)	47	1.74E-07
EPC3-20(HF)	47	1.72E-07
EPC3-20 FD %	47	9.69E-01
EPC3-21(LF)	50	1.76E-07
EPC3-21(HF)	50	1.73E-07
EPC3-21 FD %	50	1.8691
EPC3-22(LF)	53	1.68E-07
EPC3-22(HF)	53	1.66E-07
EPC3-22 FD %	53	1.3132

EPC3-23(LF)	55	1.72E-07
EPC3-23(HF)	55	1.72E-07
EPC3-23 FD %	55	-6.82E-02
EPC3-24(LF)	57	1.74E-07
EPC3-24(HF)	57	1.74E-07
EPC3-24 FD %	57	-3.42E-02
EPC3-25(LF)	60	1.76E-07
EPC3-25(HF)	60	1.72E-07
EPC3-25 FD %	60	2.0919
EPC3-26(LF)	63	1.77E-07
EPC3-26(HF)	63	1.74E-07
EPC3-26 FD %	63	1.8226
EPC3-27(LF)	65	1.81E-07
EPC3-27(HF)	65	1.80E-07
EPC3-27 FD %	65	6.70E-01
EPC3-28(LF)	68	1.78E-07
EPC3-28(HF)	68	1.79E-07
EPC3-28 FD %	68	-5.05E-01
EPC3-29(LF)	71	1.79E-07
EPC3-29(HF)	71	1.78E-07
EPC3-29 FD %	71	7.39E-01
EPC3-30(LF)	74	1.79E-07
EPC3-30(HF)	74	1.79E-07
EPC3-30 FD %	74	2.82E-02
EPC3-31(LF)	76	1.79E-07
EPC3-31(HF)	76	1.78E-07
EPC3-31 FD %	76	7.61E-01
EPC3-32(LF)	78	1.86E-07
EPC3-32(HF)	78	1.84E-07
EPC3-32 FD %	78	1.0075
EPC3-33(LF)	81	1.83E-07
EPC3-33(HF)	81	1.79E-07
EPC3-33 FD %	81	2.2088
EPC3-34(LF)	83	1.81E-07
EPC3-34(HF)	83	1.79E-07
EPC3-34 FD %	83	7.16E-01
EPC3-35(LF)	86	1.80E-07
EPC3-35(HF)	86	1.78E-07
EPC3-35 FD %	86	1.3139
EPC3-36(LF)	88	1.87E-07
EPC3-36(HF)	88	1.81E-07
EPC3-36 FD %	88	3.2579
EPC3-37(LF)	91	1.85E-07

EPC3-37(HF)	91	1.81E-07
EPC3-37 FD %	91	2.1542
EPC3-38(LF)	94	1.88E-07
EPC3-38(HF)	94	1.84E-07
EPC3-38 FD %	94	2.3684
EPC3-39(LF)	96	1.84E-07
EPC3-39(HF)	96	1.82E-07
EPC3-39 FD %	96	1.4598
EPC3-40(LF)	99	1.79E-07
EPC3-40(HF)	99	1.74E-07
EPC3-40 FD %	99	2.7608
EPC3-41(LF)	101	1.71E-07
EPC3-41(HF)	101	1.62E-07
EPC3-41 FD %	101	4.8472
EPC3-42(LF)	104	1.67E-07
EPC3-42(HF)	104	1.62E-07
EPC3-42 FD %	104	2.8214
EPC3-43(LF)	107	1.62E-07
EPC3-43(HF)	107	1.62E-07
EPC3-43 FD %	107	1.62E-01
EPC3-44(LF)	109	1.31E-07
EPC3-44(HF)	109	1.28E-07
EPC3-44 FD %	109	2.6872
EPC3-45(LF)	112	1.17E-07
EPC3-45(HF)	112	1.14E-07
EPC3-45 FD %	112	1.8728
EPC3-46(LF)	114	1.05E-07
EPC3-46(HF)	114	1.04E-07
EPC3-46 FD %	114	1.2125
EPC3-47(LF)	116	8.52E-08
EPC3-47(HF)	116	8.29E-08
EPC3-47 FD %	116	2.7226
EPC3-48(LF)	118	9.18E-08
EPC3-48(HF)	118	9.05E-08
EPC3-48 FD %	118	1.3448
EPC3-49(LF)	120	1.03E-07
EPC3-49(HF)	120	9.88E-08
EPC3-49 FD %	120	4.3454
EPC3-50(LF)	122	1.01E-07
EPC3-50(HF)	122	1.00E-07
EPC3-50 FD %	122	8.24E-01
EPC3-51(LF)	125	1.05E-07
EPC3-51(HF)	125	1.05E-07

EPC3-51 FD %	125	3.87E-01
EPC3-52(LF)	127	9.61E-08
EPC3-52(HF)	127	9.46E-08
EPC3-52 FD %	127	1.545
EPC3-53(LF)	129	8.81E-08
EPC3-53(HF)	129	8.53E-08
EPC3-53 FD %	129	3.1757
EPC3-54(LF)	132	8.07E-08
EPC3-54(HF)	132	8.01E-08
EPC3-54 FD %	132	7.06E-01
EPC3-55(LF)	135	8.18E-08
EPC3-55(HF)	135	8.05E-08
EPC3-55 FD %	135	1.5912
EPC3-56(LF)	137	8.51E-08
EPC3-56(HF)	137	8.56E-08
EPC3-56 FD %	137	-5.84E-01
EPC3-57(LF)	139	8.39E-08
EPC3-57(HF)	139	8.05E-08
EPC3-57 FD %	139	4.0131
EPC3-58(LF)	142	1.31E-07
EPC3-58(HF)	142	1.29E-07
EPC3-58 FD %	142	1.7816
EPC3-59(LF)	144	1.50E-07
EPC3-59(HF)	144	1.47E-07
EPC3-59 FD %	144	2.1163
EPC3-60(LF)	147	1.47E-07
EPC3-60(HF)	147	1.45E-07
EPC3-60 FD %	147	1.116
EPC3-61(LF)	150	1.55E-07
EPC3-61(HF)	150	1.54E-07
EPC3-61 FD %	150	7.01E-01
EPC3-62(LF)	152	1.43E-07
EPC3-62(HF)	152	1.42E-07
EPC3-62 FD %	152	4.12E-01
EPC3-63(LF)	155	1.44E-07
EPC3-63(HF)	155	1.41E-07
EPC3-63 FD %	155	2.0257
EPC3-64(LF)	157	1.45E-07
EPC3-64(HF)	157	1.44E-07
EPC3-64 FD %	157	6.94E-01
EPC3-65(LF)	160	1.24E-07
EPC3-65(HF)	160	1.22E-07
EPC3-65 FD %	160	1.6156

EPC3-66(LF)	162	8.42E-08
EPC3-66(HF)	162	8.23E-08
EPC3-66 FD %	162	2.2336
EPC3-67(LF)	165	9.40E-08
EPC3-67(HF)	165	9.06E-08
EPC3-67 FD %	165	3.6519
EPC3-68(LF)	167	1.08E-07
EPC3-68(HF)	167	1.06E-07
EPC3-68 FD %	167	1.432
EPC3-69(LF)	170	1.40E-07
EPC3-69(HF)	170	1.36E-07
EPC3-69 FD %	170	2.9448
EPC3-70(LF)	172	1.45E-07
EPC3-70(HF)	172	1.44E-07
EPC3-70 FD %	172	4.83E-01
EPC3-71(LF)	175	1.86E-07
EPC3-71(HF)	175	1.83E-07
EPC3-71 FD %	175	1.6678
EPC3-72(LF)	178	1.51E-07
EPC3-72(HF)	178	1.49E-07
EPC3-72 FD %	178	1.5307
EPC3-73(LF)	180	1.79E-07
EPC3-73(HF)	180	1.78E-07
EPC3-73 FD %	180	4.74E-01
EPC3-74(LF)	182	1.62E-07
EPC3-74(HF)	182	1.58E-07
EPC3-74 FD %	182	2.7417
EPC3-75(LF)	185	1.41E-07
EPC3-75(HF)	185	1.42E-07
EPC3-75 FD %	185	-2.32E-01
EPC3-76(LF)	188	1.51E-07
EPC3-76(HF)	188	1.51E-07
EPC3-76 FD %	188	-3.47E-01
EPC3-77(LF)	190	1.47E-07
EPC3-77(HF)	190	1.46E-07
EPC3-77 FD %	190	1.0095
EPC3-78(LF)	193	1.42E-07
EPC3-78(HF)	193	1.42E-07
EPC3-78 FD %	193	1.36E-01
EPC3-79(LF)	195	1.70E-07
EPC3-79(HF)	195	1.69E-07
EPC3-79 FD %	195	4.95E-01
EPC3-80(LF)	198	1.65E-07

EPC3-80(HF)	198	1.64E-07
EPC3-80 FD %	198	7.25E-01
EPC3-81(LF)	201	2.03E-07
EPC3-81(HF)	201	2.02E-07
EPC3-81 FD %	201	6.55E-01
EPC3-82(LF)	203	2.27E-07
EPC3-82(HF)	203	2.23E-07
EPC3-82 FD %	203	1.8024
EPC3-83(LF)	206	2.16E-07
EPC3-83(HF)	206	2.13E-07
EPC3-83 FD %	206	1.3493
EPC3-84(LF)	208	1.86E-07
EPC3-84(HF)	208	1.83E-07
EPC3-84 FD %	208	1.3175
EPC3-85(LF)	211	1.62E-07
EPC3-85(HF)	211	1.59E-07
EPC3-85 FD %	211	1.8505
EPC3-86(LF)	213	1.59E-07
EPC3-86(HF)	213	1.56E-07
EPC3-86 FD %	213	1.5221
EPC3-87(LF)	216	1.54E-07
EPC3-87(HF)	216	1.52E-07
EPC3-87 FD %	216	1.3931
EPC3-88(LF)	218	1.62E-07
EPC3-88(HF)	218	1.60E-07
EPC3-88 FD %	218	1.125
EPC3-89(LF)	221	1.32E-07
EPC3-89(HF)	221	1.30E-07
EPC3-89 FD %	221	1.4332
EPC3-90(LF)	223	1.24E-07
EPC3-90(HF)	223	1.23E-07
EPC3-90 FD %	223	3.95E-01
EPC3-91(LF)	226	1.40E-07
EPC3-91(HF)	226	1.38E-07
EPC3-91 FD %	226	1.7612
EPC3-92(LF)	228	1.29E-07
EPC3-92(HF)	228	1.25E-07
EPC3-92 FD %	228	2.7105
EPC3-93(LF)	231	1.18E-07
EPC3-93(HF)	231	1.17E-07
EPC3-93 FD %	231	1.1813
EPC3-94(LF)	233	1.16E-07
EPC3-94(HF)	233	1.14E-07

EPC3-94 FD %	233	1.5539
EPC3-95(LF)	235	1.13E-07
EPC3-95(HF)	235	1.09E-07
EPC3-95 FD %	235	3.4583
EPC3-96(LF)	238	1.22E-07
EPC3-96(HF)	238	1.20E-07
EPC3-96 FD %	238	1.7349
EPC3-97(LF)	240	1.25E-07
EPC3-97(HF)	240	1.23E-07
EPC3-97 FD %	240	1.322
EPC3-98(LF)	242	1.35E-07
EPC3-98(HF)	242	1.31E-07
EPC3-98 FD %	242	2.7981
EPC3-99(LF)	245	1.42E-07
EPC3-99(HF)	245	1.41E-07
EPC3-99 FD %	245	9.34E-01
EPC3-100(LF)	247	1.55E-07
EPC3-100(HF)	247	1.52E-07
EPC3-100 FD %	247	1.8416
EPC3-101(LF)	249	1.87E-07
EPC3-101(HF)	249	1.85E-07
EPC3-101 FD %	249	8.64E-01
EPC3-102(LF)	252	1.73E-07
EPC3-102(HF)	252	1.72E-07
EPC3-102 FD %	252	5.43E-01
EPC3-103(LF)	254	1.94E-07
EPC3-103(HF)	254	1.91E-07
EPC3-103 FD %	254	1.5025
EPC3-104(LF)	257	1.91E-07
EPC3-104(HF)	257	1.91E-07
EPC3-104 FD %	257	1.26E-01
EPC3-105(LF)	259	1.85E-07
EPC3-105(HF)	259	1.84E-07
EPC3-105 FD %	259	9.42E-01
EPC3-106(LF)	262	1.56E-07
EPC3-106(HF)	262	1.56E-07
EPC3-106 FD %	262	3.24E-01
EPC3-107(LF)	264	1.70E-07
EPC3-107(HF)	264	1.66E-07
EPC3-107 FD %	264	2.3306
EPC3-108(LF)	267	1.73E-07
EPC3-108(HF)	267	1.70E-07
EPC3-108 FD %	267	1.6514

EPC3-109(LF)	269	1.58E-07
EPC3-109(HF)	269	1.55E-07
EPC3-109 FD %	269	1.805
EPC3-110(LF)	272	1.34E-07
EPC3-110(HF)	272	1.32E-07
EPC3-110 FD %	272	1.3685
EPC3-111(LF)	275	1.46E-07
EPC3-111(HF)	275	1.43E-07
EPC3-111 FD %	275	2.4976
EPC3-112(LF)	277	1.21E-07
EPC3-112(HF)	277	1.20E-07
EPC3-112 FD %	277	2.39E-01
EPC3-113(LF)	279	9.30E-08
EPC3-113(HF)	279	9.25E-08
EPC3-113 FD %	279	4.70E-01
EPC3_114(LF)	282	8.90E-08
EPC3_114(HF)	282	8.88E-08
EPC3_114 FD %	282	2.14E-01
EPC3-115(LF)	285	1.05E-07
EPC3-115(HF)	285	1.03E-07
EPC3-115 FD %	285	1.873
EPC3-116(LF)	288	9.17E-08
EPC3-116(HF)	288	8.96E-08
EPC3-116 FD %	288	2.3747
EPC3-117(LF)	290	1.03E-07
EPC3-117(HF)	290	1.01E-07
EPC3-117 FD %	290	1.5379
EPC3-118(LF)	292	1.35E-07
EPC3-118(HF)	292	1.33E-07
EPC3-118 FD %	292	1.2997
EPC3-119(LF)	295	1.34E-07
EPC3-119(HF)	295	1.34E-07
EPC3-119 FD %	295	4.25E-01
EPC3-120(LF)	298	1.51E-07
EPC3-120(HF)	298	1.49E-07
EPC3-120 FD %	298	1.1651
EPC-121(LF)	300	1.44E-07
EPC-121(HF)	300	1.42E-07
EPC-121 FD %	300	1.3316
EPC3-122(LF)	303	1.41E-07
EPC3-122(HF)	303	1.38E-07
EPC3-122 FD %	303	2.21
EPC3-123(LF)	305	1.56E-07

EPC3-123(HF)	305	1.56E-07
EPC3-123 FD %	305	-5.22E-02
EPC3-124(LF)	308	1.56E-07
EPC3-124(HF)	308	1.55E-07
EPC3-124 FD %	308	9.25E-01
EPC3-125(LF)	310	1.48E-07
EPC3-125(HF)	310	1.47E-07
EPC3-125 FD %	310	7.33E-01
EPC3-126(LF)	313	1.45E-07
EPC3-126(HF)	313	1.46E-07
EPC3-126 FD %	313	-6.91E-01
EPC3-127(LF)	315	1.57E-07
EPC3-127(HF)	315	1.56E-07
EPC3-127 FD %	315	9.62E-01
EPC3-128(LF)	318	1.93E-07
EPC3-128(HF)	318	1.94E-07
EPC3-128 FD %	318	-4.42E-01
EPC3-129(LF)	320	1.97E-07
EPC3-129(HF)	320	1.96E-07
EPC3-129 FD %	320	7.42E-01
EPC3-130(LF)	323	1.75E-07
EPC3-130(HF)	323	1.72E-07
EPC3-130 FD %	323	1.2889
EPC3-131(LF)	326	1.69E-07
EPC3-131(HF)	326	1.67E-07
EPC3-131 FD %	326	1.0044
EPC3-132(LF)	328	1.46E-07
EPC3-132(HF)	328	1.45E-07
EPC3-132 FD %	328	3.59E-02
EPC3-133(LF)	330	1.33E-07
EPC3-133(HF)	330	1.32E-07
EPC3-133 FD %	330	1.097
EPC3-134(LF)	333	1.53E-07
EPC3-134(HF)	333	1.54E-07
EPC3-134 FD %	333	-6.72E-01
EPC3-135(LF)	335	1.49E-07
EPC3-135(HF)	335	1.49E-07
EPC3-135 FD %	335	-1.41E-01
EPC3-136(LF)	337	1.28E-07
EPC3-136(HF)	337	1.25E-07
EPC3-136 FD %	337	2.0246
EPC3-137(LF)	340	1.57E-07
EPC3-137(HF)	340	1.56E-07

EPC3-137 FD %	340	4.09E-01
EPC3-138(LF)	343	1.40E-07
EPC3-138(HF)	343	1.39E-07
EPC3-138 FD %	343	5.47E-01
EPC3-139(LF)	346	1.38E-07
EPC3-139(HF)	346	1.35E-07
EPC3-139 FD %	346	2.6068
EPC3-140(LF)	348	1.81E-07
EPC3-140(HF)	348	1.83E-07
EPC3-140 FD %	348	-7.21E-01
EPC3-141(LF)	350	1.86E-07
EPC3-141(HF)	350	1.86E-07
EPC3-141 FD %	350	4.17E-01
EPC3-142(LF)	353	1.72E-07
EPC3-142(HF)	353	1.72E-07
EPC3-142 FD %	353	1.98E-01
EPC3-143(LF)	355	1.74E-07
EPC3-143(HF)	355	1.73E-07
EPC3-143 FD %	355	2.43E-01
EPC3-144(LF)	358	1.63E-07
EPC3-144(HF)	358	1.61E-07
EPC3-144 FD %	358	1.0135
EPC3-145(LF)	360	1.63E-07
EPC3-145(HF)	360	1.61E-07
EPC3-145 FD %	360	1.4969
EPC3-146(LF)	363	1.72E-07
EPC3-146(HF)	363	1.73E-07
EPC3-146 FD %	363	-1.71E-01
EPC3-147(LF)	365	1.62E-07
EPC3-147(HF)	365	1.62E-07
EPC3-147 FD %	365	9.33E-02
EPC3-148(LF)	367	1.69E-07
EPC3-148(HF)	367	1.69E-07
EPC3-148 FD %	367	-3.41E-01
EPC3-149(LF)	370	1.72E-07
EPC3-149(HF)	370	1.73E-07
EPC3-149 FD %	370	-5.68E-01
EPC3-150(LF)	373	1.83E-07
EPC3-150(HF)	373	1.79E-07
EPC3-150 FD %	373	2.4682
EPC3-151(LF)	375	1.83E-07
EPC3-151(HF)	375	1.80E-07
EPC3-151 FD %	375	1.3924

EPC3-152(LF)	378	1.87E-07
EPC3-152(HF)	378	1.87E-07
EPC3-152 FD %	378	2.19E-01
EPC3-153(LF)	380	2.01E-07
EPC3-153(HF)	380	1.99E-07
EPC3-153 FD %	380	1.2908
EPC3-154(LF)	383	1.47E-07
EPC3-154(HF)	383	1.43E-07
EPC3-154 FD %	383	2.7096
EPC3-155(LF)	385	1.46E-07
EPC3-155(HF)	385	1.45E-07
EPC3-155 FD %	385	7.23E-01
EPC3-156(LF)	388	1.65E-07
EPC3-156(HF)	388	1.64E-07
EPC3-156 FD %	388	5.81E-01
EPC3-157(LF)	390	1.79E-07
EPC3-157(HF)	390	1.75E-07
EPC3-157 FD %	390	2.4328
EPC3-158(LF)	392	1.64E-07
EPC3-158(HF)	392	1.61E-07
EPC3-158 FD %	392	1.6945
EPC3-159(LF)	395	1.75E-07
EPC3-159(HF)	395	1.73E-07
EPC3-159 FD %	395	1.5544
EPC3-160(LF)	398	1.97E-07
EPC3-160(HF)	398	1.94E-07
EPC3-160 FD %	398	1.5531
EPC3-161(LF)	400	1.92E-07
EPC3-161(HF)	400	1.89E-07
EPC3-161 FD %	400	1.3895
EPC3-162(LF)	403	1.93E-07
EPC3-162(HF)	403	1.90E-07
EPC3-162 FD %	403	1.1906
EPC3-163(LF)	405	1.58E-07
EPC3-163(HF)	405	1.55E-07
EPC3-163 FD %	405	1.6722
EPC3-164(LF)	408	1.53E-07
EPC3-164(HF)	408	1.50E-07
EPC3-164 FD %	408	1.938
EPC3-165(LF)	410	1.47E-07
EPC3-165(HF)	410	1.46E-07
EPC3-165 FD %	410	9.58E-01
EPC3-166(LF)	413	1.64E-07

EPC3-166(HF)	413	1.61E-07
EPC3-166 FD %	413	1.5811
EPC3-167(LF)	415	1.61E-07
EPC3-167(HF)	415	1.60E-07
EPC3-167 FD %	415	5.22E-01
EPC3-168(LF)	418	1.40E-07
EPC3-168(HF)	418	1.37E-07
EPC3-168 FD %	418	2.1003
EPC3-169(LF)	420	1.45E-07
EPC3-169(HF)	420	1.44E-07
EPC3-169 FD %	420	5.70E-01
EPC3-170(LF)	423	1.48E-07
EPC3-170(HF)	423	1.45E-07
EPC3-170 FD %	423	1.7972
EPC3-171(LF)	425	1.49E-07
EPC3-171(HF)	425	1.47E-07
EPC3-171 FD %	425	1.1439
EPC3-172(LF)	428	1.49E-07
EPC3-172(HF)	428	1.49E-07
EPC3-172 FD %	428	-2.68E-01
EPC3-173(LF)	430	1.69E-07
EPC3-173(HF)	430	1.66E-07
EPC3-173 FD %	430	1.7989
EPC3-174(LF)	433	1.71E-07
EPC3-174(HF)	433	1.71E-07
EPC3-174 FD %	433	7.86E-02
EPC3-175(LF)	436	1.73E-07
EPC3-175(HF)	436	1.73E-07
EPC3-175 FD %	436	4.82E-01
EPC3-176(LF)	438	1.70E-07
EPC3-176(HF)	438	1.69E-07
EPC3-176 FD %	438	6.03E-01
EPC3-177(LF)	441	1.73E-07
EPC3-177(HF)	441	1.69E-07
EPC3-177 FD %	441	2.4977
EPC3-178(LF)	443	1.68E-07
EPC3-178(HF)	443	1.69E-07
EPC3-178 FD %	443	-4.79E-01
EPC3-179(LF)	446	1.49E-07
EPC3-179(HF)	446	1.50E-07
EPC3-179 FD %	446	-1.247
EPC3-180(LF)	448	1.45E-07
EPC3-180(HF)	448	1.33E-07

EPC3-180 FD %	448	8.6092
EPC3-181(LF)	451	1.35E-07
EPC3-181(HF)	451	1.36E-07
EPC3-181 FD %	451	-1.2436
EPC3-182(LF)	453	1.45E-07
EPC3-182(HF)	453	1.46E-07
EPC3-182 FD %	453	-2.53E-01
EPC3-183(LF)	456	1.38E-07
EPC3-183(HF)	456	1.39E-07
EPC3-183 FD %	456	-7.78E-01
EPC3-184(LF)	458	1.18E-07
EPC3-184(HF)	458	1.19E-07
EPC3-184 FD %	458	-1.1942
EPC3-185(LF)	461	1.18E-07
EPC3-185(HF)	461	1.15E-07
EPC3-185 FD %	461	2.181
EPC3-186(LF)	463	1.03E-07
EPC3-186(HF)	463	1.04E-07
EPC3-186 FD %	463	-1.3877
EPC3-187(LF)	466	7.68E-08
EPC3-187(HF)	466	7.66E-08
EPC3-187 FD %	466	1.81E-01
EPC3-188(LF)	469	7.23E-08
EPC3-188(HF)	469	7.16E-08
EPC3-188 FD %	469	1.0026
EPC3-189(LF)	471	8.86E-08
EPC3-189(HF)	471	8.50E-08
EPC3-189 FD %	471	4.115
EPC3-190(LF)	474	7.76E-08
EPC3-190(HF)	474	7.91E-08
EPC3-190 FD %	474	-2.0256
EPC3-191(LF)	476	6.67E-08
EPC3-191(HF)	476	6.86E-08
EPC3-191 FD %	476	-2.8388
EPC3-192(LF)	478	7.03E-08
EPC3-192(HF)	478	7.05E-08
EPC3-192 FD %	478	-2.37E-01
EPC3-193(LF)	481	7.59E-08
EPC3-193(HF)	481	7.56E-08
EPC3-193 FD %	481	3.70E-01
EPC3-194(LF)	484	8.24E-08
EPC3-194(HF)	484	8.20E-08
EPC3-194 FD %	484	5.30E-01

EPC3-195(LF)	486	9.94E-08
EPC3-195(HF)	486	9.71E-08
EPC3-195 FD %	486	2.3492
EPC3-196(LF)	489	1.21E-07
EPC3-196(HF)	489	1.21E-07
EPC3-196 FD %	489	1.02E-02
EPC3-197(LF)	491	8.19E-08
EPC3-197(HF)	491	8.14E-08
EPC3-197 FD %	491	5.74E-01
EPC3-198(LF)	494	6.16E-08
EPC3-198(HF)	494	6.26E-08
EPC3-198 FD %	494	-1.7229
EPC3-199(LF)	496	5.88E-08
EPC3-199(HF)	496	5.90E-08
EPC3-199 FD %	496	-2.55E-01
EPC3-200(LF)	499	5.91E-08
EPC3-200(HF)	499	6.00E-08
EPC3-200 FD %	499	-1.5023
EPC3-201(LF)	502	5.48E-08
EPC3-201(HF)	502	5.64E-08
EPC3-201 FD %	502	-2.8589
EPC3-202(LF)	504	6.23E-08
EPC3-202(HF)	504	6.16E-08
EPC3-202 FD %	504	1.1356
EPC3-203(LF)	506	5.76E-08
EPC3-203(HF)	506	5.98E-08
EPC3-203 FD %	506	-3.8053
EPC3-204(LF)	509	6.02E-08
EPC3-204(HF)	509	5.95E-08
EPC3-204 FD %	509	1.2408
EPC3-205(LF)	511	5.79E-08
EPC3-205(HF)	511	5.81E-08
EPC3-205 FD %	511	-2.75E-01
EPC3-206(LF)	513	5.38E-08
EPC3-206(HF)	513	5.34E-08
EPC3-206 FD %	513	8.63E-01
EPC3-207(LF)	516	5.31E-08
EPC3-207(HF)	516	5.54E-08
EPC3-207 FD %	516	-4.3366
EPC3-208(LF)	519	5.76E-08
EPC3-208(HF)	519	5.81E-08
EPC3-208 FD %	519	-8.40E-01
EPC3-209(LF)	521	6.45E-08

EPC3-209(HF)	521	6.30E-08
EPC3-209 FD %	521	2.3735
EPC3-210(LF)	523	6.46E-08
EPC3-210(HF)	523	6.47E-08
EPC3-210 FD %	523	-1.16E-01

* Low frequency (LF) and high frequency (HF) susceptibility are expressed in international standard units. Frequency dependence of susceptibility is expressed in percent (%). Data are formatted differently in this table due to a change in instrument output.

Table 28. EPC4 (playa center) Magnetic susceptibility*.

Sample & magnetic parameter	depth (cm)	Mag. Sus.
EPC4-1(LF)	1	7.54E-07
EPC4-1(HF)	1	7.23E-07
EPC4-1 FD %	1	4.0852
EPC4-2(LF)	3	7.81E-07
EPC4-2(HF)	3	7.67E-07
EPC4-2 FD %	3	1.7896
EPC4-3(LF)	5	8.83E-07
EPC4-3(HF)	5	8.67E-07
EPC4-3 FD %	5	1.7934
EPC4-4(LF)	7	7.05E-07
EPC4-4(HF)	7	6.88E-07
EPC4-4 FD %	7	2.3541
EPC4-5(LF)	9	6.57E-07
EPC4-5(HF)	9	6.41E-07
EPC4-5 FD %	9	2.3655
EPC4-6(LF)	11	6.57E-07
EPC4-6(HF)	11	6.45E-07
EPC4-6 FD %	11	1.8762
EPC4-7(LF)	14	6.57E-07
EPC4-7(HF)	14	6.42E-07
EPC4-7 FD %	14	2.3192
EPC4-8(LF)	16	6.57E-07
EPC4-8(HF)	16	6.25E-07
EPC4-8 FD %	16	4.977
EPC4-9(LF)	19	6.70E-07
EPC4-9(HF)	19	6.56E-07
EPC4-9 FD %	19	2.1358

EPC4-10(LF)	22	6.66E-07
EPC4-10(HF)	22	6.54E-07
EPC4-10 FD %	22	1.8672
EPC4-11(LF)	24	6.92E-07
EPC4-11(HF)	24	6.76E-07
EPC4-11 FD %	24	2.217
EPC3-12(LF)	27	6.91E-07
EPC3-12(HF)	27	6.74E-07
EPC3-12 FD %	27	2.5393
EPC4-13(LF)	29	6.85E-07
EPC4-13(HF)	29	6.65E-07
EPC4-13 FD %	29	2.9113
EPC4-14(LF)	32	6.95E-07
EPC4-14(HF)	32	6.72E-07
EPC4-14 FD %	32	3.2682
EPC4-15(LF)	34	7.07E-07
EPC4-15(HF)	34	6.83E-07
EPC4-15 FD %	34	3.3471
EPC4-16(LF)	37	7.12E-07
EPC4-16(HF)	37	6.90E-07
EPC4-16 FD %	37	3.1544
EPC4-17(LF)	39	7.17E-07
EPC4-17(HF)	39	6.99E-07
EPC4-17 FD %	39	2.5732
EPC4-18(LF)	41	7.16E-07
EPC4-18(HF)	41	6.97E-07
EPC4-18 FD %	41	2.6347
EPC4-19(LF)	44	7.24E-07
EPC4-19(HF)	44	7.06E-07
EPC4-19 FD %	44	2.5598
EPC4-20(LF)	47	7.29E-07
EPC4-20(HF)	47	7.12E-07
EPC4-20 FD %	47	2.2641
EPC4-21(LF)	49	6.72E-07
EPC4-21(HF)	49	7.14E-07
EPC4-21 FD %	49	-6.3136
EPC4-.22(LF)	52	7.40E-07
EPC4-.22(HF)	52	7.18E-07
EPC4-.22 FD %	52	2.9807
EPC4-23(LF)	54	6.95E-07
EPC4-23(HF)	54	7.36E-07
EPC4-23 FD %	54	-5.7716
EPC4-24(LF)	57	7.47E-07

EPC4-24(HF)	57	7.32E-07
EPC4-24 FD %	57	1.9895
EPC4-24(LF)	59	7.35E-07
EPC4-24(HF)	59	7.19E-07
EPC4-24 FD %	59	2.2305
EPC4-26(LF)	62	7.22E-07
EPC4-26(HF)	62	7.00E-07
EPC4-26 FD %	62	2.9761
EPC4-27(LF)	64	7.04E-07
EPC4-27(HF)	64	6.86E-07
EPC4-27 FD %	64	2.6068
EPC4-28(LF)	67	6.16E-07
EPC4-28(HF)	67	6.81E-07
EPC4-28 FD %	67	-10.5786
EPC4-29(LF)	69	7.05E-07
EPC4-29(HF)	69	6.88E-07
EPC4-29 FD %	69	2.4652
EPC4-30(LF)	72	6.99E-07
EPC4-30(HF)	72	6.85E-07
EPC4-30 FD %	72	2.1205
EPC4-31(LF)	75	6.78E-07
EPC4-31(HF)	75	6.58E-07
EPC4-31 FD %	75	2.9993
EPC4-32(LF)	78	6.71E-07
EPC4-32(HF)	78	6.54E-07
EPC4-32 FD %	78	2.4838
EPC4-33(LF)	80	6.72E-07
EPC4-33(HF)	80	6.47E-07
EPC4-33 FD %	80	3.6843
EPC4-34(LF)	82	6.56E-07
EPC4-34(HF)	82	6.39E-07
EPC4-34 FD %	82	2.5438
EPC4-35(LF)	85	5.99E-07
EPC4-35(HF)	85	5.83E-07
EPC4-35 FD %	85	2.7375
EPC4-36(LF)	88	6.06E-07
EPC4-36(HF)	88	5.90E-07
EPC4-36 FD %	88	2.6112
EPC4-37(LF)	90	5.91E-07
EPC4-37(HF)	90	5.77E-07
EPC4-37 FD %	90	2.2207
EPC4-38(LF)	93	5.83E-07
EPC4-38(HF)	93	5.70E-07

EPC4-38 FD %	93	2.2673
EPC4-39(LF)	95	5.70E-07
EPC4-39(HF)	95	5.53E-07
EPC4-39 FD %	95	3.0153
EPC4-40(LF)	97	5.53E-07
EPC4-40(HF)	97	5.42E-07
EPC4-40 FD %	97	1.9594
EPC4-41(LF)	100	5.36E-07
EPC4-41(HF)	100	5.26E-07
EPC4-41 FD %	100	1.8576
EPC4-42(LF)	102	4.35E-07
EPC4-42(HF)	102	4.31E-07
EPC4-42 FD %	102	7.84E-01
EPC4-43(LF)	105	3.59E-07
EPC4-43(HF)	105	3.47E-07
EPC4-43 FD %	105	3.6051
EPC4-44(LF)	108	4.25E-07
EPC4-44(HF)	108	4.18E-07
EPC4-44 FD %	108	1.8092
EPC4-45(LF)	110	4.16E-07
EPC4-45(HF)	110	4.14E-07
EPC4-45 FD %	110	6.06E-01
EPC4-46(LF)	113	4.20E-07
EPC4-46(HF)	113	4.15E-07
EPC4-46 FD %	113	1.2025
EPC4-47(LF)	115	4.10E-07
EPC4-47(HF)	115	4.07E-07
EPC4-47 FD %	115	5.74E-01
EPC4-48(LF)	117	4.05E-07
EPC4-48(HF)	117	3.98E-07
EPC4-48 FD %	117	1.8911
EPC4-49(LF)	120	3.90E-07
EPC4-49(HF)	120	3.85E-07
EPC4-49 FD %	120	1.0968
EPC4-50(LF)	122	3.85E-07
EPC4-50(HF)	122	3.82E-07
EPC4-50 FD %	122	6.68E-01
EPC4-51(LF)	125	3.65E-07
EPC4-51(HF)	125	3.62E-07
EPC4-51 FD %	125	7.40E-01
EPC4-52(LF)	127	4.03E-07
EPC4-52(HF)	127	4.00E-07
EPC4-52 FD %	127	7.51E-01

EPC4-53(LF)	130	3.91E-07
EPC4-53(HF)	130	3.89E-07
EPC4-53 FD %	130	5.88E-01
EPC4-54(LF)	133	4.24E-07
EPC4-54(HF)	133	4.38E-07
EPC4-54 FD %	133	-3.3261
EPC4-55(LF)	135	3.96E-07
EPC4-55(HF)	135	3.92E-07
EPC4-55 FD %	135	1.0396
EPC4-56(LF)	137	4.15E-07
EPC4-56(HF)	137	4.11E-07
EPC4-56 FD %	137	1.0028
EPC4-57(LF)	140	4.17E-07
EPC4-57(HF)	140	4.17E-07
EPC4-57 FD %	140	-2.14E-02
EPC4-58(LF)	142	4.56E-07
EPC4-58(HF)	142	4.51E-07
EPC4-58 FD %	142	1.051
EPC4-59(LF)	145	4.63E-07
EPC4-59(HF)	145	4.61E-07
EPC4-59 FD %	145	5.28E-01
EPC4-60(LF)	147	4.98E-07
EPC4-60(HF)	147	4.91E-07
EPC4-60 FD %	147	1.3333
EPC4-61(LF)	150	4.71E-07
EPC4-61(HF)	150	4.68E-07
EPC4-61 FD %	150	5.95E-01
EPC4-62(LF)	152	5.07E-07
EPC4-62(HF)	152	5.08E-07
EPC4-62 FD %	152	-1.01E-01
EPC4-63(LF)	155	5.34E-07
EPC4-63(HF)	155	5.30E-07
EPC4-63 FD %	155	7.91E-01
EPC4-64(LF)	158	3.80E-07
EPC4-64(HF)	158	3.82E-07
EPC4-64 FD %	158	-6.81E-01
EPC4-65(LF)	160	3.94E-07
EPC4-65(HF)	160	3.93E-07
EPC4-65 FD %	160	2.29E-01
EPC4-66(LF)	163	3.71E-07
EPC4-66(HF)	163	3.71E-07
EPC4-66 FD %	163	-7.40E-02
EPC4-67(LF)	165	3.54E-07

EPC4-67(HF)	165	3.45E-07
EPC4-67 FD %	165	2.5612
EPC4-68(LF)	168	3.79E-07
EPC4-68(HF)	168	3.76E-07
EPC4-68 FD %	168	8.47E-01
EPC4-69(LF)	170	3.40E-07
EPC4-69(HF)	170	3.41E-07
EPC4-69 FD %	170	-1.89E-01
EPC4-70(LF)	173	3.41E-07
EPC4-70(HF)	173	3.40E-07
EPC4-70 FD %	173	3.31E-01
EPC4-71(LF)	175	3.58E-07
EPC4-71(HF)	175	3.58E-07
EPC4-71 FD %	175	-6.38E-02
EPC4-72(LF)	178	3.36E-07
EPC4-72(HF)	178	3.34E-07
EPC4-72 FD %	178	5.20E-01
EPC4-73(LF)	180	3.45E-07
EPC4-73(HF)	180	3.46E-07
EPC4-73 FD %	180	-2.00E-01
EPC4-74(LF)	182	3.86E-07
EPC4-74(HF)	182	3.85E-07
EPC4-74 FD %	182	2.57E-01
EPC4-75(LF)	185	4.11E-07
EPC4-75(HF)	185	4.07E-07
EPC4-75 FD %	185	1.0698
EPC4-76(LF)	188	3.13E-07
EPC4-76(HF)	188	3.12E-07
EPC4-76 FD %	188	4.20E-01
EPC4-77(LF)	190	3.63E-07
EPC4-77(HF)	190	3.60E-07
EPC4-77 FD %	190	8.98E-01
EPC4-78(LF)	192	3.95E-07
EPC4-78(HF)	192	3.96E-07
EPC4-78 FD %	192	-1.55E-01
EPC4-79(LF)	195	3.95E-07
EPC4-79(HF)	195	3.94E-07
EPC4-79 FD %	195	2.70E-01
EPC4-80(LF)	198	3.14E-07
EPC4-80(HF)	198	3.59E-07
EPC4-80 FD %	198	-14.3922
EPC4-81(LF)	200	2.92E-07
EPC4-81(HF)	200	2.89E-07

EPC4-81 FD %	200	1.0065
EPC4-82(LF)	203	3.21E-07
EPC4-82(HF)	203	3.27E-07
EPC4-82 FD %	203	-1.8909
EPC4-83(LF)	205	3.06E-07
EPC4-83(HF)	205	3.05E-07
EPC4-83 FD %	205	2.65E-01
EPC4-84(LF)	207	3.14E-07
EPC4-84(HF)	207	3.08E-07
EPC4-84 FD %	207	2.014
EPC4-85(LF)	210	3.80E-07
EPC4-85(HF)	210	3.77E-07
EPC4-85 FD %	210	7.98E-01
EPC4-86(LF)	213	3.16E-07
EPC4-86(HF)	213	3.14E-07
EPC4-86 FD %	213	3.62E-01
EPC4-87(LF)	215	2.53E-07
EPC4-87(HF)	215	2.58E-07
EPC4-87 FD %	215	-1.9934
EPC4-88(LF)	218	3.79E-07
EPC4-88(HF)	218	3.76E-07
EPC4-88 FD %	218	9.24E-01
EPC4-89(LF)	220	3.91E-07
EPC4-89(HF)	220	3.88E-07
EPC4-89 FD %	220	8.53E-01
EPC4-90(LF)	223	2.73E-07
EPC4-90(HF)	223	2.73E-07
EPC4-90 FD %	223	5.11E-02
EPC4-91(LF)	225	2.77E-07
EPC4-91(HF)	225	2.69E-07
EPC4-91 FD %	225	3.0595
EPC4-92(LF)	228	3.80E-07
EPC4-92(HF)	228	3.77E-07
EPC4-92 FD %	228	9.10E-01
EPC4-93(LF)	230	4.74E-07
EPC4-93(HF)	230	4.67E-07
EPC4-93 FD %	230	1.3191
EPC4-94(LF)	233	4.48E-07
EPC4-94(HF)	233	4.12E-07
EPC4-94 FD %	233	7.9758
EPC4-95(LF)	235	4.64E-07
EPC4-95(HF)	235	4.62E-07
EPC4-95 FD %	235	4.85E-01

EPC4-96(LF)	238	5.11E-07
EPC4-96(HF)	238	5.28E-07
EPC4-96 FD %	238	-3.3226
EPC4-97(LF)	240	4.53E-07
EPC4-97(HF)	240	4.50E-07
EPC4-97 FD %	240	5.63E-01
EPC4-98(LF)	243	3.85E-07
EPC4-98(HF)	243	3.82E-07
EPC4-98 FD %	243	6.61E-01
EPC4-99(LF)	247	4.91E-07
EPC4-99(HF)	247	4.90E-07
EPC4-99 FD %	247	3.53E-01
EPC4-100(LF)	249	4.53E-07
EPC4-100(HF)	249	4.50E-07
EPC4-100 FD %	249	6.09E-01
EPC4-101(LF)	251	4.42E-07
EPC4-101(HF)	251	4.38E-07
EPC4-101 FD %	251	8.86E-01
EPC4-102(LF)	254	3.56E-07
EPC4-102(HF)	254	3.54E-07
EPC4-102 FD %	254	6.49E-01
EPC4-103(LF)	256	3.73E-07
EPC4-103(HF)	256	3.76E-07
EPC4-103 FD %	256	-7.17E-01
EPC4-104(LF)	259	3.58E-07
EPC4-104(HF)	259	3.54E-07
EPC4-104 FD %	259	1.1058
EPC4-105(LF)	261	3.21E-07
EPC4-105(HF)	261	3.18E-07
EPC4-105 FD %	261	7.39E-01
EPC4-106(LF)	263	3.15E-07
EPC4-106(HF)	263	3.16E-07
EPC4-106 FD %	263	-1.08E-01
EPC4-107(LF)	266	3.23E-07
EPC4-107(HF)	266	3.21E-07
EPC4-107 FD %	266	6.63E-01
EPC4-108(LF)	268	2.94E-07
EPC4-108(HF)	268	2.93E-07
EPC4-108 FD %	268	6.01E-01
EPC4-109(LF)	271	3.12E-07
EPC4-109(HF)	271	3.12E-07
EPC4-109 FD %	271	-2.37E-01
EPC4-110(LF)	273	3.54E-07

EPC4-110(HF)	273	3.52E-07
EPC4-110 FD %	273	5.82E-01
EPC4-111(LF)	276	3.44E-07
EPC4-111(HF)	276	3.44E-07
EPC4-111 FD %	276	1.25E-02
EPC4-112(LF)	278	3.18E-07
EPC4-112(HF)	278	3.16E-07
EPC4-112 FD %	278	4.92E-01
EPC4-113(LF)	281	3.46E-07
EPC4-113(HF)	281	3.45E-07
EPC4-113 FD %	281	1.72E-01
EPC4-114(LF)	284	3.51E-07
EPC4-114(HF)	284	3.44E-07
EPC4-114 FD %	284	2.0127
EPC4-116(LF)	288	3.13E-07
EPC4-116(HF)	288	3.12E-07
EPC4-116 FD %	288	1.31E-01
EPC4-117(LF)	291	3.03E-07
EPC4-117(HF)	291	3.00E-07
EPC4-117 FD %	291	7.45E-01
EPC4-118(LF)	293	2.54E-07
EPC4-118(HF)	293	2.53E-07
EPC4-118 FD %	293	2.83E-01
EPC4-119(LF)	296	1.58E-07
EPC4-119(HF)	296	1.58E-07
EPC4-119 FD %	296	4.90E-02
EPC4-120(LF)	298	1.38E-07
EPC4-120(HF)	298	1.36E-07
EPC4-120 FD %	298	1.1219
EPC4-121(LF)	301	1.83E-07
EPC4-121(HF)	301	1.81E-07
EPC4-121 FD %	301	9.72E-01
EPC4-122(LF)	304	1.94E-07
EPC4-122(HF)	304	1.94E-07
EPC4-122 FD %	304	-1.07E-01
EPC4-123(LF)	306	1.56E-07
EPC4-123(HF)	306	1.56E-07
EPC4-123 FD %	306	-2.34E-01
EPC-124(LF)	308	1.37E-07
EPC-124(HF)	308	1.33E-07
EPC-124 FD %	308	2.5886
EPC4-125(LF)	311	1.27E-07
EPC4-125(HF)	311	1.25E-07

EPC4-125 FD %	311	1.7307
EPC4-126(LF)	313	1.56E-07
EPC4-126(HF)	313	1.54E-07
EPC4-126 FD %	313	1.4844
EPC4-127(LF)	316	1.72E-07
EPC4-127(HF)	316	1.68E-07
EPC4-127 FD %	316	2.2356
EPC4-128(LF)	318	1.49E-07
EPC4-128(HF)	318	1.48E-07
EPC4-128 FD %	318	1.0164
EPC4-129(LF)	321	1.35E-07
EPC4-129(HF)	321	1.34E-07
EPC4-129 FD %	321	7.41E-01
EPC4-130(LF)	323	1.38E-07
EPC4-130(HF)	323	1.39E-07
EPC4-130 FD %	323	-7.66E-01
EPC4-131(LF)	325	1.29E-07
EPC4-131(HF)	325	1.29E-07
EPC4-131 FD %	325	5.29E-01
EPC4-132(LF)	328	1.41E-07
EPC4-132(HF)	328	1.43E-07
EPC4-132 FD %	328	-1.9182
EPC4-133(LF)	330	1.49E-07
EPC4-133(HF)	330	1.51E-07
EPC4-133 FD %	330	-1.3848
EPC4-134(LF)	333	1.68E-07
EPC4-134(HF)	333	1.65E-07
EPC4-134 FD %	333	1.306
EPC4-135(LF)	335	1.81E-07
EPC4-135(HF)	335	1.82E-07
EPC4-135 FD %	335	-6.46E-01
EPC4-136(LF)	337	1.85E-07
EPC4-136(HF)	337	1.85E-07
EPC4-136 FD %	337	-2.45E-01
EPC4-137(LF)	340	1.62E-07
EPC4-137(HF)	340	1.61E-07
EPC4-137 FD %	340	4.85E-01
EPC4-138(LF)	343	1.74E-07
EPC4-138(HF)	343	1.74E-07
EPC4-138 FD %	343	-3.55E-03
EPC4-139(LF)	345	2.24E-07
EPC4-139(HF)	345	2.23E-07
EPC4-139 FD %	345	5.65E-01

EPC4-140(LF)	348	2.06E-07
EPC4-140(HF)	348	2.04E-07
EPC4-140 FD %	348	7.15E-01
EPC4-141(LF)	350	1.83E-07
EPC4-141(HF)	350	1.85E-07
EPC4-141 FD %	350	-9.67E-01
EPC4-142(LF)	353	1.65E-07
EPC4-142(HF)	353	1.66E-07
EPC4-142 FD %	353	-4.41E-01
EPC4-143(LF)	355	1.95E-07
EPC4-143(HF)	355	1.94E-07
EPC4-143 FD %	355	2.97E-01
EPC4-144(LF)	358	2.98E-07
EPC4-144(HF)	358	2.98E-07
EPC4-144 FD %	358	1.40E-01
EPC4-145(LF)	362	2.42E-07
EPC4-145(HF)	362	2.41E-07
EPC4-145 FD %	362	2.93E-01
EPC4-146(LF)	364	2.08E-07
EPC4-146(HF)	364	2.09E-07
EPC4-146 FD %	364	-6.94E-01
EPC4-147(LF)	366	1.88E-07
EPC4-147(HF)	366	1.87E-07
EPC4-147 FD %	366	2.83E-01
EPC4-148(LF)	369	1.91E-07
EPC4-148(HF)	369	1.89E-07
EPC4-148 FD %	369	1.1218
EPC4-149(LF)	371	2.37E-07
EPC4-149(HF)	371	2.36E-07
EPC4-149 FD %	371	3.40E-01
EPC4-150(LF)	374	2.03E-07
EPC4-150(HF)	374	2.01E-07
EPC4-150 FD %	374	8.29E-01
EPC4-151(LF)	376	2.16E-07
EPC4-151(HF)	376	2.12E-07
EPC4-151 FD %	376	1.8102
EPC4-152(LF)	379	1.89E-07
EPC4-152(HF)	379	1.87E-07
EPC4-152 FD %	379	1.3264
EPC4-153(LF)	381	1.61E-07
EPC4-153(HF)	381	1.63E-07
EPC4-153 FD %	381	-1.0015
EPC4-154(LF)	383	1.58E-07

EPC4-154(HF)	383	1.58E-07
EPC4-154 FD %	383	6.64E-02
EPC4-155(LF)	386	1.58E-07
EPC4-155(HF)	386	1.57E-07
EPC4-155 FD %	386	7.16E-01
EPC4-156(LF)	388	1.42E-07
EPC4-156(HF)	388	1.41E-07
EPC4-156 FD %	388	6.63E-01
EPC4-157(LF)	391	1.34E-07
EPC4-157(HF)	391	1.34E-07
EPC4-157 FD %	391	3.38E-01
EPC4-158(LF)	393	1.26E-07
EPC4-158(HF)	393	1.26E-07
EPC4-158 FD %	393	6.13E-01
EPC4-159(LF)	396	1.17E-07
EPC4-159(HF)	396	1.17E-07
EPC4-159 FD %	396	-6.14E-01
EPC4-160(LF)	398	1.27E-07
EPC4-160(HF)	398	1.23E-07
EPC4-160 FD %	398	3.0281
EPC4-161(LF)	401	1.26E-07
EPC4-161(HF)	401	1.23E-07
EPC4-161 FD %	401	2.0442
EPC4-162(LF)	403	1.29E-07
EPC4-162(HF)	403	1.28E-07
EPC4-162 FD %	403	6.70E-01
EPC4-163(LF)	406	1.39E-07
EPC4-163(HF)	406	1.36E-07
EPC4-163 FD %	406	1.9654
EPC4-164(LF)	408	1.53E-07
EPC4-164(HF)	408	1.53E-07
EPC4-164 FD %	408	3.64E-01
EPC4-165(LF)	411	1.51E-07
EPC4-165(HF)	411	1.57E-07
EPC4-165 FD %	411	-4.3289
EPC4-166(LF)	413	1.60E-07
EPC4-166(HF)	413	1.59E-07
EPC4-166 FD %	413	1.2036
EPC4-167(LF)	415	1.55E-07
EPC4-167(HF)	415	1.57E-07
EPC4-167 FD %	415	-1.1943
EPC4-168(LF)	418	1.61E-07
EPC4-168(HF)	418	1.59E-07

EPC4-168 FD %	418	1.0526
EPC4-169(LF)	421	2.01E-07
EPC4-169(HF)	421	2.00E-07
EPC4-169 FD %	421	4.73E-01
EPC4-170(LF)	423	1.86E-07
EPC4-170(HF)	423	1.82E-07
EPC4-170 FD %	423	1.8961
EPC4-171(LF)	425	1.95E-07
EPC4-171(HF)	425	1.96E-07
EPC4-171 FD %	425	-6.55E-01
EPC4-172(LF)	427	1.97E-07
EPC4-172(HF)	427	1.94E-07
EPC4-172 FD %	427	1.7198
EPC4-173(LF)	430	2.01E-07
EPC4-173(HF)	430	1.99E-07
EPC4-173 FD %	430	8.42E-01
EPC4-174(LF)	432	2.00E-07
EPC4-174(HF)	432	2.00E-07
EPC4-174 FD %	432	9.11E-02
EPC4-175(LF)	435	2.11E-07
EPC4-175(HF)	435	2.04E-07
EPC4-175 FD %	435	3.1368
EPC4-176(LF)	437	2.01E-07
EPC4-176(HF)	437	1.97E-07
EPC4-176 FD %	437	1.8899
EPC4-177(LF)	440	2.19E-07
EPC4-177(HF)	440	2.16E-07
EPC4-177 FD %	440	1.0788
EPC4-178(LF)	442	1.93E-07
EPC4-178(HF)	442	2.13E-07
EPC4-178 FD %	442	-10.3623
EPC4-179(LF)	445	1.53E-07
EPC4-179(HF)	445	1.48E-07
EPC4-179 FD %	445	3.5739
EPC4-180(LF)	447	1.18E-07
EPC4-180(HF)	447	1.17E-07
EPC4-180 FD %	447	1.2545
EPC4-181(LF)	450	9.69E-08
EPC4-181(HF)	450	7.86E-08
EPC4-181 FD %	450	18.8154
EPC4-182(LF)	452	8.58E-08
EPC4-182(HF)	452	9.52E-08
EPC4-182 FD %	452	-10.9075

EPC4-183(LF)	454	9.51E-08
EPC4-183(HF)	454	9.30E-08
EPC4-183 FD %	454	2.2121
EPC4-184(LF)	457	1.12E-07
EPC4-184(HF)	457	1.11E-07
EPC4-184 FD %	457	9.73E-01
EPC4-185(LF)	459	1.47E-07
EPC4-185(HF)	459	1.46E-07
EPC4-185 FD %	459	1.2463
EPC4-186(LF)	462	1.54E-07
EPC4-186(HF)	462	1.56E-07
EPC4-186 FD %	462	-8.90E-01
EPC4-187(LF)	464	1.55E-07
EPC4-187(HF)	464	1.55E-07
EPC4-187 FD %	464	-6.79E-02
EPC4-188(LF)	467	1.78E-07
EPC4-188(HF)	467	1.87E-07
EPC4-188 FD %	467	-5.0031
EPC4-189(LF)	469	1.52E-07
EPC4-189(HF)	469	1.50E-07
EPC4-189 FD %	469	1.6357
EPC4-190(LF)	472	1.66E-07
EPC4-190(HF)	472	1.63E-07
EPC4-190 FD %	472	1.6214
EPC4-191(LF)	474	1.43E-07
EPC4-191(HF)	474	1.69E-07
EPC4-191 FD %	474	-18.4114
EPC4-192(LF)	477	1.51E-07
EPC4-192(HF)	477	1.48E-07
EPC4-192 FD %	477	2.083
EPC4-193(LF)	479	1.57E-07
EPC4-193(HF)	479	1.56E-07
EPC4-193 FD %	479	4.88E-01
EPC4-194(LF)	482	1.72E-07
EPC4-194(HF)	482	2.02E-07
EPC4-194 FD %	482	-17.1902
EPC4-195(LF)	484	1.52E-07
EPC4-195(HF)	484	1.46E-07
EPC4-195 FD %	484	3.6736
EPC4-196(LF)	487	1.53E-07
EPC4-196(HF)	487	1.53E-07
EPC4-196 FD %	487	-1.12E-01
EPC4-197(LF)	489	1.80E-07

EPC4-197(HF)	489	1.80E-07
EPC4-197 FD %	489	2.30E-01
EPC4-198(LF)	492	1.81E-07
EPC4-198(HF)	492	1.83E-07
EPC4-198 FD %	492	-1.3279
EPC4-199(LF)	494	1.72E-07
EPC4-199(HF)	494	1.68E-07
EPC4-199 FD %	494	2.3618
EPC4-200(LF)	497	1.66E-07
EPC4-200(HF)	497	1.68E-07
EPC4-200 FD %	497	-1.0893
EPC4-201(LF)	499	1.50E-07
EPC4-201(HF)	499	1.47E-07
EPC4-201 FD %	499	1.8258
EPC4-202(LF)	501	1.61E-07
EPC4-202(HF)	501	1.61E-07
EPC4-202 FD %	501	1.02E-02
EPC4-203(LF)	504	1.54E-07
EPC4-203(HF)	504	1.56E-07
EPC4-203 FD %	504	-7.28E-01
EPC4-204(LF)	506	1.35E-07
EPC4-204(HF)	506	1.26E-07
EPC4-204 FD %	506	6.2843
EPC4-205(LF)	509	1.21E-07
EPC4-205(HF)	509	1.23E-07
EPC4-205 FD %	509	-1.6152
EPC4-206(LF)	512	1.53E-07
EPC4-206(HF)	512	1.55E-07
EPC4-206 FD %	512	-1.3505
EPC4-207(LF)	514	1.54E-07
EPC4-207(HF)	514	1.54E-07
EPC4-207 FD %	514	1.36E-01
EPC4-208(LF)	517	1.80E-07
EPC4-208(HF)	517	1.80E-07
EPC4-208 FD %	517	3.29E-01
EPC4-209(LF)	519	1.72E-07
EPC4-209(HF)	519	1.70E-07
EPC4-209 FD %	519	1.0444
EPC4-210(LF)	522	2.08E-07
EPC4-210(HF)	522	2.07E-07
EPC4-210 FD %	522	4.07E-01
EPC4-211(LF)	524	1.91E-07
EPC4-211(HF)	524	1.91E-07

EPC4-211 FD %	524	-1.72E-01
EPC4-212(LF)	527	1.99E-07
EPC4-212(HF)	527	1.96E-07
EPC4-212 FD %	527	1.619
EPC4-213(LF)	530	2.06E-07
EPC4-213(HF)	530	2.05E-07
EPC4-213 FD %	530	2.73E-01
EPC4-214(LF)	532	2.05E-07
EPC4-214(HF)	532	2.03E-07
EPC4-214 FD %	532	9.76E-01
EPC4-215(LF)	535	1.91E-07
EPC4-215(HF)	535	1.93E-07
EPC4-215 FD %	535	-9.87E-01
EPC4-216(LF)	537	1.79E-07
EPC4-216(HF)	537	1.75E-07
EPC4-216 FD %	537	1.7923
EPC4-217(LF)	540	1.99E-07
EPC4-217(HF)	540	1.99E-07
EPC4-217 FD %	540	-2.94E-01
EPC4-218(LF)	542	2.10E-07
EPC4-218(HF)	542	2.08E-07
EPC4-218 FD %	542	7.24E-01
EPC4-219(LF)	544	2.15E-07
EPC4-219(HF)	544	2.18E-07
EPC4-219 FD %	544	-1.5716
EPC4-220(LF)	547	2.01E-07
EPC4-220(HF)	547	2.00E-07
EPC4-220 FD %	547	4.07E-01
EPC4-221(LF)	549	1.90E-07
EPC4-221(HF)	549	1.94E-07
EPC4-221 FD %	549	-2.1211
EPC4-222(LF)	552	1.90E-07
EPC4-222(HF)	552	1.86E-07
EPC4-222 FD %	552	2.1575
EPC4-223(LF)	554	1.85E-07
EPC4-223(HF)	554	1.94E-07
EPC4-223 FD %	554	-5.1293
EPC4-224(LF)	557	2.00E-07
EPC4-224(HF)	557	1.97E-07
EPC4-224 FD %	557	1.1245
EPC4-225(LF)	559	2.15E-07
EPC4-225(HF)	559	2.14E-07
EPC4-225 FD %	559	6.40E-01

EPC4-226(LF)	562	1.88E-07
EPC4-226(HF)	562	1.89E-07
EPC4-226 FD %	562	-4.39E-01
EPC4-227(LF)	564	2.37E-07
EPC4-227(HF)	564	2.34E-07
EPC4-227 FD %	564	1.3191
EPC4-228(LF)	567	2.38E-07
EPC4-228(HF)	567	2.36E-07
EPC4-228 FD %	567	9.40E-01
EPC4-229(LF)	569	2.18E-07
EPC4-229(HF)	569	2.18E-07
EPC4-229 FD %	569	6.08E-02
EPC4-230(LF)	572	2.09E-07
EPC4-230(HF)	572	2.12E-07
EPC4-230 FD %	572	-1.103
EPC4-231(LF)	574	2.02E-07
EPC4-231(HF)	574	2.06E-07
EPC4-231 FD %	574	-1.8068
EPC4-232(LF)	577	2.09E-07
EPC4-232(HF)	577	2.11E-07
EPC4-232 FD %	577	-9.26E-01
EPC4-233(LF)	579	2.14E-07
EPC4-233(HF)	579	2.11E-07
EPC4-233 FD %	579	1.4219
EPC4-234(LF)	582	1.88E-07
EPC4-234(HF)	582	1.85E-07
EPC4-234 FD %	582	1.4338
EPC4-235(LF)	584	2.02E-07
EPC4-235(HF)	584	2.06E-07
EPC4-235 FD %	584	-1.8482
EPC4-236(LF)	587	2.10E-07
EPC4-236(HF)	587	2.08E-07
EPC4-236 FD %	587	9.07E-01
EPC4-237(LF)	589	2.12E-07
EPC4-237(HF)	589	2.20E-07
EPC4-237 FD %	589	-3.6812
EPC4-238(LF)	592	1.90E-07
EPC4-238(HF)	592	1.90E-07
EPC4-238 FD %	592	-1.72E-01
EPC4-239(LF)	594	2.03E-07
EPC4-239(HF)	594	2.02E-07
EPC4-239 FD %	594	5.01E-01
EPC4-240(LF)	597	1.93E-07

EPC4-240(HF)	597	1.97E-07
EPC4-240 FD %	597	-2.2805
EPC4-241(LF)	600	1.98E-07
EPC4-241(HF)	600	2.10E-07
EPC4-241 FD %	600	-5.8894
EPC4-242(LF)	602	2.07E-07
EPC4-242(HF)	602	2.05E-07
EPC4-242 FD %	602	5.92E-01
EPC4-243(LF)	604	2.29E-07
EPC4-243(HF)	604	2.25E-07
EPC4-243 FD %	604	1.7364
EPC4-244(LF)	607	1.95E-07
EPC4-244(HF)	607	1.96E-07
EPC4-244 FD %	607	-4.57E-01
EPC4-245(LF)	609	1.24E-07
EPC4-245(HF)	609	1.25E-07
EPC4-245 FD %	609	-4.30E-01
EPC4-246(LF)	612	1.53E-07
EPC4-246(HF)	612	1.53E-07
EPC4-246 FD %	612	1.26E-01
EPC4-247(LF)	614	1.38E-07
EPC4-247(HF)	614	1.37E-07
EPC4-247 FD %	614	1.99E-01
EPC4-248(LF)	616	1.22E-07
EPC4-248(HF)	616	1.21E-07
EPC4-248 FD %	616	1.371
EPC4-249(LF)	619	1.26E-07
EPC4-249(HF)	619	1.24E-07
EPC4-249 FD %	619	1.8234
EPC4-250(LF)	621	1.15E-07
EPC4-250(HF)	621	1.14E-07
EPC4-250 FD %	621	9.07E-01
EPC4-251(LF)	624	9.76E-08
EPC4-251(HF)	624	9.60E-08
EPC4-251 FD %	624	1.669
EPC4-252(LF)	626	6.63E-08
EPC4-252(HF)	626	6.42E-08
EPC4-252 FD %	626	3.1856
EPC4-253(LF)	629	7.13E-08
EPC4-253(HF)	629	7.13E-08
EPC4-253 FD %	629	-7.38E-02
EPC4-254(LF)	631	7.47E-08
EPC4-254(HF)	631	7.42E-08

EPC4-254 FD %	631	6.26E-01
EPC4-255(LF)	634	6.52E-08
EPC4-255(HF)	634	6.62E-08
EPC4-255 FD %	634	-1.6259
EPC4-256(LF)	636	6.52E-08
EPC4-256(HF)	636	6.55E-08
EPC4-256 FD %	636	-4.38E-01
EPC4-257(LF)	639	1.02E-07
EPC4-257(HF)	639	1.02E-07
EPC4-257 FD %	639	-4.43E-02
EPC4-258(LF)	641	7.84E-08
EPC4-258(HF)	641	8.47E-08
EPC4-258 FD %	641	-7.997
EPC4-259(LF)	644	7.58E-08
EPC4-259(HF)	644	7.49E-08
EPC4-259 FD %	644	1.0908
EPC4-260(LF)	646	7.25E-08
EPC4-260(HF)	646	7.97E-08
EPC4-260 FD %	646	-9.8658
EPC4-261(LF)	649	6.73E-08
EPC4-261(HF)	649	6.85E-08
EPC4-261 FD %	649	-1.8903
EPC4-262(LF)	651	7.55E-08
EPC4-262(HF)	651	7.55E-08
EPC4-262 FD %	651	-1.02E-01
EPC4-263(LF)	653	4.91E-08
EPC4-263(HF)	653	5.01E-08
EPC4-263 FD %	653	-2.0887
EPC4-264(LF)	656	6.59E-08
EPC4-264(HF)	656	6.85E-08
EPC4-264 FD %	656	-3.8692
EPC4-265(LF)	659	7.63E-08
EPC4-265(HF)	659	7.74E-08
EPC4-265 FD %	659	-1.4506
EPC4-266(LF)	661	7.81E-08
EPC4-266(HF)	661	7.80E-08
EPC4-266 FD %	661	1.91E-01
EPC4-267(LF)	664	8.19E-08
EPC4-267(HF)	664	8.16E-08
EPC4-267 FD %	664	3.81E-01
EPC4-268(LF)	666	7.76E-08
EPC4-268(HF)	666	7.96E-08
EPC4-268 FD %	666	-2.5571

EPC4-269(LF)	669	7.61E-08
EPC4-269(HF)	669	7.43E-08
EPC4-269 FD %	669	2.327
EPC4-270(LF)	671	6.90E-08
EPC4-270(HF)	671	6.96E-08
EPC4-270 FD %	671	-7.48E-01
EPC4-271(LF)	674	8.57E-08
EPC4-271(HF)	674	8.48E-08
EPC4-271 FD %	674	1.0649
EPC4-272(LF)	676	9.48E-08
EPC4-272(HF)	676	9.50E-08
EPC4-272 FD %	676	-1.74E-01
EPC4-273(LF)	679	9.75E-08
EPC4-273(HF)	679	9.58E-08
EPC4-273 FD %	679	1.6933
EPC4-274(LF)	681	5.96E-08
EPC4-274(HF)	681	6.07E-08
EPC4-274 FD %	681	-1.951
EPC4-275(LF)	684	7.20E-08
EPC4-275(HF)	684	7.31E-08
EPC4-275 FD %	684	-1.529
EPC4-276(LF)	686	7.85E-08
EPC4-276(HF)	686	8.13E-08
EPC4-276 FD %	686	-3.5441
EPC4-277(LF)	689	8.62E-08
EPC4-277(HF)	689	8.65E-08
EPC4-277 FD %	689	-3.06E-01
EPC4-278(LF)	691	9.20E-08
EPC4-278(HF)	691	8.98E-08
EPC4-278 FD %	691	2.3411
EPC4-279(LF)	693	1.02E-07
EPC4-279(HF)	693	1.03E-07
EPC4-279 FD %	693	-3.56E-01
EPC4-280(LF)	696	9.94E-08
EPC4-280(HF)	696	9.88E-08
EPC4-280 FD %	696	6.52E-01
EPC4-281(LF)	698	9.36E-08
EPC4-281(HF)	698	9.29E-08
EPC4-281 FD %	698	7.28E-01
EPC4-282(LF)	701	8.97E-08
EPC4-282(HF)	701	9.03E-08
EPC4-282 FD %	701	-6.09E-01
EPC4-283(LF)	703	1.06E-07

EPC4-283(HF)	703	1.05E-07
EPC4-283 FD %	703	3.76E-01
EPC4-284(LF)	706	9.53E-08
EPC4-284(HF)	706	1.01E-07
EPC4-284 FD %	706	-6.3926
EPC4-285(LF)	708	1.10E-07
EPC4-285(HF)	708	1.10E-07
EPC4-285 FD %	708	6.07E-01
EPC4-286(LF)	711	1.25E-07
EPC4-286(HF)	711	1.27E-07
EPC4-286 FD %	711	-1.7707
EPC4-287(LF)	713	1.23E-07
EPC4-287(HF)	713	1.23E-07
EPC4-287 FD %	713	2.33E-01
EPC4-288(LF)	716	1.42E-07
EPC4-288(HF)	716	1.41E-07
EPC4-288 FD %	716	7.23E-01
EPC4-289(LF)	718	1.37E-07
EPC4-289(HF)	718	1.43E-07
EPC4-289 FD %	718	-3.9424
EPC4-290(LF)	720	1.41E-07
EPC4-290(HF)	720	1.40E-07
EPC4-290 FD %	720	5.41E-01
EPC4-291(LF)	723	1.59E-07
EPC4-291(HF)	723	1.63E-07
EPC4-291 FD %	723	-2.0129
EPC4-292(LF)	725	1.63E-07
EPC4-292(HF)	725	1.68E-07
EPC4-292 FD %	725	-3.4101

* Low frequency (LF) and high frequency (HF) susceptibility are expressed in international standard units. Frequency dependence of susceptibility is expressed in percent (%). Data are formatted differently in this table due to a change in instrument output.

Table 29. EPC5 (playa center) magnetic susceptibility

Sample ID	depth (cm)	LF mag. Sus.	Frequency dep.
EPC 5-1	5	2.46E-07	1.3354
EPC 5-2	45	2.10E-07	1.4032
EPC 5-3	65	1.95E-07	1.30E-01
EPC 5-4	94	2.21E-07	6.80E-01
EPC 5-5	123	1.20E-07	2.8479
EPC 5-6	155	1.55E-07	2.1476
EPC 5-7)	179	1.43E-07	1.3964
EPC 5-8	195	1.23E-07	1.5149
EPC 5-9	227	1.44E-07	1.7244
EPC 5-10	252	1.47E-07	3.013
EPC 5-11	276	1.53E-07	1.9915
EPC 5-12	294	1.30E-07	8.01E-01
EPC 5-13	309	1.65E-07	2.8715
EPC 5-14	345	1.61E-07	1.7753
EPC 5-15	373	1.64E-07	-9.32E-01
EPC 5-16	406	1.08E-07	2.2145
EPC 5-17	428	1.48E-07	1.2028
EPC 5-18	454	1.33E-07	3.91E-01
EPC 5-19	473	7.13E-08	4.099
EPC 5-20	500	5.63E-08	2.7753
EPC 5-21	616	8.84E-08	2.1942
EPC 5-22	630	8.17E-08	2.6416
EPC 5-23	665	1.34E-07	5.30E-01
EPC 5-24	684	4.71E-08	9.85E-01
EPC 5-25	696	2.06E-07	1.6554
EPC 5-26	725	8.81E-08	9.96E-01
EPC 5-27	738	6.41E-08	5.85E-01
EPC 5-28	755	1.99E-07	2.0773
EPC 5-29	775	4.50E-07	1.8747
EPC 5-30	791	3.60E-07	1.5613
EPC 5-31	804	3.27E-07	1.4216
EPC 5-32	818	2.29E-07	7.72E-01
EPC 5-33	856	3.01E-07	1.9518
EPC 5-34	880	5.33E-08	5.4817
EPC 5-35	906	1.11E-07	2.6587
EPC 5-36	921	9.57E-08	3.6119
EPC 5-37	972	1.11E-07	3.2859
EPC 5-38	1028	2.32E-07	2.14E-01
EPC 5-39	1062	2.07E-07	2.0944

EPC 5-40	1073	2.52E-07	2.7114
EPC 5-41	1084	2.78E-07	8.88E-01
EPC 5-42	1137	2.20E-07	1.9587
EPC 5-43	1157	3.72E-07	1.5874
EPC 5-44	1207	3.07E-07	9.67E-01

* Low frequency (LF) and high frequency (HF) susceptibility are expressed in international standard units. Frequency dependence of susceptibility is expressed in percent (%).

Table 30. EPC 7 (interplaya north) magnetic susceptibility*.

Sample	depth (cm)	LF mag. Sus.	Frequency dep.
EPC 7-1	9	7.95E-07	2.7223
EPC 7-2	49	6.96E-07	2.1832
EPC 7-3	73	5.79E-07	1.3235
EPC 7-4	105	6.72E-07	1.274
EPC 7-5	119	5.83E-07	1.4036
EPC 7-6	134	6.62E-07	1.2201
EPC 7-7	177	6.86E-07	9.07E-01
EPC 7-8	192	6.71E-07	1.1351
EPC 7-9	232	7.29E-07	1.927
EPC 7-10	247	7.43E-07	1.2364
EPC 7-11	256	7.52E-07	1.4926
EPC 7-12	297	7.57E-07	1.4903
EPC 7-13	314	5.57E-07	1.3427
EPC 7-14	352	3.66E-07	2.5388
EPC 7-15	365	4.96E-07	1.6564
EPC 7-16	378	5.34E-07	9.93E-01
EPC 7-17	423	5.80E-07	1.4113
EPC 7-18	438	5.73E-07	1.3254
EPC 7-19	475	5.89E-07	1.5242
EPC 7-20	496	4.56E-07	1.3186
EPC 7-21	534	3.88E-07	1.5089
EPC 7-22	547	3.92E-07	2.3008
EPC 7-23	561	3.68E-07	1.5431
EPC 7-24	594	4.35E-07	1.0148
EPC 7-25	608	3.95E-07	2.5026
EPC 7-26	619	4.97E-07	2.138

EPC 7-27	647	5.35E-07	9.63E-01
EPC 7-28	659	5.51E-07	1.9069
EPC 7-29	675	5.65E-07	1.3566
EPC 7-30	710	4.96E-07	1.3507
EPC 7-31	724	6.14E-07	2.1416
EPC 7-32	742	6.42E-07	1.6644
EPC 7-33	789	5.06E-07	1.7702
EPC 7-34	800	3.90E-07	1.947
EPC 7-35	844	4.70E-08	-1.721
EPC 7-36	862	2.40E-08	2.6856
EPC 7-37	892	1.33E-07	1.4747
EPC 7-38	907	5.37E-08	-1.1889
EPC 7-39	924	1.15E-07	1.1241
EPC 7-40	1039	8.64E-08	2.7815
EPC 7-41	1076	1.87E-07	8.93E-01
EPC 7-42	1091	1.89E-07	2.14E-01
EPC 7-43	1106	2.60E-07	2.7996
EPC 7-44	1155	2.71E-07	3.174
EPC 7-45	1167	1.12E-07	1.66E-01
EPC 7-46	1199	3.46E-08	1.1277
EPC 7-47	1210	1.06E-07	2.60E-01
EPC 7-48	1226	1.69E-07	1.6975
EPC 7-49	1266	2.04E-07	7.01E-01
EPC 7-50	1285	2.65E-07	1.0016
EPC 7-51	1303	3.24E-07	3.4756
EPC 7-52	1316	3.68E-07	1.296
EPC 7-53	1330	3.16E-07	2.1567
EPC 7-54	1343	2.82E-07	3.0168

* Low frequency (LF) and high frequency (HF) susceptibility are expressed in international standard units. Frequency dependence of susceptibility is expressed in percent (%).

Table 31. EPC3 (playa center) stable C isotope ($\delta^{13}\text{C}$), stable N isotope ($\delta^{15}\text{N}$), organic C content (OC), N content, and C:N ratio.

sample	depth (cm)	$\delta^{13}\text{C}$ (‰)	N (%)	OC (%)	C:N
EPC 3-1	1	-21.44	0.2	1.5	9.8
EPC 3-3	5	-21.78	0.1	1.2	10.0
EPC 3-5	10	-21.65	0.1	1.0	9.9
EPC 3-7	14	-22.49	0.1	0.9	10.2
EPC 3-9	20	-22.00	0.1	0.9	10.1
EPC 3-11	25	-22.24	0.1	0.9	10.2
EPC 3-13	29	-21.89	0.1	0.8	11.1
EPC 3-15	35	-22.03	0.1	0.6	10.9
EPC 3-17	40	-21.82	0.1	0.7	10.8
EPC 3-19	45	-21.91	0.1	0.6	10.7
EPC 3-21	50	-21.84	0.1	0.6	10.6
EPC 3-23	55	-22.03	0.1	0.6	11.0
EPC 3-25	60	-21.80	0.1	0.6	10.5
EPC 3-27	65	-21.74	0.1	0.7	10.7
EPC 3-29	71	-21.90	0.1	0.6	10.9
EPC 3-31	76	-21.92	0.1	0.6	10.7
EPC 3-33	81	-21.13	0.0	0.5	10.1
EPC 3-35	86	-21.32	0.1	0.6	10.3
EPC 3-37	91	-21.12	0.1	0.5	9.9
EPC 3-39	96	-21.43	0.0	0.5	10.1
EPC 3-41	101	-21.17	0.0	0.3	8.7
EPC 3-43	107	-20.36	0.0	0.3	7.5
EPC 3-45	112	-21.33	0.0	0.2	7.3
EPC 3-47	116	-20.60	0.0	0.2	6.4
EPC 3-50	122	-23.03	0.0	0.2	7.2
EPC 3-55	135	-24.35	0.0	0.2	5.9
EPC 3-60	147	-24.53	0.0	0.1	4.9
EPC 3-65	160	-26.37	0.0	0.1	5.2
EPC 3-70	172	-26.22	0.0	0.1	5.1
EPC 3-75	185	-26.88	0.0	0.1	5.4
EPC 3-80	198	-26.57	0.0	0.1	5.1
EPC 3-85	211	-27.24	0.0	0.1	4.5
EPC 3-90	223	-27.05	0.0	0.1	3.9
EPC 3-95	235	-27.75	0.0	0.1	4.4
EPC 3-100	247	-27.41	0.0	0.1	3.9
EPC 3-105	259	-27.42	0.0	0.1	4.2
EPC 3-110	272	-27.55	0.0	0.1	4.0
EPC 3-115	285	-26.67	0.0	0.1	3.4

EPC 3-120	298	-25.97	0.0	0.1	4.4
EPC 3-125	310	-24.95	0.0	0.1	3.5
EPC 3-130	323	-25.34	0.0	0.1	4.3
EPC 3-135	335	-25.95	0.0	0.1	4.7
EPC 3-140	348	-24.55	0.0	0.1	4.8
EPC 3-145	360	-25.00	0.0	0.2	4.9
EPC 3-150	373	-23.81	0.0	0.1	4.0
EPC 3-155	385	-23.68	0.0	0.1	4.2
EPC 3-160	398	-23.95	0.0	0.2	5.7
EPC 3-165	410	-22.52	0.0	0.1	4.3
EPC 3-170	423	-23.47	0.0	0.2	5.3
EPC 3-175	436	-23.33	0.0	0.2	4.7
EPC 3-180	448	-24.52	0.0	0.2	5.3
EPC 3-185	461	-22.04	0.0	0.1	4.5
EPC 3-190	474	-21.95	0.0	0.3	6.7
EPC 3-195	486	-23.29	0.0	0.3	6.7
EPC 3-200	499	-23.52	0.04	0.3	6.5
EPC 3-205	511	-23.95	0.05	0.4	7.8
EPC 3-210	523	-23.71	0.05	0.3	7.2

Table 32. EPC5 (playa center) stable C isotope ($\delta^{13}\text{C}$), stable N isotope ($\delta^{15}\text{N}$), organic C content (OC), N content, and C:N ratio.

sample	depth (cm)	$\delta^{13}\text{C}$ (‰)	N (%)	OC (%)	C:N
EPC5-1	5	-23.84	0.10	1.00	10.3
EPC5-2	45	-22.52	0.06	0.57	10.3
EPC5-3	65	-21.21	0.07	0.70	9.5
EPC5-4	94	-20.77	0.05	0.46	9.3
EPC5-5	123	-20.91	0.04	0.23	5.9
EPC5-6	155	-20.61	0.03	0.18	5.5
EPC5-7	179	-23.17	0.03	0.14	4.9
EPC5-8	195	-24.70	0.04	0.22	6.4
EPC5-9	227	-25.84	0.02	0.07	3.4
EPC5-10	252	-25.07	0.02	0.08	3.8
EPC5-11	276	-26.09	0.02	0.06	3.2
EPC5-12	294	-24.53	0.03	0.10	3.6
EPC5-13	309	-23.41	0.02	0.07	3.0
EPC5-14	345	-23.66	0.02	0.06	2.8
EPC5-15	373	-22.60	0.03	0.12	3.7

EPC5-16	406	-22.42	0.03	0.11	3.7
EPC5-17	428	-21.75	0.03	0.09	3.5
EPC5-18	454	-21.21	0.04	0.15	4.3
EPC5-19	473	-22.91	0.03	0.19	5.7
EPC5-20	500	-23.46	0.04	0.29	6.6
EPC5-21	616	-23.04	0.04	0.26	6.7
EPC5-22	630	-22.97	0.04	0.23	6.3
EPC5-23	665	-24.67	0.01	0.03	4.7
EPC5-24	684	-25.30	0.01	0.03	5.9
EPC5-25	696	-25.19	0.01	0.03	5.1
EPC5-26	725	-25.66	0.01	0.04	6.3
EPC5-27	738	-18.01	0.01	0.05	8.3
EPC5-28	755	-27.27	0.01	0.03	4.3
EPC5-29	775	-26.43	0.01	0.02	3.1
EPC5-30	791	-28.12	0.01	0.03	4.8
EPC5-31	804	-30.57	0.00	0.02	4.1
EPC5-32	818	-27.39	0.01	0.02	3.7
EPC5-33	856	-26.55	0.01	0.03	6.5
EPC5-34	880	-23.34	0.01	0.07	5.1
EPC5-35	906	-27.16	0.01	0.03	4.1
EPC5-36	921	-23.88	0.01	0.04	4.8
EPC5-37	972	-23.78	0.01	0.05	6.7
EPC5-38	1028	-28.52	0.01	0.02	4.1
EPC5-39	1062	-26.61	0.00	0.03	5.4
EPC5-40	1073	-30.47	0.00	0.01	3.6
EPC5-41	1084	-25.40	0.00	0.02	5.1
EPC5-42	1137	-23.31	0.01	0.05	7.3
EPC5-43	1157	-24.11	0.01	0.03	3.9
EPC5-44	1207	-25.86	0.01	0.06	7.4

Table 33. EPC7 (interplaya north) stable C isotope ($\delta^{13}\text{C}$), stable N isotope ($\delta^{15}\text{N}$), organic C content (OC), N content, and C:N ratio.

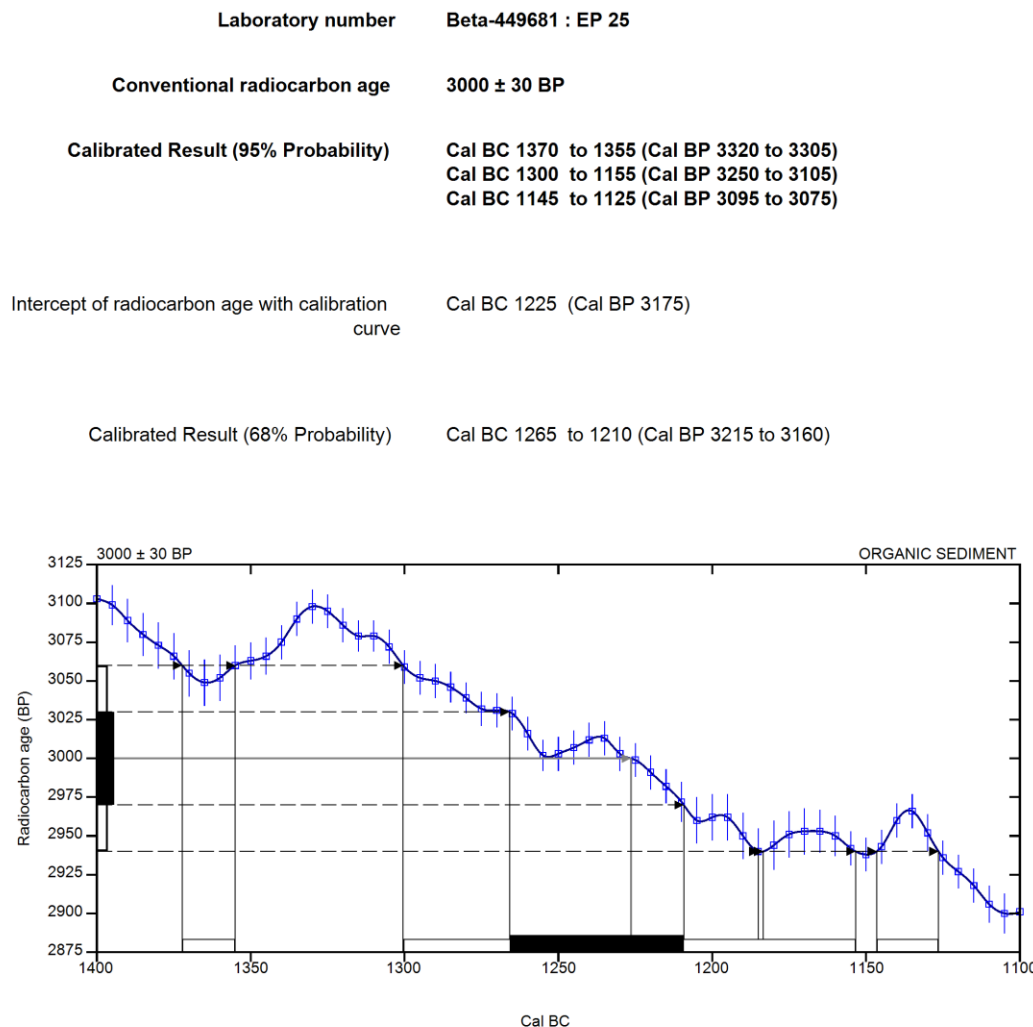
Sample	Depth (cm)	$\delta^{13}\text{C}$ (‰)	N (%)	OC (%)	C:N
1	9	-14.82	0.14	1.21	8.7
2	49	-15.51	0.10	0.81	8.5
3	73	-19.48	0.04	0.22	5.9
4	105	-21.13	0.04	0.28	7.0
5	119	-21.23	0.03	0.16	5.2
6	134	-22.60	0.04	0.22	6.2
7	177	-22.55	0.04	0.27	6.9
8	192	-22.61	0.04	0.23	6.5
9	232	-23.16	0.04	0.24	6.8
10	247	-22.44	0.04	0.27	7.0
11	256	-21.64	0.04	0.24	6.9
12	297	-21.38	0.03	0.23	6.8
13	314	-21.57	0.03	0.19	6.7
14	352	-23.19	0.03	0.20	7.2
15	365	-22.34	0.03	0.24	7.0
16	378	-19.75	0.04	0.24	6.5
17	423	-19.57	0.03	0.19	6.2
18	438	-19.59	0.03	0.19	5.9
19	475	-17.60	0.03	0.15	5.2
20	496	-18.26	0.04	0.25	6.3
21	534	-16.97	0.04	0.24	6.4
22	547	-17.02	0.04	0.28	7.6
23	561	-15.16	0.04	0.33	4.8
24	594	-16.71	0.03	0.16	5.8
25	608	-17.70	0.02	0.10	4.5
26	619	-18.02	0.03	0.12	4.3
27	647	-18.57	0.02	0.08	4.2
28	659	-20.74	0.02	0.07	3.6
29	675	-20.58	0.01	0.04	3.3
30	710	-21.09	0.02	0.06	3.3
31	724	-23.84	0.01	0.05	4.1
32	742	-22.77	0.01	0.04	2.9
33	789	-23.92	0.01	0.03	3.0
34	800	-24.32	0.01	0.03	4.0
35	844	-25.00	0.01	0.04	4.1
37	892	-26.12	0.01	0.04	3.8
38	907	-26.00	0.01	0.04	4.7
39	924	-26.21	0.01	0.04	4.8

40	1039	-24.50	0.01	0.04	5.9
41	1076	-23.31	0.00	0.02	6.1
42	1091	-26.96	0.00	0.02	4.0
43	1106	-25.01	0.01	0.03	5.3
44	1155	-25.88	0.01	0.03	4.9
45	1167	-23.49	0.01	0.07	6.0
46	1199	-24.60	0.01	0.07	7.1
47	1210	-23.91	0.01	0.05	6.3
48	1226	-25.17	0.01	0.05	6.0
49	1266	-25.56	0.01	0.03	4.3
50	1285	-18.41	0.01	0.05	9.5
51	1303	-27.89	0.01	0.03	2.9
52	1316	-27.65	0.01	0.02	2.5
53	1330	-27.71	0.01	0.03	4.1
54	1343	-26.56	0.01	0.03	4.4

B2. Accelerator mass spectrometry ^{14}C age data

CALIBRATION OF RADIOCARBON AGE TO CALENDAR YEARS

(Variables: C13/C12 = -20.4 o/oo : lab. mult = 1)



Database used
INTCAL13

References

Mathematics used for calibration scenario

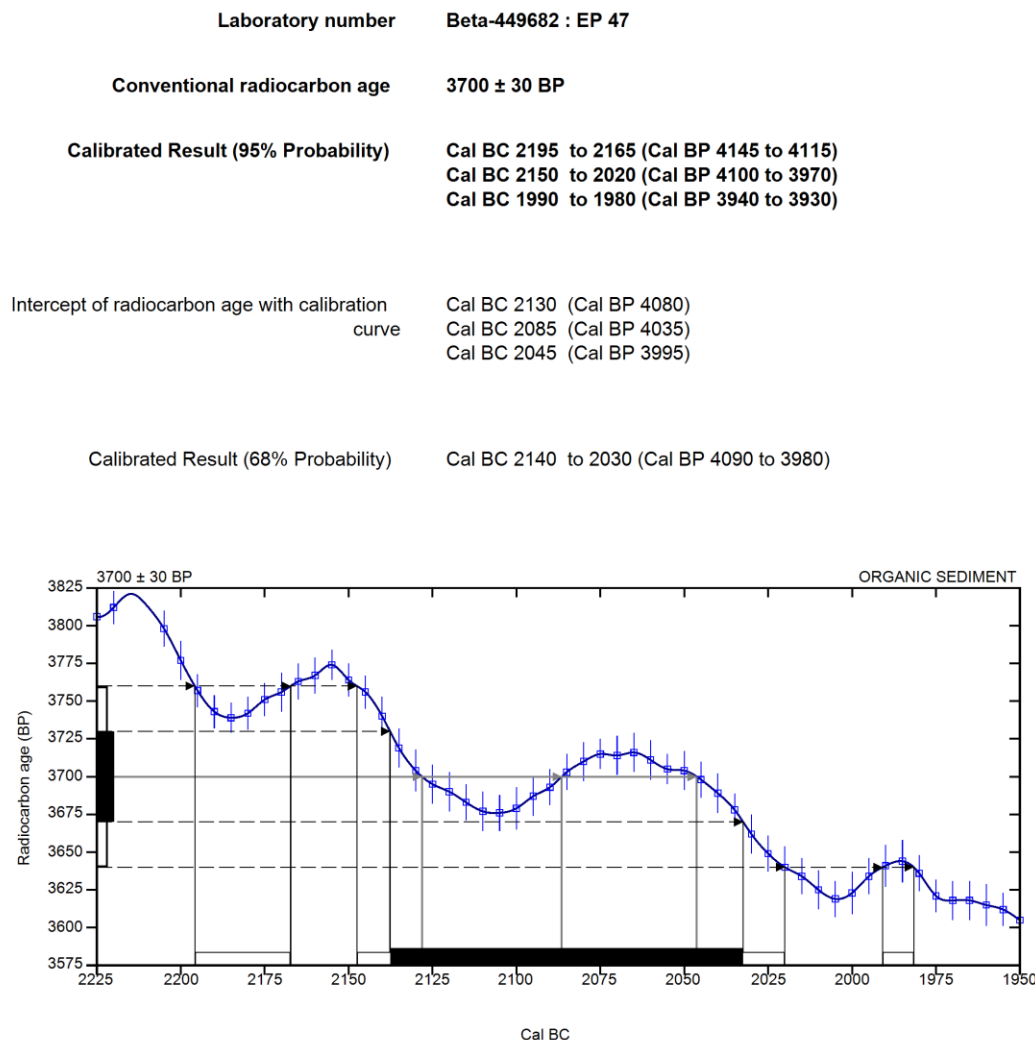
A Simplified Approach to Calibrating C14 Dates, Talma, A. S., Vogel, J. C., 1993, Radiocarbon 35(2):317-322

References to INTCAL13 database

Reimer PJ et al. IntCal13 and Marine13 radiocarbon age calibration curves 0–50,000 years cal BP. Radiocarbon 55(4):1869–1887., 2013.

CALIBRATION OF RADIOCARBON AGE TO CALENDAR YEARS

(Variables: C13/C12 = -20.4 ‰ : lab. mult = 1)



Database used
INTCAL13

References

Mathematics used for calibration scenario

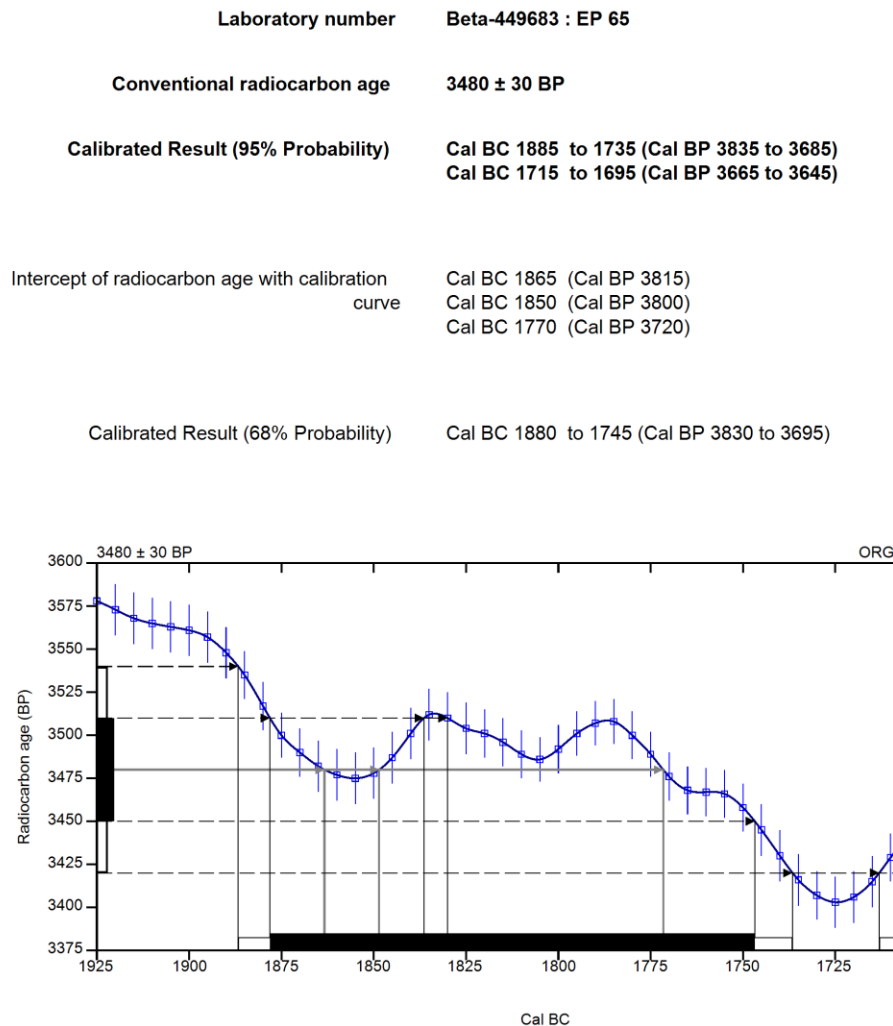
A Simplified Approach to Calibrating C14 Dates, Talma, A. S., Vogel, J. C., 1993, Radiocarbon 35(2):317-322

References to INTCAL13 database

Reimer PJ et al. IntCal13 and Marine13 radiocarbon age calibration curves 0–50,000 years cal BP. Radiocarbon 55(4):1869–1887., 2013.

CALIBRATION OF RADIOCARBON AGE TO CALENDAR YEARS

(Variables: C13/C12 = -20.4 ‰ : lab. mult = 1)



Database used
INTCAL13

References

Mathematics used for calibration scenario

A Simplified Approach to Calibrating C14 Dates, Talma, A. S., Vogel, J. C., 1993, Radiocarbon 35(2):317-322

References to INTCAL13 database

Reimer PJ et al. IntCal13 and Marine13 radiocarbon age calibration curves 0–50,000 years cal BP. Radiocarbon 55(4):1869–1887., 2013.

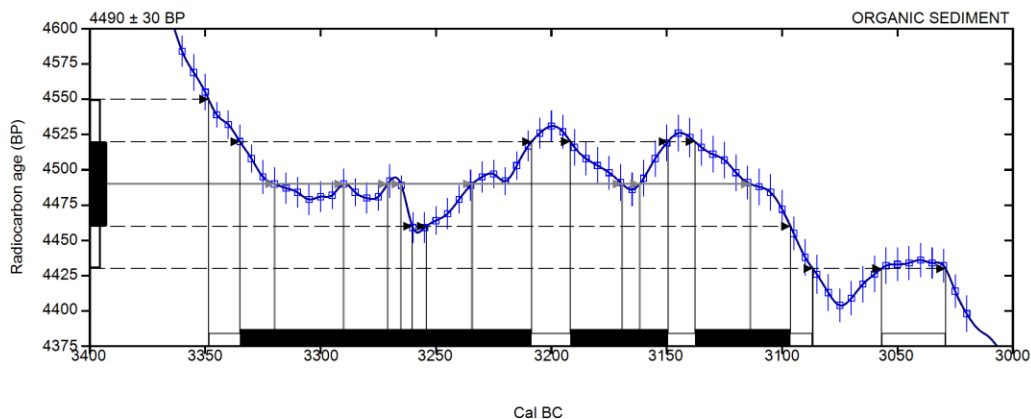
Beta Analytic Radiocarbon Dating Laboratory

4985 S.W. 74th Court, Miami, Florida 33155 • Tel: (305)667-5167 • Fax: (305)663-0964 • Email: beta@radiocarbon.com

CALIBRATION OF RADIOCARBON AGE TO CALENDAR YEARS

(Variables: C13/C12 = -19.9 ‰ : lab. mult = 1)

Laboratory number	Beta-449684 : EP 85
Conventional radiocarbon age	4490 ± 30 BP
Calibrated Result (95% Probability)	Cal BC 3350 to 3085 (Cal BP 5300 to 5035) Cal BC 3055 to 3030 (Cal BP 5005 to 4980)
Intercept of radiocarbon age with calibration curve	Cal BC 3320 (Cal BP 5270) Cal BC 3290 (Cal BP 5240) Cal BC 3270 (Cal BP 5220) Cal BC 3265 (Cal BP 5215) Cal BC 3235 (Cal BP 5185) Cal BC 3170 (Cal BP 5120) Cal BC 3160 (Cal BP 5110) Cal BC 3115 (Cal BP 5065)
Calibrated Result (68% Probability)	Cal BC 3335 to 3210 (Cal BP 5285 to 5160) Cal BC 3190 to 3150 (Cal BP 5140 to 5100) Cal BC 3140 to 3095 (Cal BP 5090 to 5045)



Database used
INTCAL13

References

Mathematics used for calibration scenario

A Simplified Approach to Calibrating C14 Dates, Talma, A. S., Vogel, J. C., 1993, Radiocarbon 35(2):317-322

References to INTCAL13 database

Reimer PJ et al. IntCal13 and Marine13 radiocarbon age calibration curves 0–50,000 years cal BP. Radiocarbon 55(4):1869–1887., 2013.

Beta Analytic Radiocarbon Dating Laboratory

4985 S.W. 74th Court, Miami, Florida 33155 • Tel: (305)667-5167 • Fax: (305)663-0964 • Email: beta@radiocarbon.com

B3. Hydrology, fluid-flux, and geochemical data from the vadose zone

Table 2. Playa anion concentrations in pore water (mg L^{-1}) and field water contents for EPC 1, 2, and 5.

Core Sample	Average Depth (m)	Chloride (mg L^{-1})	Bromide (mg L^{-1})	Nitrate-N (mg L^{-1})	Sulfate (mg L^{-1})	Fluoride (mg L^{-1})	θ_G	θ_V
EPC 1-1	0.025	81	5.4	<0.2	450	6.9	0.13	0.14
EPC 1-1	0.775	22	4.5	<0.2	170	14	0.14	0.17
EPC 1-2	1.695	42	4.2	<0.2	220	5.3	0.08	0.09
EPC 1-2	1.995	140	<0.1	<0.2	360	14	0.05	0.06
EPC 1-3	2.575	25	3.2	<0.2	170	4.2	0.10	0.16
EPC 1-3	3.025	16	<0.1	<0.2	130	<0.2	0.15	0.17
EPC 1-3	3.325	14	1.9	<0.2	110	2.7	0.18	0.21
EPC 1-4	4.085	16	1.7	<0.2	200	10	0.19	0.19
EPC 1-4	4.685	31	1.7	<0.2	190	14	0.19	0.20
EPC 1-5	5.125	60	1.7	0.83	270	8.0	0.24	0.30
EPC 2-1	0.025	96	6.5	<0.2	370	8.8	0.12	0.14
EPC 2-1	0.765	16	3.2	<0.2	120	1.3	0.15	0.15
EPC 2-2	1.715	21	3.0	<0.2	150	16	0.12	0.16
EPC 2-2	2.015	25	<0.1	<0.2	130	12	0.12	0.18
EPC 2-3	2.615	19	2.7	<0.2	170	8.2	0.12	0.14
EPC 2-3	3.075	14	<0.1	<0.2	150	9.7	0.16	0.16
EPC 2-3	3.365	12	2.0	<0.2	190	10	0.18	0.19
EPC 2-4	4.115	15	2.0	<0.2	220	16	0.18	0.22
EPC 2-4	4.725	37	2.0	<0.2	210	11	0.18	0.18
EPC 2-5	5.185	78	1.8	<0.2	310	9.5	0.22	0.25
EPC 5-2	0.515	51	<0.1	<0.2	110	2.8	0.18	0.31
EPC 5-3	1.015	35	<0.1	<0.2	83	3.4	0.21	0.29
EPC 5-4	2.015	37	<0.1	<0.2	110	5.3	0.16	0.26
EPC 5-6	3.015	27	<0.1	<0.2	180	7.0	0.19	0.29
EPC 5-8	4.015	29	<0.1	<0.2	190	13	0.21	0.25
EPC 5-9	5.015	46	<0.1	<0.2	330	18	0.24	0.31
EPC 5-11	6.015	19	<0.1	<0.2	82	17	0.16	0.26
EPC 5-12	7.015	34	<0.1	1.5	120	29	0.23	0.34
EPC 5-14	8.015	37	<0.1	2.4	78	40	0.11	0.18
EPC 5-15	9.015	72	<0.1	3.4	120	60	0.06	0.10
EPC 5-16	10.015	63	<0.1	2.4	58	47	0.10	0.16
EPC 5-18	11.015	55	<0.1	2.1	63	27	0.19	0.33
EPC 5-19	11.685	34	<0.1	<0.2	82	17	0.21	0.28

Table 3. Interplaya anion concentrations in pore water (mg L^{-1}) and field water contents for EPC 7.

Core Sample	Average Depth (m)	Chloride (mg L^{-1})	Bromide (mg L^{-1})	Nitrate-N (mg L^{-1})	Sulfate (mg L^{-1})	Fluoride (mg L^{-1})	θG	θV
EPC 7-2	0.515	59	<0.1	<0.2	59	11	0.13	0.22
EPC 7-3	1.015	220	0.91	<0.2	1100	44	0.15	0.18
EPC 7-4	2.015	3900	18	<0.2	2600	4.0	0.13	0.17
EPC 7-6	3.015	1400	6.5	3.5	1200	15	0.13	0.17
EPC 7-8	4.015	860	5.0	4.7	850	30	0.13	0.20
EPC 7-9	5.015	640	3.0	7.6	500	48	0.16	0.20
EPC 7-11	6.015	450	2.6	7.1	380	63	0.16	0.25
EPC 7-12	7.015	340	1.5	<0.2	360	66	0.12	0.23
EPC 7-14	7.905	260	1.0	<0.2	270	43	0.11	0.21
EPC 7-15	9.015	270	1.1	<0.2	230	35	0.12	0.21
EPC 7-16	10.675	85	<0.1	<0.2	130	21	0.22	0.30
EPC 7-17	11.415	58	<0.1	<0.2	140	29	0.09	0.18
EPC 7-18	12.655	31	<0.1	<0.2	94	22	0.13	0.20
EPC 7-19	14.065	41	<0.1	<0.2	140	38	0.11	0.15
EPC 7-21	15.515	46	<0.1	<0.2	220	56	0.11	0.22
EPC 7-22	16.015	45	<0.1	<0.2	83	32	0.12	0.20
EPC 7-23	16.745	42	<0.1	<0.2	69	25	0.28	0.34

Table 4. Playa anion vadose zone ratios from pore water (mass ratio, mg L⁻¹) for EPC 1, 2, and 5. Some ratios are reported as not-applicable (NA) due to certain measurements of bromide and nitrate that are below the instrument quantification limit.

Core Sample	Average Depth (m)	Bromide/ Chloride	Nitrate/ Chloride	Sulfate/ Chloride	Fluoride/ Chloride
EPC 1-1	0.025	0.068	NA	5.6	0.085
EPC 1-1	0.775	0.20	NA	7.6	0.64
EPC 1-2	1.695	0.099	NA	5.2	0.13
EPC 1-2	1.995	NA	NA	2.7	0.10
EPC 1-3	2.575	0.13	NA	6.9	0.17
EPC 1-3	3.025	NA	NA	8.3	0
EPC 1-3	3.325	0.14	NA	8.0	0.20
EPC 1-4	4.085	0.11	NA	12	0.62
EPC 1-4	4.685	0.056	NA	6.2	0.44
EPC 1-5	5.125	0.029	0.014	4.4	0.13
EPC 2-1	0.025	0.068	NA	3.8	0.091
EPC 2-1	0.765	0.20	NA	7.8	0.084
EPC 2-2	1.715	0.14	NA	7.1	0.74
EPC 2-2	2.015	NA	NA	5.2	0.48
EPC 2-3	2.615	0.14	NA	9.3	0.44
EPC 2-3	3.075	NA	NA	10	0.67
EPC 2-3	3.365	0.16	NA	16	0.84
EPC 2-4	4.115	0.13	NA	15	1.1
EPC 2-4	4.725	0.055	NA	5.7	0.30
EPC 2-5	5.185	0.023	NA	4.0	0.12
EPC 5-2	0.515	NA	NA	2.2	0.054
EPC 5-3	1.015	NA	NA	2.4	0.099
EPC 5-4	2.015	NA	NA	2.9	0.15
EPC 5-6	3.015	NA	NA	6.8	0.26
EPC 5-8	4.015	NA	NA	6.6	0.46
EPC 5-9	5.015	NA	NA	7.1	0.38
EPC 5-11	6.015	NA	NA	4.4	0.91
EPC 5-12	7.015	NA	0.046	3.7	0.85
EPC 5-14	8.015	NA	0.064	2.1	1.1
EPC 5-15	9.015	NA	0.047	1.6	0.82
EPC 5-16	10.015	NA	0.039	0.92	0.74
EPC 5-18	11.015	NA	0.038	1.1	0.50
EPC 5-19	11.685	NA	NA	2.4	0.51

Table 5. Interplaya anion vadose zone ratios from pore water (mass ratio, mg L⁻¹) for EPC 7. Some ratios are reported as not-applicable (NA) due to certain measurements of bromide and nitrate that are below the instrument quantification limit.

Core Sample	Average Depth (m)	Bromide/ Chloride	Nitrate/ Chloride	Sulfate/ Chloride	Fluoride/ Chloride
EPC 7-2	0.515	NA	NA	0.99	0.18
EPC 7-3	1.015	0.0041	NA	4.7	0.20
EPC 7-4	2.015	0.0046	NA	0.67	0.0010
EPC 7-6	3.015	0.0046	0.0024	0.83	0.01
EPC 7-8	4.015	0.0059	0.0055	1.00	0.04
EPC 7-9	5.015	0.0047	0.012	0.78	0.07
EPC 7-11	6.015	0.0059	0.016	0.85	0.14
EPC 7-12	7.015	0.0045	NA	1.1	0.19
EPC 7-14	7.905	0.0040	NA	1.0	0.17
EPC 7-15	9.015	0.0040	NA	0.86	0.13
EPC 7-16	10.675	NA	NA	1.6	0.25
EPC 7-17	11.415	NA	NA	2.5	0.49
EPC 7-18	12.655	NA	NA	3.1	0.72
EPC 7-19	14.065	NA	NA	3.6	0.93
EPC 7-21	15.515	NA	NA	4.9	1.2
EPC 7-22	16.015	NA	NA	1.8	0.71
EPC 7-23	16.745	NA	NA	1.6	0.60

Table 6. Depth-weighted mass averages (mg L⁻¹) for vadose zone anion concentrations and water contents.

Core	Total Depth (m)	Chloride (mg L ⁻¹)	Bromide (mg L ⁻¹)	Nitrate-N (mg L ⁻¹)	Sulfate (mg L ⁻¹)	Fluoride (mg L ⁻¹)	θG	θV
EPC 1	5.1	35	2.5	0.33	200	8.3	0.14	0.17
EPC 2	5.2	26	2.2	0.28	180	11	0.16	0.18
EPC 5	11.7	42	<0.1	1.2	130	24	0.17	0.25
EPC 7	16.7	520	2.4	1.5	480	35	0.14	0.22

Table 7. Groundwater well surface elevations, total depths below ground surface (bgs), and measured water levels bgs.

Well Name	Land Surface Elevation (m)	Total Well Depth (m bgs)	Measured Water Levels (m bgs)			
			6/25/2016	7/28/2016	6/12/2017	8/21/2017
Well 1	867.84	31.53	11.56	11.55	11.49	11.48
Well 2	871.60	30.13	16.08	16.09	15.97	16.03
Well 3	874.16	29.98	16.45	16.50	16.43	16.44

Table 8. Groundwater anion concentrations (mg L^{-1}) collected in August, 2017.

Well Name	Chloride	Bromide	Nitrate-N	Sulfate	Fluoride
Well 1	21	<0.1	1.1	71	2.7
Well 2	24	0.14	1.5	65	2.4
Well 3	26	0.11	1.5	82	2.9
East Windmill Well	20	0.20	1.0	48	1.8

Table 9. Groundwater well anion concentration ratios (mass ratio, mg L^{-1}) collected in August, 2017. The bromide/chloride ratio in Well 1 is not-applicable (NA) due to bromide concentrations below the instrument quantification limit.

Well Name	Bromide/ Chloride	Nitrate/ Chloride	Sulfate/ Chloride	Fluoride/ Chloride
Well 1	NA	0.054	3.4	0.13
Well 2	0.0058	0.060	2.7	0.10
Well 3	0.0040	0.056	3.1	0.11
East Windmill Well	0.010	0.051	2.5	0.09

Table 9. GPS locations of monitoring wells, soil borings, and infiltrometer measurements.

Name	Type	Latitude	Longitude
Well 1	Groundwater Monitoring Well	38.44240	-100.60301
Well 2	Groundwater Monitoring Well	38.43879	-100.59441
Well 3	Groundwater Monitoring Well	38.43908	-100.61197
EPC 1	2016 Soil Core	38.44236	-100.60289
EPC 2	2016 Soil Core	38.44236	-100.60289
EPC 3	2016 Soil Core	38.44232	-100.60303
EPC 4	2016 Soil Core	38.43947	-100.60292
EPC 5	2017 Soil Core	38.44238	-100.60295
EPC 6	2017 Soil Core	38.44238	-100.60297
EPC 7	2017 Soil Core	38.44693	-100.60084
Inf 1	Infiltrometer Measurement	38.44256	-100.60284
Inf 2	Infiltrometer Measurement	38.44204	-100.60268
Inf 3	Infiltrometer Measurement	38.44693	-100.60104
Inf 4	Infiltrometer Measurement	38.44695	-100.60055

Table 10. Playa anion concentrations in bulk soil (mg kg^{-1}) for EPC 1, 2, and 5. Instrument quantification limits (IQLs) are displayed in Table 14.

Core Sample	Average Depth (m)	Chloride (mg kg^{-1})	Bromide (mg kg^{-1})	Nitrate-N (mg kg^{-1})	Sulfate (mg kg^{-1})	Fluoride (mg kg^{-1})
EPC 1-1	0.025	10	0.70	<IQL	58	0.88
EPC 1-1	0.775	3.0	0.61	<IQL	23	1.9
EPC 1-2	1.695	3.4	0.34	<IQL	18	0.43
EPC 1-2	1.995	6.9	<IQL	<IQL	18	0.71
EPC 1-3	2.575	2.6	0.33	<IQL	18	0.43
EPC 1-3	3.025	2.4	<IQL	<IQL	20	<IQL
EPC 1-3	3.325	2.5	0.34	<IQL	20	0.49
EPC 1-4	4.085	3.0	0.32	<IQL	37	1.9
EPC 1-4	4.685	6.0	0.33	<IQL	37	2.6
EPC 1-5	5.125	14	0.41	0.20	63	1.9
EPC 2-1	0.025	12	0.78	<IQL	44	1.1
EPC 2-1	0.765	2.4	0.48	<IQL	18	0.20
EPC 2-2	1.715	2.6	0.36	<IQL	18	1.9
EPC 2-2	2.015	3.1	<IQL	<IQL	16	1.5
EPC 2-3	2.615	2.3	0.33	<IQL	22	1.0
EPC 2-3	3.075	2.4	<IQL	<IQL	24	1.6
EPC 2-3	3.365	2.2	0.35	<IQL	34	1.8
EPC 2-4	4.115	2.6	0.35	<IQL	39	2.8

EPC 2-4	4.725	6.7	0.37	<IQL	38	2.0
EPC 2-5	5.185	18	0.40	<IQL	70	2.1
EPC 5-2	0.515	9.5	<IQL	<IQL	21	0.51
EPC 5-3	1.015	7.2	<IQL	<IQL	17	0.71
EPC 5-4	2.015	6.0	<IQL	<IQL	17	0.87
EPC 5-6	3.015	5.2	<IQL	<IQL	35	1.3
EPC 5-8	4.015	6.1	<IQL	<IQL	40	2.8
EPC 5-9	5.015	11	<IQL	<IQL	79	4.2
EPC 5-11	6.015	2.9	<IQL	<IQL	13	2.7
EPC 5-12	7.015	7.6	<IQL	0.35	28	6.5
EPC 5-14	8.015	4.0	<IQL	0.26	8.4	4.4
EPC 5-15	9.015	4.1	<IQL	0.19	6.6	3.3
EPC 5-16	10.015	6.1	<IQL	0.24	5.6	4.5
EPC 5-18	11.015	10	<IQL	0.39	12	5.1
EPC 5-19	11.685	7.0	<IQL	<IQL	17	3.5

Table 11. Interplaya anion concentrations in bulk soil (mg kg^{-1}) for EPC 7. Instrument quantification limits (IQLs) are displayed in Table 14.

Core Sample	Average Depth (m)	Chloride (mg kg^{-1})	Bromide (mg kg^{-1})	Nitrate-N (mg kg^{-1})	Sulfate (mg kg^{-1})	Fluoride (mg kg^{-1})
EPC 7-2	0.515	8.0	<IQL	<IQL	7.9	1.4
EPC 7-3	1.015	34	0.14	<IQL	160	6.6
EPC 7-4	2.015	490	2.2	<IQL	330	0.50
EPC 7-6	3.015	190	0.86	0.46	160	2.1
EPC 7-8	4.015	110	0.67	0.63	110	4.0
EPC 7-9	5.015	100	0.47	1.2	78	7.4
EPC 7-11	6.015	70	0.41	1.1	59	10
EPC 7-12	7.015	43	0.19	<IQL	45	8.3
EPC 7-14	7.905	29	0.12	<IQL	30	4.9
EPC 7-15	9.015	33	0.13	<IQL	28	4.4
EPC 7-16	10.675	18	<IQL	<IQL	28	4.6
EPC 7-17	11.415	5.4	<IQL	<IQL	13	2.6
EPC 7-18	12.655	4.0	<IQL	<IQL	12	2.9
EPC 7-19	14.065	4.6	<IQL	<IQL	16	4.3
EPC 7-21	15.515	5.1	<IQL	<IQL	25	6.2
EPC 7-22	16.015	5.5	<IQL	<IQL	10	4.0
EPC 7-23	16.745	12	<IQL	<IQL	19	7.1

Table 12. Depth-weighted mass averages (mg kg^{-1}) for vadose zone anion concentrations.

Core	Total Depth (m)	Chloride (mg kg^{-1})	Bromide (mg kg^{-1})	Nitrate-N (mg kg^{-1})	Sulfate (mg kg^{-1})	Fluoride (mg kg^{-1})
EPC 1	5.1	4.5	0.33	0.017	28	1.2
EPC 2	5.2	4.4	0.33	0	30	1.7
EPC 5	11.7	6.6	0	0.12	24	3.3
EPC 7	16.7	69	0.31	0.20	64	4.8

Table 13. Daily rain and corresponding day in Hydrus 1D model simulation.

Date	Rain (mm)	Model Day	Date	Rain (mm)	Model Day	Date	Rain (mm)	Model Day	Date	Rain (mm)	Model Day
12/27/2016	0	1	2/7/2017	0	43	3/21/2017	0	85	5/2/2017	0	127
12/28/2016	0	2	2/8/2017	0	44	3/22/2017	0	86	5/3/2017	4.064	128
12/29/2016	0	3	2/9/2017	0	45	3/23/2017	0	87	5/4/2017	0	129
12/30/2016	0	4	2/10/2017	0	46	3/24/2017	12.45	88	5/5/2017	0	130
12/31/2016	0	5	2/11/2017	0	47	3/25/2017	0.254	89	5/6/2017	0	131
1/1/2017	0	6	2/12/2017	0	48	3/26/2017	0	90	5/7/2017	0	132
1/2/2017	0	7	2/13/2017	0	49	3/27/2017	0.508	91	5/8/2017	0	133
1/3/2017	0	8	2/14/2017	2.54	50	3/28/2017	0	92	5/9/2017	0	134
1/4/2017	0	9	2/15/2017	0	51	3/29/2017	35.81	93	5/10/2017	0	135
1/5/2017	0	10	2/16/2017	0	52	3/30/2017	18.03	94	5/11/2017	22.1	136
1/6/2017	0	11	2/17/2017	0	53	3/31/2017	0	95	5/12/2017	3.302	137
1/7/2017	0	12	2/18/2017	0	54	4/1/2017	0	96	5/13/2017	0	138
1/8/2017	0	13	2/19/2017	0	55	4/2/2017	12.95	97	5/14/2017	0	139
1/9/2017	0	14	2/20/2017	0	56	4/3/2017	0	98	5/15/2017	0	140
1/10/2017	0	15	2/21/2017	0	57	4/4/2017	0	99	5/16/2017	0	141
1/11/2017	0	16	2/22/2017	0	58	4/5/2017	11.43	100	5/17/2017	0.254	142
1/12/2017	0	17	2/23/2017	0	59	4/6/2017	0	101	5/18/2017	0	143
1/13/2017	0	18	2/24/2017	0	60	4/7/2017	0	102	5/19/2017	0	144
1/14/2017	0	19	2/25/2017	0	61	4/8/2017	0	103	5/20/2017	2.286	145
1/15/2017	0.762	20	2/26/2017	0	62	4/9/2017	0	104	5/21/2017	0	146
1/16/2017	2.286	21	2/27/2017	0	63	4/10/2017	0	105	5/22/2017	0	147
1/17/2017	11.18	22	2/28/2017	0	64	4/11/2017	0	106	5/23/2017	0.762	148
1/18/2017	2.286	23	3/1/2017	0	65	4/12/2017	0	107	5/24/2017	0	149
1/19/2017	0	24	3/2/2017	0	66	4/13/2017	79.25	108	5/25/2017	0	150
1/20/2017	0	25	3/3/2017	0	67	4/14/2017	0	109	5/26/2017	0	151
1/21/2017	0	26	3/4/2017	0	68	4/15/2017	0	110	5/27/2017	0	152
1/22/2017	0	27	3/5/2017	0	69	4/16/2017	0	111	5/28/2017	0.254	153
1/23/2017	0	28	3/6/2017	0	70	4/17/2017	0	112	5/29/2017	0	154
1/24/2017	0	29	3/7/2017	0	71	4/18/2017	0	113	5/30/2017	0	155
1/25/2017	0	30	3/8/2017	0	72	4/19/2017	0	114	5/31/2017	0	156
1/26/2017	0	31	3/9/2017	0	73	4/20/2017	0	115	6/1/2017	0	157
1/27/2017	0	32	3/10/2017	0	74	4/21/2017	0	116	6/2/2017	1.524	158
1/28/2017	0	33	3/11/2017	0	75	4/22/2017	5.588	117	6/3/2017	0	159
1/29/2017	0	34	3/12/2017	0	76	4/23/2017	0	118	6/4/2017	0	160
1/30/2017	0	35	3/13/2017	0	77	4/24/2017	0	119	6/5/2017	0	161
1/31/2017	0	36	3/14/2017	0	78	4/25/2017	0	120	6/6/2017	0	162
2/1/2017	0	37	3/15/2017	0	79	4/26/2017	0	121	6/7/2017	1.016	163
2/2/2017	0	38	3/16/2017	0	80	4/27/2017	0	122	6/8/2017	0	164
2/3/2017	0	39	3/17/2017	0	81	4/28/2017	6.604	123	6/9/2017	10.16	165
2/4/2017	0	40	3/18/2017	0	82	4/29/2017	4.318	124	6/10/2017	0	166
2/5/2017	0	41	3/19/2017	0	83	4/30/2017	20.32	125	6/11/2017	0	167
2/6/2017	0	42	3/20/2017	0	84	5/1/2017	10.92	126	6/12/2017	0	168
									6/13/2017	0	169

Table 14. Ion chromatograph instrument quantification limit (IQL) and R² value from linear regression. Values are based on two high and two low standards for each run. Detector response (area under the curve, $\mu\text{S} \cdot \text{min}$) is plotted against the calculated standard quantities (mg L^{-1}) for the calculation of root mean square error (Corley, 2003).

Value	Fluoride	Chloride	Bromide	Nitrate-N	Phosphate-P	Sulfate
Run 1						
IQL	0.12	0.10	0.20	0.05	0.13	1.16
R ²	0.92	1.00	0.85	1.00	0.99	1.00
Run 2						
IQL	0.26	0.48	0.03	0.39	0.12	3.31
R ²	0.91	1.00	0.97	0.99	1.00	1.00
Average of Runs 1 and 2						
IQL	0.2	0.3	0.1	0.2	0.1	2.2
R ²	0.91	1.00	0.91	1.00	1.00	1.00

Table 15. Results for the four Infiltrometer measurements collected in August, 2017.

Test Name	Location	K _{sat} (cm sec ⁻¹)	K _{sat} (mm yr ⁻¹)	K _{sat} Error (cm sec ⁻¹)
Inf 1	Playa	7.84E-04	247,000	1.50E-04
Inf 2	Playa	1.62E-04	51,100	1.86E-05
Inf 3	Interplaya	2.33E-04	73,500	2.57E-04
Inf 4	Interplaya	7.21E-04	227,00	6.78E-05

Table 16. Fluid fluxes calculated from the date and time that each sensor reached field capacity (-33 kPa).

Sensor Depth (cm)	Date Field Capacity was Reached at Sensor	Time Elapsed Between Reaching Field Capacity (days)	Fluid Flux (mm yr ⁻¹)
12	3/29/17 11:30 AM	NA	NA
47	4/12/17 10:30 PM	14.46	8,800
96	4/13/17 9:20 AM	0.45	400,000
152	4/14/17 3:20 AM	0.75	270,000

Table 17. Maximum Fluid Flux calculated by the Hydrus 1D model at each of the four nodes.

Node (cm)	Max Flux (mm yr ⁻¹)
Surface	28,900
39	9,600
160	470
510	2.9E-06
1150	2.9E-06